FLUORINATED EMITTER MOLECULES FOR TRIPLET-TRIPLET ANNIHILATION UP-CONVERSION MEDIA

HOPE, ADAM,JOHN

DURHAM UNIVERSITY

A THESIS ENTITLED

FLUORINATED EMITTER MOLECULES FOR TRIPLET-TRIPLET ANNIHILATION UP-CONVERSION MEDIA

SUBMITTED BY

ADAM JOHN HOPE

A CANDIDATE FOR THE DEGREE OF DOCTOR OF PHILOSOPHY

DEPARTMENT OF CHEMISTRY

2013

Abstract

This thesis details the synthesis, characterisation and photophysical properties of various fluorinated emitters for triplet-triplet annhilation up-conversion systems. The theory and mechanism of TTAUC is evaluated and the molecular design of the annihilating emitter molecule reviewed to allow improvement of the external up-conversion quantum yield and overall energy efficiency of the process.

Three main series of chromaphores were investigated, based on diphenylanthracenes, bisphenylperylenes, and 3,5,8-triphenylBODIPYs. These were synthesised by metal catalysed aryl-aryl coupling (Suzuki-Miyaura) or nucleophilic substitution reactions and, when paired with appropriate sensitizing molecules, allowed the up-conversion of green to blue; red to green; and near IR/red to orange respectively.

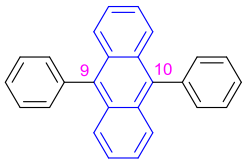

anthracene core

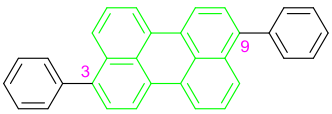

perylene core

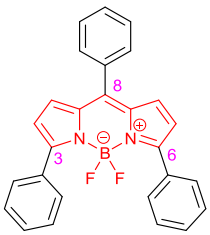

BODIPY core

The effect of increasing fluorination on the ease of synthesis and photophysical properties of these emitter systems was studied with a view to their application in up-conversion systems. Fluorinated emitter molecules were shown to be highly resistant to degradation by UV light compared to their non-fluorinated analogues, for example 9,10-bis(2,3,5,6-tetrafluoro-4-(trifluoromethyl)phenyl)anthracene was over 50 times more resistant to 4 hours of direct UV irradiation that its analogue 9,10-diphenylanthracene. The up-conversion ability of these systems was evaluated, and a system containing the highly fluorinated bisphenylperylene analogue 3,9(10)-bis(2,3,5,6-tetrafluoro-4-(trifluoromethyl)phenyl)perylene was shown to have extremely high external quantum yield (16%) and energy efficiency (21%), with a very low onset of the strong up-conversion limit of 0.1 $W.cm^{-2}$. Novel fluorinated BODIPY based dyes were produced that have high fluorescence quantum yields of over 90%. Finally the up-conversion of up-converting nanoparticles incorporating fluorinated emitters was evaluated, with the best showing an external up-conversion yield of 1%, which is higher that comparable lanthanide based up-converting nanoparticles.

Acknowledgements

I would like to thank my supervisor, Professor Graham Sandford, for the opportunity to study for a PhD, and also for his continued guidance and faith.

Thank you to everyone at Sony MSL, Stuttgart, particularly Dr Gabrielle Nelles, Dr Tzenka Miteva, Dr Vladimir Yakutkin and Mr Tony Roberts, for both funding and support, without which this thesis would not have been possible.

I would like to thank the denizens of CG 115, both past and present, for their friendship during my time at Durham.

The chemistry department would not function without the aid of the technical staff, and thank you to those who have helped me in the production of this thesis, including Dr Alan Kenwright, Mr Ian McKeag and Mrs Catherine Heffernan (NMR), Dr Jackie Mosely, Dr Dave Parker and Peter Stokes (MS), Dr Dima Yufit (Crystallography), Mr Malcolm Richardson and Mr Aaron Brown (Glassblowing), Mr Dave Hunter (High pressure laboratory), and members of the chromatography service, the stores, and the administration and secretarial staff.

Thank you to my family, particularly my mother for her continuing love and support, without which I would be very little and to Lauren – thank you, always.

Memorandum

The work described within this thesis was carried out at Durham University between October 2010 and December 2013. This thesis is the work of the author, except where acknowledged by reference and has not been submitted for any other degree. The copyright of this thesis lies solely with the author and no quotation from it should be published without prior written consent and information derived from it should be acknowledged. No part of this thesis may be reproduced by any means, nor transmitted, nor translated into any machine language without the express written permission of the author.

Nomenclature and abbreviations

In figures an F in the centre of a ring denotes that all hydrogen atoms have been replaced by fluorine atoms.

The following abbreviations are used throughout the thesis.

AIBN	Azobis(isobutyro)nitrile	MP	Melting Point
ASAP	Atmospheric Solids Analysis probe	MS	Mass spectrometry
COSY	Correlated spectroscopy	NMR	Nuclear magnetic resonance
DCM	Dichloromethane	OLED	Organic light emitting diode
Dppf	1,1'-bis(diphenylphosphino)ferrocene	RT	Room temperature
DSSC	Dye sensitized solar cell	S_NAR	Nucleophilic aromatic substitution
GC	Gas chromatography	TFA	Trifluoroacetic acid
GCMS	Gas chromatography-mass spectrometry	TGA	Thermogravimetric Analysis
HMBC	Heteronuclear multiple bond correlation	THF	Tetrahydrofuran
HRMS	High resolution mass spectrometry	TLC	Thin-layer chromatography
HSQC	Heteronuclear single quantum correlation	TTA	Triplet-triplet annihilation
IR	Infrared	TTAUC	Triplet-triplet annihilation up-conversion
ISC	Intersystem Crossing	TTAUCS	TTAUC system
IUPAC	International Union of Pure and Applied Chemistry	TTT	Triplet-triplet transfer
MeCN	Acetonitrile	UC	Up-conversion
MeOH	Methanol	UV	Ultraviolet

Appendices, containing x-ray crystallography data, HPLC and NMR traces are contained in the accompanying compact disc.

A note on the numbering of compounds

In this project four series of target compounds were produced, based on 4 molecular scaffolds. For clarity these four scaffolds are numbered 1-4, as shown below. The derivitisation of the scaffolds is indicated by a letter following their number. The least fluorinated derivative is numbered with the scaffold number and suffix **a**, and more highly fluorinated compounds have later alphabetical letters, for example compound **2a** is 9,10-diphenylanthracene.

1

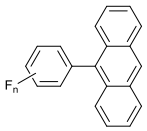

9-phenylanthracene scaffold

2

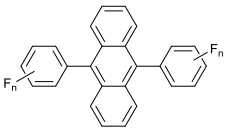

diphenylanthracene scaffold

3

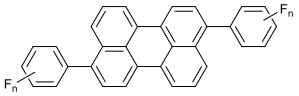

bisphenylperylene scaffold

4

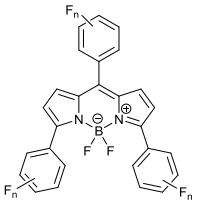

tri-aryl BODIPY scaffold

Compounds that were intermediates or byproducts in forming the target compounds are numbered sequentially throughout the thesis.

Contents

1. Introduction

The energy up-conversion of light by triplet-triplet annihilation up-conversion (TTAUC) has been gaining increasing interest over the past ten years, with particular reference to it's potential in third generation solar technology.[1,2] Up-conversion systems (UCSs) chemically convert incident low energy light to a higher energy emission, by receiving two or more low energy photons, either simultaneously or sequentially, and expelling a photon with the summed higher energy.[3]

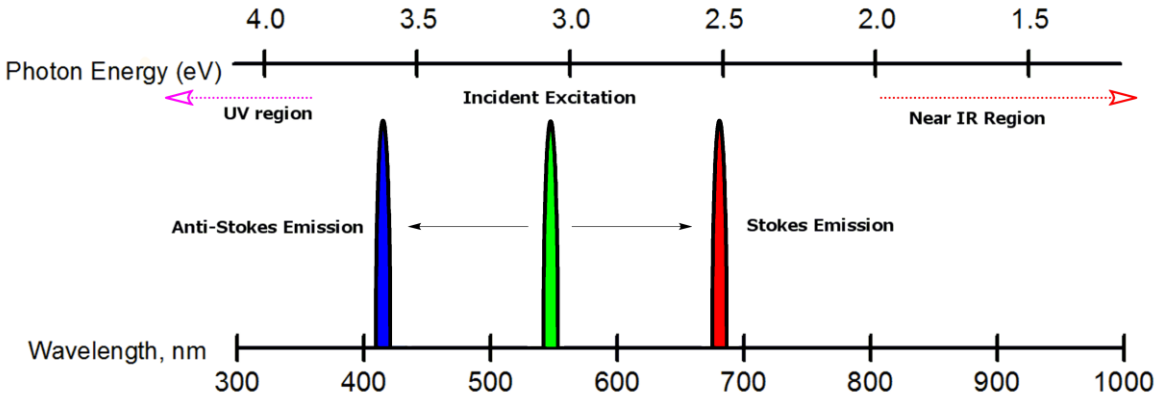

Figure 1.1 : Stokes and Anti-Stokes emission

As the world's population continues to grow the issue of producing sufficient energy in a secure, environmentally considerate manner is becoming increasingly important. Over reliance on fossil fuels decreases energy security and has grave effects upon the climate, causing environmental, social and economic damage.[4] Energy of the order of tens of petawatts (10^{15} W) falls upon the earth from the sun and harnessing this energy with solar photovoltaic (PV) panels could allow clean, renewable energy production. Current PV technology does not efficiently use the whole spectrum of the sun's rays falling on the earth:[5] triplet–triplet annihilation up-conversion systems (TTAUCSs) could utilize a larger proportion of this light than ever before.[6]

Population increase has been greatly influenced by improved disease diagnosis and treatment since the advent of modern medical science. Bio-nanophotonic imaging, nanotherapies and fluorescence image guided surgery have the potential to further improve human health, and TTAUCSs could play an instrumental part in this endeavour by allowing less damaging low energy light to illuminate less invasive injected fluorescent probes.[7]

Across the world display technology is now ubiquitous – there are now almost as many mobile phone subscriptions as people.[8] As devices become smaller display technology must adapt – TTAUCSs can produce low cost, extremely thin, transparent displays with low power requirements and high resolution.

For single photon events, where absorption is followed by a fluorescent or phosphorescent emission, the incident light must be greater or equal to that emitted – energy cannot be gained in the process. This "Stokes shift" is based on the thermodynamic necessity that energy is not created or destroyed and is universal. The overall effect of the UCS is that light is emitted with an "anti-Stokes shift", seemingly gaining energy in violation of thermodynamic expectation (Figure 1.1). However, since two photons are absorbed their combined energies are greater than that of the single emitted photon, thus the maximum external photon quantum yield of this process is 50%: energy is conserved and not created. Therefore, the energy of the emitted photon can only be a maximum of double that of the incident photons, for a two photon process. This theoretical scope allows bridging the visible spectrum by producing ultraviolet (UV) light from incident near-infrared (NIR) photons, which would be very useful for many optoelectronic applications.

Triplet-triplet annihilation (TTA) is a form of P-type delayed fluorescence, where the fluorescence lifetime is half that of the phosphorescence lifetime. For E-type delayed fluorescence the lifetime is equal to the associated phosphorescence of the molecule. These differ by their routes of producing excited singlets from triplet states. Recombination delayed fluorescence allows the population of the first excited state by recombination of radical chromaphore species with electrons or radical ions of opposite charge.[9]

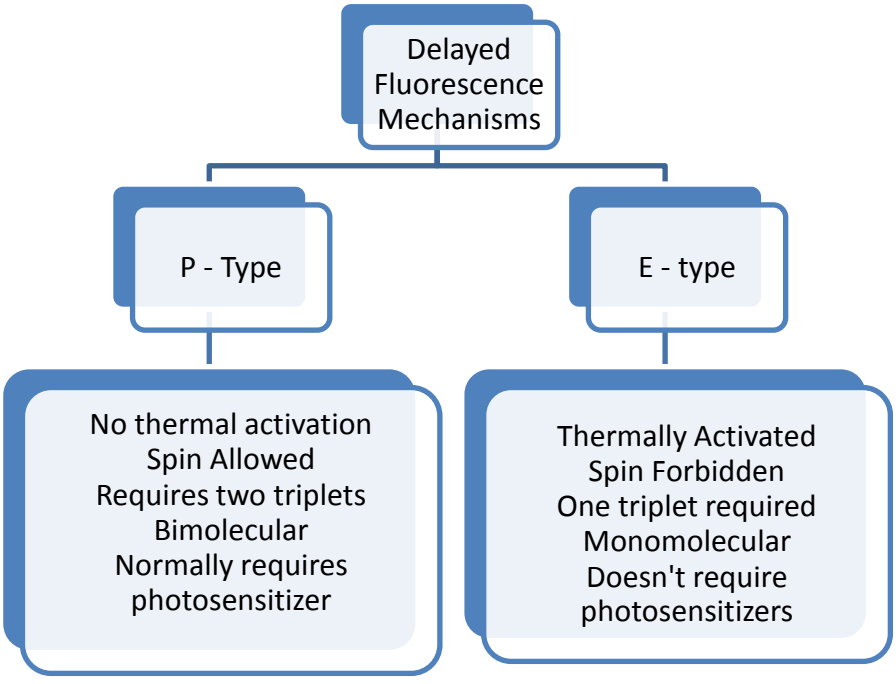

Figure 1.2 : Delayed Fluorescence Mechanisms

Other mechanisms for generation of high energy light from low energy incident light include: two-photon absorption, where two photons are absorbed at the same time and a single photon emitted; and multistage absorption, involving the population of an intermediate excited state followed by the absorption of another photon.[10,11] Rare-earth-ion doping[12,13] and two-photon adsorption[5] generally

require high density above 1 sun (0.1 $W.cm^{-2}$) and coherent light to function, whereas TTA up-conversion systems can efficiently use low density incoherent light, such as solar light.[14]

The first instances of TTAUC were reported by Parker and Hatchard in the 1960s,[15,16] but little practical use was made of this discovery for four decades, other than reports of delayed fluorescence in polymers.[11,17] However, with the realisation that metal-ligand charge transfer compounds can be used as stable sensitizers that possess high intersystem crossing (ISC) yields interest in these systems has increased dramatically.[10,18] Recently a number of reviews have been published in the area: by Castellano *et al*.,[19] by Zhao *et al.* surveying the various sensitizers in use,[20] by Ceroni looking at the supramolecular aspects of TTAUC,[21] by Monguzzi *et al*.,[22] and by Simon and Weder on triplet-triplet annihilation in polymers.[23]

Molecules used in TTAUCSs are commonly polyaromatic hydrocarbons, which are susceptible to thermal and photodegradation. The substitution of hydrogen by fluorine in hydrocarbons can confer vastly altered properties for the fluorinated derivative, including increased stability and bioactivity.[24] The use of fluorinated hydrocarbons in electronic devices is becoming more widespread due to the high strength of the carbon-fluorine bond (~480 $kJ.mol^{-1}$) which allows high thermal and oxidative stability as well as the electronic interactions that are provided by the substitution of hydrogen (Pauling scale EN = 2.20) with highly electronegative fluorine (Pauling scale EN = 3.98).[25] Within materials chemistry, organofluorine compounds and polymers have been increasingly used for their exceptional stabilities and useful properties.[25–27] Fluorine is associated with greatly improved thermal stability, as well as reducing the degrading effects UV light and oxygen.[28] Applications which make use of the optical and electrical properties of these fluorinated compounds include dye-sensitized solar cells (DSSCs),[29] organic thin film transistors (OFETs),[30] and organic light emitting diodes (OLEDs).[31,32] Previously within our group we have shown that highly fluorinated biphenyl ether systems can be used as dopants for fast-response liquid crystal display applications.[33,34] By applying fluorinated derivatives to the TTAUC arena it is possible that more stable, efficient systems may be produced.

In this thesis we assess the use of fluorinated aromatic systems in various TTAUC processes, and the following discussion introduces the current state-of-the-art in TTAUC systems and fluorine chemistry techniques that underpin the synthetic work carried out.

1.1. The Triplet-triplet Annihilation Up-conversion (TTAUC) Mechanism

The triplet-triplet annihilation up-conversion (TTAUC) process has the overall effect of combining the energy from two low power photons into a single high power photon by using bimolecular energy transfer and annihilation. This anti-Stokes delayed fluorescence is carried out by adsorption

by a sensitizer molecule (S) of an incident low energy photon (1.1 below) which possesses a high intersystem crossing (ISC) yield to the triplet state (1.2), which then transfers (1.3) the triplet energy to an emitter molecule (E).

$$S_S{}^0 \xrightarrow{Excitation} S_S{}^1 \quad (1.1)$$

$$S_S{}^0 \xrightarrow{ISC} S_T{}^1 \quad (1.2)$$

$$S_T{}^1 + E_S{}^0 \xrightarrow{TTT} S_S{}^0 + E_T{}^1 \quad (1.3)$$

$$E_T{}^1 + E_T{}^1 \xrightarrow{TTA} E_S{}^0 + E_S{}^1 \quad (1.4)$$

$$E_S{}^1 \xrightarrow{Emission} E_S{}^0 \quad (1.5)$$

If two triplet excited emitters annihilate (1.4) one may form an excited singlet and thus fluoresce a photon of increased energy compared to the photon that was adsorbed (1.5).

A Jablonski diagram may be used to follow the TTAUC process in more detail. First the sensitiser molecule is excited by incident light to $S_S{}^1$ and relaxes to a triplet state $S_T{}^1$ via intersystem crossing. Then the sensitizer in this triplet state may transfer energy via triplet-triplet transfer (TTT) to the emitter molecule $E_T{}^1$ rather than phosphoresce. If two emitter molecules in the triplet state encounter each other then triplet-triplet annihilation may occur, where one emitter molecule gains energy and reaches the excited singlet level $E_S{}^1$, while the other is quenched to the ground state $E_S{}^0$. The excited emitter molecule may then fluoresce, emitting a photon of increased energy compared to one of the incident photons. This means that blue or green light may be emitted from incident safe and cheap NIR or red light. The sensitizer must easily undergo intersystem crossing to produce a high triplet level population to then allow triplet-triplet annihilation to take place. The emitter and sensitizer may be tailored by altering their molecular structures (and thus energy levels) allowing an efficient pairing.

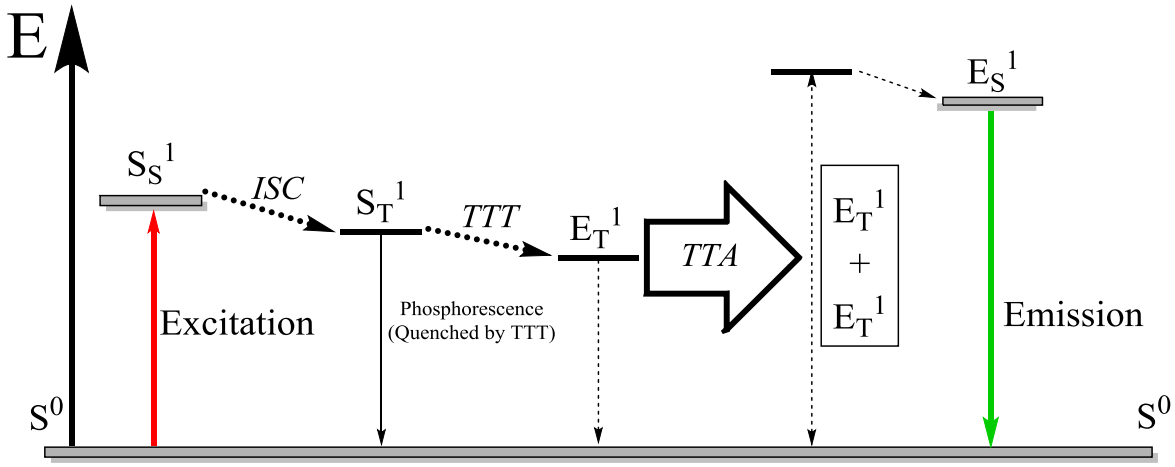

Figure 1.3 : Jablonski diagram of TTA up-conversion The vertical axis Energy (E) is unitless. Dotted lines indicate non-radiative transitions - intersystem crossing (ISC) and triplet-triplet transfer (TTT). Triplet-triplet annihilation (TTA) is shown by the open arrow. Solid arrows represent radiative transitions. Energy levels are represented by S_S^1 (first excited sensitizer singlet level), S_T^1 (first excited sensitizer triplet level), E_T^1 (first excited emitter triplet level), E_S^1 (first excited emitter singlet level).

Each of the photochemical processes: absorption, intersystem crossing (ISC), triplet-triplet transfer (TTT), triplet-triplet annihilation (TTA) and emission must be maximised for up-conversion to occur most effectively. The up-conversion quantum efficiency is a product of the efficiency of all the internal processes.

$$\Phi_{UC} = \Phi_{ISC} \times \Phi_{TTT} \times \Phi_{TTA} \times \Phi_F \qquad (1.6)$$

The bi-molecular processes (TTT and TTA) are promoted by close spatial relation between the emitter and acceptor molecules and this should ideally occur at a rate close to the diffusion limit, thus efficiencies tend to be greater in solution state TTA up-conversion than in films or polymers.[35]

In general, the sensitizer must readily absorb incident light and show a high degree of intersystem crossing to produce a long-lived triplet. Compounds that meet these requirements include metal complexes based on porphyrins: transition metals used in such metal ligand charge transfer (MLCT) compounds include ruthenium,[18,36,37] palladium,[6,10,38–40] iridium,[41] and platinum.[3,10,42–44] A fully organic sensitizer and emitter TTA up-conversion system producing near-white light has also been reported.[45]

The high energy difference between emitter singlet and triplet energy levels required for TTA up-conversion systems has caused polyaromatic hydrocarbons (PAHs) to be commonly employed as the emitter components. These are often selected for their high quantum yield of fluorescence, indicating a minimisation of non-radiative relaxation and examples include anthracene;[18] 9,10-diphenylanthracene;[6,18,38,40,45] 9,10-dimethylanthracene (DMA);[36] 2-chloro-bis-phenylethynylanthracene;[42] pyrene and 3,8-di-*tert*-butylpyrene;[41] rubrene[39] and perylene.[44] Recently boron dipyrromethene chromophores have been used as emitters rather than a PAH molecule.[43]

TTAUCSs may be processed relatively easily as they are generally small molecules dissolved in an organic solvent; they may be spincoated, screen printed, or evaporated as films onto substrates, as well as functioning in nanoparticles, rubbery solids and solutions, and there are many potential devices and applications that make use of high energy light produced from low energy light, thus TTAUC has great potential to disrupt current technologies.

1.2. The utility of photon TTAUC

Triplet-triplet annihilation up-conversion may be utilized in any situation where high energy photons are required from a low energy. Commonly explored applications include 3rd generation photovoltaic systems, display technologies and bioimaging.

TTA up-conversion techniques have many potentially useful applications such as in artificial photosynthesis, photocatalysis, photoelectrochemistry, optics and photovoltaic devices.[46] Recent reviews concerning TTA up-conversion indicate a growing interest in the field.[19,20,21] In particular, the Castellano group reported up-conversion of a range of emitters, their incorporation into solid polymer matrices and behaviour at varying power densities.[18,19,44,46,47] Another group at Milan-Bicocca University has reported studies using commercially available porphyrins with various emitters, measured their behaviour in solid films and nanoparticles and investiged the theoretical aspects of up-conversion.[22,35,48] Schmidt *et al.* have investigated the kinetic aspects of TTA up-conversion systems with commercial emitters such as rubrene.[1,49–53] A working photovoltaic system has been reported using a TTA up-conversion solution, which compared favourably to lanthanide up-conversion examples.[50] The Sony MSL group collaborating on this project has in the past investigated commercial sensitizers and emitters, as well as synthesising novel molecules for relevant applications and their use in solid matrices. Previously Sony MSL have shown that non-coherent light with intensity as low as 1 $W.cm^{-2}$ may be used in TTA systems composed of a metal ligand charge transfer sensitizer and an emitter.[6,10,14,54–57]

1.2.1. 3rd Generation Photovoltaics

Worldwide energy requirements are rising as both population and per capita energy consumption increase – this causes an increased strain on both the environment and energy security concerns.[58] Generating energy from the sun's solar radiation is generally accepted to be an important part of the energy production landscape, however efficiencies need to be improved to make photovoltaic technology more cost effective, viable and sustainable. While 1st generation solar energy production based on silicon semiconductors has been available for around 50 years and 2nd generation technology (such as DSSCs and thin film solar cells) is coming to fruition, more innovation is required in order that these become viable commercial alternatives to conventional

energy sources, such as fossil fuels. In single junction photovoltaic devices the band gap energy defines if a photon has sufficient energy to drive the cell; photons that are too low in energy are not adsorbed, while photons of higher energy produce the same amount of electrical power but their excess energy is lost as heat. Through both these effects the efficiency of the solar cell is greatly reduced. 3rd generation solar power technology is based on harnessing as much of the suns solar spectrum as possible, by, in effect, splitting high energy photons or combining low energy photons in such a way that the cell receives a smaller range of energies that it can use more efficiently.[5]

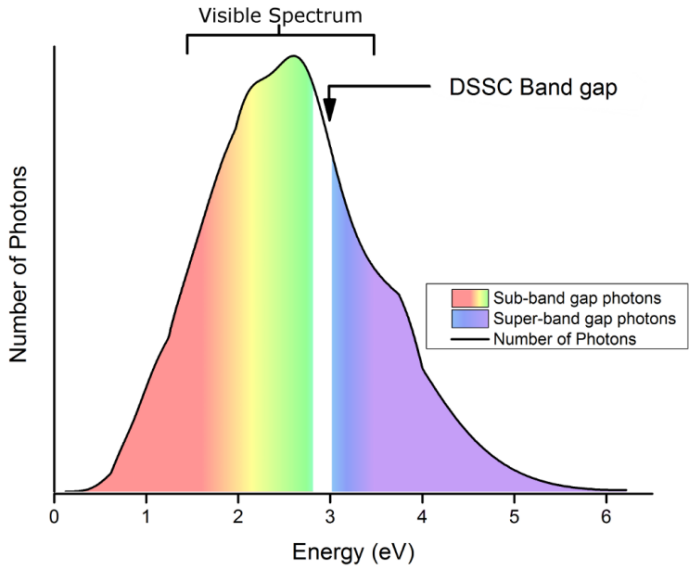

Figure 1.4 : A cartoon of the solar spectrum, with DSSC band gap marked. The area to the left of the band gap is not harnessed by DSSC cells, the area to the right is used inefficiently.

If super-band gap photons could be broken up into separate photons with lower energy (down-converted), and sub-band gap photons combined to form a single photon of increased energy (up-converted) the overall efficiency of the cell could be greatly increased.[5] Examples where up-conversion systems have been incorporated in cells have been reported.[46,59] In silicon photovoltaic cells the band-gap is quite low (*circa* 1.1 eV), making down-conversion an important consideration. However, Grätzel dye-sensitized cells generally have a band-gap in the visible spectrum (*circa* 3 eV), making efficiency gains from up-conversion potentially very valuable.

As well as the possibilities in harvesting energy from the sun, TTA up-conversion may also be used to promote photochemical reactions that require high energy photons. By up-converting low energy light these reactions may be carried out using cheaper low power light, for example the [4+4] cycloaddition dimerization of anthracene.[37]

The great majority of up-conversion systems in the literature, and discussed in this review, are in solution - most commonly degassed toluene. However, the incorporation of up-conversion systems into solids, particularly polymers, is of great interest for applications. Due to the bimolecular nature of the TTT and TTA processes some diffusion allowance is required by the substance, so rubbery

solids have been commonly investigated, as well as nanoparticles[48,60] and films.[40] The incorporation of up-conversion systems into solids is associated with the decrease in the up-conversion efficiencies by several orders of magnitude, and cooling of the solids to glass transition temperatures often results in the almost complete cessation of the up-conversion phenomena: there is a clear correlation between glass transition temperature of the polymer host and the magnitude of up-conversion phenomena within.[19,23] A recent review by Simon and Weder has discussed the incorporation of up-conversion systems into polymers including nanoparticles.[23]

1.2.2. Up-conversion display media

The use of organic molecules for display media has been under investigation for many years, for example multi-layered organic light emitting diodes (OLEDs) were proposed by Tang *et al.* more than 20 years ago.[61] OLED research is now coming to fruition in modern display media including televisions and mobile phones, where their bright, efficient, high resolution screens are popular. One area of consumer display research that has not been investigated in depth to date is the use of "up-conversion systems" (UCSs), which could have lower power requirements than current LCD and OLED displays. UCS displays can produce bright, saturated colours while retaining long working lifetimes, and produce exceptionally thin, transparent, borderless displays by using refraction and internal reflection within the material to project the image from the side onto a viewing area.[62]

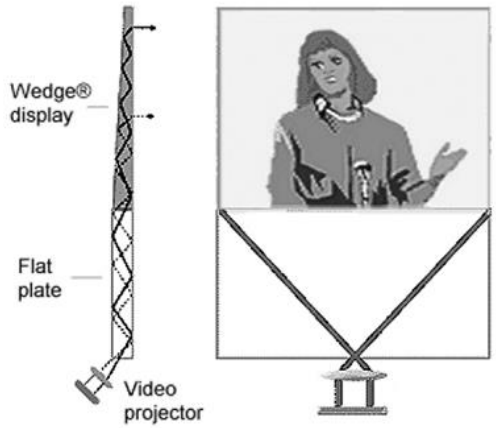

Figure 1.5 : Example side projection display (Cambridge Flat Projections Display Ltd.)[62]

Previous work on UCS displays has been on the use of inorganic materials; however the use of organic materials with high processability would have clear advantages in the production of such devices.

1.2.3. Bio-nanophotonic Imaging

Continuing improvement in medical imaging now allows earlier and more accurate diagnosis of diseases than ever before. Bio-nanophotonic imaging is a discipline that describes nanoscale optical science and technology when applied to biological systems, and has the potential to improve upon currently used medical imaging techniques due to its minimally invasive methods, high resolution and specificity. Current technologies suffer from disadvantages such as harmful ionizing radiation, inability to distinguish between benign and malignant tumours, harmful radioactivity and low resolution. Optical imaging methods, such as bio-nanophotonic imaging, overcome these difficulties and have many advantages since they:

- are not harmful
- can resolve objects from tens of nm in size
- give high resolution images, so can detect smaller tumours
- may be used for *in vitro, in vivo,* and *ex vivo* specimens
- can give information on cellular processes
- allow rapid and real time measurements
- allow multidimensional imaging
- are minimally invasive
- can detect precancerous conditions in a cell, before it becomes cancerous

Bio-nanophotonics is at a meeting point between medicinal sciences, nanotechnology[1] and photonics. Materials that are used for bio-nanophotonic applications are produced by chemical reactions that allow precise control over the composition size and shape of the objects formed. Such materials show interesting electronic, optical and physical properties that are dependent on these properties.

Photons may interact with biological materials by being absorbed or scattered. As well as decreasing the amount of light reaching the desired area this also causes problems. Light that is absorbed by tissue may cause autofluorescence - the tissue itself may re-emit light. This decreases the resolution, sensitivity and selectivity of the image by increased background interference. Adsorbed light may also cause damage to biological tissue by non-radiative interactions - these may cause thermal heating (roasting) or unwanted chemical reactions (due to oxygen radicals) within the tissue. Scattering of the light upon the tissue decreases the focus of the light that arrives at the desired target, lowering the brightness of the emission.

While tissue is clearly seen by the human eye due to its interactions with the visible portion of the electromagnetic spectrum, it is transparent to lower energy light in the infrared portion of the

[1] Formally, one nanometre (nm) is a billionth of a metre, but ‘nanotechnology' is normally taken to be the range from 1 to 100nm.

electromagnetic spectrum. The region between 800 - 1300 nm is known as the biological window, here photons may move to the desired target with greatly decreased unwanted tissue interaction. Bio-nanophotonics must harness this area of the electromagnetic spectrum.

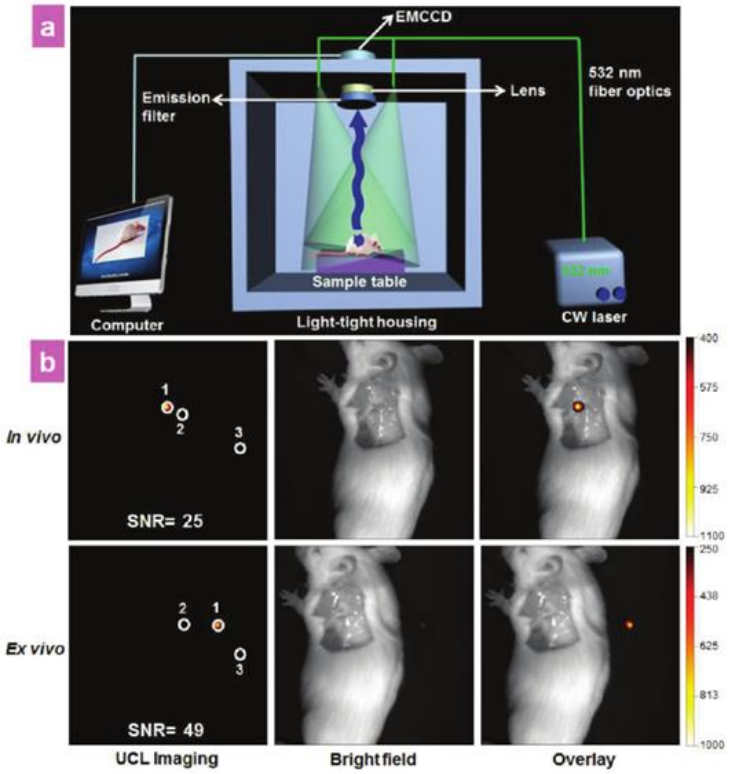

Figure 1.6 : a) Schematic layout of experimental setup. b) *In vivo* and *ex vivo* upconversion luminescence lympthatic imaging at 30 min postinjection of 20 µl of TTAUC nanoparticles in paw (adapted from Li *et al.*[60])

Up-converting nanoparticles use low energy light and produce high energy light. This allows them to make use of the so-called "biological window", the region in the electro-magnetic spectrum which does not interact strongly with biological tissue. Unwanted damage by lasers upon the tissue is prevented and any unwanted auto-fluorescent background signal can be filtered from the imaging system using short pass optical filters.

Whereas rare-earth-doped nanoparticles are the most widely investigated form of up-converting nanoparticle, triplet-triplet annhilation up-converting nanoparticles is a thriving area of research. Rare earth nanoparticles use inorganic lanthanide compounds that produce visible light from NIR light. A weakness of rare-earth-doped nanoparticles is that they phosphoresce, and thus cannot be used for short lifetime applications - they also require much higher coherent laser power densities than triplet-triplet annihilation up-conversion nanoparticles.[60]

TTAUC nanoparticles make use of molecular interactions between sensitizer molecules that can pass energy to emitter molecules within a nanoparticle.

Up-conversion systems could be used as biomarkers, since illumination with a NIR or red source would cause a clear emission of up-converted light that could only arise from TTA, greatly improving the signal to noise ratio.[56] The UCSs would be delivered within marked nanoparticles (designed to accumulate at certain positions within the body) allowing unambiguous marking of the extent of tumours for excision. Up-converting nanoparticles using diphenylanthracene have been employed for the marking of cells, as well as *in vivo* lymphatic node imaging.[60] Recently both BODIPY and perylene emitters have been used in nanocapsules for cell imaging.[63]

In summary, the potential applications of TTAUC require low energy light to be converted into high energy light in an efficient manner, conserving as much of the incident energy as possible.

1.3. Spectral properties of TTAUC systems

The most important properties of UCSs are the anti-Stokes shift, ($\Delta E = E_{obs} - E_{exc}$) and the external up-conversion quantum yield (Φ_{UC}). In both cases, the considered transitions are the sensitizer ${S_S}^0 \rightarrow {S_S}^1$ event and the emitter ${E_S}^1 \rightarrow {E_S}^0$ event. A Stokes shift is easily accessed by measurement of the incident and emitted photon wavelengths, but the absolute quantum yield is difficult to quantify accurately due to photon scattering during the experiment. A measurement of the unknown quantum yield (Φ_x) may be taken by comparison to a reference of known quantum yield (Φ_r), provided the emission integral (*F*), light intensity at excitation wavelength (*I*), absorbance of the substrate at excitation wavelength (*A*), refractive index of the substrate (*n*) and energy of the excitation photons ($h\upsilon$) are known. Under most experimental procedures the refractive index is kept constant.

$$\Phi_x = \Phi_r \frac{F_x}{F_r} \times \frac{I_r}{I_x} \times \frac{A_r}{A_x} \times \frac{n_x^2}{n_r^2} \times \frac{h\upsilon_x}{h\upsilon_r} \qquad (1.7)$$

A survey of up-conversion literature shows that the reporting of up-conversion quantum yield is not always consistent. Where up-conversion quantum yield data is presented it is confused by the incorporation (or lack) of a conversion factor. As the quantum yield is commonly used to compare different systems the calculation must be consistently explained or discrepancies may occur. Due to the annihilation step in the up-conversion sequence the maximum external quantum yield is 0.5, but in the literature quantum yields have commonly, and somewhat erroneously, been doubled to produce a maximum of 100%. The IUPAC approved definition of quantum yield is shown.[64]

$$\Phi = \frac{\text{number of events}}{\text{number of photons absorbed}} \qquad (1.8)$$

If the event measured is the emission of a photon then the doubling factor should not be applied, and the maximum possible value is 0.5, while if the event measured is the consumption of triplet

emitters in the TTA mechanism the maximum value is 1. In this work the measurements quoted are external up-conversion quantum yields (Φ_{UC}), calculated from the number of photons emitted ($N_{emitted}^{photons}$) and the number of photons absorbed ($N_{absorbed}^{photons}$) **without a doubling conversion factor**, in keeping with the IUPAC definition above. This aids comparison and allows the calculation of the energy efficiency of the overall process.

$$\Phi_{UC} = \frac{N_{emitted}^{photons}}{N_{absorbed}^{photons}} \tag{1.9}$$

Since the TTA is an "all or nothing" process there is a limit on the maximum energy of the up-converted photons for a given excitation energy: the combination of energy from two excited triplets into a singlet emitter requires that $2E_T^1 > E_S^1$, therefore since $S_S^1 > S_T^1$ then $E_S^1 < 2S_S^1$, meaning that the energy of the up-converted photons produced can never be more than twice the energy of the incident photons. This, however, may still theoretically cover the entire visible spectrum 700 → 350 nm, but energy losses due to non-radiative transitions and bi-molecular processes will greatly reduce this scope. Whereas an anti-Stokes emission is a strong indicator of up-conversion, there are a number of different mechanisms whereby this phenomenon may occur, the presence of TTAUC requires certain accompanying clues.

1.3.1. Measurement of TTAUC: Methods and Proofs

Before considering the detailed theory of up-conversion we must look at the methods by which it is measured, what proofs are considered for its presence, and how we can compare different molecular systems. Proofs are required because while the emission of light of higher energy than the incident is a strong indication of up-conversion, other mechanisms, such as two-photon absorption, could be taking place. It is generally assumed that if it can be proved that energy is being passed from the sensitizer molecule to the emitter molecule, and that the relationship between the emitted light intensity and the incident power density is quadratic, then TTAUC is the mechanism in action.

1.3.1.1. Proof of TTAUC I: Quadratic intensity relationship

A commonly used proof of the presence of TTA up-conversion in a molecular system is the quadratic relationship between incident power and external emission. However recently this has been shown to not be the case for all samples as linear and quartic relationships have also been reported.[38,51,52,65]

The number of photons emitted by the up-conversion system is an integral of the emission over all time, and this is dependent on the number of S_1 emitters produced by the mechanism of TTA.

$$2E_T^1 \xrightarrow{TTA} E_S^1 + E_S^0 \tag{1.10}$$

$$N_F = \int_0^\infty I_F(t)dt = \int_0^\infty \Phi_F k_{TTA}\left[{E_T}^1\right]_t^{\,2} \tag{1.11}$$

The fluorescence quantum yield (Φ_F) is taken as a constant for the emitter species, while the change in concentration of the emitter triplets over time is due to: spin forbidden non-radiative relaxation to the ground state (first order w.r.t. the emitter triplet); and the formation of an encounter complex capable of annhilation (second order w.r.t. the emitter triplet).

$${E_T}^1 + {E_T}^1 \rightarrow [{E_T}^1.{E_T}^1] \tag{1.12}$$

Thus k_T is the rate at which triplet emitters are consumed by decay to the ground state, while k_{TTA} is the rate at which they are consumed by annihilation.

$$\frac{d\left[{E_T}^1\right]_t}{dt} = -k_T\left[{E_T}^1\right]_t - k_{TTA}\left[{E_T}^1\right]_t^2 \tag{1.13}$$

Integration of this function gives the concentration of the emitter triplet at time t, as a function of the initial number of triplets formed:

$$\left[{E_T}^1\right]_t = \left[{E_T}^1\right]_0 \frac{1-\beta}{e^{k_T t} - \beta} \tag{1.14}$$

Where β gives the fraction of initial decay that occurs through the second order channel.[66]

$$\beta = \frac{k_{TTA}\left[{E_T}^1\right]_0}{k_t + k_{TTA}\left[{E_T}^1\right]_0} \tag{1.15}$$

At low power densities, $k_T > k_{TTA}[E_1^T]$; the triplet emitter molecules do not encounter each other rapidly enough for TTA to occur before they decay to the ground state, thus, the proportion of second order decay (β) very small. Therefore, the concentration of triplet emitter molecules at time *t* is proportional to the initial number of triplet emitter molecules.

$$\left[{E_T}^1\right]_t = \left[{E_T}^1\right]_0 e^{-k_T t} \tag{1.16}$$

When this is inserted into equation (1.11) to find the total number of emitted photons it is clear that this is proportional to the initial number of emitter triplet molecules squared.

$$N_F = \frac{\Phi_F k_{TTA} \left[{E_T}^1\right]_0^{\ 2}}{2k_T} \quad (1.17)$$

$$N_F \propto \left[{E_T}^1\right]_0^{\ 2} \propto (N_I)^2 \quad (1.18)$$

Thus, the number of photons emitted by the up-conversion device is proportional to the square of the triplet emitters produced by the incident light.[19] This relationship has been reported experimentally in most papers on TTAUC.

1.3.1.2. Proof of TTAUC II: Stern Volmer quenching constants

Within the TTAUC process, the TTT step involves a bimolecular quenching of the triplet sensitizer molecule by the singlet emitter molecule. This can be measured by the Stern-Volmer relationship, where in practice the fluorescence lifetime of the sensitizer is measured in combination with various emitter concentrations.

$$\tau_0/\tau = I_0/I = 1 + K_{SV}[Q] \quad (1.19)$$

The Stern-Volmer quenching coefficient (K_{SV}) is calculated from the ratios of: I_0 - the emission intensity in the absence of the quencher; and I - the emission intensity in the presence of molar concentration of quencher $[Q]$, alternatively the emission lifetime of the sensitizer (τ) may be used.[44] The bimolecular quenching coefficient (k_q) can be calculated (1.20).

$$K_{SV} = k_q \tau_0 \quad (1.20)$$

Where τ_0 is the lifetime in the absence of the quencher. The values of K_{SV} are normally around 10^5 M^{-1} and the values of k_q are in the region of 10^9 M^{-1} s^{-1}. The presence of bimolecular quenching is instrumental to the TTAUC process and shows that energy is being passed from the sensitizer to the emitter. If k_q is close to the diffusion rate then the quenching can be said to be efficient. However, other quenching pathways may also have an effect.

1.3.2. Comparing TTAUC systems

It is very difficult to compare different up-conversion systems as different testing apparatus, solvents (or solid incorporation) and preparation methods (including the rigorous exclusion of oxygen) return different results from similar systems. Differing the molar ratio of the sensitizers and emitters also has an effect. Added to this, the fact that up-conversion quantum yields are quoted with or without doubling factors (as explained above) makes direct comparison difficult.

Zhao *et al.* proposed that up-conversion systems could be evaluated by the use of an up-conversion capability parameter (η), calculated by multiplying the up-conversion quantum yield and the extinction coefficient of the sensitizer.

$$\eta = \varepsilon \times \Phi_{UC} \tag{1.21}$$

This is intended to give a measure of both how well the sensitizer can adsorb incident photons and what proportion of these are then emitted by the up-conversion system. While a useful measure of how efficiently the system may use incident photons, it does not take into account the energy of the photons emitted.

$$\Xi = \frac{\Phi_x \times E_{obs}}{E_{exc}} \tag{1.22}$$

Clearly for applications such as solar cells the overall energy conserved in the process, and thus available for power generation, is important. Consequently, this thesis proposes an "up-conversion energy efficiency" parameter (Ξ) which is calculated from the quantum yield of the emitter and the incident and emission photon energies.

This value is a measure of how much usable energy has been retained by the up-conversion system for possible use. For example, if no energy is lost in the transitions and the external quantum yield is 50% the energy efficiency would be 100%. The most energy efficient system to date is tetrakisquinoxalinoporphyrin palladium(II) and rubrene, producing almost 20% energy efficiency.[52]

Sensitizer	**Emitter**	**$\lambda_{(ex)}$ (nm)**	**$\lambda_{(obs)}$ (nm)**	**$E_{(obs)} - E_{(ex)}$ (eV)**	**Φ_{UC} %**	**Ξ %**
PQ_4Pd	Rubrene	670	560	0.36	16.5[52]	19.7
PdTBP	perylene/bodipy dyad	635	550	0.30	11.0[67]	12.7
Pt-3	DPA	445	410	0.24	9.1[68]	9.8
PtTBP	Perylene	635	451	0.80	6.5[44]	9.2
PtTBP	BD-2	635	556	0.28	7.5[43]	8.9
B4	1CBPEA	635	490	0.58	6.1[69]	7.9
Pt-2	DPA	445	410	0.24	7.1[68]	7.7
C-2	Perylene	532	490	0.20	7.0[70]	7.6
B4	Perylene	532	451	0.42	6.1[69]	7.2
$[Ru(dmb)_3]^{2+}$	DMA	515	431	0.47	4.0[36]	4.8
B-1	Perylene	532	451	0.42	4.1[71]	4.8
PdTBP	BPEA	635	490	0.58	3.2[6]	4.2
PtTBP	BD-1	635	527	0.40	3.1[43]	3.8
PdTAP	Rubrene	780	560	0.62	1.2[55]	1.7
Biacetyl	PPO	442	360	0.64	0.6[72]	0.7

Table 1: Up-conversion quantum yield (Φ_{UC}), anti-Stokes shift and energy efficiency (Ξ) of reported TTAUC systems, structures see figure 1.15 and associated references

The energy efficiency may be used to compare up-conversion systems composed of different types of emitter and sensitizer pairings. It does not take into account the proportion of incident source photons that are initially adsorbed by the sensitizer but, provided the adsorption at the incident wavelength is constant, provides a useful comparison. Indeed, the two parameters are complimentary, since the up-conversion capability (η) is of more utility to assess the effect of the sensitizer, while the up-conversion energy efficiency (Ξ) is useful to probe emitter efficiency. It should be noted that the use of the up-conversion energy efficiency parameter assumes monochromatic excitation and emission – in reality this will not be the case, and so results are affected by the shape of the emission spectrum. For example, a spectral shape where the peak wavelength is skewed to the higher energy side will have an artificially inflated efficiency parameter. This could be solved by integration across the spectrum, however this data is not commonly available. Since energy efficiencies can differ by significant amounts the measure can be used as an indicator of efficient sensitizer / emitter pairings.

There are a number of processes that a TTAUCS must realise to allow efficient and effective up-conversion, governed by the sensitizer and emitter molecules, as well as their environment.

1.3.3. Running the gauntlet of TTAUC effectiveness

While the general up-conversion scheme described by the Jablonski diagram (Figure 1.3) is widely accepted, there has been some discussion in the literature regarding a few of the facets of the model, including the maximum possible external up-conversion quantum yield. These encompass spin-statistical arguments and kinetic arguments, including altering the relationship between incident power and up-conversion efficiency, as well as the mode of intermolecular triplet transfer. Each of these considerations creates an additional method by which TTA up-conversion may be perturbed, so a "gauntlet" is created, through which the system must be guided to produce the maximum up-conversion quantum efficiency.

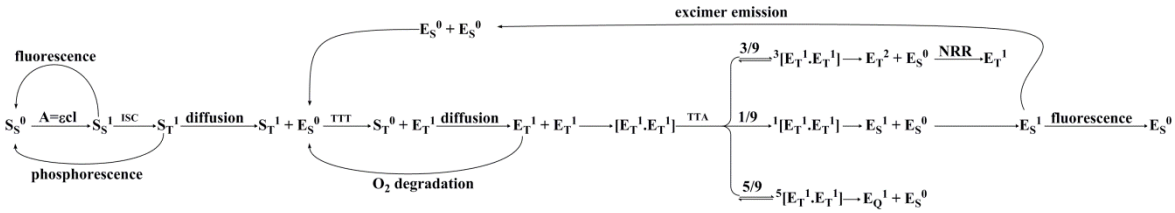

Figure 1.7 : The up-conversion "gauntlet"

It is clear that the limiting part of the TTAUC system is the emitter compound, since its energy levels define the TTT, TTA and fluorescence efficiencies, and its ability to withstand aggregation will prevent any excimer emission. We can assess each step in the process individually.

1.3.3.1. Solely Sensitizer dependent steps: adsorption and ISC

The first two steps that the system undergoes in the TTAUC process, the adsorption and intersystem crossing, are entirely dependent on the sensitizer molecule and its surroundings, and are well understood. The adsorption relies on the concentration and extinction coefficient of the sensitizer, as well as the path length of the container ($A = \varepsilon cl$). Maximising the initial adsorption step requires the use of an efficient chromaphore at sufficient concentration, in an architecture that presents a long enough pathlength for a high optical density. The intersystem crossing step has been improved by the use of transition metal cation containing complexes, which possess an intersystem crossing yield close to 1.[22] Other reviews have investigated the effect that sensitizer design has on the TTA up-conversion system.[20]

1.3.3.2. Triplet-triplet transfer

Experimentally it has been shown that the efficiency of the TTT step (Φ_{TTT}) is affected by the molar concentration ratio of the sensitizer triplets and ground state emitter molecules, as well as the temperature and excitation intensity.[67]

Clearly a long lived triplet state for the sensitizer is a necessary consideration, as this increases the proportion of sensitizers in the T^1 state ready to undergo TTT.[68] TTT is observed provided the accepting energy level is lower than the donating level: ${E_T}^1 < {S_T}^1$. While an increase in this energy difference represents a greater "driving force" to TTT, and prevents TTT back transfer from the emitter to the sensitizer, it also represents an energy loss in the system – ideally TTT would proceed immediately with zero energy loss. Experimentally this situation is generally created by using a 20 fold excess of emitter,[67] which decreases the effect of the sensitizer T^1 lifetime, and prevents any back-transfer by TTT. A system utilizing 2.0 equivalents of emitter to a sensitizer possessing a long-lived T^1 has been shown to be effective.[68]

The exact nature of the triplet-triplet transfer (TTT) from the sensitizer to the emitter is assumed to be a mixture of Dexter-type (electron transfer) and Förster-type (resonant energy transfer). It has been shown by Monguzzi *et al.* that the Dexter-type transfer is dominant at low temperatures, while at room temperature diffusion has a major effect.[35] This then allows the Perrin approximation to be used, where within the active sphere of the sensitizer the transfer occurs with an efficiency of unity, while outside this sphere the transfer does not occur. It follows from this that the concentration of the two species must be sufficient to allow an emitter to always be within the Perrin limit of the sensitizer, allowing most efficient TTT.[23]

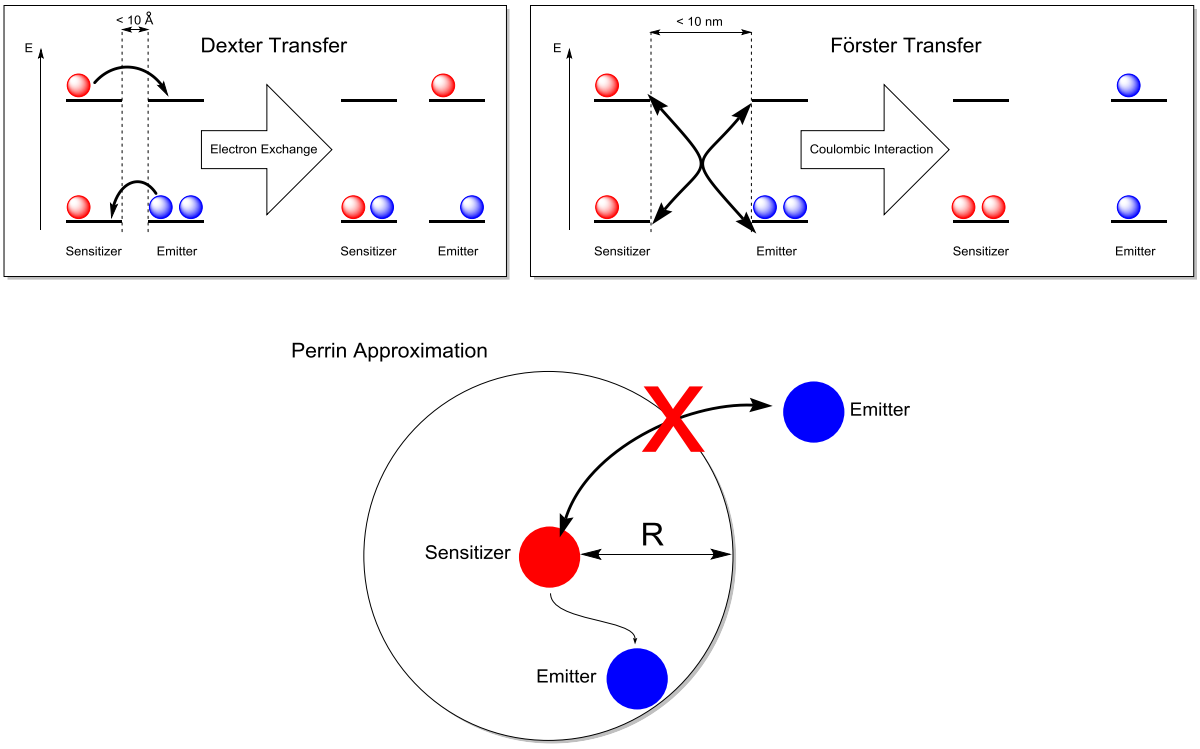

Figure 1.8 : Dexter Transfer, Förster Transfer and the Perrin Approximation, adapted from[23]

For molecular design the solubility of the emitter and sensitizer chromaphores must be as high as possible to facilitate high concentrations, to create the largest optical density in the sample, and their energies must effectively overlap, with ${E_T}^1 < {S_T}^1$.

1.3.3.3. TTA: Does spin statistical theory define the UC efficiency?

Since the TTAUC process crucially must form a single photon from two incident photons a limit for the external quantum yield of 0.5 is clear, however, it was thought that spin-statistics reduced this greatly.

When two molecules, for example two emitter molecules, collide in solution the number of encounter complexes possible is the product of their multiplicities, and in the absence of a magnetic field they are populated equally.[73,74] Following the Clebsch-Gordon series for the interaction for two triplets, nine encounter complexes may be formed, of which one is a singlet, three are triplets and five are quintets.

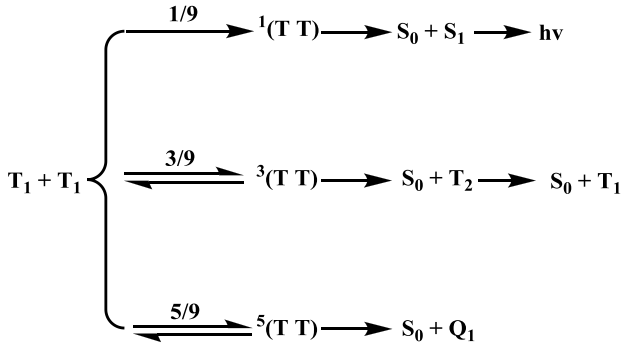

Figure 1.9 : Spin statistics of triplet encounter complexes in TTA

Only the singlet encounter complex is capable of undergoing TTA to produce fluorescence. Since each of these nine is equally likely to occur the possibility of the desired singlet complex forming is 1/9 or 11%. For some time it was thought that this limited the theoretical yield of the TTA step to 11%, making 0.055 the maximum external quantum yield for TTAUC as a whole. However, this assumes that the triplet and quintet encounter complexes do not return triplet emitters to the reaction bath either by forming reversibly, or via their decomposition products. In fact, as anthracene quintet encounter complexes have a 92% chance of decomposing back to their constituent triplets,[74] and the triplet encounter complex decays to a T_1 and an S_0, triplet emitters are being returned to the reaction bath to perpetuate the TTA process. For every photon expelled by the system 5 T_1 molecules are consumed, and 13 T_1 molecules returned to the bath. Because of this the TTA yield, i.e. the probability that one singlet emitter is formed from an encounter complex has been quoted at 40%,[2] making 0.2 the overall maximum external quantum yield.[49]

The initial 11% barrier has been experimentally disproved on many occasions.[43,51] It is likely that positioning of the singlet, triplet and quintet energy levels is a factor.

As the quintet encounter complex has been found to be reversible, by virtue of its decomposition products requiring excess energy to form, it can be theorised that by making the T^2 energy level inaccessible the triplet encounter complex will be formed reversibly. This would have the effect of forcing all encounter complexes to proceed by the singlet path, increasing the theoretical TTA limit to 100%, and making 0.5 the external quantum yield maximum. In this possibility, the efficiency maximum is "beyond any spin statistical limit".[51] So, by correctly designing the emitter such that the quintet and second triplet levels are inaccessible by TTA, the highest efficiencies may be reached.[51,52]

[2] If we assume that adsorption, ISC, TTT and emission are 100% efficient: 200 photons → 200T_1 → 100 (T_1+T_1) → 40 ^{1}(T-T) → 40S_1 + 40S_0 → 40 photons.

1.3.3.4. Linear, quadratic or quartic power relationships

The quadratic relationship between incident power density and the emission intensity has been used as a strong indication that TTAUC is occurring. However, if this relationship could be altered, increased up-conversion efficiencies could be realised. First the Castellano group showed that by incorporation of two photon excitation (TPE) processes into a TTA up-conversion regime a quartic light dependence could be realised, however, this behaviour is not general across all sensitizers.[65]

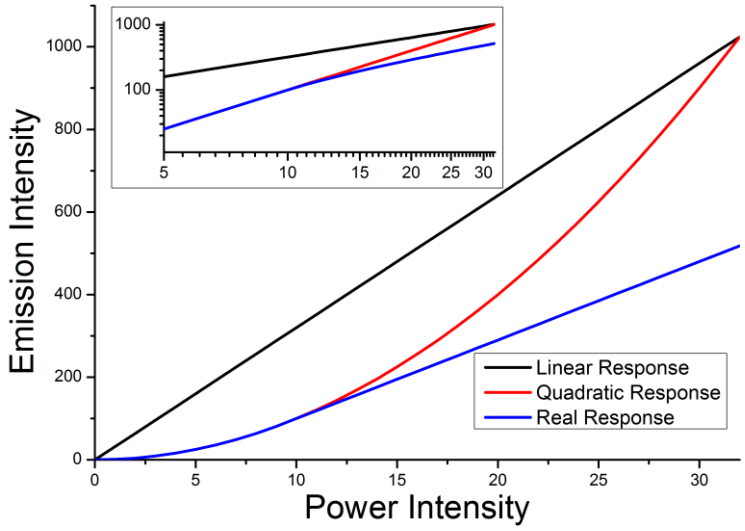

Figure 1.10 : Increase of emission intensity with increasing illumination power intensity, with linear (black), quadratic (red) and commonly observed real response (blue), and log scaled plot (inset)

A kinetic model of TTA UC has been shown by Schmidt *et al.* to agree with the conclusion that TTAUC systems could be designed which do not possess spin statistical limits.[49] By analysing the steady state conditions of a model TTA system they showed that the efficiency was determined by the competition between the unimolecular non-radiative relaxation of the emitter triplet ($k_T[{E_T}^1]$) and bi-molecular TTA ($k_{TTA}[{E_T}^1]^2$). When the non-radiative transition was promoted the normal quadratic dependance of TTAUC was modelled (see above – Proof I). However, when the non-radiative process was retarded a completely linear model between irradiation intensity and efficiency was observed, with a smooth change from quadratic to linear with partial retardation.[49]

The authors postulated that dioxygen could be a major cause of non-radiative relaxation of the emitter triplet molecules and its exclusion would provide a route to a linear mode where the overall efficiency would be much improved. Building on this theoretical work the same group investigated the up-converted emission of rubrene sensitized by PQ_4Pd, showing that the emitter quenched the sensitizer effectively in agreement with the theory.[51] This would be especially useful in low power density applications, such as photovoltaic cells utilising non-concentrated solar light. In the cases where the possibility of a linear relationship have been developed at low power densities there has been an initial quadratic relationship, labelled the weak up-conversion limit, and at higher power

densities there has been a movement to the linear relationship, labelled the strong up-conversion limit.

Building on the work by Monguzzi *et al.* and Schmidt *et al.*[49] demonstrating that quadratic dependence can be altered to a linear scheme the Castellano group tried using non-coherent sources to increase the efficiency of the up-conversion system.[38] Using the sensitizer Pd(II) octaethylporphyrin and diphenylanthracene (DPA) they found that a linear region is accessible with irradiation at higher power density in accordance with previous findings. However when a solar lamp was used as the excitation source the concentration of the sample had to be increased in order to access the strong annihilation limit. The onset of the strong up-conversion limit was shown to be 10 mW/cm^2, which may be accessible by 1 sun.[38] From Proof 1 (1.3.1.1), by minimizing the non-radiative relaxation of the triplet emitter such that $k_T \ll k_{TTA}[E_1^T]$ then:

$$\left[{E_T}^1\right]_t = \frac{\left[{E_T}^1\right]_0}{1 + k_{TTA}\left[{E_T}^1\right]_0} \tag{1.23}$$

So the number of observed photons is directly proportional to the number of triplet emitters.[38]

$$N_F = \Phi_F\left[{E_T}^1\right]_0 \tag{1.24}$$

From these reports it is clear that the molecules involved in TTAUC must allow fast TTT and TTA, preventing the phosphorescence of the sensitizer and relaxation of the emitter. The importance of sample preparation has been shown in many articles, TTA up-conversion often uses metal complex sensitizers that are very oxygen sensitive, but the emitter compound may also be oxygen sensitive. This is clearly the case with anthracene[19] and rubrene,[39,55] and is likely to play a significant role for all emitter molecules. As k_T must be minimised the emitter should have a long lived T^1 state to prevent intersystem crossing; previously this has been obtained by the use of highly symmetrical polyaromatic molecules such as anthracene[19] and rubrene.[39,55] In order to prevent *pseudo* first order oxygen degredation of the emitter triplets the systems should be prepared with rigorous exclusion of oxygen.

The linear relationship between incident power and emission intensity has been shown for up-conversion systems incorporating platinum bis(arylacetylide) complexes with long-lived excited states.[68]

Various molecules have been used in TTAUCSs, with a diverse selection of both sensitizers and emitters. These have generally been commercially available molecules, and have shown various degrees of success in quantum yields and efficiencies.

1.4. Evolution in TTA up-conversion emitter chromaphores

Polyaromatic hydrocarbon chromaphores were traditionally found to meet the energy requirements of TTA emitters (large energy difference between singlet and triplet levels) and, to-date, the emitter used when researching TTA up-conversion has most commonly been diphenylanthracene (DPA), due to its high quantum yield of fluorescence and commercial availability.[6,18,38,40,45] Unlike the sensitizers, whose derivatives have seen larger degree of investigation, the commercial availability of an emitter has often been the sole selection criterion, and relatively few "bespoke" structures have been developed. If TTAUC research is to mature into devices stable, efficient emitters must be found. There has been some innovation in the area, most obviously by the production of the following Class A, B and most recently Class C emitters. Class A emitters were developed initially and are PAH structures joined covalently to a sensitizer moiety. Type B emitters are single molecules, commonly with high commercial availability and fluorescence quantum yield, and are the usual choice in TTA up-conversion systems. The most recent structure is the covalent linkage of two Class B emitter molecules producing a Class C emitter.

1.4.1. Class A Emitters: Sensitizer – Emitter Dyads

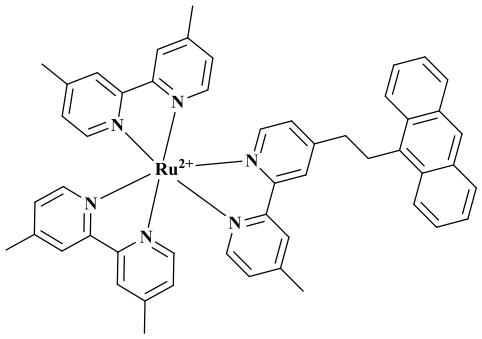

Figure 1.11 : Ruthenium MLCT - Anthracene dyad

The first compound used in modern TTAUC was studied by Castellano, and composed of a Ruthenium MLCT complex covalently bonded to anthracene, likely as a result of a serendipitous discovery of a previous study into similar structures.[75] Following excitation by a laser pulse at a wavelength of 450 nm delayed fluorescence was observed in a solution of the ruthenium MLCT - anthracene dyad (Figure 1.11) in deaerated acetonitrile, with peaks at 390 nm and 410 nm, matching those of directly excited anthracene (360 nm excitation).[47] At this stage it was understood TTA was likely to be the mechanism in action, and this hypothesis was borne out by the prevention of anti-Stokes fluorescence in glycerol where diffusion is reduced. This study found that the up-

conversion was 2.9 times more efficient when the analogous non-covalently bonded separate (i.e. Class B) system was used.

1.4.2. Class B Emitters: Free Single Molecule Emitters

Class B emitters have been found to be superior to their analogous covalently bonded Class A counterparts, as described above this is most likely due to a decrease in singlet-singlet energy transfer and increased mobility of the molecules allowing better intermolecular interactions.[47] Since anthracene has a low quantum yield of fluorescence (0.36)[76] it was hypothesised that this could hinder the overall efficiency of the TTAUC process, thus diphenylanthracene (DPA) was selected for use. DPA has a much greater fluorescence quantum yield (0.95).[18] In fact DPA produced an improvement of almost 25 times over anthracene with the same sensitiser. The Stern-Volmer and bimolecular quenching constants were similar for both emitter molecules, showing that fluorescence quantum yield was an important factor in TTAUC emitter selection. There are other concerns when using anthracene in TTAUC systems, such as its ability to decay via a non-radiative pathway,[77] and the quenching of the anthracene triplet by ground state sensitizers.[47] Other detrimental pathways include the irreversible formation of photochemical anthracene dimers in the absence of oxygen, while under air the endoperoxide is formed. Neither the anthracene dimers nor anthracene endoperoxide undergo TTA.

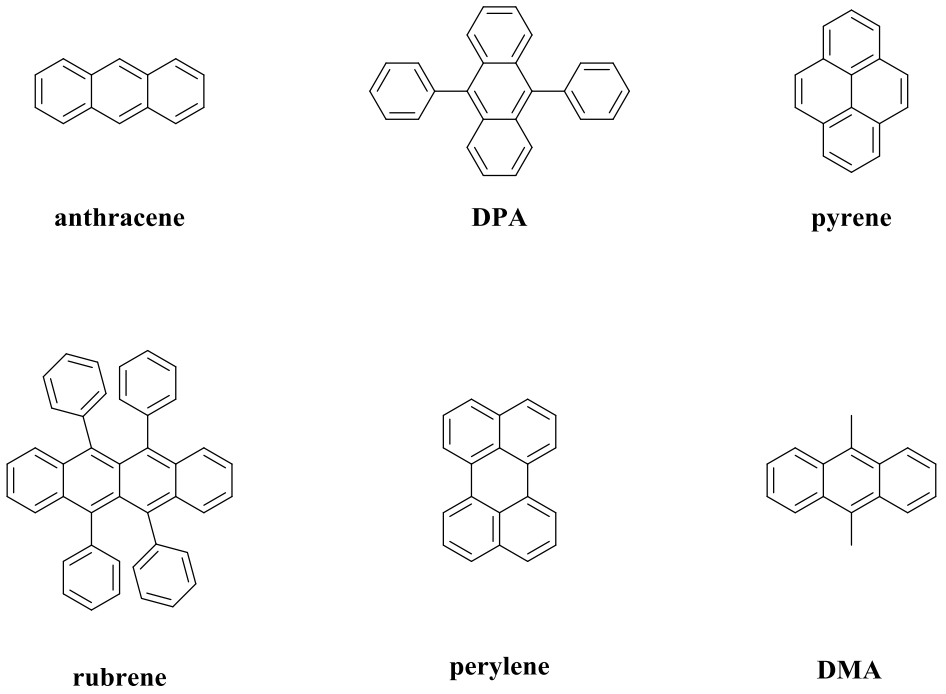

Figure 1.12 : PAH molecules

1.4.2.1. High fluorescence quantum yield emitters: DPA, Rubrene and Perylene

Since DPA, with its high fluorescence quantum yield, had seen success in TTAUC systems, similar molecules have been investigated. However, DPA has continued to be the molecule of choice, and is currently the standard molecule used in TTA investigations due to its wide commercial availability and effective properties.

DPA has been used in TTAUC systems investigating: up-converting nanoparticles for *in vivo* and *in vitro* bioimaging,[60] the strong up-conversion limit,[38] an up-conversion powered photoelectrochemical cell,[46] polymer nanoparticles,[48] a white-light emitter,[45] rigid polymer films,[78] solar light up-conversion,[6] Dexter energy transfer in the TTT step,[35] and solid polymer films.[40]

Rubrene has a high fluorescence quantum yield, close to unity,[79] it is also commercially available due to its use in organic light emitting diodes (OLEDS).[80] It is a PAH that is similar structurally to DPA, with the addition of a second 1,4-diphenylbenzene structure in its centre. It has been used in a range of TTA up-conversion studies including the investigation of: an integrated up-conversion solar cell device;[50] breaking spin statistical up-conversion limits;[51] up-conversion from the IR region;[55] up-conversion in thin films;[39] and up-conversion with more than one sensitizer.[54]

Rubrene fits the molecular design requirements for the positions of the singlet and triplet energy levels outlined above, as TTA of two of its first level triplets ($2 \times 1.15 = 2.30\ eV$) can endothermically reach the S_1 level ($2.39\ eV$) but the T_2 level may also be accessed ($2.38\ eV$).[51] Under investigation it has been found to have high TTA and external up-conversion yields (~30% and 16% respectively).[51]

Rubrene has some problems for use in TTAUC, it is even more air sensitive than the metal sensitizer complexes as it photooxidizes to the endoperoxide in a similar manner to anthracene, resulting in a measurable decrease in up-conversion ability over a period of days when incorporated into a thin film.[39]

Perylene is another molecule that posesses a quantum yield of fluorescence close to unity (0.94),[76] so is another candidate for TTAUC. It was used in the first investigations of sensitised delayed fluorescence.[16] When used in a TTA up-conversion system with PdTPBP it has been shown to possess a high anti-Stokes shift of 0.8 eV.[44] The measured energy levels of perylene are in the region of 1.53 eV for T_1, while the S_1 is around 2.76 eV (emission at 450 nm).[44,70] The T_2 level has not been reported, but it would be expected to be in the region of 2.8-3.0 eV, as it is likely that the competing TTA pathway is a source of the low external up-conversion quantum yield observed (6.5%).[44]Another source of the decreased quantum yield is the clear excimer emission observed at ~560 nm,[44] a known effect for this molecule.[81] Perylene has been used to study up-conversion mechanisms[82] and a range of organic sensitizers.[69,70]

1.4.3. Class C Emitters: Emitter – Emitter Dyads

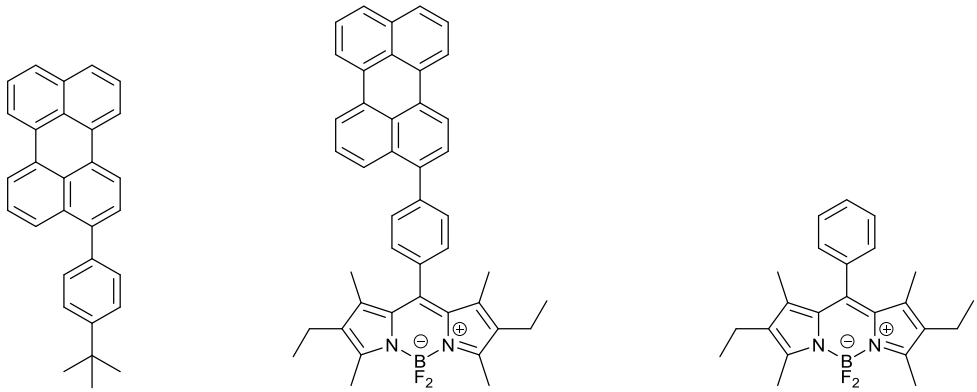

Figure 1.13 : Class B and Class C emitter stuctures

More recently a dyad type emitter, composed of a linked perylene and BODIPY moiety, has been used in an upconversion system, aiming to optimise the overall upconversion process by using different parts of the molecule for the TTT and TTA steps. This provided a system with an upconversion quantum yield of 0.11, and anti-Stokes shift of 0.30eV.[67]

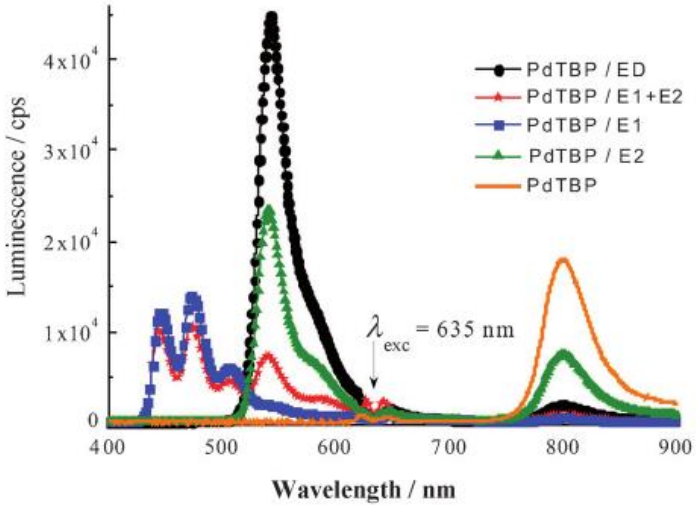

Figure 1.14 : Luminescence Spectrum for the UC systems: PdTBP / E1 (blue), PdTBP / E2 (green), physical mixture of PdTBP / (E1+E2) (red), and PdTBP / ED (black), Phosphorescence of neat PdTBP (orange).[67]

These dyad type emitters are composed of two molecules whose base structures have previously been investigated as Class B emitter chromaphores such as 3-(4-tert-butylphenyl)perylene (a perylene derivative)[44,69] and 1,3,5,7-tetramethyl-8-phenyl-2,6-diethyl dipyrromethane-BF_2 (a BODIPY derivative)[43] covalently linked through a phenyl group. Class C emitters aim to allow

simultaneous optimization of TTA and TTT by ascribing each mechanism to a different portion of the molecule. This is facilitated via the chromaphore portion with the lowest triplet energy readily undergoing TTT, while the portion of the molecule with the lowest singlet energy fluorescing, so energy is transferred from one part of the molecule to the other. Baluschev *et al.* make the assumption that the chromaphore portion with the lowest singlet energy also undergoes the TTA step. Experimentally they proved that the perylene based emitter more efficiently quenched the sensitizer phosphorescence than the BODIPY derivative and so was more effective in the energy transfer step, whereas the reverse was the case for the annihilation step.

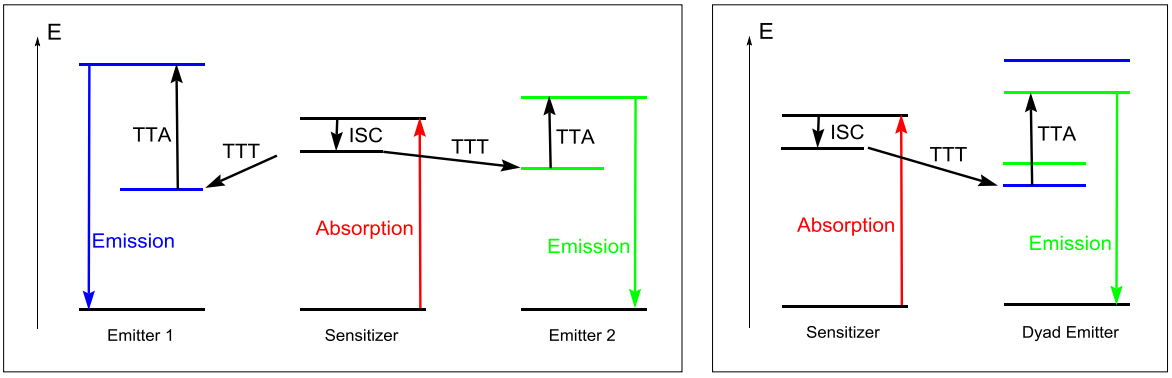

Figure 1.15 : Jablonski Diagrams for seperate emitters (left), and the dyad emitter (right, adapted from [67])

Using the dyad emitter energy that was passed from the sensitizer to the BODIPY chromaphore via the perylene system, the low quenching and annihilation efficiencies commonly seen for the BODIPY emitters was surpassed. This allowed a quantum yield of 0.11 to be realised, much higher than that previously seen for BODIPY Class B emitter systems.

1.4.4. Sensitizers

In general, the sensitizer must readily absorb incident light and show a high degree of intersystem crossing to produce a long-lived triplet.

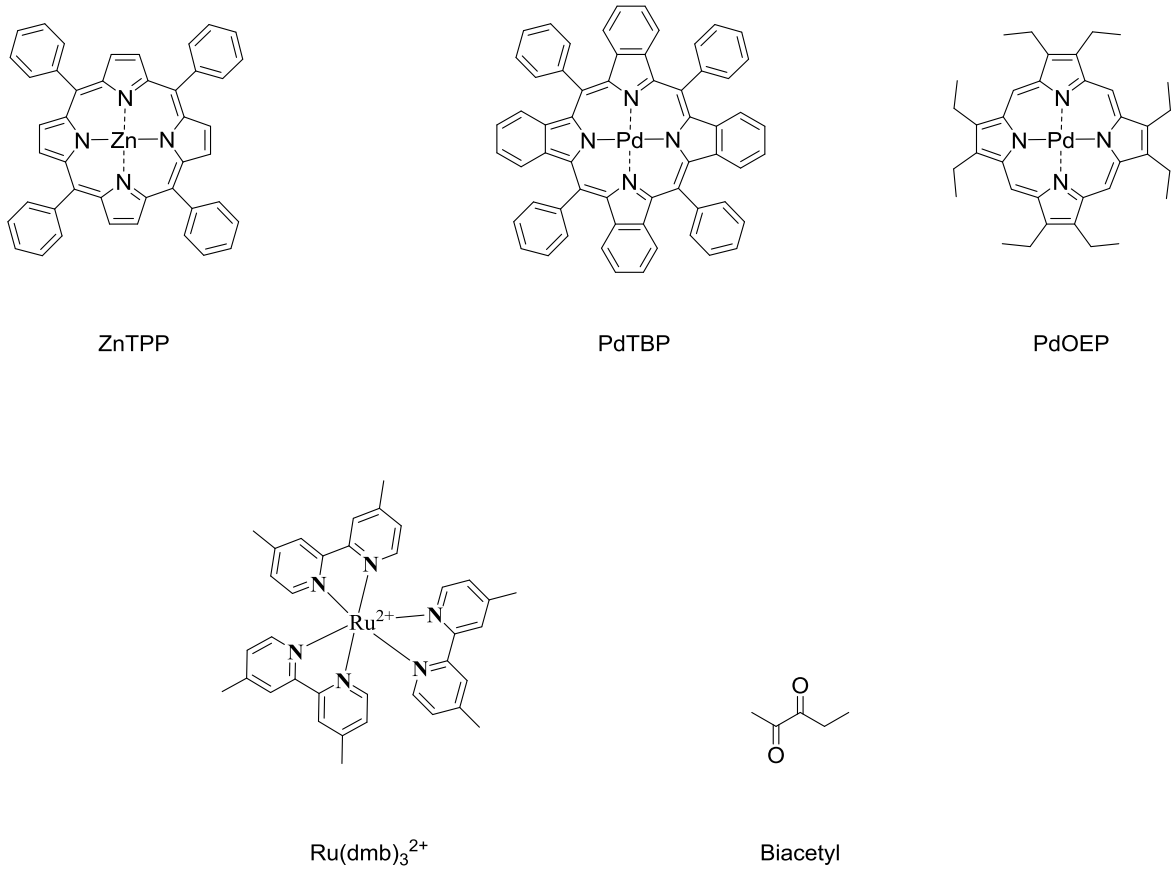

Figure 1.16 : Example porphyrin sensitizers for TTAUC systems

One class of compounds that meets these requirements are metal complexes based on porphyrins: transition metals used in these metal ligand charge transfer (MLCT) compounds include ruthenium,[18,36,37] palladium,[6,10,38–40] iridium,[41] zinc[82], and platinum.[3,10,42–44,68] A fully organic sensitizer and emitter TTA up-conversion system producing near-white light has also been reported.[45] A review by Zhao *et al.* has shown the influence of organometallic chemistry in this area,[20] and the same group has investigated BODIPY structures as organic sensitizer molecules.[69] Sensitizer molecules modified with pendant PAHs have been reported to increase their effectiveness in TTAUC systems.[19]

The range of sensitizers absorb across a large portion of the visible spectrum, from NIR to blue. The movement of the sensitizing band into the NIR and IR-A regions would increase the utility of TTAUC for silicon based photovoltaic applications.

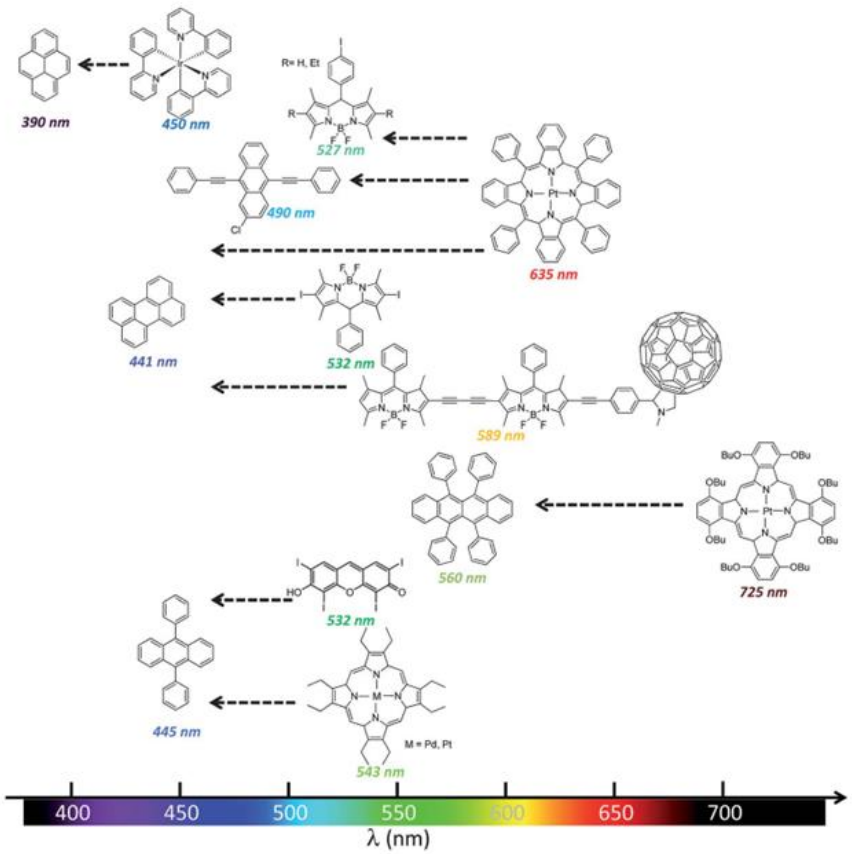

Figure 1.17 : Examples of sensitizer and emitter combinations with absorption and emission maxima, adapted from Simon *et al.*[23]

In conclusion, in the TTAUC arena the porphyrin sensitizers are normally paired with commercially available emitters, diphenylanthracene being the most common. For future device applications the stability, processibility and efficiency of the TTAUC system relies heavily upon the properties and energy levels of the emitter molecule - bespoke tuning of energy levels is required. One strategy to adjust the energy levels of the emitter would be to replace hydrogen with fluorine and introduce fluorine containing functional groups. These functional groups could increase the up-conversion efficiency, as well as the increasing the stability of the emitter to thermal, chemical, and photo degradation, and so could be essential for long device lifetimes. Consequently, methodologies for the fluorination of aromatic molecules are highly relevant to the experimental part of this thesis.

1.5. Organofluorine Chemistry

Due its extreme reactivity fluorine is very rarely found in its elemental gaseous state in nature, but in ores, most commonly as the mineral fluorite. Despite the high abundance of fluorine in natural minerals,[83] it is very rare to find fluorine in biological molecular products. Indeed out of over 3000 known halogenated natural products only around a dozen are fluorinated and the most common of these (fluoroacetate, produced by some plants) is toxic to humans.[84] The comparative lack of

fluorocarbon compounds in nature allows organic chemistry to produce completely synthetic substances. The incorporation of fluorine into molecules often gives unique properties. It is the most electronegative element known, 4.0 on the Pauling scale, but is very small with a van der Waals radius of 1.35 Å (close to hydrogen 1.20 Å).[85]

Element	$\Delta H_{dissociation}$ / kJ.mol^{-1}	Bond	$\Delta H_{dissociation}$ / kJ.mol^{-1}
F_2	159	C-F	490
Cl_2	243	O-H	460
Br_2	193	C-H	410
I_2	151	C-C	~350
H_2	436	C-Cl	331

C-F bonds are always polar, with a large proportion of ionic character, and are stronger than other carbon halogen bonds due to fluorine's higher electronegativity and the orbital overlap with carbon 2s and 2p producing very stable bonds.[86] Due to fluorine's high electronegativity it inductively produces a dipole through sigma type bonds, but it may donate electrons into a pi system when attached to one.

Figure 1.18 : Fluorine's dual affect upon carbon

1.5.1. The discovery and utility of fluorine

Hydrogen fluoride was isolated before F_2, in 1771, but its chemical composition was at this time unknown, despite having been used to decoratively etch glass since the 17th Century.[87] The name fluorine comes from the mineral fluorite (or fluorspar) which was the original source of hydrogen fluoride – fluorite was itself named for its low melting point and thus its ability to flow (fluor from the Latin *fluo*), it was used as flux in metal smelting and smithing.[88] Fluorite is also the source of the word fluorescence, due to fluorite's exhibition of a blue tinge under illumination.

Elemental fluorine was finally isolated by Moissan in 1886 by the electrolysis of a solution of potassium fluoride in liquid hydrogen fluoride using apparatus made from an alloy of platinum-iridium, work which won him a Nobel Prize in 1906.[89]

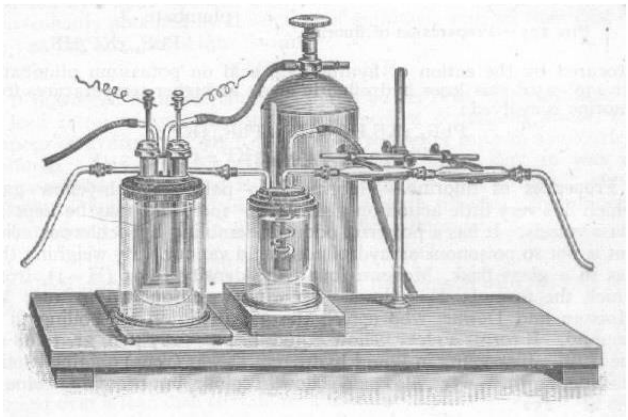

Figure 1.19 : Moissan's apparatus for the preparation of Fluorine, adapted from [88]

The first organic compounds of fluorine were investigated by Dumas and Péligot before elemental fluorine had been isolated, they synthesised methyl fluoride from methanol in 1835. Nucleophilic substitution by fluorine was the main method of fluorination, with halogen substitution reactions being a major portion of these. Fluorination of aromatics was also undertaken, initially using diazo compounds.

Elemental fluorine is difficult to work with however, and the use of metal fluoride exchange reactions pioneered by Swarts produced the first organofluorine compounds in 1892.[90] The reaction, now named after him, makes use of HF and antimony trifluoride to substitute fluorine for other halogens, and he is credited with the first CFC, trichlorofluoromethane (CFC-11) as well as the production of fluorinated analogues of many common chemicals.[91] Swarts found that these compounds were generally more volatile than their non-fluorinated analogues, research which indicated to later workers that they could have application as refrigerants. The CFCs are in many ways Swarts' legacy, as it was using a modification of his processes that the "Freons" were produced by Midgley and Henne in 1930, and this was the first commercial application of fluorinated compounds.[92]

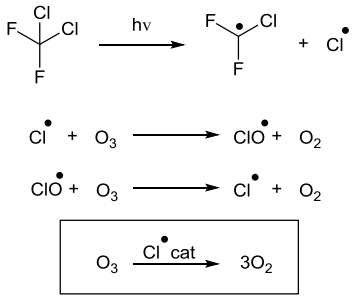

Figure 1.20 : Delpletion of ozone by CFCs

The Freon family of chlorofluorocarbons was used widely throughout the 20th century as refrigerant gases. However their excellent properties as refrigerants - high stability and volatility -

allow them to permeate the stratosphere without reaction. Once in the stratosphere they react with short range UV rays, producing radical species that convert ozone into oxygen.

While organofluorine chemistry up until World War Two was concerned mainly with the CFCs and their use as refrigerants, inorganic fluorine chemistry leapt ahead, with the production of inorganic fluorides across the periodic table (although noble gas fluorides were not yet discovered at this time).

The destructive end of the Second World War in the Pacific was aided by fluorine chemistry, both inorganic and organic. The use of inorganic fluorine chemistry allowed uranium hexafluoride to be produced, which allowed the separation of fissionable uranium 235 by gas diffusion or centrifuge separation.

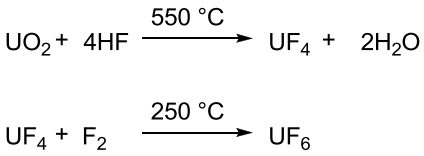

Figure 1.21 : Synthesis of UF_6

Uranium hexafluoride is a highly toxic and corrosive solid and its production and containment was a major problem in the production of an atomic bomb. Since it reacts vigorously with most metals, and explosively with water, poly(tetrafluoroethylene) (PTFE) was used to contain the UF_6.

Since these early advances, fluorinated molecules are used in all sectors of the chemical industries. For example, within pharmaceutical compounds, Atorvastatin (Lipitor©), is the highest grossing drug ever made, and of the 100 top selling non protein based drugs a quarter contain one or more fluorine atom.[93] This is due to the increased in bioavailability, biological activity, potency and resistance to metabolism that fluorine substituents give. Most common anaesthetics, including halothane and desflurane contain fluorine, and Flucloxicillin was an early antibiotic that contained fluorine. Agrocultural chemicals, including perticides, commonly contain fluorine.

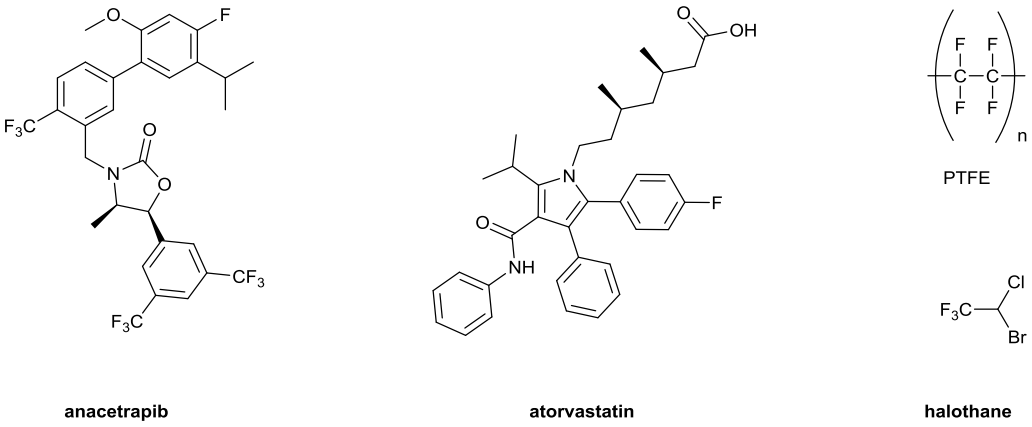

Figure 1.22 : Common commercial fluorinated compounds

1.6. Fluorination of organic molecules

In general, fluorination methods make use of either nucleophlic fluoride ions, or electrophilic "F^+" reagents. There are a number of methods that use fluoride, these generally replace a halogen (halogen exchange, HALEX), hydrogen (oxidative fluorination) or oxygen (deoxyfluorination). "F^+" reagents allow a nucleophile to attack a δ+ fluorine atom, nucleophiles include aromatic π systems and carbocations.

Nucleophilic Fluorinating Agents		**Electrophilic Fluorinating Agents**	
Hydrogen Fluoride	H-F	Elemental Fluorine	F_2
Alkali Fluorides	CsF > KF >> NaF > LiF	N-F reagents	Selectfluor
Organic Fluorides	TAS, TBAF	O-F reagents	
Oxidative	CoF_3	Xe-F	
Deoxyfluorinating	DAST, Deoxyfluor		

Since the emitter molecules synthesised for this project are aromatic in nature, the production of fluorinated aromatics will be the focus of the thesis' discussion.

1.6.1. Nucleophilic Fluorine: F^- Reagents

Alkali metal fluorides are widely used due to their commercial availability, ease of handling and low price. The action of the fluoride ion is regulated by its dissociation from the cation, and the lack of subsequent solvation of the fluoride to allow an available nucleophile.

The small fluoride ion will dissociate more readily from soft diffuse cations such as cesium, thus the reactivity of the alkali metal fluorides is in proportion to the cation size: CsF > KF >> NaF > LiF. Using polar solvents encourages the dissociation by solvation of the metal cation. However solvation of the fluoride ion by water or protic solvents greatly decreases its fluorinating strength, making aprotic solvents a better choice. Common aprotic solvents include diglyme, sulfolane, DMF and DMA. Potassium fluoride is a widely available, commercially viable, fluoride ion source, with good reactivity and so is used most frequently in industrial processes.

Alkali metal fluorides, as well as other fluoride reagents, undergo halogen exchange (HALEX) reactions. Reactions may proceed by S_N1, S_N2 or S_NAr mechanisms.

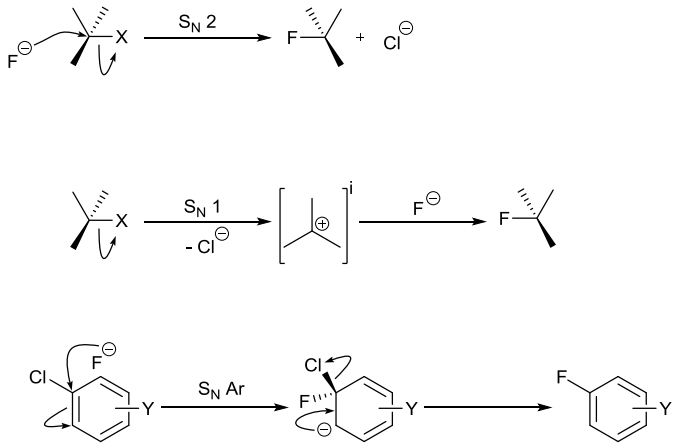

Figure 1.23 : HALEX reactions

Aromatic substrates are good reagents for this reaction, and proceed by S_NAr in many HALEX procedures.

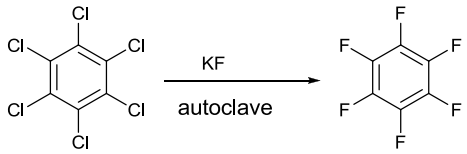

Figure 1.24 : Perfluorobenzene synthesis

1.6.1.1. Oxidative fluorination agents

Oxidative fluorination is so called due to the change in oxidation state of the carbon atom. For example a transformation that allowed methane to be singularly fluorinated to fluoromethane would cause an increase in the oxidation state of the carbon atom.

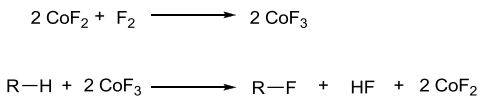

Figure 1.25 : Cobalt fluoride process

Cobalt trifluoride (CoF_3) is a commonly used oxidative fluorination agent, produced by reaction of elemental fluorine and cobalt diflouride. Cobalt trifluoride may then react with C-H bond containing species to replace the hydrogen atom, producing HF as a by product.

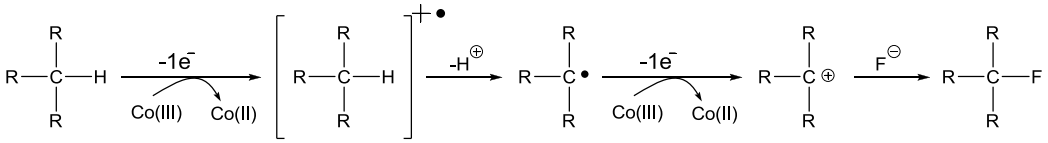

Figure 1.26 : Cobalt fluoride radical reaction

If the reaction is carried out in the presence of elemental fluorine the cobalt trifluoride may be regenerated and used catalytically. The process uses a one electron radical mechanism, where the cobalt trifluoride is both oxidising agent and fluoride ion supply. Cobalt trifluoride is generally not selective, and will fluorinate most hydrocarbons to saturation, these may then be reduced to produce perfluorinated aromatic molecules.

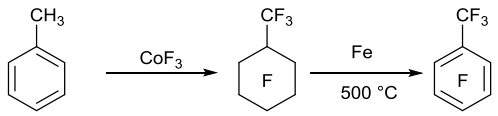

Figure 1.27 : Cobalt fluoride and aromatics

1.6.2. Electrophilic Fluorine: F^+ reagents

As well as fluoride (F^-) reagents, under the right conditions electrophilic "F^+" reagents may be used to provide fluorine attachment to electron rich carbon centres.

The simplest F^+ reagent is elemental fluorine. When diluted with nitrogen and used in combination with solvents such as acetonitrile electrophilic fluorination reactions may be carried out. Fluorine gas allows the production of large quantities of fluorinated compounds that would be difficult to synthesise by other methods.

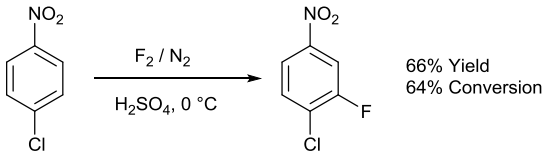

Figure 1.28 : Direct fluorination of aromatics

Although elemental fluorine can be used in increasingly safe and controlled ways, bench stable F+ reagents are attractive for small scale synthesis. These complex a fluorine atom using highly electronegative counter-ions ligands to produce a fluorine atom that is susceptible to nucleophilic attack.

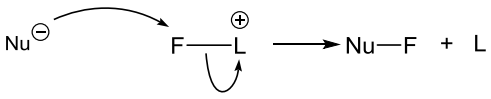

Figure 1.29 : Nucleophilic attack upon fluorine

Classical compounds of this nature include $FClO_3$, XeF_2, CF_3OF and $CsSO_4F$, however they are often unstable as well as difficult to handle and prepare, so have been supplanted by nitrogen - fluorine reagents. In NF compounds a fluorine atom is complexed with a nitrogen ligand, forming a stable, crystalline electrophilic fluorinating reagent.

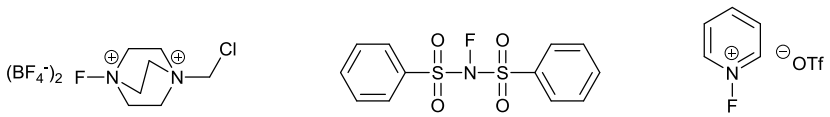

Figure 1.30 : NF fluorinating agents

NF compounds are produced by the action of elemental fluorine on amine parent compounds. 1-Chloromethyl-4-fluoro-1,4-diazoniabicyclo[2.2.2]octane bis(tetrafluoroborate) (Selectfluor) has come to the fore as the most widely used NF reagent.[94]

In conclusion, organofluorene chemistry allows the production of a range of fluorinated aromatic molecules using reagents as diverse as gaseous elemental fluorine to solid, bench stable Selectfluor™. Octafluorotoluene, a key reagent in this project, is produced by oxidative fluorination with cobalt trifluoride followed by reduction over hot iron.

Since up-conversion emitter structures are composed of PAH systems with aromatic ring connected by carbon sp^2-sp^2 bonds, a short review of aryl-aryl bond forming reactions with reference to fluorinated aromatic substrates now follows, particularly the metal catalysed Suzuki-Miyaura system and nucleophilic aromatic substitution (S_NAr).

1.7. Aryl-aryl coupling methods

Formation of bonds connecting two aromatic units has long been investigated as a method of building conjugated molecular scaffolds and was one of the earliest applications of transition metal catalysis. Palladium catalysed cross coupling reactions are a particularly valuable and robust technique, and include symmetrical (Ullmann) or asymetrical (Stille, Suzuki) methods. Reviews of the literature for the separate methods have been published,[95] and also reviews of the aryl-aryl bond forming field in the laboratory,[96] and in industry.[97]

Palladium catalysts are expensive when compared to nickel, copper or iron, but are in most wide spread use, because less reactive substrates and lower temperatures may be used, with higher turnovers. Of the possible aryl-aryl coupling methods the Suzuki reaction is the most common, indeed a great many pharmaceutical products make use of this transformation.[97]

1.7.1. Suzuki Coupling Reaction

The well-established Suzuki reaction is widely used due to its easy to handle components, lack of toxic byproducts and functional group tolerance and the boronic acid partners are readily available and stable.[98] The coordination of a negatively charged base to the boron atom increases the already

weak nucleophilicity of the organic group allowing migration to the metal centre, this had been explored before with a variety of metal halides.[99]

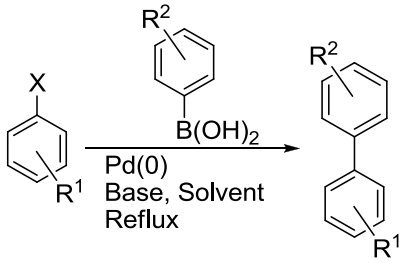

Figure 1.31 : General scheme for Suzuki coupling reactions

The discovery by Suzuki and Miyaura that sp^2 centres could be joined with facile and reasonably mild reaction conditions has allowed aromatic frameworks to be constructed much more easily than previously possible.[95]

The catalyst most often used for this process is tetrakis(triphenylphosphine)palladium(0), but palladium acetate, bis(diphenylphosphino)ferrocene-palladium(II)dichloride and other, more expensive ligands such as SPhos or XPhos are used for difficult substrates. Normally the Suzuki-Miyaura reaction is carried out under reflux, and reaction times may be in excess of 72 hours; however, the use of microwave assisted reactions may reduce the reaction time greatly.[100]

Whereas the role of the Suzuki-Miyaura reaction is to replace Grignard and Organolithium chemistry, the production of Suzuki precursors requires these methods.

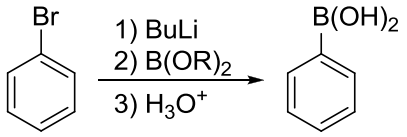

Figure 1.32: Boronic acid formation

This means that the atom efficiency of the reaction from raw materials is worse for the palladium coupling reaction than using the more traditional chemistry, but the merit of the cross-coupling route is that common building blocks may be combined to produce increasingly complex molecules. Although the reaction is widely used in research and industry, the precise mechanism is disputed, the literature offers some variants.

1.7.1.1. Competing Mechanisms of the Suzuki-Miyaura Reaction

The general understanding of the cross-coupling reaction involves three steps: oxidative addition (a) of an aryl halide to a palladium(0) complex gives the palladium(II) complex, base catalysed transmetallation (b) of the organoboronic acid gives a second palladium complex which undergoes

reductive elimination (c) producing the cross-coupled product and reforming the active palladium(0) catalyst species.

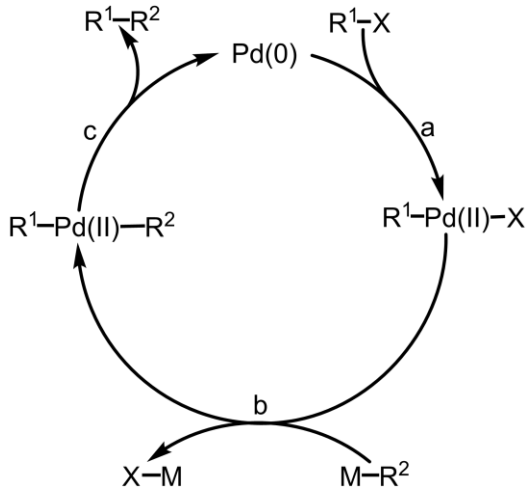

Figure 1.33: Cross-coupling mechanism

There is some disagreement over the fine details of the mechanism, producing some alternative cycles – these should be considered to ensure clean, efficient reactions. The first step is well understood, as is the final step – these are general to many metal catalysed systems as a whole. Between the initial and last steps there are various additions and substitutions that may occur as well as the transmetallation step that involves a number of sub-steps; the exact route is contested in the literature. The original reaction scheme relies on the production of a quarternary boron reactive species, as shown.

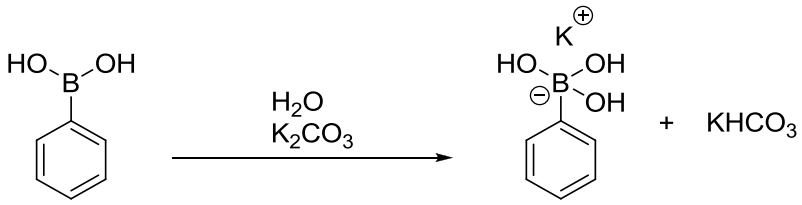

Figure 1.34 : Formation of trihydroxy anion with base

The requirement for the trihydroxy anion has been supported by the detection of intermediates,[101] for this anion to form bases with pKa above 10 are often vital.[102] This species then coordinates to the palladium centre, allowing the reaction to continue. Following various investigations the base has been shown to coordinate to the boron or palladium first.[102,103]

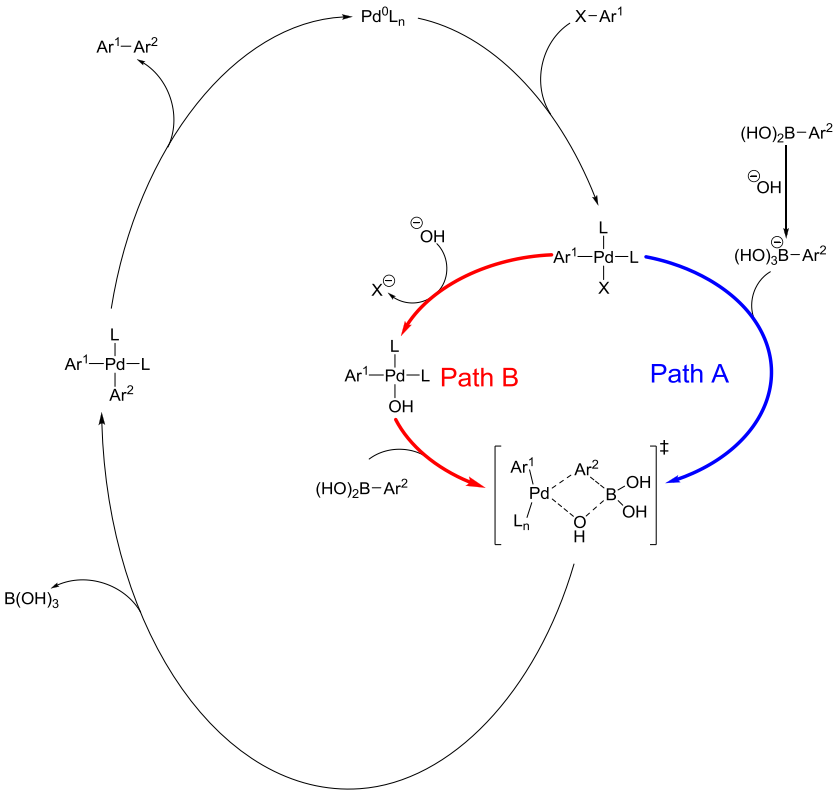

Figure 1.35 : Suzuki Cross coupling mechanism with trihydroxyborate (Path A) or palladium hydroxyl (Path B) transmetallation

The mechanism first proposed involves a base driven mechanism (Path A), where the hydroxyl reacts with the boronic acid first, this then coordinates to the palladium centre, forming the transition state as shown. Evidence for this route includes experimental[102] and computational[103] studies. The competing Path B, where the hydroxyl displaces the halide on the palladium centre also has experimental evidence, although Amatore and Jutand's work remarks on the unreactivity of the trihydroxylborate,[104]which is not borne out by other studies.[105] The literature does agree that the use of the Suzuki coupling reaction in the lab requires some optimisation, since certain aryl-halide substrates and boronic acid coupling partners are more problematic than others.

The use of palladium cross-coupling reagents with fluorine containing molecules produces some unique problems, due to the extreme electronegativity of fluorine acting as a highly electron withdrawing group.

1.7.1.2. Suzuki-Miyaura reactions of fluorinated substrates

It is useful to consider an ideal reaction system, in order to illustrate the strengths and flaws of the Suzuki-Miyaura reaction, by moving stepwise through the reaction any problems will be identified. As with most metal catalysed reactions, oxidative addition is often rate limiting, and the ease of this step is directly related to the halide in use, with the relative reactivity as follows: I > OTf > Br >> C1.[95] Thus cheap, readily available and stable aryl chlorides are difficult to use, although some

examples have been reported.[106,107] No Suzuki-Miyaura reaction has been reported with the oxidative addition in place of a fluorine atom. The oxidative addition step is promoted by electron withdrawing groups on the aryl substrate - but sterically encumbered systems, such as those with *ortho* substituents, greatly decrease the rate.[108] When sterically impeded arylhalides are employed the coupling proceeds slowly, allowing arylhalide homocoupling, or protodehalogenation to occur, this may be reduced by the use of aprotic solvents.

The next step after oxidative addition involves boron mediated transmetallation and is unique to the Suzuki reaction, generally using boronic acids. Catalytic homocoupling of the boronic acid occurs in the presence of oxygen, and this has been used to produce symmetrical biaryl systems, and has been found to occur at room temperature with copper chloride in methanol.[109]

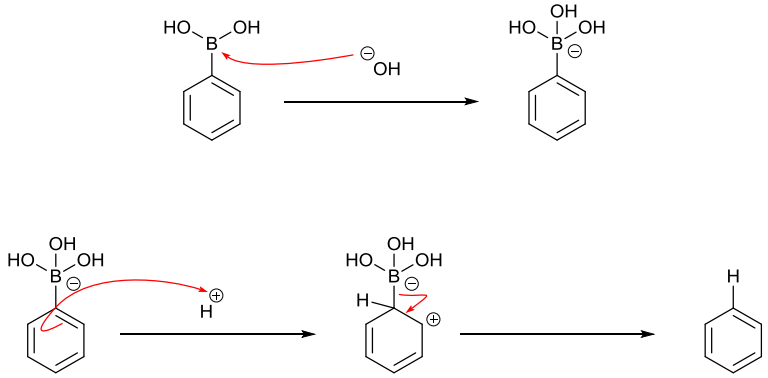

Figure 1.36 : Deboronation of phenyl boronic acid

Along with homocoupling another important problem is facile deboronation, requiring relatively high loading of the boronic acid in normal reactions.[110–114] Protodeboronation of phenylboronic acid occurs spontaneously in water at 150 °C, and is catalysed by many different routes, including the presence of base. Due to the excess of base in Suzuki reactions, this is the mechanism of most interest in this case, and was investigated by Kuivila.[111]

The reaction is an electrophilic substitution reaction and the normal substituent effects apply, the intermediate carbocation may be stabilised by electron donating groups. Thus to retard protodeboronation electron withdrawing groups that deactivate the aromatic ring would be present in the ideal coupling partner.

With fluorinated arylboronic acid coupling partners this is difficult to quantify since fluorine is σ withdrawing and π donating. From Kuivala's data the rate of protodeboronation of the *ortho* and *meta* fluorinated analogues are the highest, much greater than for the *para* fluorinated compound.

Thus the protodeborination is dominated by inductive withdrawl of electrons by fluorine from the aromatic ring, increasing the rate of protodeboronation. It can then be theorised that increasing the number fluorine sites on the ring will increase the rate of protodeboronation to the point where coupling reactions may not proceed. Indeed the difficulty in using pentafluorophenyl boronic acid

in Suzuki cross couplings is well known, with facile deboronation occurring, while the fluorine atom is not very much bigger than a hydrogen atom the *ortho* substituents prevent efficient couplings due to electronic effects, in a similar manner to the larger arylhalides.

Boronic Acid	**10^{10} K_a**
Benzeneboronic acid	7.59
4-fluorobenzeneboronic acid	9.33
2-fluorobenzeneboronic acid	56.2
3-fluorobenzeneboronic acid	57.5

Table 2 : Comparison of the rate of protodeboronation of benzeneboronic acids

Due to the many problems in the use of boronic acids in difficult systems, such as those that have electron withdrawing boronic acid substiutents, much work has involved the use of protected boronic acids that couple rather than deboronate. Among these are boronate esters (pinacol ester being the most prevalent), protected forms of boronic acids, which do themselves not deboronate, but will slowly hydrolyse under reaction conditions back to the boronic acid. Production of boronic esters is expensive and purification is non-trivial since they hydrolise under column chromatography.

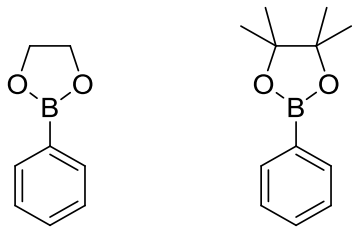

Figure 1.37 : Phenyl boronic acid trimethylene glycol ester, Phenyl boronic acid pinacol ester

All trivalent boron compounds are susceptible to degradation under common organic synthsis conditions, and so must be used “straight from the bottle” without any modification. However, quarternary boron compounds are more stable and so may have additional functionalization before the Suzuki reaction takes place.[115] Quarternary boron compounds such as trifluoroboronate salts have been known for over half a century[116] but an easy and extremely high yielding synthesis using KHF_2 was only discovered in 1995,[117,118] and the ability of the salts to be used in Suzuki coupling reactions was realised soon after.[114]

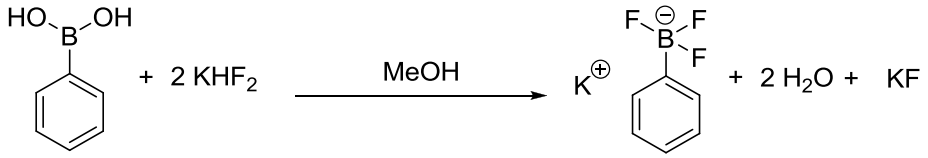

Figure 1.38 : Formation of potassium (phenyl)trifluoroborate

The advantages of these salts over the boronic acids are legion: protodeboronation is decreased, they are crystalline, free flowing powders, they are easy to isolate and require little purification for coupling reactions.[118] They are also far cheaper to produce than the competing protecting groups such as pinacol esters and are stable under a wide range of reaction conditions.

Another crucial advantage of using trifluoroborate salts in Suzuki couplings is that normally problematic couplings, such as those using sterically hindered boron reagents or electron withdrawing substituents may be carried out. Trifluoroborate salts have been found to couple to all the common Suzuki substrates in good yield, in some case under "ligandless" (ie. no phosphine ligands) conditions in air. It should be noted that as well as the striking successes in aryl aryl couplings, the trifluoroborate salts of alkyl, alkene and alkyne boronic acids have been successfully coupled. These pseudo Suzuki reactions greatly enhance the scope of coupling reations.[115]

The mechanism of the trifluoroborate coupling had not been investigated until recently, and it has been shown that the active species in this coupling is the same as in the normal Suzuki coupling – the trihydroxy boronate anion.[119]

Therefore the reason that the trifluoroboronate salts give increased yields in reactions is due to the prevention of protodeboronation, the active boron species is formed *in situ* and then couples before it can break down. It has been found that three equivalents of base is required to produce the necessary coupling species. Finally, following the transmetallation, reductive elimination occurs.

To conclude, Suzuki reactions in ideal conditions use iodoaryl coupling substrates with potassium trifluoroborate salts in a degassed solution of water and aprotic organic solvent with a minimum of three equivalents of base, producing a cross-coupled product with no homocoupled, deboronated or dehalogenated undesired contaminants. However in some cases, especially using highly fluorinated substrates, even these conditions are not sufficient and other routes must be considered. C-H activation chemistry has shown promise for constructing aryl-aryl bonds.

1.7.2. C-H Activation

Suzuki cross coupling reactions traditionally carried out between arylhalides and boronic acids require prefunctionalisation of the structures to promote the reaction. The aim of C-H activation processes is to allow the reaction to occur without prefunctionalisation of the molecules and simply

replace the C-H bond - this would allow greater atom efficiency and decreased waste. It is common for these reactions to be one-sided, i.e. one molecule have functionalization at the desired coupling atom while the other does not, but in some cases the reaction may proceed without any prefunctionalisation of either molecule. A potential problem of this method is that the lack of direction may cause the reaction to proceed without specificity. Initial C-C bond forming C-H activated coupling stratagies involved addition of aromatic C-H bonds across olefins,[120,121] but have branched out into a large range of synthetic routes.

Pentafluorobenzene has been successfully C-H activation coupled with aryl halides by Lafrance *et al.*[122] This used the air-stable boronate salt of di-tert-butylmethylphosphine to allow excellent yield.

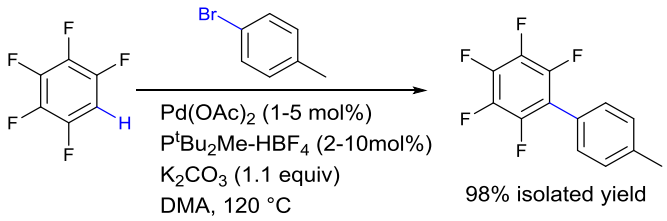

Figure 1.39 : C-H Activated coupling of perfluorobenzenes with aryl halides

This system was successful with a range of perfluoroarenes and was possible with aryl chlorides and iodides as well as bromides. A reversal in reactivity when compared to normal arylhalide coupling reactions was observed, with decreased fluorine functionalization causing a decreased yield. Similar systems have been employed, including a bi-phasic solvent system that allows room temperature reactions of aryl iodides. It should be noted that there was no attempt in this work to couple an arylhalide with an *ortho* steric group, meaning that its relative usefulness in the coupling of anthracene is difficult to assess.

Arylboronic acids have also been successfully coupled with highly fluorinated aryl systems, again using a palladium catalyst, as shown.[123]

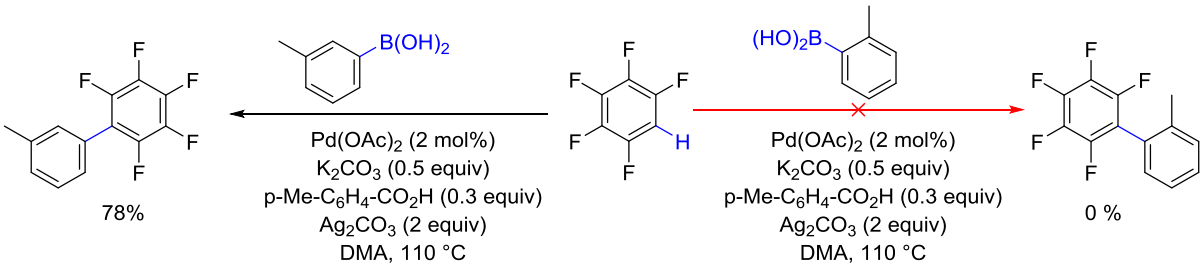

Figure 1.40 : Effect of ortho groups on C-H activated couplings of boronic acids and pentafluorobenzene

This system uses silver carbonate and palladium acetate, as well as a solution of weak acid (to supress boronic acid homocoupling) and weak base (to promote C-H bond cleavage).

Unfortunately, this system is of little use to the current investigation, since groups *ortho* to the boronic acid moiety cause no conversion to occur.

Recently a "naked coupling" of pentafluorobenzene with arenes has been carried out, without any prefunctionalisation on either molecule.[124]

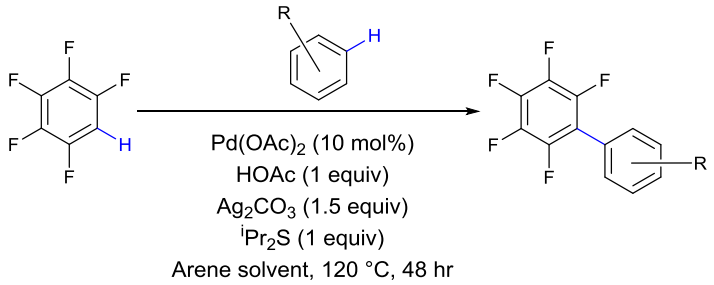

Figure 1.41 : "Naked" C-H activated coupling of pentafluorobenzene and arenes

This again uses silver carbonate and palladium acetate, and an acid, but also uses an "additive" diisopropyl sulphide which was found to be necessary for any reaction to occur. When the reaction was carried out using toluene *meta* and *para* isomers were formed, but not *ortho*. The lack of an *ortho* isomer is presumably due to steric effects, the reported coupling of chlorobenzene with these conditions produced *meta*, *para* and *ortho* isomers in ratios 1.4 : 1.0 : 0.1, indicating that the coupling sterically hindered systems is possible, but not favourable. This indicates that an attempt to couple anthracene at the 9 or 10 positions would likely fail.

C-H activation is a promising area of contemporary chemistry, with a large amount of research going into these potentially efficient and high yielding reactions. Although they are not well understood and currently only in their infancy if they could be used to produce complex aromatic structures their development would be a major breakthrough in modern chemistry. While C-H activation methodology has great potential, another, more traditional, method of producing highly fluorinated aryl systems is aromatic nucleophilic substitution.

1.7.3. Aromatic Nucleophilic Substitution (S_NAr)

Aromatic molecules often undergo electrophilic substitution, however if the aromatic system is sufficiently deactivated with electron withdrawing groups a nucleophilic substitution reaction may take place. These make use of highly electron deficient aromatic systems that have the ability to stabilise a carbanion following attack by a nucleophile.

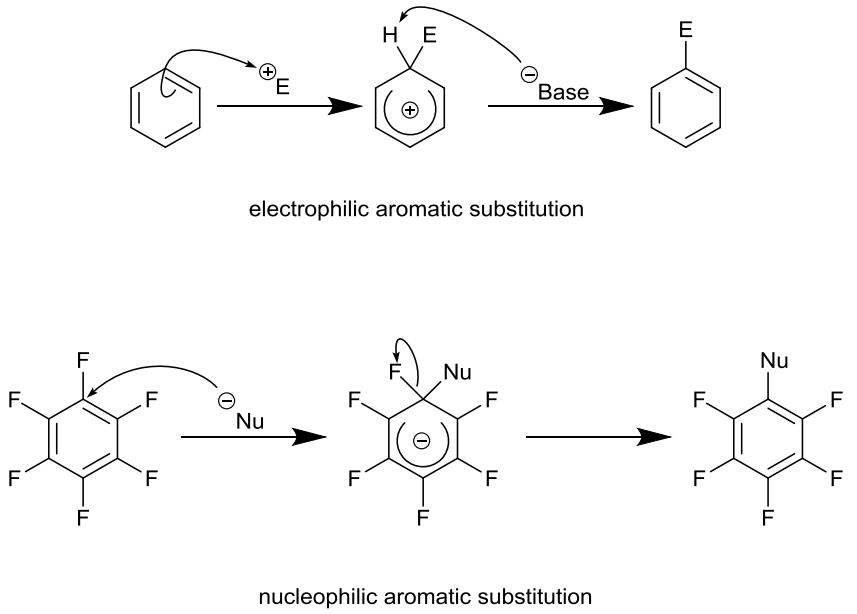

Figure 1.42 Aromatic Substitution Reactions

The nucleophilic attack produces a stabilised anion known as the Meisenheimer intermediate, and a fluoride ion acts as a leaving group. Perfluorinated aromatics readily undergo nucleophilic substitution, for example perfluorobenzene and octafluorotoluene are often used in these reactions.

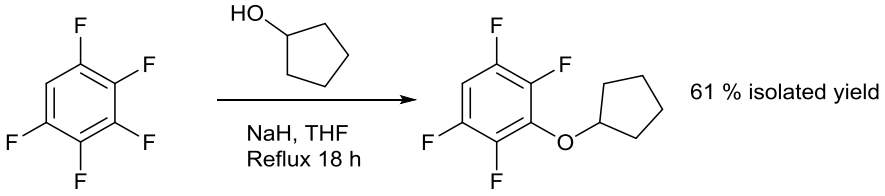

Figure 1.43 : Reaction of pentafluorobenzene and cyclopentanol (adapted from *Cargill et al.*[33])

In the case of aryl-aryl bond forming reactions an "aryl carbanion", produced using either Grignard chemistry or organolithium reagents from a halogenated aromatic, may attack a sufficiently activated system, displacing a leaving group.

1.8. Summary

This review has highlighted the key aspects of TTAUCSs: they up-convert incident light to a higher energy emission, and they possess possible advantages over current display media including lower power requirements, may be used to improve the efficiency of photovoltaic power generation, and can be used for effective bioimaging.

There is a large amount of processes that may occur to impede effective TTA up-conversion, and many of these are associated with the selection of an inappropriate emissive molecule. As the body of work in this area has increased it has become clear that the use of "off the shelf" chromaphores designed for other applications may not be sufficient to run the gauntlet of TTA up-conversion. A

number of processes must proceed effectively to ensure efficient up-conversion, the molecular design of the emitter portion can disfavour routes which would allow energy loss.

Fluorination of organic emitters is commonly associated with increased stability – by incorporating fluorinated TTA emitters into UCSs device lifetime and efficiency may potentially be increased. An overview of fluorine chemistry is presented with this ability in mind. Due to the sp^2 hybridised structures of the emitters aryl-aryl bond forming reactions are essential, and a short review of methods by which aromatic scaffolds may be formed in the presence of fluorine moieties has been prevented, to investigate methods that might allow the production of highly fluorinated polyaromatic hydrocarbon TTA emitter molecules.

(1) Schmidt, T. Molecular approaches to next-generation photovoltaic-energy conversion. *SPIE Newsroom* **2010**, *1*, 1–2.

(2) Farrell, D. J.; Ekins-Daukes, N. J. Routes to High-efficiency Photovoltaic Conversion of Solar Energy. *Modern Energy Review* **2011**, *3*, 84–88.

(3) Laquai, F.; Wegner, G.; Im, C.; Büsing, A.; Heun, S. Efficient upconversion fluorescence in a blue-emitting spirobifluorene-anthracene copolymer doped with low concentrations of Pt (II) octaethylporphyrin. *J. Chem. Phys.* **2005**, *123*, 074902 .

(4) Hope, C.; Hope, M. The social cost of CO2 in a low-growth world. *Nature Clim. Change* **2013**, *3*, 722–724.

(5) Green, M. A. *Third generation photovoltaics: advanced solar energy conversion*; Springer Verlag, 2006; Vol. 12.

(6) Baluschev, S.; Yakutkin, V.; Miteva, T.; Wegner, G.; Roberts, T.; Nelles, G.; Yasuda, A.; Chernov, S.; Aleshchenkov, S.; Cheprakov, A. A general approach for non-coherently excited annihilation up-conversion: transforming the solar-spectrum. *New J. Phys.* **2008**, *10*, 013007.

(7) Cheng, L.; Wang, C.; Liu, Z. Upconversion nanoparticles and their composite nanostructures for biomedical imaging and cancer therapy. *Nanoscale* **2013**, *5*, 23–37.

(8) ITU *Measuring the Information Society Executive Summary*; International Telecommunication Union, 2012.

(9) McNaught, A. D.; Wilkinson, A. *IUPAC compendium of chemical terminology*; Blackwell Scientific Publications, 1997; Vol. 2.

(10) Keivanidis, P. E.; Baluschev, S.; Miteva, T.; Nelles, G.; Scherf, U.; Yasuda, A.; Wegner, G. Up-Conversion Photoluminescence in Polyfluorene Doped with Metal (II)-Octaethyl Porphyrins. *Adv. Mater.* **2003**, *15*, 2095–2098.

(11) Gerhard, A.; Bässler, H. Delayed fluorescence of a poly (p-phenylenevinylene) derivative: Triplet-triplet annihilation versus geminate pair recombination. *J. Chem. Phys.* **2002**, *117*, 7350 – 7356.

(12) Auzel, F. Upconversion and anti-Stokes processes with f and d ions in solids. *Chem. Rev.* **2004**, *104*, 139–174.

(13) Trupke, T.; Shalav, A.; Richards, B.; Würfel, P.; Green, M. Efficiency enhancement of solar cells by luminescent up-conversion of sunlight. *Sol. Energ. Mat. Sol. C.* **2006**, *90*, 3327–3338.

(14) Baluschev, S.; Miteva, T.; Yakutkin, V.; Nelles, G.; Yasuda, A.; Wegner, G. Up-conversion fluorescence: Noncoherent excitation by sunlight. *Phys. Rev. Lett.* **2006**, *97*, 143903.

(15) Parker, C.; Hatchard, C. In *Proc. Chem. Soc., London*; 1962; pp. 386–387.

(16) Parker, C.; Hatchard, C.; Joyce, T. A. Sensitised delayed fluorescence as an analytical method. Some preliminary experiments. *Analyst* **1965**, *90*, 1–8.

(17) Hertel, D.; Bässler, H.; Guentner, R.; Scherf, U. Triplet-triplet annihilation in a poly (fluorene)-derivative. *J. Chem. Phys.* **2001**, *115*, 10007 – 10013.

(18) Islangulov, R. R.; Kozlov, D. V.; Castellano, F. N. Low power upconversion using MLCT sensitizers. *Chem. Commun.* **2005**, 3776–3778.

(19) Singh-Rachford, T. N.; Castellano, F. N. Photon upconversion based on sensitized triplet-triplet annihilation. *Coordin. Chem. Rev.* **2010**, *254*, 2560–2573.

(20) Zhao, J.; Ji, S.; Guo, H. Triplet-triplet annihilation based upconversion: from triplet sensitizers and triplet acceptors to upconversion quantum yields. *R. Soc. Chem. Adv.* **2011**, *1*, 937–950.

(21) Ceroni, P. Energy Up-Conversion by Low-Power Excitation: New Applications of an Old Concept. *Chem - Eur. J.* **2011**, *17*, 9560–9564.

(22) Monguzzi, A.; Tubino, R.; Hoseinkhani, S.; Campione, M.; Meinardi, F. Low power, non-coherent sensitized photon up-conversion: modelling and perspectives. *Phys. Chem. Chem. Phys.* **2012**, *14*, 4322 – 4332.

(23) Simon, Y. C.; Weder, C. Low-power photon upconversion through triplet-triplet annihilation in polymers. *J. Mater. Chem.* **2012**, *22*, 20817–20830.

(24) Chambers, R. D. *Fluorine in organic chemistry*; CRC Press, 2004.

(25) Babudri, F.; Farinola, G. M.; Naso, F.; Ragni, R. Fluorinated organic materials for electronic and optoelectronic applications: the role of the fluorine atom. *Chem. Commun.* **2007**, 1003–1022.

(26) Pagliaro, M.; Ciriminna, R. New fluorinated functional materials. *J. Mater. Chem.* **2005**, *15*, 4981–4991.

(27) Tang, M. L.; Bao, Z. Halogenated Materials as Organic Semiconductors. *Chem. Mater.* **2011**, *23*, 446–455.

(28) Ono, K.; Totani, H.; Hiei, T.; Yoshino, A.; Saito, K.; Eguchi, K.; Tomura, M.; Nishida, J.; Yamashita, Y. Photooxidation and reproduction of pentacene derivatives substituted by aromatic groups. *Tetrahedron* **2007**, *63*, 9699–9704.

(29) Chen, B. S.; Chen, D. Y.; Chen, C. L.; Hsu, C. W.; Hsu, H. C.; Wu, K. L.; Liu, S. H.; Chou, P. T.; Chi, Y. Donor-acceptor dyes with fluorine substituted phenylene spacer for dye-sensitized solar cells. *J. Mater. Chem.* **2011**, *21*, 1937–1945.

(30) Ie, Y.; Umemoto, Y.; Nitani, M.; Aso, Y. Perfluoroalkyl-annelated conjugated systems toward n-type organic semiconductors. *Pure Appl. Chem.* **2008**, *80*, 589–598.

(31) Zheng, Y.; Eom, S. H.; Chopra, N.; Lee, J.; So, F.; Xue, J. Efficient deep-blue phosphorescent organic light-emitting device with improved electron and exciton confinement. *Appl. Phys. Lett.* **2008**, *92*, 223301.

(32) Zhang, Q.; Li, J.; Shizu, K.; Huang, S.; Hirata, S.; Miyazaki, H.; Adachi, C. Design of Efficient Thermally Activated Delayed Fluorescence Materials for Pure Blue Organic Light Emitting Diodes. *J. Am. Chem. Soc.* **2012**, *134*, 14706–14709.

(33) Cargill, M. R.; Sandford, G.; Tomlinson, D. J.; Hollfelder, N.; Pleis, F.; Nelles, G.; Kilickiran, P. Polyfluorinated cycloalkoxyphenyl ether systems as dopants for liquid crystal display applications. *J. Fluorine Chem.* **2011**, *132*, 829–833.

(34) Cargill, M. R.; Sandford, G.; Tadeusiak, A. J.; Love, G. D.; Hollfelder, N.; Pleis, F.; Nelles, G.; Kilickiran, P. Highly fluorinated biphenyl ether systems as dopants for fast-response liquid crystal display applications. *Liq. Cryst.* **2011**, *38*, 1069–1078.

(35) Monguzzi, A.; Tubino, R.; Meinardi, F. Upconversion-induced delayed fluorescence in multicomponent organic systems: Role of Dexter energy transfer. *Phys. Rev. B* **2008**, *77*, 155122.

(36) Singh-Rachford, T. N.; Islangulov, R. R.; Castellano, F. N. Photochemical Upconversion Approach to Broad-Band Visible Light Generation. *J. Phys. Chem. A* **2008**, *112*, 3906–3910.

(37) Islangulov, R. R.; Castellano, F. N. Photochemical Upconversion: Anthracene Dimerization Sensitized to Visible Light by a RuII Chromophore. *Angew. Chem. Int. Edit.* **2006**, *118*, 6103–6105.

(38) Haefele, A.; Blumhoff, J.; Khnayzer, R. S.; Castellano, F. N. Getting to the (Square) Root of the Problem: How to Make Non-Coherent Pumped Upconversion

Linear. *J. Phys. Chem. Lett.* **2012**, *3*, 299–303.

(39) Singh-Rachford, T. N.; Castellano, F. N. Pd (II) phthalocyanine-sensitized triplet-triplet annihilation from rubrene. *J. Phys. Chem. A* **2008**, *112*, 3550–3556.

(40) Islangulov, R. R.; Lott, J.; Weder, C.; Castellano, F. N. Noncoherent low-power upconversion in solid polymer films. *J. Am. Chem. Soc.* **2007**, *129*, 12652–12653.

(41) Zhao, W.; Castellano, F. N. Upconverted emission from pyrene and di-tert-butylpyrene using Ir (ppy) 3 as triplet sensitizer. *J. Phys. Chem. A* **2006**, *110*, 11440–11445.

(42) Singh-Rachford, T. N.; Castellano, F. N. Supra-Nanosecond Dynamics of a Red-to-Blue Photon Upconversion System. *Inorg. Chem.* **2009**, *48*, 2541–2548.

(43) Singh-Rachford, T. N.; Haefele, A.; Ziessel, R.; Castellano, F. N. Boron Dipyrromethene Chromophores: Next Generation Triplet Acceptors/Annihilators for Low Power Upconversion Schemes. *J. Am. Chem. Soc.* **2008**, *130*, 16164–16165.

(44) Singh-Rachford, T. N.; Castellano, F. N. Triplet Sensitized Red-to-Blue Photon Upconversion. *J. Phys. Chem. Lett.* **2009**, *1*, 195–200.

(45) Chen, H. C.; Hung, C. Y.; Wang, K. H.; September, W. S. F. D.; Chien, F. C.; Chen, P.; Chow, T. J.; Hsu, C. P.; Sun, S. S.; others White-light emission from an upconverted emission with an organic triplet sensitizer. *Chem. Commun.* **2009**, 4064–4066.

(46) Khnayzer, R. S.; Blumhoff, J.; Harrington, J. A.; Haefele, A.; Deng, F.; Castellano, F. N. Upconversion-powered photoelectrochemistry. *Chem. Commun.* **2012**, *48*, 209–211.

(47) Kozlov, D. V.; Castellano, F. N. Anti-Stokes delayed fluorescence from metal-organic bichromophores. *Chem. Commun.* **2004**, 2860–2861.

(48) Monguzzi, A.; Frigoli, M.; Larpent, C.; Tubino, R.; Meinardi, F. Low-Power-Photon Up-Conversion in Dual-Dye-Loaded Polymer Nanoparticles. *Adv. Funct. Mater.* **2012**, *22*, 139–143.

(49) Auckett, J. E.; Chen, Y. Y.; Khoury, T.; Clady, R. G. C. R.; Ekins-Daukes, N.; Crossley, M. J.; Schmidt, T. W. In *Journal of Physics: Conference Series*; 2009; Vol. 185, p. 012002.

(50) Cheng, Y. Y.; Fueckel, B.; MacQueen, R. W.; Khoury, T.; Clady, R. G. R. C.; Schulze, T. F.; Ekins-Daukes, N.; Crossley, M. J.; Stannowski, B.; Lips, K.; Schmidt, T. W. Improving the light-harvesting of amorphous silicon solar cells with photochemical upconversion. *Energ. Environ. Sci.* **2012**, *5*, 6953–6959.

(51) Cheng, Y. Y.; Fückel, B.; Khoury, T.; Clady, R. G. C. R.; Tayebjee, M. J. Y.; Ekins-Daukes, N.; Crossley, M. J.; Schmidt, T. W. Kinetic Analysis of

Photochemical Upconversion by Triplet- Triplet Annihilation: Beyond Any Spin Statistical Limit. *J. Phys. Chem. Lett.* **2010**, *1*, 1795–1799.

(52) Cheng, Y. Y.; Khoury, T.; Clady, R. G. C. R.; Tayebjee, M. J. Y.; Ekins-Daukes, N.; Crossley, M. J.; Schmidt, T. W. On the efficiency limit of triplet-triplet annihilation for photochemical upconversion. *Phys. Chem. Chem. Phys.* **2009**, *12*, 66–71.

(53) Ekins-Daukes, N.; Schmidt, T. A molecular approach to the intermediate band solar cell: The symmetric case. *Appl. Phys. Lett.* **2008**, *93*, 063507.

(54) Baluschev, S.; Yakutkin, V.; Wegner, G.; Miteva, T.; Nelles, G.; Yasuda, A.; Chernov, S.; Aleshchenkov, S.; Cheprakov, A. Upconversion with ultrabroad excitation band: Simultaneous use of two sensitizers. *Appl. Phys. Lett.* **2007**, *90*, 181103.

(55) Yakutkin, V.; Aleshchenkov, S.; Chernov, S.; Miteva, T.; Nelles, G.; Cheprakov, A.; Baluschev, S. Towards the IR Limit of the Triplet-Triplet Annihilation-Supported Up-Conversion: Tetraanthraporphyrin. *Chem. Eur. J.* **2008**, *14*, 9846–9850.

(56) Miteva, T.; Nelles, G. Polymeric nanoparticles comprising a medium for photon up-conversion. *United States Patent Application Publication* **2011**.

(57) Miteva, T.; Fuhrmann, G.; Nelles, G.; Yakutkin, V.; Balouchev, S. Organic Polymeric Photon Up-Conversion Nanoparticles for Biological Applications. *United States Patent Application Publication* **2010**, 20100330026.

(58) BP *Statistical Review of World Energy 2012*; BP, Ed.; British Petroleum: London, 2012.

(59) Schulze, T. F.; Cheng, Y. Y.; Fückel, B.; MacQueen, R. W.; Danos, A.; Davis, N. J. L. K.; Tayebjee, M. J. Y.; Khoury, T.; Clady, R. G. C. R.; Ekins-Daukes, N.; others Photochemical Upconversion Enhanced Solar Cells: Effect of a Back Reflector. *Aust. J. Chem.* **2012**, *65*, 480–485.

(60) Liu, Q.; Yang, T.; Feng, W.; Li, F. Blue-emissive upconversion nanoparticles for low-power-excited bioimaging in vivo. *J. Am. Chem. Soc.* **2012**, *134*, 5390–5397.

(61) Tang, C.; VanSlyke, S. Organic electroluminescent diodes. *Appl. Phys. Lett.* **1987**, *51*, 913.

(62) Rapaport, A.; Milliez, J.; Bass, M.; Cassanho, A.; Jenssen, H. Review of the properties of up-conversion phosphors for new emissive displays. *J. Disp. Technol.* **2006**, *2*, 68–78.

(63) Wohnhaas, C.; Mailänder, V.; Dröge, M.; Filatov, M. A.; Busko, D.; Avlasevich, Y.; Baluschev, S.; Miteva, T.; Landfester, K.; Turshatov, A. Triplet-Triplet Annihilation Upconversion Based Nanocapsules for Bioimaging Under Excitation

by Red and Deep-Red Light. *Macromol Biosci* **2013**, *13*, 1422–1430.

(64) Braslavsky, S. Glossary of Terms Used in Photochemistry 3rd Edition. *Pure Appl. Chem* **2007**, *79*, 293–465.

(65) Singh-Rachford, T. N.; Castellano, F. N. Nonlinear Photochemistry Squared: Quartic Light Power Dependence Realized in Photon Upconversion. *J. Phys. Chem. A* **2009**, *113*, 9266–9269.

(66) Bachilo, S. M.; Weisman, R. B. Determination of triplet quantum yields from triplet-triplet annihilation fluorescence. *J. Phys. Chem. A* **2000**, *104*, 7711–7714.

(67) Turshatov, A.; Busko, D.; Avlasevich, Y.; Miteva, T.; Landfester, K.; Baluschev, S. Synergetic Effect in Triplet-Triplet Annihilation Upconversion: Highly Efficient Multi-Chromophore Emitter. *ChemPhysChem* **2012**, *13*, 3112–3115.

(68) Ji, S.; Wu, W.; Zhao, J.; Guo, H.; Wu, W. Efficient Triplet-Triplet Annihilation Upconversion with Platinum (II) Bis (arylacetylide) Complexes That Show Long-Lived Triplet Excited States. *Eur. J. Inorg. Chem.* **2012**, *2012*, 3183–3190.

(69) Wu, W.; Guo, H.; Wu, W.; Ji, S.; Zhao, J. Organic Triplet Sensitizer Library Derived from a Single Chromophore (BODIPY) with Long-Lived Triplet Excited State for Triplet-Triplet Annihilation Based Upconversion. *J. Org. Chem* **2011**, *76*, 7056–7064.

(70) Wu, W.; Zhao, J.; Sun, J.; Guo, S. Light Harvesting Fullerene Dyads as Organic Triplet Photosensitizers for Triplet-triplet Annihilation Upconversions. *J. Org. Chem.* **2012**, *77*, 5305–5312.

(71) Zhang, C.; Zhao, J.; Wu, S.; Wang, Z.; Wu, W.; Ma, J.; Guo, S.; Huang, L. Intramolecular RET Enhanced Visible light-Absorbing Bodipy Organic Triplet Photosensitizers and Application in Photooxidation and Triplet-triplet-annihilation Upconversion. *J. Am. Chem. Soc.* **2013**, *135*, 10566–10578.

(72) Singh-Rachford, T. N.; Castellano, F. N. Low Power Visible-to-UV Upconversion. *J. Phys. Chem. A* **2009**, *113*, 5912–5917.

(73) Saltiel, J.; Atwater, B. W. Spin-Statistical Factors in Diffusion-Controlled Reactions. *Adv. Photochem.* **2007**, *14*, 1–90.

(74) Saltiel, J.; March, G. R.; Smothers, W. K.; Stout, S. A.; Charlton, J. L. Spin-statistical factor in the triplet-triplet annihilation of anthracene triplets. *J. Am. Chem. Soc.* **1981**, *103*, 7159–7164.

(75) Trouts, T. D.; Tyson, D. S.; Pohl, R.; Kozlov, D. V.; Waldron, A. G.; Castellano, F. N. Dinuclear Metal-Organic Material for Binary Optical Recording. *Adv. Funct. Mater.* **2003**, *13*, 398–402.

(76) Berlman, I. B. *Handbook of Fluorescence Spectra of Aromatic Molecules*; ACS Publications, 1971.

(77) Weinheimer, C.; Choi, Y.; Caldwell, T.; Gresham, P.; Olmsted, J. Effect of a steric spacer on chromophoric interactions of ruthenium complexes containing covalently bound anthracene. *J. Photochem. Photobiol. A* **1994**, *78*, 119–126.

(78) Merkel, P. B.; Dinnocenzo, J. P. Low-power green-to-blue and blue-to-UV upconversion in rigid polymer films. *J. Lumin.* **2009**, *129*, 303–306.

(79) Montalti, M.; Credi, A.; Prodi, L.; Gandolfi, M. T. *Handbook of photochemistry*; Taylor & Francis, Ed.; CRC, 2006.

(80) Kytka, M.; Gerlach, A.; Schreiber, F.; Kovac, J. Real-time observation of oxidation and photo-oxidation of rubrene thin films by spectroscopic ellipsometry. *Appl. Phys. Lett.* **2007**, *90*, 131911.

(81) Katoh, R.; Sinha, S.; Murata, S.; Tachiya, M. Origin of the stabilization energy of perylene excimer as studied by fluorescence and near-IR transient absorption spectroscopy. *J. Photochem. Photobiol. A* **2001**, *145*, 23–34.

(82) Sugunan, S. K.; Tripathy, U.; Brunet, S. M. K.; Paige, M. F.; Steer, R. P. Mechanisms of Low-Power Noncoherent Photon Upconversion in Metalloporphyrin- Organic Blue Emitter Systems in Solution. *J. Phys. Chem. A* **2009**, *113*, 8548–8556.

(83) Banks, R. E. *Fluorine: the first hundred years (1886-1986)*; Elsevier Science Ltd, 1986.

(84) O'Hagan, D.; B Harper, D. Fluorine-containing natural products. *J. Fluorine Chem.* **1999**, *100*, 127–133.

(85) Welch, J. T.; Eswarakrishnan, S. *Flourine in Bioorganic Chemistry*; Wiley New York, 1991.

(86) Dolbier Jr, W. R.; Battiste, M. A. Structure, synthesis, and chemical reactions of fluorinated cyclopropanes and cyclopropenes. *Chem. Rev.* **2003**, *103*, 1071–1098.

(87) Hudlicky, M. *Chemistry of Organic Fluorine Compounds* ; Ellis Harwood, Chichester, UK, 1976.

(88) Partington, J. R. *A Text-Book Of Inorganic Chemistry*; Macmillan And Co., London, 1950.

(89) Moissan, H. Action d'un courant électrique sur l'acide fluorhydrique anhydre. *CR Acad. Sci* **1886**, *102*, 1543–1544.

(90) Swarts, F. Note sur un nouveau dérivé fluoré du carbone. *Bull. Soc. Chim. Belg* **1892**, *24*, 309–310.

(91) Kauffman, G. B. Frederic Swarts: Pioneer in organic fluorine chemistry. *J. Chem. Educ.* **1955**, *32*, 301–301.

(92) Midgley Jr, T.; Henne, A. L. Organic Fluorides as Refrigerants1. *Ind. Eng. Chem.* **1930**, *22*, 542–545.

(93) Swallow, S. *Fluorine-Containing Pharmaceuticals*; World Scientific Publishing Company, 2012; p. 141.

(94) Banks, R. E. Selectfluor^{TM} reagent F-TEDA-BF4 in action: tamed fluorine at your service. *J. Fluorine. Chem* **1998**, *87*, 1–17.

(95) Miyaura, N.; Suzuki, A. Palladium-catalyzed cross-coupling reactions of organoboron compounds. *Chem. Rev.* **1995**, *95*, 2457–2483.

(96) Hassan, J.; Sévignon, M.; Gozzi, C.; Schulz, E.; Lemaire, M. Aryl-aryl bond formation one century after the discovery of the Ullmann reaction. *Chem. Rev.* **2002**, *102*, 1359–470.

(97) Magano, J.; Dunetz, J. R. Large-scale applications of transition metal-catalyzed couplings for the synthesis of pharmaceuticals. *Chem. Rev.* **2011**, *111*, 2177–250.

(98) Casado, M. A.; Stobart, S. R. Modular Construction of Dendritic Carbosilanes. Organization of Dendrimer Connectivity around Bifunctional Precursors That Are Adapted for Sequential Convergent and Divergent Propagative Steps. *Org. Lett.* **2000**, *2*, 1549–1552.

(99) Gardner, J. H.; Borgstrom, P. A Method of Coupling Organic Radicals by Means of the Grignard Reagent. *J. Am. Chem. Soc.* **1929**, *51*, 3375–3377.

(100) Leadbeater, N. E. Fast, easy, clean chemistry by using water as a solvent and microwave heating: the Suzuki coupling as an illustration. *Chem. Commun. (Camb.)* **2005**, 2881–902.

(101) Aliprantis, A. O.; Canary, J. W. Observation of catalytic intermediates in the Suzuki reaction by electrospray mass spectrometry. *J. Am. Chem. Soc.* **1994**, *116*, 6985–6986.

(102) Smith, G. B.; Dezeny, G. C.; Hughes, D. L.; King, A. O.; Verhoeven, T. R. Mechanistic studies of the Suzuki cross-coupling reaction. *J. Org. Chem.* **1994**, *59*, 8151–8156.

(103) Braga, A. A.; Morgon, N. H.; Ujaque, G.; Maseras, F. Computational characterization of the role of the base in the Suzuki-Miyaura cross-coupling reaction. *J. Am. Chem. Soc.* **2005**, *127*, 9298–9307.

(104) Amatore, C.; Jutand, A.; Le Duc, G. Kinetic Data for the Transmetalation/Reductive Elimination in Palladium-Catalyzed Suzuki-Miyaura Reactions: Unexpected Triple Role of Hydroxide Ions Used as Base. *Chem. Eur. J.*

2011, *17*, 2492–2503.

(105) Carrow, B. P.; Hartwig, J. F. Distinguishing between pathways for transmetalation in Suzuki-Miyaura reactions. *J. Am. Chem. Soc.* **2011**, *133*, 2116–9.

(106) Seechurn, C. C. C. J.; Kitching, M. O.; Colacot, T. J.; Snieckus, V. Palladium-Catalyzed Cross-Coupling: A Historical Contextual Perspective to the 2010 Nobel Prize. *Angew. Chem. Int. Ed.* **2012**, *51*.

(107) Littke, A. F.; Fu, G. C. Palladium-catalyzed coupling reactions of aryl chlorides. *Angew. Chem. Int. Ed.* **2002**, *41*, 4176–4211.

(108) Walker, S. D.; Barder, T. E.; Martinelli, J. R.; Buchwald, S. L. A rationally designed universal catalyst for Suzuki-Miyaura coupling processes. *Angew. Chem. Int. Ed. Engl.* **2004**, *43*, 1871–1876.

(109) Cheng, G.; Luo, M. Homocoupling of Arylboronic Acids Catalyzed by CuCl in Air at Room Temperature. *Eur. J. Org. Chem.* **2011**, *2011*, 2519–2523.

(110) Kuivila, H. G.; Nahabedian, K. Electrophilic Displacement Reactions. X. General Acid Catalysis in the Protodeboronation of Areneboronic Acids1-3. *J. Am. Chem. Soc.* **1961**, *83*, 2159–2163.

(111) Kuivila, H. G.; Reuwer Jr, J. F.; Mangravite, J. A. Electrophilic Displacement Reactions: XV. Kinetics and Mechanism of the Base-Catalyzed Protodeboronation of Areneboronic Acids. *Can. J. Chem.* **1963**, *41*, 3081–3090.

(112) Kuivila, H. G.; Nahabedian, K. Electrophilic Displacement Reactions. XI. Solvent Isotope Effects in the Protodeboronation of Areneboronic Acids1-3. *J. Am. Chem. Soc.* **1961**, *83*, 2164–2166.

(113) Kuivila, H. G.; Reuwer, J. F.; Mangravite, J. A. Electrophilic Displacement Reactions. XVI. Metal Ion Catalysis in the Protodeboronation of Areneboronic Acids1-3. *J. Am. Chem. Soc.* **1964**, *86*, 2666–2670.

(114) Nahabedian, K.; Kuivila, H. G. Electrophilic Displacement Reactions. XII. Substituent Effects in the Protodeboronation of Areneboronic Acids1-3. *J. Am. Chem. Soc.* **1961**, *83*, 2167–2174.

(115) Molander, G. A.; Ellis, N. Organotrifluoroborates: Protected boronic acids that expand the versatility of the Suzuki coupling reaction. *Acc. Chem. Res.* **2007**, *40*, 275–286.

(116) Chambers, R.; Clark, H.; Willis, C. Some Salts of Trifluoromethylfluoroboric Acid. *J. Am. Chem. Soc.* **1960**, *82*, 5298–5301.

(117) Vedejs, E.; Chapman, R.; Fields, S.; Lin, S.; Schrimpf, M. Conversion of arylboronic acids into potassium aryltrifluoroborates: Convenient precursors of arylboron difluoride lewis acids. *J. Org. Chem.* **1995**, *60*, 3020–3027.

(118) Molander, G. A.; Canturk, B. Organotrifluoroborates and monocoordinated palladium complexes as catalysts-a perfect combination for Suzuki-Miyaura coupling. *Angew. Chem. Int. Ed. Engl.* **2009**, *48*, 9240–61.

(119) Butters, M.; Harvey, J. N.; Jover, J.; Lennox, A. J. J.; Lloyd-Jones, G. C.; Murray, P. M. Aryl trifluoroborates in Suzuki-Miyaura coupling: the roles of endogenous aryl boronic acid and fluoride. *Angew. Chem. Int. Ed. Engl.* **2010**, *49*, 5156–60.

(120) Kakiuchi, F.; Murai, S. Catalytic C-H/Olefin Coupling. *Acc. Chem. Res.* **2002**, *35*, 826–834.

(121) Murai, S.; Kakiuchi, F.; Sekine, S.; Tanaka, Y.; Kamatani, A.; Sonoda, M.; Chatani, N. Efficient catalytic addition of aromatic carbon-hydrogen bonds to olefins. *Nature* **1993**, *366*, 529–531.

(122) Lafrance, M.; Rowley, C. N.; Woo, T. K.; Fagnou, K. Catalytic intermolecular direct arylation of perfluorobenzenes. *J. Am. Chem. Soc.* **2006**, *128*, 8754–8756.

(123) Wei, Y.; Kan, J.; Wang, M.; Su, W.; Hong, M. Palladium-catalyzed direct arylation of electron-deficient polyfluoroarenes with arylboronic acids. *Org. Lett.* **2009**, *11*, 3346–3349.

(124) Li, H.; Liu, J.; Sun, C.-L.; Li, B.-J.; Shi, Z.-J. Palladium-Catalyzed Cross-Coupling of Polyfluoroarenes with Simple Arenes. *Org. Lett.* **2010**, *13*, 276–279.

2.Synthesis of anthracene based emitter molecules

In TTAUC emitter molecules the substitution of hydrogen with fluorine atoms would be expected to depress the HOMO and LUMO levels, and thus reduce the singlet and triplet energy levels. This would red shift the emission when compared to non-fluorinated derivatives. However, ideally the triplet level would be lowered to a greater extent than the singlet, spreading these levels and giving an increased potential anti-Stokes shift to the system. Movement of the energy levels may also cause the second triplet level to become inaccessible by annihilation, making the system more efficient for TTA up-conversion. The ability of fluorine to tune energy levels in this way may allow design of efficient up-conversion systems.

2.1. Aims and Approach

In general the structure of the proposed triplet-triplet annihilation up-conversion (TTAUC) emitter molecule uses an emissive core moiety that is modified by the addition of a single or multiple periphery aromatic systems (Figure 2.1). The functionalization of the core and periphery portions of the molecule, especially with fluorine containing functional groups, is of major interest in this project since this allows fine tuning of the chromaphore's energy levels and physical properties. It was hoped that these structures would have properties and energy levels tuned to match a porphyrin sensitizer, making these highly efficient and stable bespoke emitters suitable for use in TTAUC systems.

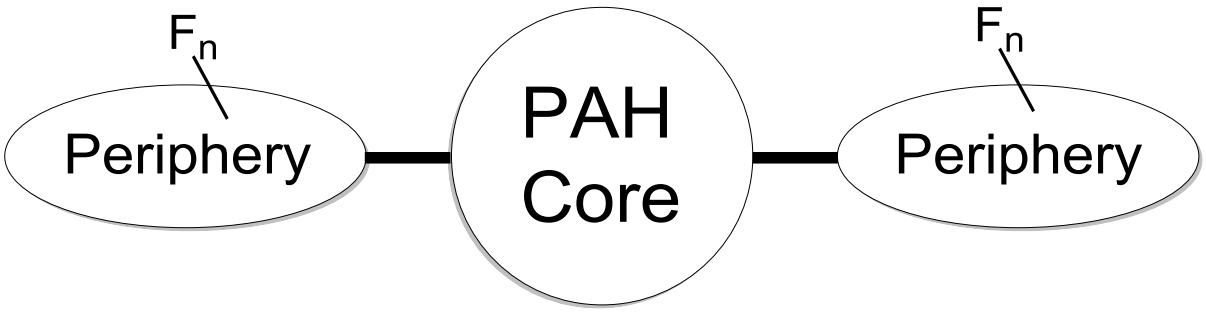

Figure 2.1: Idealised structure of TTAUC emitter molecule

The core structure, normally a polyaromatic hydrocarbon (PAH), will define the basic properties of the molecule, but careful selection of the periphery structures and functionalisation will allow tuning of solubility and emission.

We selected the most commonly used TTA up-conversion emitter, diphenylanthracene (DPA), for initial fluorination investigation - DPA has been used in papers by many different groups, including our collaborators.[1–6] Anthracene and its derivatives are widely used in organic light emitting diode (OLED) applications, as organic field-effect transistors (OFETs), and may act as scaffolds for electron transfer species due to its conjugation. A route in the literature to 9-substituted anthracenes was via ring forming reactions;[7] however these are not suitable for bissubstituted anthracenes. 9,10-substituted anthracenes were first prepared using Grignard or organolithium techniques from anthraquinone, followed by deoxygenation with potassium iodide.[8,9]

An anthracene emitter that is functionalised in the 9- and 9,10- positions, in a similar manner to the common chromaphore diphenylanthracene (DPA), would produce chromaphores that emit in the blue region of the visible spectrum.

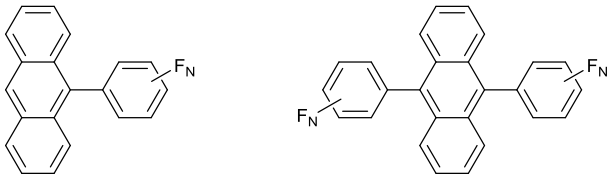

1 2

Figure 2.2 : Proposed structures for anthracene based emitters

Anthracene core based molecules functionalised with fluorinated aryl groups at the 9- position and at 9,10- positions were targeted as appropriate targets for emitters in up-conversion systems.

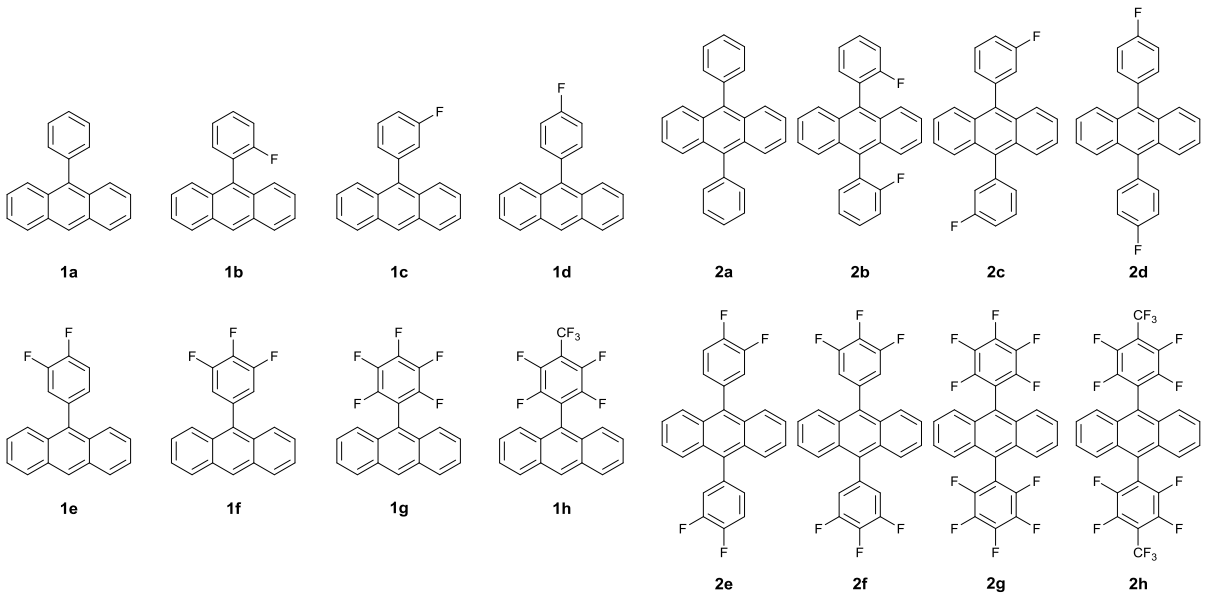

Figure 2.3 : 9-phenylanthracene and 9,10-diphenylanthracene targets

The diphenylanthracene targets were chosen due to the availability of the required reagents and the useful continuous series of increasing fluorination. A number of routes could be used, a

retrosynthetic analysis is shown for 9,10-diphenylanthracenes. The same steps could be used to produce 9-phenylanthracenes.

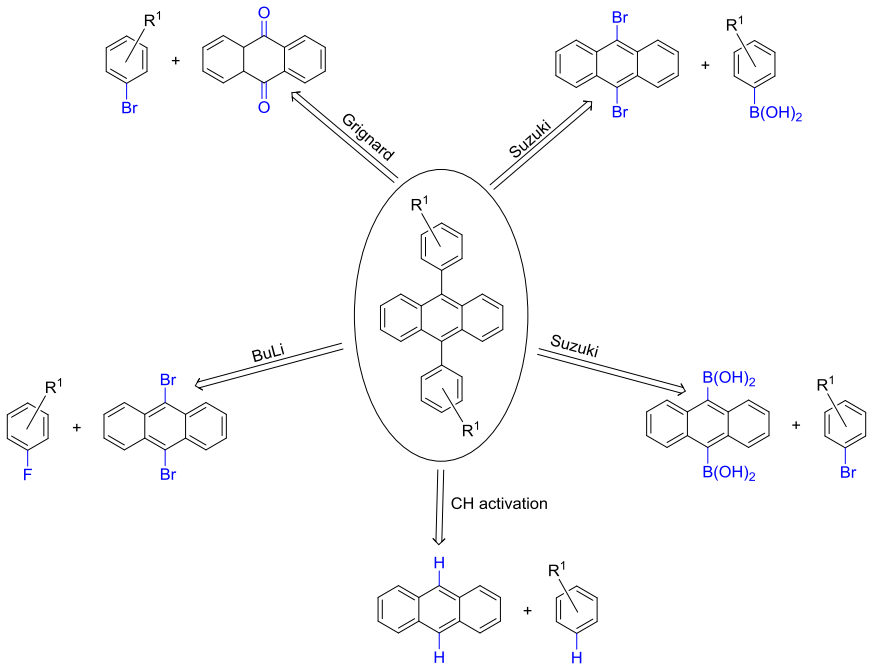

Figure 2.4 : Retrosynthetic analysis of 9,10-diphenyl anthracenes

2.2. Boronic acid couplings with 9,10-dibromoanthracene

It was necessary to investigate a model reaction initially, that of 4-fluorophenylboronic acid and 9,10-dibromoanthracene, chosen due to the commercial availability of the required reagents.

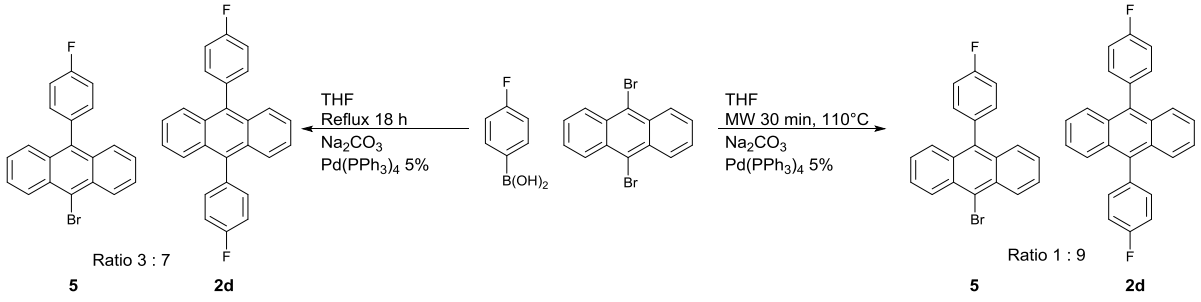

Figure 2.5: Microwave and standard reaction of 9,10-dibromoanthracene with 4-fluorophenyl boronic acid

This was carried out under conditions reported by Kotha et al but was only partly successful, analysis by ^{19}F NMR showing a large proportion of 9-bromo-10-(4-fluorophenyl)anthracene, the monocoupled product, compared to 9,10-bis(4-fluorophenyl)anthracene, the dicoupled product. The equivalent reaction carried out under microwave conditions from literature, and using standard

conditions was also unsuccessful in producing the pure symmetrical product, with both starting materials isolated, with a low conversion.

The monocoupled product, 9-bromo-10-(4-fluorophenyl)anthracene, was successfully isolated and analysed. It was hypothesised that the boronic acid was not forming the quarternary anion required for the reaction due to either the poor solubility of the base or that protodeborylation was occuring before the coupling reaction could take place. In the Suzuki reaction where the boronic acid is polyfluorinated or a heterocycle, protodeborylation of the reagent is a common problem, causing the boronic acid to be used in great excess. These problems could be probed by a base and solvent survey, the results of which are shown. Na_2CO_3 was not tested as this it would be expected to have extremely poor solubility in the organic solvents. The standard conditions for these reactions were a microwave reaction for 1 hr at 110°C of 4-fluorophenylboronic acid, 9,10-dibromoanthracene and the base (2:1:3) using $Pd(PPh_3)_4$ (2%) in the degassed reaction solvent (2 ml) under inert atmosphere. These were then analysed by ^{19}F NMR as before to give the conversion (percentage of boronic acid that has reacted) and the product ratio (percentage dicoupled compared to other products).

	THF	Dioxane	DMSO
Cs_2CO_3	50 (4:1)	60 (9:1)	
K_2CO_3	30 (9:1)		
K_3PO_4	30 (6:1)		
KO-tBu	60 (11:9)	80 (7:3)	40 (3:1)

Figure 2.6 : Base and solvent survey: conversion %, (ratio mono:disubstituted)

From the data above it can be seen that potassium tert-butoxide is the most suitable base for this reaction, it is more soluble in organic solvents than potassium carbonate, and that the best solvents are THF and Dioxane. Dioxane was chosen because 9,10-bis(4-fluorophenyl)anthracene has a low solubility in this solvent, while the monosubstituted 9-bromo-10-(4-fluorophenyl)anthracene stays in solution.

An experiment was carried out to evaluate if increasing the temperature would increase the rate of the reaction thus allowing it to go to completion before protodeborylation; however the more elevated temperatures of 130 °C resulted in increased speed of deborylation of the starting materials, producing samples with more impurities and a worse conversion percentage. Following the test reaction syntheses of compounds **1a-h** and **2a-h** were carried out concurrently.

The coupling of 3-fluorophenylboronic acid with 9,10-dibromoanthracene was unsuccessful, instead multiple products are formed, as well as homocoupled boronic acid, giving low yields of the desired product which could not be separated. The high loading of boronic acid means that this is not an efficient procedure and it was clear that it the reaction conditions required improvement.

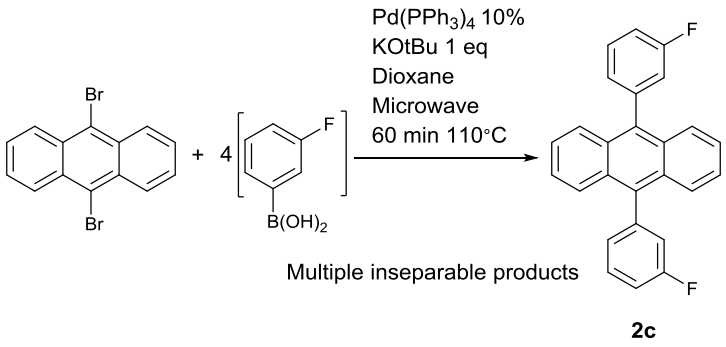

Figure 2.7 : Microwave Suzuki cross coupling of 9,10-dibromoanthracene with (3-fluorophenyl)boronic acid

While the use of boronic acids in coupling reactions is common they have disadvantages. Unwanted by-products may be formed by catalytic homocoupling of the boronic acid which occurs in the presence of oxygen, decreasing yield. The major problem with Suzuki reactions lies in the facile deboronation of the boronic acid coupling partner, requiring relatively high loading in normal reactions.[10–14]

Loadings of over 2 equivalents of boronic acid were required to produce any yield of the intended products, and even these reactions produced poor yields. For this reason it was beneficial to explore alternatives to the boronic acid coupling partner to avoid deboronation.

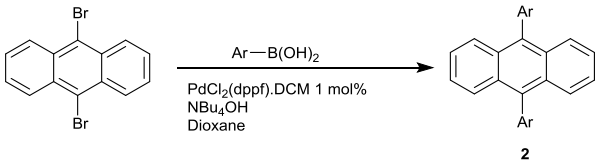

Boronic Acid	Diphenylanthracene Product	Yield	Boronic Acid	Diphenylanthracene Product	Yield
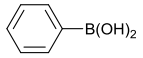	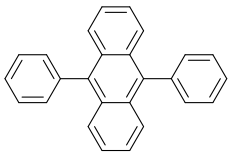	**2a**, 34%	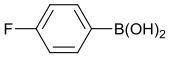	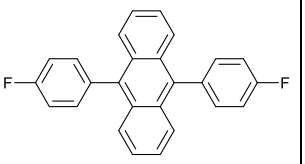	**2d**, 73%
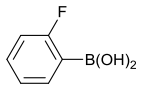	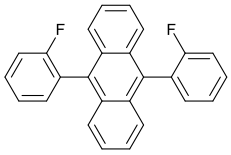	**2b**, 0%	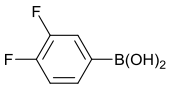	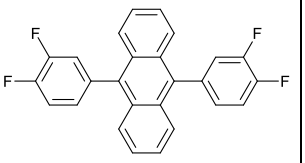	**2e**, 15%
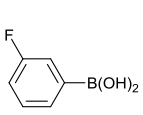	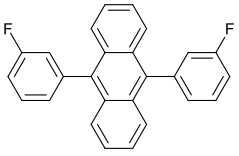	**2c**, 54%	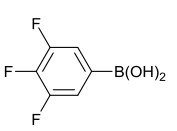	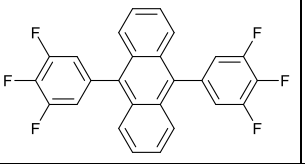	**2f**, 0%
			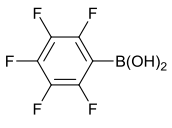	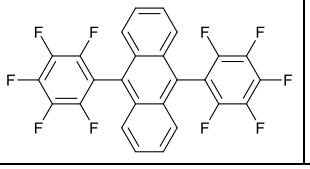	**2g**, 0%

Figure 2.8 : Suzuki coupling reactions of 9,10-dibromoanthracene and boronic acids using dppf catalyst

The isolation of these products has proved non trivial due to the formation of debrominated monosubstituted by-products (in this example 9-(3,4,5-trifluorophenyl)anthracene), these are difficult to seperate by chromatography from the desired product. 9,10-di(3,4,5-trifluorophenyl)anthracene was purified by chromatography (silica, toluene), co-eluting the disubstituted and monosubstituted products. Due to the difference in polarity of the two products they were separated by recrystallization of the crude solid from methanol.

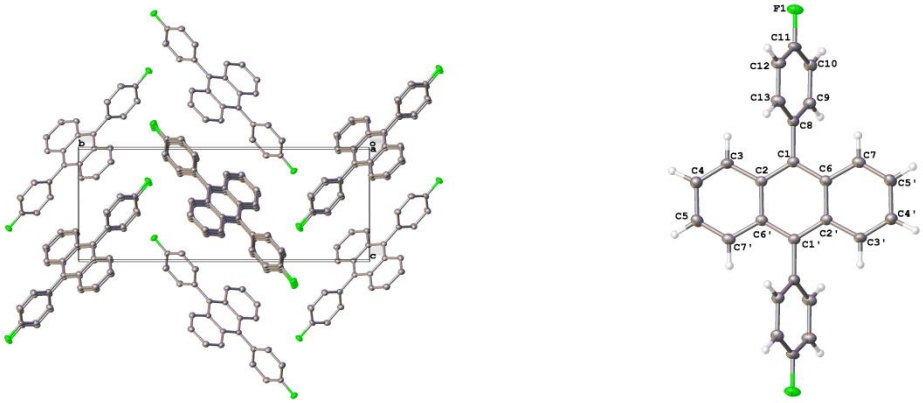

Figure 2.9 : Unit cell (left) and molecular structure (right) of **2d,** obtained by x-ray crystallography

In the case of **2d** and **2e** crystals of sufficient quality for analysis by x-ray crystallography were obtained.

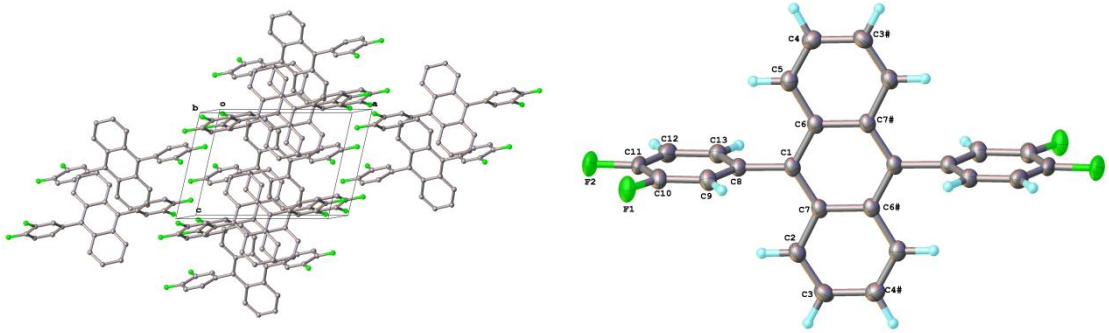

Figure 2.10 : Unit cell (left) and molecular structure (right) of **2e,** obtained by x-ray crystallography

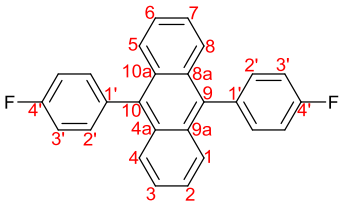

Figure 2.11 : IUPAC numbering of **2d**

Assignment of the NMR spectra of compound **2d** begins with the fluorine peak and the subsequent assignment of C4', C3', C2' and C1' by the *J* coupling.

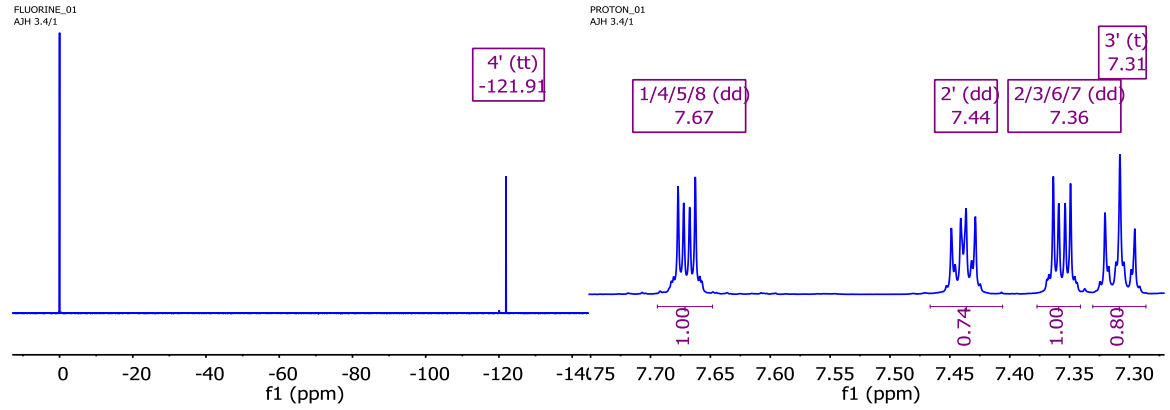

Figure 2.12 : ^{19}F (left) and ^{1}H (right) spectra of **2d**

With the phenyl ring assigned, the remaining anthracene environments are found by the HMBC spectrum where C9 couples to the phenyl protons and equivalent protons H1/4/5/8, thus equivalent protons H2/3/6/7 are found by elimination, their associated carbon atoms are assigned by HSQC.

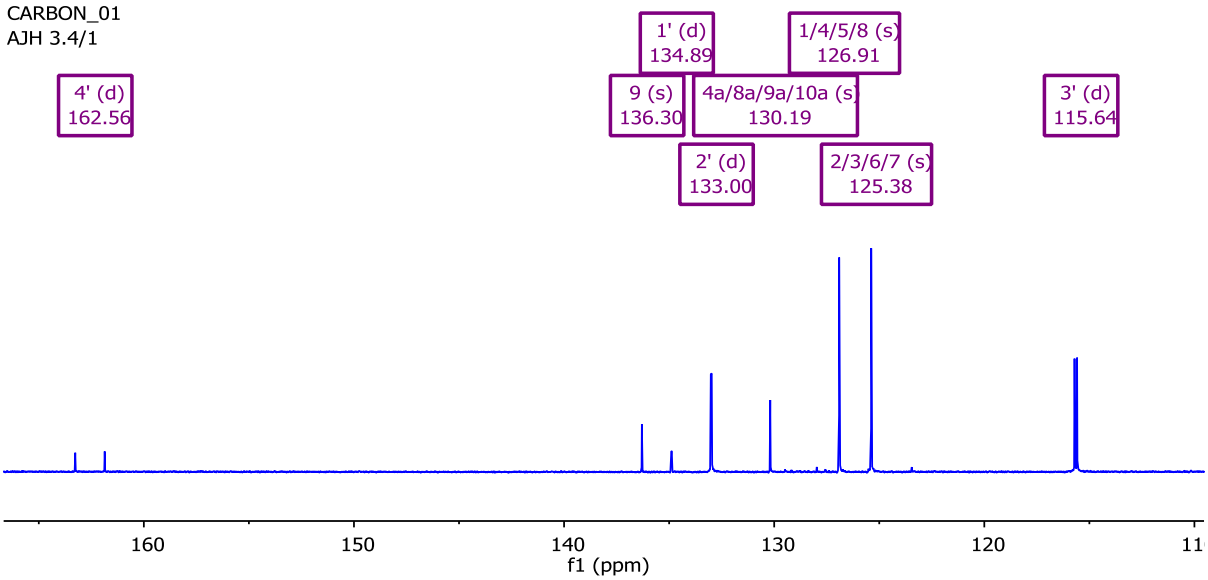

Figure 2.13 : ^{13}C NMR spectrum of **2d**

Equivalent bridge carbons C4a/8a/9a/10a are found by elimination of C-H HMBC correlations.

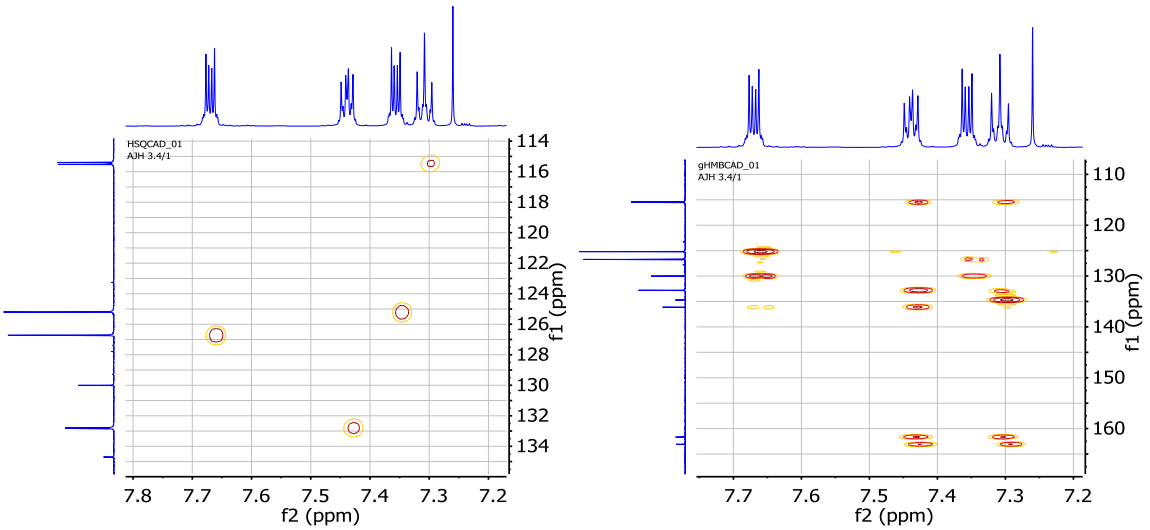

Figure 2.14 : HSQC (left) and HMBC (right) spectra of **2d**

All attempts to synthesise 9,10-di(2-fluorophenyl)anthracene, **2b**, were unsuccessful and syntheses of highly fluorinated products **2f-g** were also unsuccessful. In the course of synthesising **2f** mixtures of the desired product, along with monosubstituted side products and anthracene were obtained. The competing dehalogenation causes the formation of **1f**.

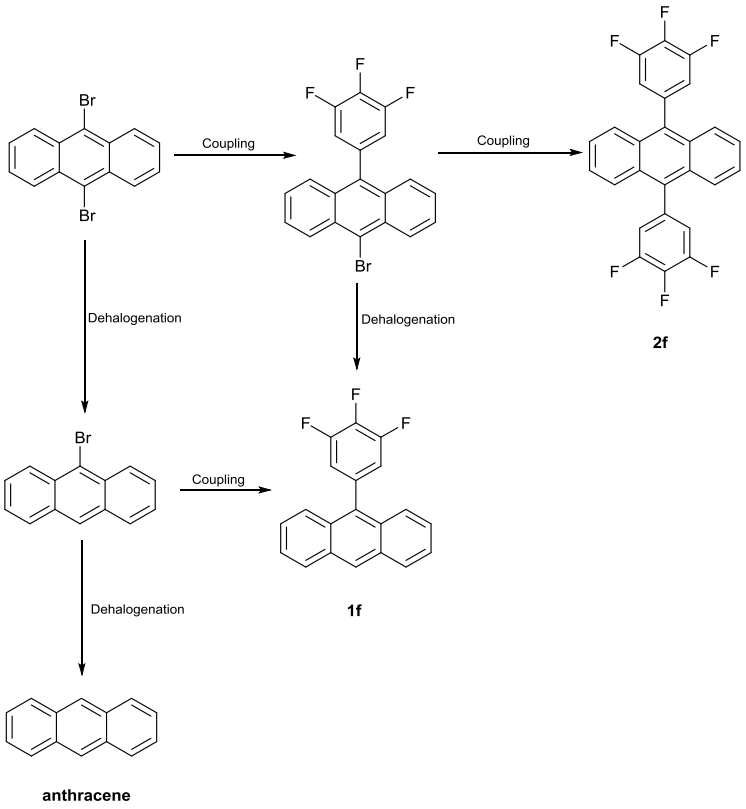

Figure 2.15: The competing routes of dehalogenation and cross coupling

Clearly dehalogenation is much slower than the cross coupling mechanism, because less than 1 % of anthracene compared to the desired product is detected by GC, therefore it can be assumed that the rate of coupling is 10 times that of the dehalogenation when using these reagents.

Another attempt to synthesise **2b** using an altered Suzuki-Miyaura protocol, found to be successful in the production of 2-arylpyrroles (Chapter 6), was undertaken. A suspension of boronic acid, 9,10-dibromoanthracene, $Pd(PPh_3)_4$, in toluene, methanol and 2 M aq. K_2CO_3 was degassed by three freeze-pump-thaw cycles and then stirred at 85 °C for 36 h, allowed to cool and eluted with ethyl acetate through a silica plug on a bed of celite. After evaporation *en vacuo* and recrystallization from hexane / ethyl acetate yellow crystals were collected.

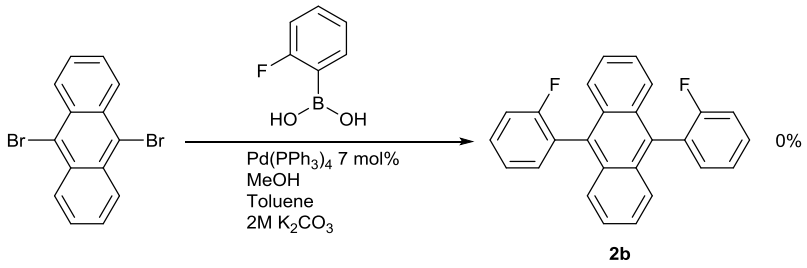

Figure 2.16 : Attempted synthesis of 9,10-bis-(2-fluorophenyl)anthracene

Rather than the desired product, 9,10-bis-(2-fluorophenyl)anthracene, debrominated anthracene was isolated. Again the facile deboronation of the 2-fluorophenylboronic acid coupling partner has prevented the coupling reaction, allowing debromination of the starting material. Fluorobenzene is volatile, and so was lost during reduction *en vacuo.* Traces of fluorobenzene were nevertheless detected by GCMS, and ^{19}F NMR.

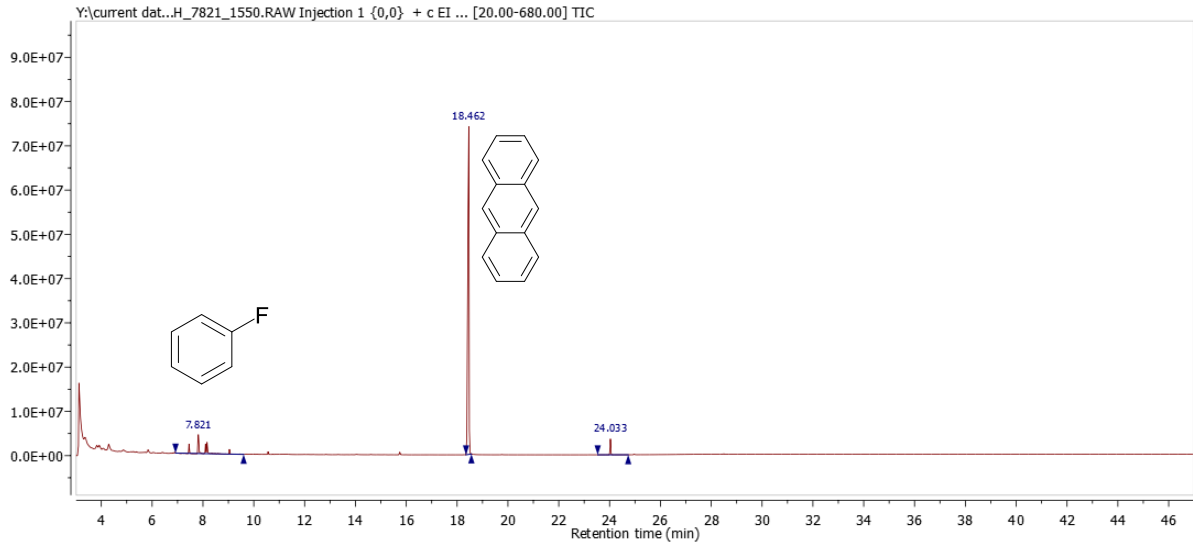

Figure 2.17 : GC trace of attempted synthesis of **3b**

It was clear that another method was required to allow the synthesis of highly fluorinated diphenylanthracenes, where deboronation and debromination of the starting materials was reduced.

2.3. Coupling of potassium trifluoroborate salts with 9,10-dibromoanthracene

One method to prevent protodeboronation of the boron coupling partner is to make use of trifluoroborate salts. Quarternary boron compounds such as trifluoroborate salts have been known for over half a century[15] but an easy and extremely high yielding synthesis using KHF_2 was discovered in 1995,[16] and their utility in Suzuki-Miyaura coupling reactions has been shown by Molander and other groups.[17] For these reasons the potassium trifluoroborate salts were synthesised and tested in a coupling reaction.

The useful qualities of potassium trifluoroborate salts have been outlined above, and the conversion of the fluorophenyl boronic acids to the equivalent salt was undertaken with a view to their use in coupling reactions. This normally occurs in excellent yield.

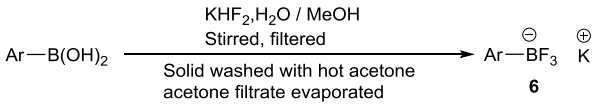

Boronic Acid	Trifluoroborate Product	Yield	Boronic Acid	Trifluoroborate Product	Yield
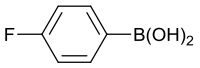	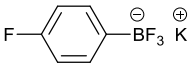	**6d**, 99%	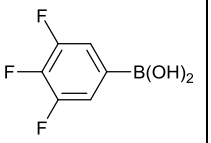	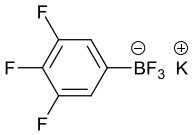	**6f**, 99%
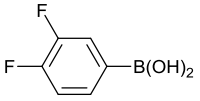	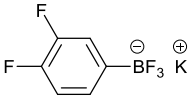	**6e**, 35%	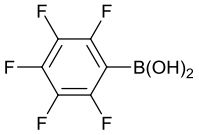	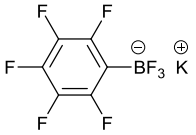	**6g**, 75%

Figure 2.18 : Synthesis of phenyl potassium trifluoroborate salts

Using this coupling procedure the reactions of boronic acids with brominated anthracenes were undertaken, to investigate if it was necessary to produce the potassium trifluoroborate salts, extending the number of required steps.

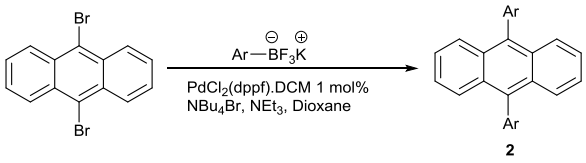

Trifluoroborate	Diphenylanthracene	Yield	Trifluoroborate	Diphenylanthracene	Yield
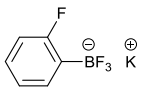	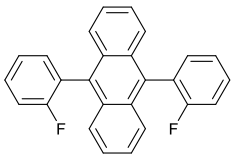	**2b**, 0%	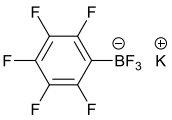	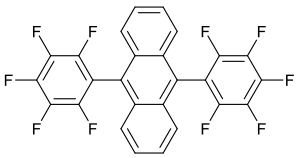	**2g**, 0%
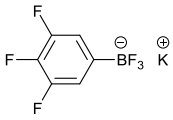	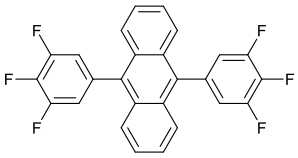	**2f**, 40%			

Figure 2.19: Suzuki coupling reactions of 9,10-dibromoanthracene and potassium trifluoroborates using dppf catalyst

The synthesis of **2f** was successful, and crystals of sufficient quality for x-ray crystallography were obtained from hexane.

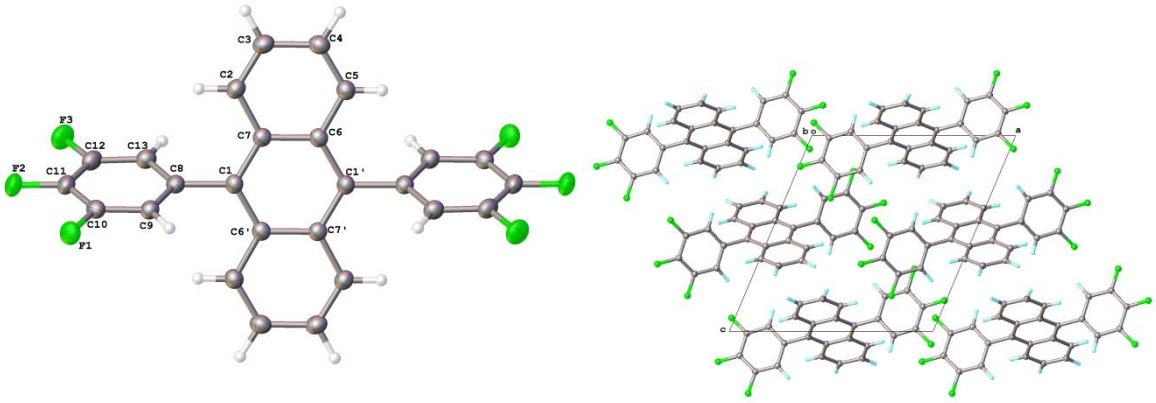

Figure 2.20 : Molecular structure (left) and unit cell structure (right) of **2f**

Highly fluorinated boronic acids are susceptible to deboronation under Suzuki-Miyaura coupling conditions which may require higher than desired loading.[10] The yields of products clearly decrease with the increasing fluorination of the phenyl boronic acid.

As well as diphenylanthracenes the synthesis of a series of 9-phenylanthracene molecules was desired for photophysical investigation.

2.4. Boronic Acid couplings with 9-bromoanthracene

Microwave reactions at 110°C using $Pd(PPh_3)_4$ in Dioxane were carried out, these conditions have produced the target compounds, but in low yields.

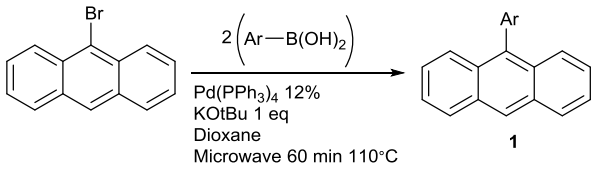

Boronic Acid	9-arylanthracene Product	Yield	Boronic Acid	9-arylanthracene Product	Yield
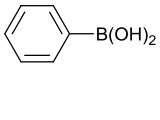	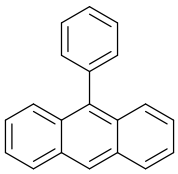	**1a**, 17%	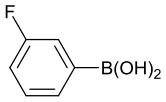	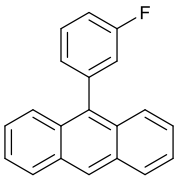	**1c**, 20%
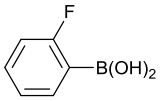	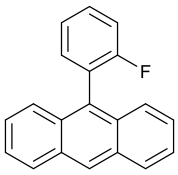	**1b**, 43%	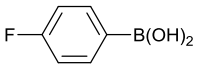	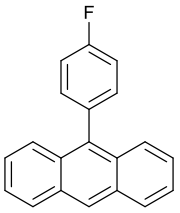	**1d**, 40%

Figure 2.21 : Microwave synthesis of 9-arylanthracene. **3b** required 4 equivalents of boronic acid

Due to deboronation an excess of boronic acid was required for the reaction to proceed, and even with large excesses this system fails for coupling 9,10-dibromoanthracene or highly fluorinated phenylboronic acids.

The products were isolated by crystallisation, crystals of **1a-c** were obtained in sufficient quality for analysis by x-ray crystallography. Interestingly, the crystal structures of these compounds show differing unit cells despite their similarity in structure; 9-phenylanthracene forms angled columns while 9-(2-fluoro)phenylanthracene forms dimers. The *ortho* fluorine substitution has greatly altered the intermolecular packing of the phenylanthracene system. The *meta* fluorine substitution has the same effect as the *ortho*.

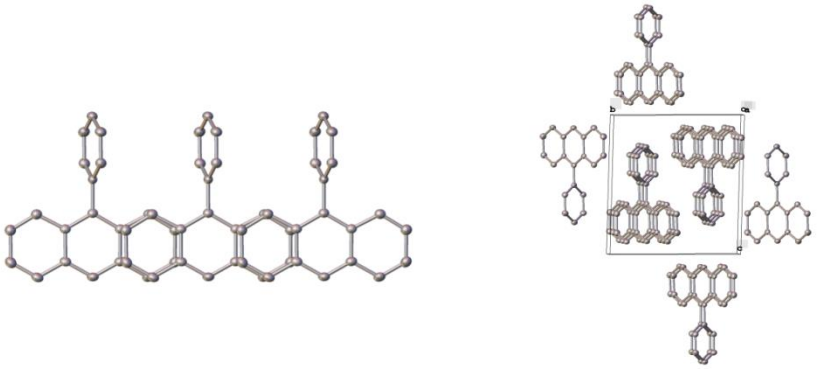

Figure 2.22 Double layer (left) and stacked columns (right) of **1a**

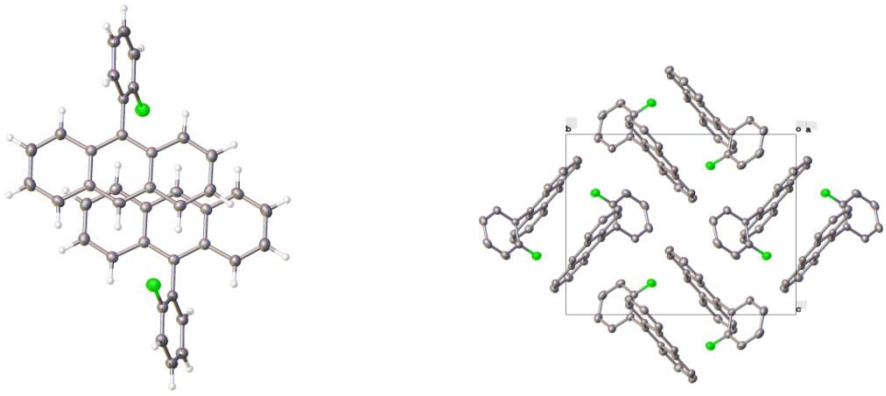

Figure 2.23 : Double layer (left) and unit cell (right) of **1b**

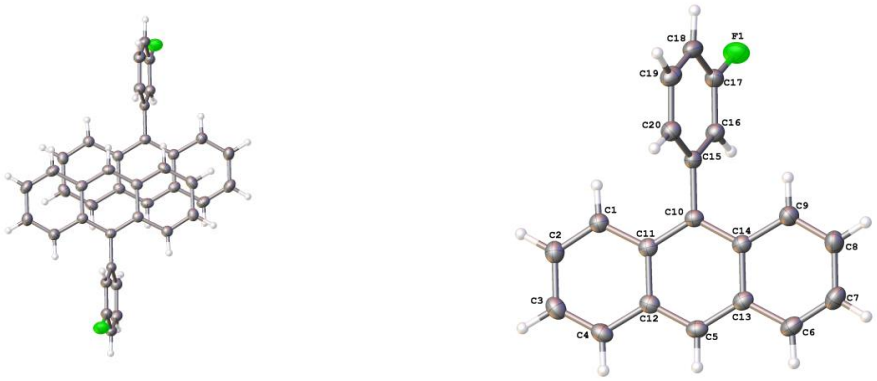

Figure 2.24 : Double layer (left) and molecular structure (right) of **1c**

The yields of the compounds may be accounted for by the protodeboronation of the boronic acid starting material reducing the available coupling reagent – when four equivalents of the boronic acid are used the yield is increased. The homocoupled biphenyl was isolated from the reaction mixture with ortho fluorine substituent.

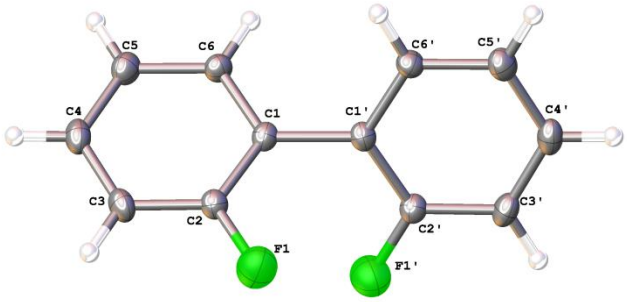

Figure 2.25 : Molecular structure of 2,2'-difluorbiphenyl

Again deboronation was having an effect, and another strategy was required for the production of the desired 9-phenylanthracene series.

2.5. Coupling of potassium trifluoroborate salts with 9-bromoanthracene

Trifluoroboronate salts have been found to couple to all the common Suzuki substrates in good yield, in some case under "ligandless" (ie. no phosphine ligands) conditions in air,[17] for this reason the reaction shown was undertaken. However, following reflux for 21 hours no product was detected by mass spectrometry or NMR spectroscopy.

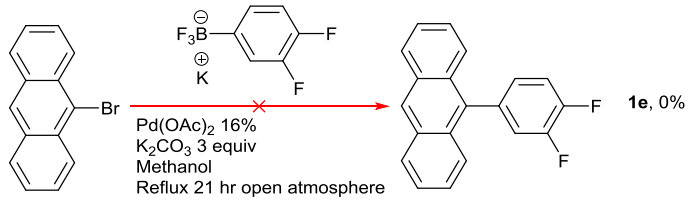

Figure 2.26: Suzuki cross coupling of 9-bromoanthracene with potassium (3,4-difluorophenyl)trifluoroborate under ligandless conditions

In contrast to the above reaction when the same reagents were heated in a microwave at 100°C for 60 min multiple compounds were detected, including the product. Clearly there are many competing mechanisms at work here, but for a clean reaction a different catalyst system was required.

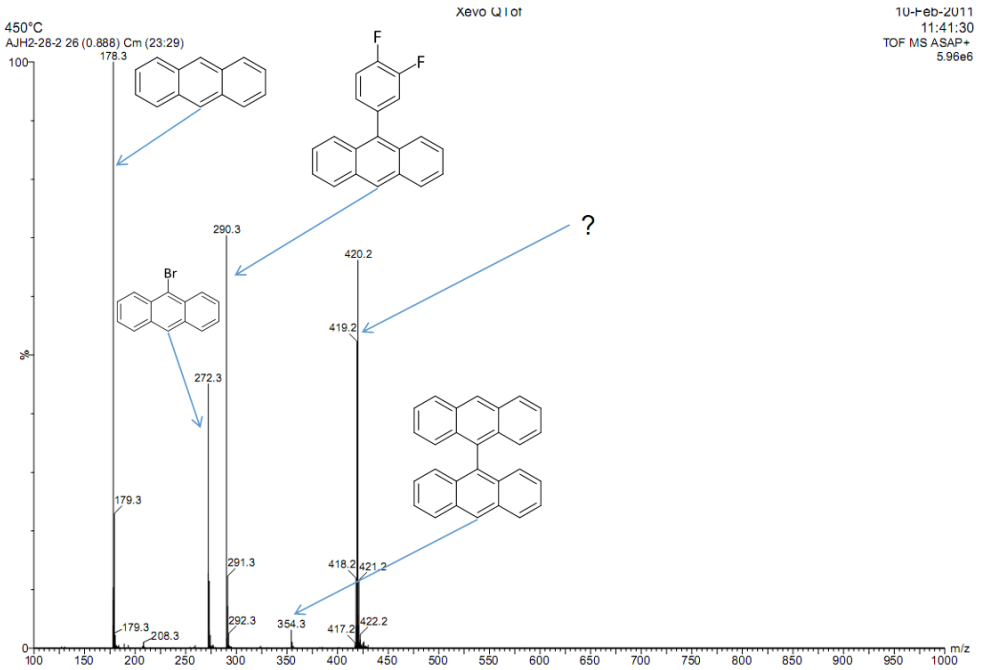

Figure 2.27: ASAP spectrograph of products of Suzuki coupling of 9-bromoanthracene with potassium (3,4-difluorophenyl)trifluoroborate under microwave heating and ligandless conditions

A promising catalyst for use with trifluoroborate salts is [1,1'-Bis(diphenylphosphino)ferrocene] palladium(II) dichloride which is commercially available. Advantageously to this project its use

with ethanol and Hunig's base or triethylamine allows coupling of boronate salts with fluorinated moieties. This prompted the investigation of the system shown below which has shown promise.[18]

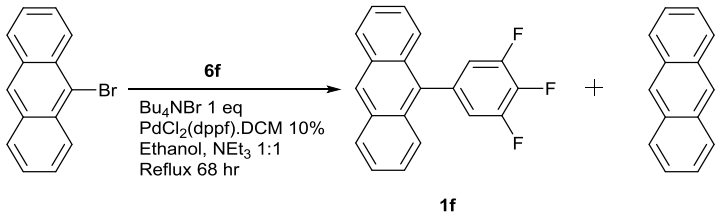

Figure 2.28: Suzuki cross coupling of 9-bromoanthracene and potassium (3,4,5-trifluorophenyl)trifluoroborate

A competing mechanism caused debromination and forms anthracene as an unwanted by-product. The debromination forced us to explore the use of an aprotic solvent such as dioxane, which seems to slow dehalogenation enough for the intended reaction to occur. The slow coupling reaction allows deboronation to a small extent, preventing full conversion, but potassium carbonate in water causes less dehalogenation than amine bases.

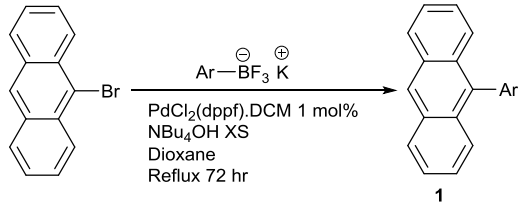

Trifluoroborate	9-arylanthracene product	Yield	Trifluoroborate	9-arylanthracene product	Yield
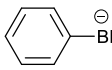	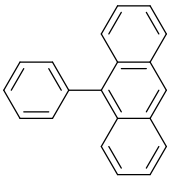	**1a**, 32%[a]	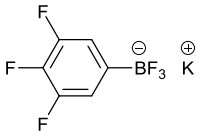	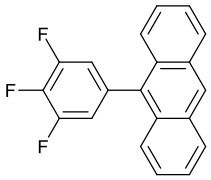	**1f**, 22%
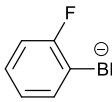	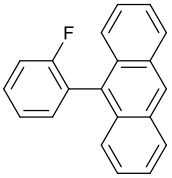	**1b**, 0%	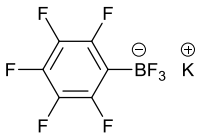	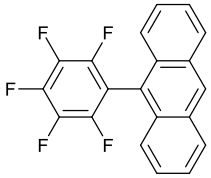	**1g**, 0%
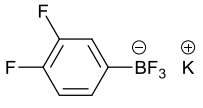	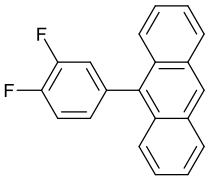	**1e**, 54%[b]			

Figure 2.29: Suzuki coupling reactions of 9,10-dibromoanthracene and potassium trifluoroborates using dppf catalyst

Once isolated the product **1f** was analysed by x-ray crystallography.

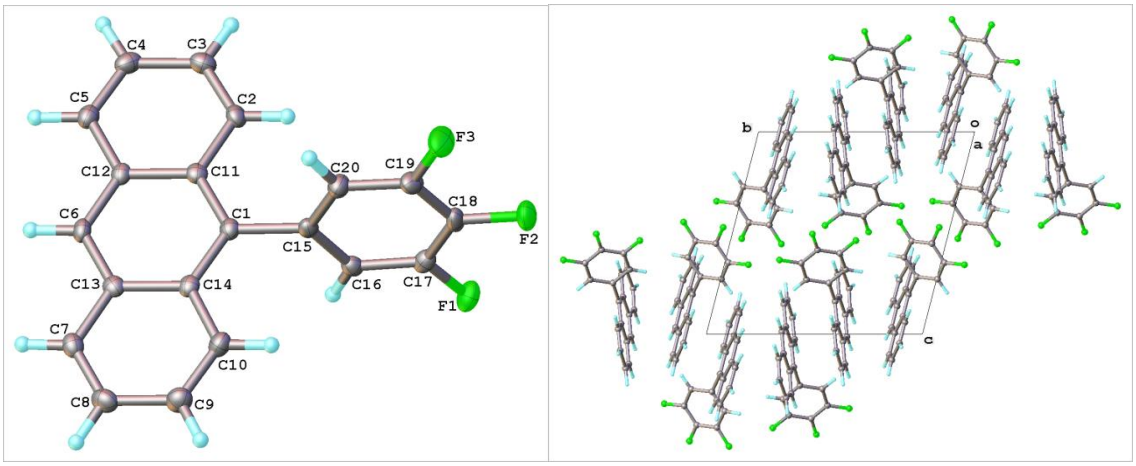

Figure 2.30: Molecular structure (left) and unit cell (right) of **1f**

The products were characterised by NMR spectroscopy, mass spectrometry, melting point and elemental analysis. The assignment of the NMR spectrum was similar for each compound, and atoms are numbered according to IUPAC numbering. For example the assignment of compound **1c** is as follows.

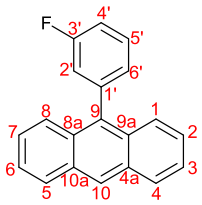

Figure 2.31 : Compound **1c** with IUPAC numbered atoms

Assignment begins with the fluorine substituent at the 3’ position to the single peak in the fluorine spectrum (0 ppm corresponds to the $CFCl_3$ internal standard).

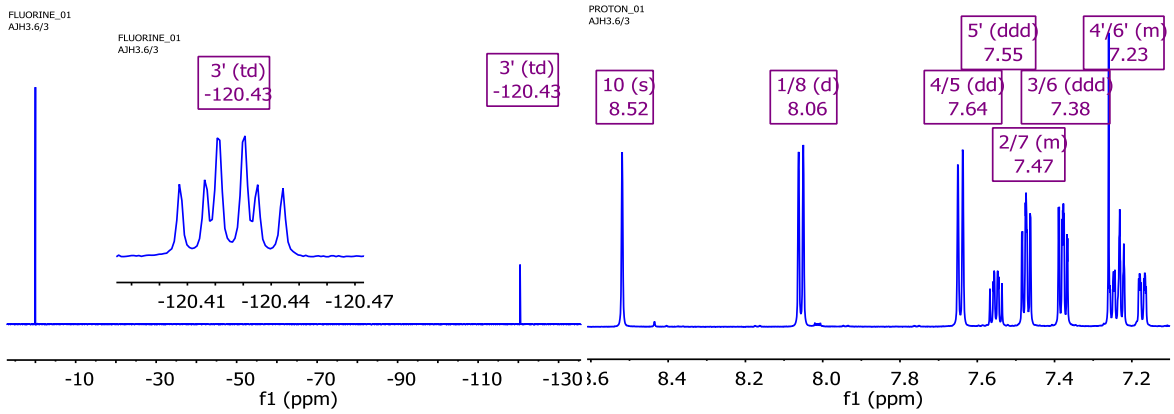

Figure 2.32 : 19F and 1H NMR spectra of 1c

Assignment of fluorine environment allows assignment of its nearest carbon atom neighbours. The α carbon atom, C3’, is that with the largest coupling constant, the two β carbon atoms have the next

largest *J* coupling, and so on. This allows us to assign C6', but since C2' and C4' have the same *J* coupling, as do C1' and C5' these cannot be distinguished between from *J* coupling alone.

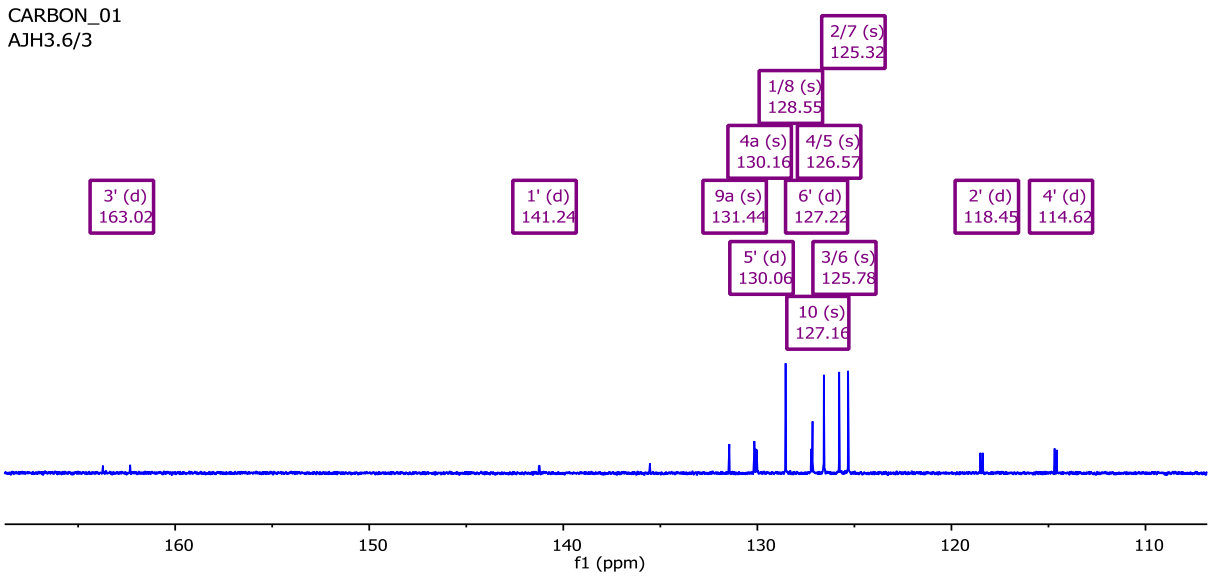

Figure 2.33 : 13C NMR spectrum of **1c**

From the HSQC spectrum H6' may be assigned, and its coupling to H5' (elucidated by the COSY spectrum), and the lack of H-H coupling by H2' allows these protons and their respective carbon environments to be assigned, C1' is found by process of eliminating C5'. With the phenyl ring finished the assignment of the anthracene structure begins with the assignment of the singlet, lone proton, H10.

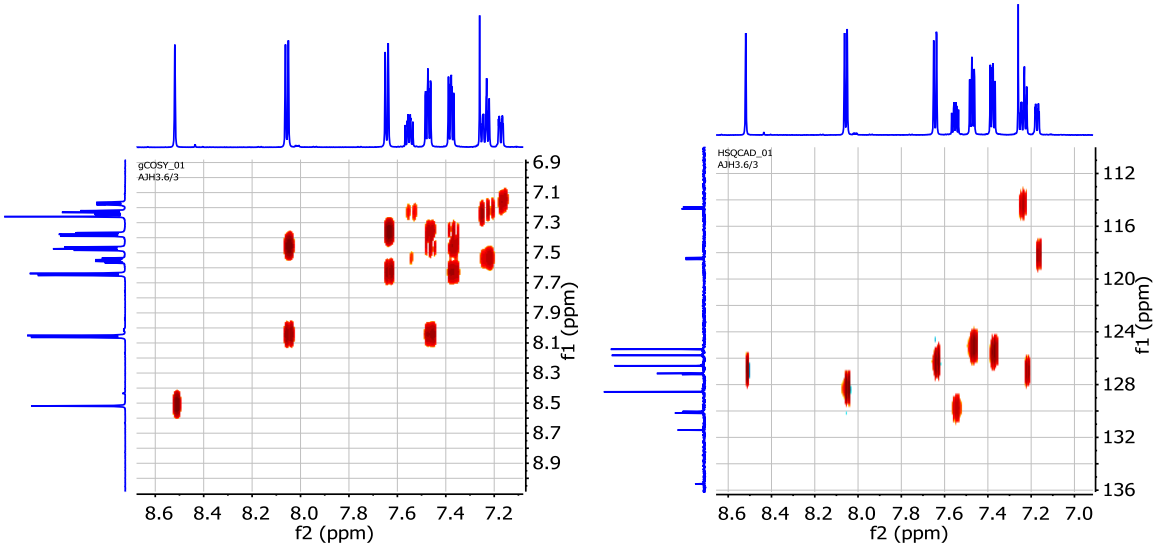

Figure 2.34 : COSY (left) and HSQC (right) spectra of **1c**

Using the HMBC spectrum and faint long range H-H coupling allows assignment of equivalent protons H4/5, and coupling round the ring gives the anthracene protons, and their carbon atoms via the HSQC spectrum.

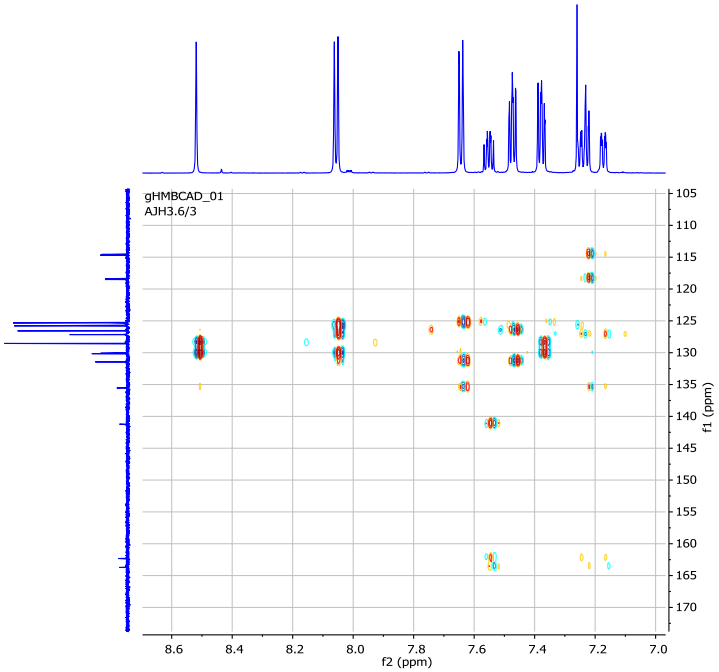

Figure 2.35 : HMBC spectrum of **1c**

Finally, the anthracene carbon environments without bonded hydrogen atoms must be assigned by the HMBC spectrum where the small signal C9 couples to the phenyl ring protons, equivalent carbons C8a/9a faintly couple to H6' and H2' and equivalent carbons C4a/10a only couple to anthracene protons. This general method of assignment has been used for each 9-phenylanthracene product, regardless of their synthesis route.

The debromination of the arylhalide had been experienced previously when Molander *et al.* attempted similar reactions using this catalyst and they found that dry THF gave the best result, and also concluded that the use of the boronic acid, rather than trifluoroborate salt gave very little conversion. They found that when sterically impeded aryl-halides are employed the coupling may proceed slowly, and arylhalide homocoupling or protodehalogenation may occur. The use of aprotic conditions discourages the dehalogenation of the aryl-halide, this is in agreement with the experience of this project.

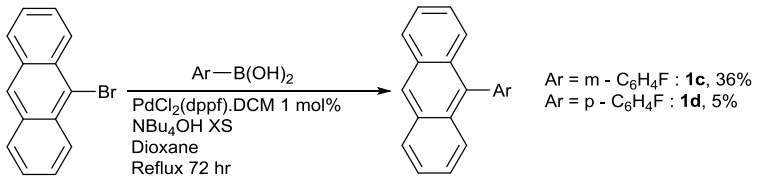

Figure 2.36 : Suzuki coupling reactions of 9,10-dibromoanthracene and boronic acids using dppf catalyst

This system was used with a view to coupling 9-bromoanthracenes with boronic acids, to deduce if potassium trifluoroborate salts are required in these couplings. The yields using boronic acids are lower, and highly fluorinated partners are more likely to fail, separation is also more difficult causing more losses. Again the synthesis of highly fluorinated systems was unsuccessful. Another synthesis route was required to produce these molecules.

2.6. Synthesis of pentafluorophenyl anthracene systems

Pentafluorophenylboronic acid and its trifluoroborate salt are well known to be poor coupling partners and this has been borne out by the results of this project. Attempted coupling reactions using potassium (pentafluorophenyl)trifluoroborate using both ethanol and dioxane have produced only anthracene, with no fluorinated product detected by NMR spectroscopy.

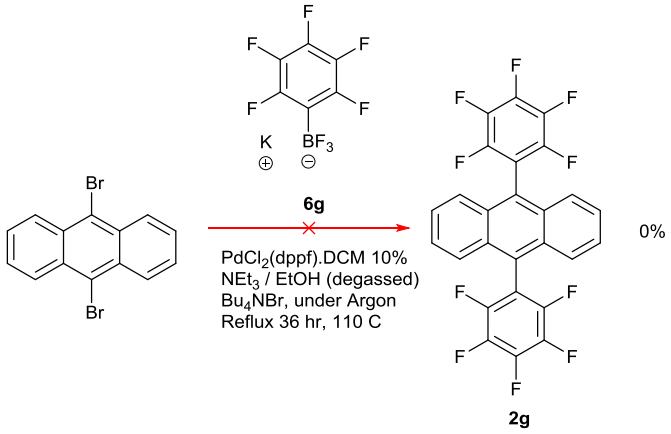

Figure 2.37: Suzuki cross coupling of 9,10-dibromoanthracene with potassium (pentafluorophenyl)trifluoroborate

It is clear that increasing fluorination of the boron coupling partner retards the reaction, so it may be theorised by reversing the functionality, such that the anthracene possesses the boronic acid moiety and the pentafluorophenyl acts as the aryl halide, then the reaction may be encouraged.[19,20]

Indeed, this may be beneficial since ideally the aryl halide should possess electron withdrawing groups to promote oxidative addition. While pentafluorobromobenzene is commercially available anthracene-9,10-diyldiboronic acid and anthracen-9-ylboronic acid must be synthesised. They may be produced by using butyl lithium to form the required carbon anion and then reaction with a borate ester.

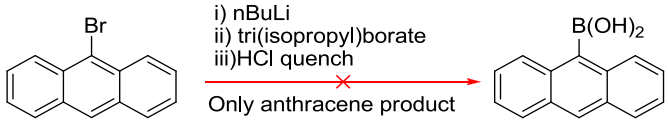

Figure 2.38: Formation of anthracen-9-ylboronic acid using BuLi

A first attempt at this was unsuccessful, and only anthracene was isolated. The reaction was repeated with the more reactive trimethylborate, and with also with fresh tri(isopropyl)borate, neither with success.

Another approach to this coupling is by using CH activation chemistry, the pseudo-directed naked coupling of pentafluorobenzene with anthracene was investigated. A trial coupling with toluene using literature procedures was successful. This reaction is carried out in the microwave, and has a large number of different reactants.

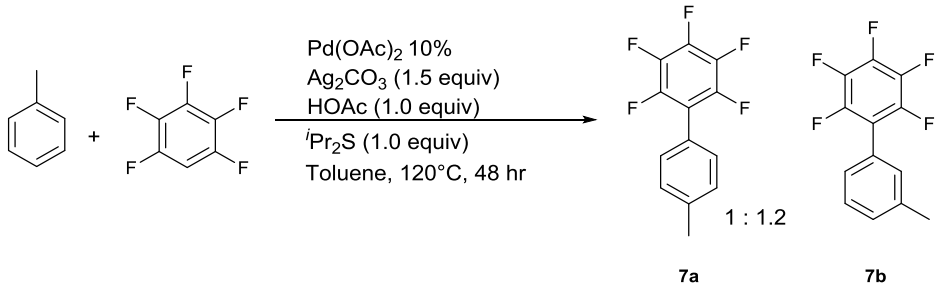

Figure 2.39: CH activated coupling of toluene with pentafluorobenzene

The reaction produced two isomers, pentafluorophenyl substituent located on *meta* and *para* positions, with ratios 1:1.2, in complete agreement with the literature. The lack of an *ortho* isomer is due to the large steric bulk of the pentafluorophenyl moiety, in the original work the coupling of chlorobenzene with these conditions produced *meta*, *para* and *ortho* isomers in ratios 1.4 : 1.0 : 0.1, indicating that the coupling sterically hindered systems is possible, but not favourable.[21] The reaction was tested with naphthalene as a substrate, and the reaction was less efficient, and substitution was seen in the least hindered beta position.

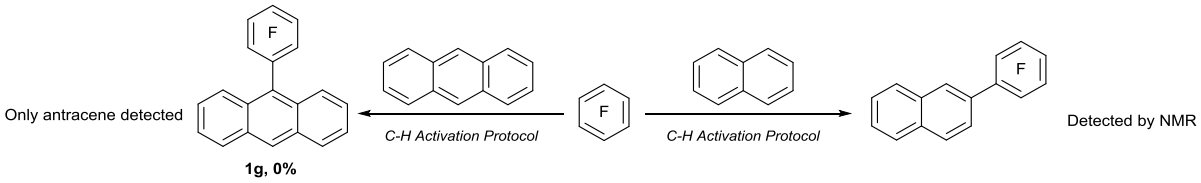

Figure 2.40 : CH activated protcols to perflurophenyl bonded PAHs

A similar reaction was conducted using the same conditions with pentafluorobenzene and anthracene but this did not produce any of the required coupling product, likely due to the high degree of steric bulk associated with anthracene. The reaction was repeated, but continued for a week rather than 48 hours and followed via ^{19}F NMR, but this also produced no yield. Only anthracene was detected by GCMS and NMR in both cases. It can therefore be concluded that anthracene is too sterically hindered, or not sufficiently reactive, to allow the coupling to proceed.

A nucleophilic attack by an aryl group upon an anthraquinone, followed by reduction of the resulting diol, is another method for producing diphenylanthracene molecules. However, when this was attempted using pentafluorobromobenzene the desired diol intermediate was not detected.

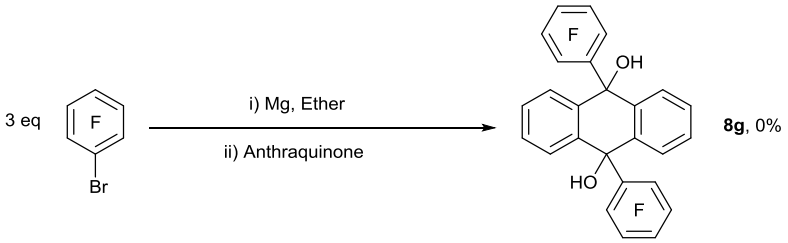

Figure 2.41 : Attempted syntesis of diol intermediate

Following experimentation, it was found that the synthesis of highly fluorinated emitters may be facilitated by the facile nucleophilic aromatic substitution (S_NAr) that perfluorinated aromatic systems undergo.

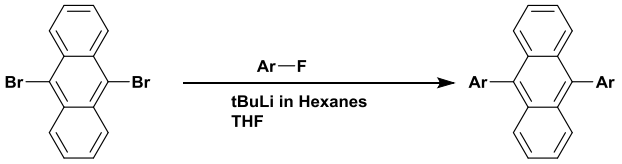

Fluorophenyl	Diphenylanthracene	Yield	Fluorophenyl	Diphenylanthracene	Yield
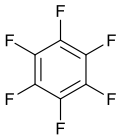	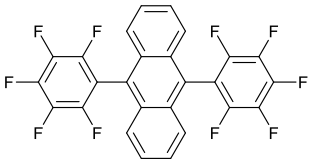	**2g**, 10%	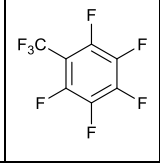	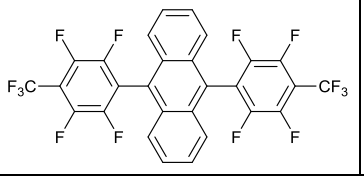	**2h**, 22%

Figure 2.42 : Synthesis of diphenylanthracenes with highly fluorinated periphery

Commercially available 9,10-dibromoanthracene in dry THF under argon was cooled by a dry-ice/acetone bath to −78 °C and ^{t}butyl-lithium added to form the required carbanion. The desired product was formed by the addition of highly fluorinated aromatic to this solution. Following work up the crude sample (~80% yield) was purified by column chromatography and then recrystallized from methanol and ethyl acetate yielding, in the case of **2h**, x-ray crystallography quality crystals.

The sample was recrystallized from hot hexane to provide the highest purity possible, as impurities have been shown to greatly decrease the effectiveness of TTA systems. The yield of **2g** is lower than that of **2h** as polymeric products may be formed by attack by the anthracene carbanion on the para-fluorine of the product.

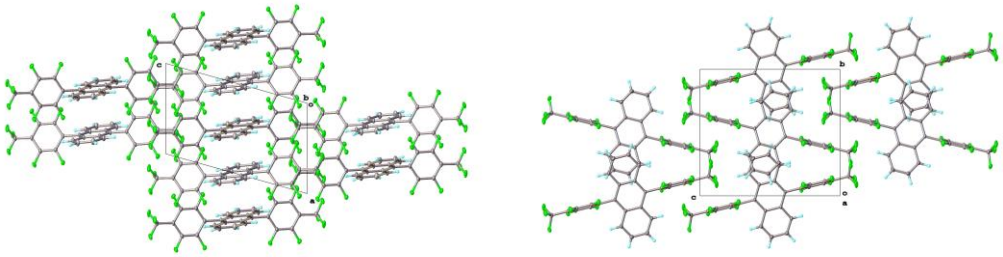

Figure 2.43 : X-ray crystallography of 9,10-di(4-trifluotomethylperfluorophenyl)anthracene

In a similar manner the 9-phenylanthracene analogues **1g-h** were synthesised by S_NAr methods, allowing the desired products.

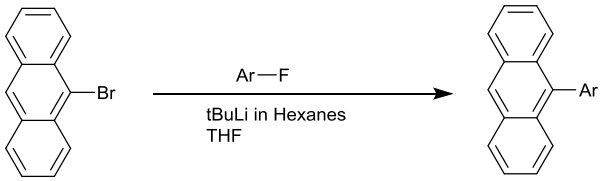

1

Fluorophenyl	9--arylanthracene	Yield	Fluorophenyl	9--arylanthracene	Yield
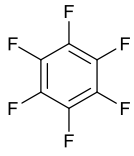	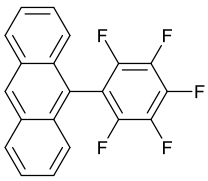	**1g**, 6%	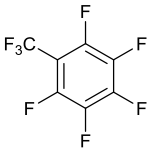	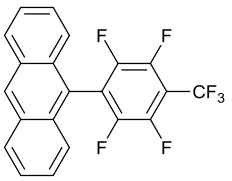	**1h**, 56%

Figure 2.44 : Synthesis of 9-phenylanthacenes with highly fluorinated periphery

Obtained crystals of **1g** were of sufficient quality for analysis by x-ray crystallography.

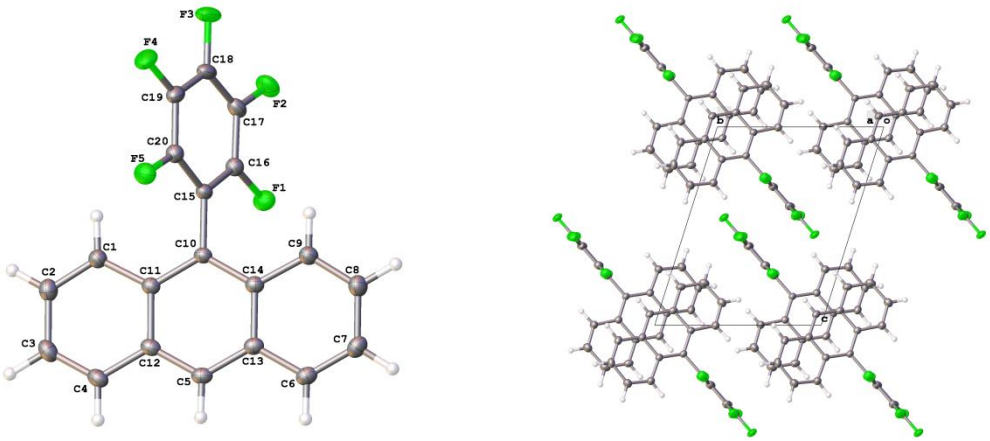

Figure 2.45 : Molecular structure (left) and unit cell of **2g**

Again for **1g** additional nuclephilic attack was found, and the di substituted product **9** was isolated.

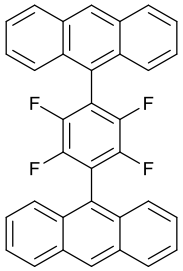

9

Figure 2.46 : di substituted 1,4-di(9'-anthracenyl)perfluorobenzene byproduct

2.7. Conclusion

As would be expected, increasing the fluorination of the desired product can cause a difficulty in using "traditional" C-C bond forming reactions between aryl groups. A clear trend of decreasing utility of the Suzuki-Miyaura cross coupling protocol can be seen as the number of fluorine atoms on the boron containing partner increases from none to three, requiring a move from boronic acids to more stable trifluoroboronate salts to produce useful yields. Above this point the palladium cross coupling method is not of use. While C-H activated protocols can produce perfluorophenyl appendages on simple model aryls, such as toluene, this requires a large excess of the aryl substrate, and the C-H activated system fails with increased steric bulk. An attempt to make the desired highly fluorinated phenylanthracenes via the diol was also unsuccessful.

Finally, a route using S_NAr chemistry was used. This makes use of the excellent electron withdrawing capability of fluorine, whereby highly fluorinated systems are activated to pathways normally closed to standard aryl functionality. Here the extremely strong C-F bond is broken, allowing fluoride to act as a leaving group. It should be noted that the perfluorophenyl derivatives are difficult to produce due to the increased reactivity of the para substituted product to nucleophilic attack, causing the production of polymeric byproducts. These were detected by MS.

Octafluorotoluene is an excellent partner in the S_NAr scheme, since the reactive para site is blocked to further nucleophililic attack, and the electron withdrawing trifluoromethyl group further activates the ring to the initial attack. The yield of the associated product is increased due to these factors.

Analysis of the products by NMR is aided by correlation spectra, and the products may be fully assigned. The crystal structures of the compounds gives an indication of their intermolecular relationships, with varying degrees of pi-pi interactions across the series.

2.8. Experimental

All palladium-catalyzed reactions were performed under an atmosphere of argon with magnetic stirring. ^{1}H, ^{19}F, ^{13}B, and ^{13}C NMR data were reported as follows: chemical shift in ppm compared to an internal standard, multiplicity (s = singlet, d = doublet, t = triplet, q = quartet, and m = multiplet), coupling constant (*J*, in Hz), integration (for ^{1}H) and assignment.

GC-MS analysis was performed on a Trace GC-MS device (Thermo-Finnigan Corp.) operating in electron impact ionisation (EI^{+}) mode and accurate mass analysis was achieved with a Xevo QtoF mass spectrometer (Waters Ltd, UK) equipped with an accurate solids analysis probe (ASAP).

ASAP Mass spectrometry and accurate mass analysis was achieved with a Xevo QtoF mass spectrometer (Waters Ltd, UK) equipped with an accurate solids analysis probe (ASAP). Infra-red spectra were recorded on a Perkin Elmer Spectrum RX1 fitted with an ATR attachment. Crystallographic data was recorded with a Rigaku R-Axis SPIDER IP diffractometer equipped with Cryostream (Oxford Cryosystems) low-temperature device at 120 K with graphite-monochromated MoK_{alpha}-radiation (λ = 0.71073 Å). Melting points were measured with a Gallenkamp apparatus at atmospheric pressure and are uncorrected.

Commercially available reagents were used without purification unless otherwise stated. Solvents used for palladium catalysed reactions were dried using an Innovative Technology Onc. Solvent Purification System fitted with a Metrohm 831 Karl Fischer Coulometric Tirtrator and degassed by three sequential freeze-pump-thaw cycles before use. Chromatography was carried out using Fluorochem Silicagel LC60A (40-63 micron).

C,H and N elemental analysis was collected with an Exeter Analytical CE-440 Elemental Analyser. Infra-red spectra were recorded on a Perkin Elmer Spectrum RX1 fitted with an ATR attachment.

Crystallographic data was recorded with a Rigaku R-Axis SPIDER IP diffractometer equipped with Cryostream (Oxford Cryosystems) low-temperature device at 120 K with graphite-monochromated MoK_{alpha}-radiation (λ = 0.71073 Å).

Melting points were measured with a Gallenkamp apparatus at atmospheric pressure and are uncorrected.

***1a**, 9-phenylanthracene*

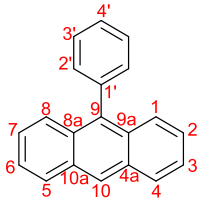

In a microwave vial 9-bromoanthracene (0.131 g, 0.509 mmol), phenyl boronic acid (0.128 g, 1.069 mmol), potassium t-butoxide (0.118 g, 1.069 mmol) and $Pd(PPh_3)_4$ (65 mg, 0.056 mmol) in degassed dioxane (5 ml) were heated to 110 °C under inert atmosphere in a Biotage microwave for 1 hr. The reaction mixture was diluted with ethyl acetate/ hexane (3:7), filtered through silica gel and the filtrate evaporated to dryness. Recrystallization gave 9-phenylanthracene (0.0211 g, 17%) as yellow crystals; MP 154 - 155 °C (hexane, lit;[22] 153 – 154 °C); Anal. Calcd for $C_{20}H_{14}$: C, 94.45; H, 5.55. Found: C, 94.46; H, 5.58; IR ν_{max} / cm^{-1} 3050, 1596, 1494, 1443, 1410, 1357, 1160; ^{1}H NMR (700 MHz, $CDCl_3$) δ 8.51 (1H, s, **10**), 8.06 (2H, d, *J* 8.4, **1/8**), 7.68 (2H, d, *J* 8.8, **4/5**), 7.59 (2H, dd, *J* 1.2, 4.3, **3'**), 7.54 (1H, t, *J* 6.9, **4'**), 7.49 – 7.43 (4H, m, **2'/2/7**), 7.38 – 7.34 (2H, m, **3/6**); ^{13}C NMR (176 MHz, $CDCl_3$) δ 138.93 (**1'**), 137.18 (**9**), 131.51 (**8a/9a**), 131.38 (**2'**), 130.35 (**4a/10a**), 128.49 (**3'**), 128.46 (**1/8**), 127.58 (**4'**), 126.98 (**4/5**), 126.68 (**10**), 125.45 (**3/6**), 125.23 (**2/7**); MS (GCMS) *m/z*: 254 (M^+, 100%), 126 (53), 113 (42).

1b, *9-(2-fluorophenyl)anthracene*

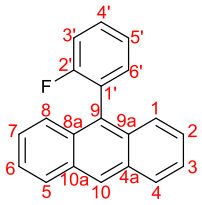

In a microwave vial 9-bromoanthracene (0.127 g, 0.495 mmol), 2-fluorophenyl boronic acid (0.287 g, 2.09 mmol), potassium t-butoxide (0.181 g, 1.634 mmol) and $Pd(PPh_3)_4$ (103 mg, 0.0891mmol) in degassed dioxane (5 ml) were heated to 110 °C under inert atmosphere in a Biotage microwave for 1 hr. The reaction mixture was diluted with ethyl acetate/ hexane (3:7), filtered through silica gel and and the filtrate evaporated to dryness. Recrystallization gave 9-(2-fluorophenyl)anthracene (0.0587 g, 43%) as yellow crystals; MP 153.5 °C (hexane, lit;[7] 143 – 144 °C); Anal. Calcd for $C_{20}H_{13}F$: C, 88.21; H, 4.81. Found: C, 87.91; H, 4.96; IR ν_{max} /cm^{-1} 3085, 2360, 1684, 1558, 1506, 1494, 1480, 1442; ^{1}H (700 MHz, $CDCl_3$) δ 8.57 (1H, s, **10**), 8.10 (2H, d, *J* 8.4, **1/8**), 7.70 (2H, d, *J* 8.7, **4/5**), 7.61 – 7.55 (1H, m, **4'**), 7.53 – 7.49 (2H, m, **2/7**), 7.46 – 7.42 (3H, m, **3/6/6'**), 7.42 – 7.36 (2H, m, **3'/5'**); ^{13}C (176 MHz, $CDCl_3$) δ 160.91 (d, $^1J_{CF}$ 246, **2'**), 133.57 (d, $^3J_{CF}$ 3.5, **6'**), 131.50 (**4a/10a**), 130.56 (**8a/9a**), 130.34 (**9**), 129.99 (d, $^3J_{CF}$ 8, **4'**), 128.65 (**1/8**), 127.58 (**10**), 126.31 (**4/5**), 126.08 (d, $^2J_{CF}$ 17.4, **1'**), 125.93 (**3/6**), 125.30 (**2/7**), 124.30 (d, *J* 4, **5'**), 116.03 (d, $^2J_{CF}$ 22, **3'**); ^{19}F (658 MHz, $CDCl_3$) δ -113.73 – -113.81 (m); MS (GCMS) *m/z*: 272 (M^+, 100%), 250(41), 135(57), 125(48).

1c, *9-(3-fluorophenyl)anthracene*

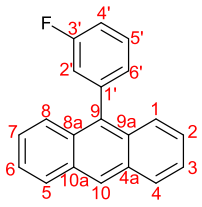

In a microwave vial 9-bromoanthracene (0.129 g, 0.500 mmol), 3-fluorophenyl boronic acid (0.147 g, 1.05 mmol), potassium t-butoxide (0.127 g, 1.15 mmol) and $Pd(PPh_3)_4$ (0.0667 g, 0.06 mmol) in degassed dioxane (5 ml) were heated to 110 °C under inert atmosphere in a Biotage microwave for 1 hr. The reaction mixture was diluted with ethyl acetate/ hexane (3:7), filtered through silica gel and the filtrate evaporated to dryness. Recrystallization gave 9-(3-fluorophenyl)anthracene (0.0506 g, 37%) as yellow crystals; MP 147-152 °C (hexane, lit;[23] 143.5 – 144.5 °C); Anal. Calcd for $C_{20}H_{13}F$: C, 88.21; H, 4.81. Found: C, 88.22; H, 4.85; IR ν_{max} /cm^{-1} 3048, 1611, 1581, 1492, 1477, 1420; ^{1}H NMR (700 MHz, CDCl3) δ 8.52 (1H, s, **10**), 8.06 (2H, d, *J* 8.5, **1/8**), 7.64 (2H, d, *J* 8.8, **4/5**), 7.55 (1H, dd, *J* 14.1, 7.8, **5'**), 7.49 – 7.45 (2H, m, **2/7**), 7.38 (2H, dd, *J* 8.1, 7.1, **3/6**), 7.23 (2H, m, **4'/6'**), 7.17 (1H, dd, *J* 9.4, 1.3, **2'**); ^{13}C NMR (176 MHz, $CDCl_3$) δ 163.02 (d, $^1J_{CF}$ 247, **3'**), 141.23 (d, $^3J_{CF}$ 8, **1'**), 135.54 (**9**), 131.44 (**9a**), 130.15 (**4a**), 130.06 (d, $^3J_{CF}$ 8, **5'**), 128.55 (**1/8**), 127.22 (d, $^3J_{CF}$ 2.9, **6'**), 127.16 (**10**), 126.57 (**4/5**), 125.78 (**3/6**), 125.32 (**2/7**), 118.45 (d, $^2J_{CF}$ 21, **2'**), 114.62 (d, $^2J_{CF}$ 21, **4'**); ^{19}F (658 MHz, $CDCl_3$) δ -113.92 (td, *J* 9.0, 6.1); MS (GCMS) m/z: 272 (M^+, 100%), 250 (23), 135 (90), 122 (42).

1d, *9-(4-fluorophenyl)anthracene*

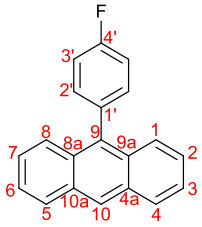

In a microwave vial 9-bromoanthracene (0.142 g, 0.554 mmol), 4-fluorophenyl boronic acid (0.146 g, 1.05 mmol), potassium t-butoxide (0.113 g, 0.997 mmol) and $Pd(PPh_3)_4$ (0.0601 g, 0.056mmol) in degassed dioxane (5 ml) were heated to 110 °C under inert atmosphere in a Biotage microwave for 1 hr. The reaction mixture was diluted with ethyl acetate/ hexane (3:7), filtered through silica gel and the filtrate evaporated to dryness. Recrystallization gave 9-(4-fluorophenyl)anthracene (0.0529 g, 40%) as yellow crystals; MP 174-175 °C (hexane, lit;[24] 168.5 – 169.5 °C); Anal. Calcd for $C_{20}H_{13}F$: C, 88.21; H, 4.81. Found: C, 87.67; H, 4.97; IR ν_{max} /cm^{-1} 3050(w), 1621(w), 1439(m). ^{1}H (700 MHz, $CDCl_3$) δ 8.51 (1H, s, **10**), 8.05 (2H, d, *J* 8.5, **1/8**), 7.63 (2H, d, *J* 8.8, **4/5**), 7.49 – 7.45 (2H, m, **2/7**), 7.42 – 7.38 (2H, m, **2'**), 7.38 – 7.35 (2H, m, **3/6**), 7.28 (2H, t, *J* 8.5, **3'**); ^{13}C (176 MHz, $CDCl_3$) δ 162.53 (d, $^1J_{CF}$ 246, **4'**), 135.92 (**9**), 134.71 (d, $^3J_{CF}$ 3, **1'**), 132.95 (d, $^3J_{CF}$ 8, **2'**),

131.49 (**8a/9a**), 130.51 (**4a/10a**), 128.55 (**1/8**), 126.96 (**10**), 126.68 (**4/5**), 125.66 (**3/6**), 125.28 (**2/7**), 115.56 (d, $^{2}J_{CF}$ 21, **3'**); ^{19}F (188 MHz, $CDCl_3$) δ -115.57 (tt, *J* 8.7, 5.6); MS (GCMS) *m/z*: 272 (M^+, 100%), 250 (22), 135 (57), 122 (40).

***1e**, 9-(3,4-difluorophenyl)anthracene*

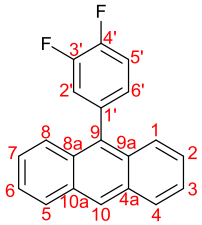

Potassium trifluoroborate salt **6e** (0.2664 g, 1.216 mmol), 9-dibromoanthracene (0.257 g, 1.00 mmol), K_2CO_3 (0.542 g, 3.6 mmol) and $PdCl_2$(dppf).DCM (0.0198 g, 0.0244 mmol) in degassed dioxane (8 ml) and H_2O (0.5 ml) were heated to reflux for 48 h. The solution was diluted with H_2O, and extracted with toluene. The organics were combined, washed and dried ($MgSO_4$), and filtered through celite. The solution was evaporated to dryness and the solid dissolved in ethyl acetate and the solution taken through silica gel before purification by chromatography (silica, hexane, ethyl acetate, toluene 2:2:1) and evaporated to give 9-(3,4-difluorophenyl)anthracene (0.158 g, 54%) as a yellow solid; MP 91.4 °C (hexane); Anal. Calcd for $C_{20}H_{12}F_2$: 82.75; H, 4.17. Found: C, 82.53; H, 4.18; IR ν_{max} /cm^{-1} 3054, 2364, 1602, 1511, 1482; ^{1}H NMR (700 MHz, $CDCl_3$) δ 8.52 (1H, s, **10**), 8.06 (2H, d, *J* 8.5, **4/5**), 7.63 (2H, d, *J* 8.8, **1/8**), 7.48 (2H, dd, *J* 11.2, 3.7, **2/7**), 7.43 – 7.36 (3H, m, **3/6/6'**), 7.30 – 7.26 (1H, m, **2'**), 7.19 – 7.13 (1H, m, **5'**); ^{13}C NMR (176 MHz, $CDCl_3$) δ 150.84 (dd, $^{1}J_{CF}$ 64, $^{2}J_{CF}$ 13, **3'**), 149.43 (dd, $^{1}J_{CF}$ 63, $^{2}J_{CF}$ 13, **4'**), 135.62 (dd, $^{3}J_{CF}$ 6, $^{3}J_{CF}$ 4, **1'**), 134.34 (**9**), 131.25 (**8a/9a**), 130.12 (**4a/10a**), 128.46 (**4/5**), 127.43 (dd, $^{3}J_{CF}$ 6, $^{3}J_{CF}$ 4, **5'**), 127.26 (**10**), 126.13 (**1/8**), 125.81 (**3/6**), 125.20 (**2/7**), 120.27 (d, $^{2}J_{CF}$ 17, **2'**), 117.33 (d, $^{2}J_{CF}$ 17, **6'**); ^{19}F NMR (658 MHz, $CDCl_3$) δ -144.78 – -144.91 (1F, **4'**), -146.43 – -146.55 (1F, **3'**); MS (ASAP$^+$) *m/z*: 290 (M^+, 100%).

***1f**, 9-(3,4,5-trifluorophenyl)anthracene*

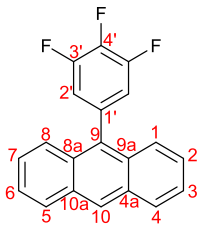

Potassium trifluoroborate salt **6f** (0.405 g, 1.70 mmol), 9-dibromoanthracene (0.341 g, 1.33 mmol) and $PdCl_2$(dppf).DCM (0.0211g, 0.034 mmol) in degassed dioxane (10 ml) and Bu_4NOH (5 ml 0.5 M) were heated to reflux for 72 h. The solution was concentrated, filtered and washed with H_2O, and the solid purified by column chromatography (silica, hexane: toluene: ethyl acetate 2:1:1) and

evaporated to give 9-(3,4,5-trifluorophenyl)anthracene (0.677 g, 22%) as a yellow solid; MP = 122 °C (hexane); IR ν_{max} /cm^{-1} 3049(w), 1609(m), 1521(s), 1417(m), 1379(m), 1235(m); ^{1}H NMR (700 MHz, $CDCl_3$) δ 8.53 (1H, s, **10**), 8.07 (2H, d, *J* 8.4, **1/8**), 7.63 (2H, d, *J* 8.7, **4/5**), 7.51 (2H, dd, *J* 14.0, 5.6, **2/7**), 7.44 (2H, dd, **3/6**), 7.09 (2H, t, *J* 7.0, **2'**); ^{13}C NMR (176 MHz, $CDCl_3$) δ 151.42 (ddd, $^{1}J_{CF}$ 251, $^{2}J_{CF}$ 10, $^{2}J_{CF}$ 4, **4'**), 139.52 (dt, $^{1}J_{CF}$ 252, $^{2}J_{CF}$ 15, **3'**), 135.01 (dd, $^{3}J_{CF}$ 13, $^{3}J_{CF}$ 8, **1'**), 133.32 (**9**), 131.32 (**4a/10a**), 130.02 (**8a/9a**), 128.70 (**1/8**), 127.84 (**10**), 126.27 (**3/6**), 125.88 (**4/5**), 125.42 (**2/7**), 115.68 (dd, $^{2}J_{CF}$ 16, 4, **2'**); ^{19}F NMR (658 MHz, $CDCl_3$) δ -141.42 (2F, dd, $^{1}J_{CF}$ 21, $^{2}J_{CF}$ 8, **3'**), -168.77 (1F, tt, $^{1}J_{CF}$ 21, $^{2}J_{CF}$ 7, **4'**); MS (GCMS) *m/z*: 308 (M^+, 100%), 288 (56), 144 (50), 128 (35); HRMS (TOF ASAP$^+$), Calcd for $[C_{20}H_{11}F_3]^+$: 308.0402, found *m/z*: 308.0408.

1g *9-(perfluorophenyl)anthracene*

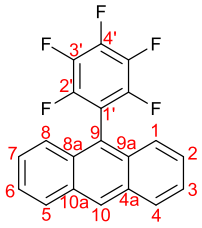

9-bromoanthracene (1.28 g, 4.9 mmol) in dry, degassed THF (30 ml) was cooled to -78 °C and ^{n}BuLi in hexanes (5.5 mmol) added dropwise over 15 min. After stirring at -78 °C for 2 h hexafluorobenzene (1.86 g, 1.2 ml, 10 mmol) was added over 10 s and the resulting solution stirred overnight to room temperature, heated to 40 °C for 2 h then allowed to cool. Following quenching with water the organic portion extracted with DCM, washed with water and brine, dried ($MgSO_4$) and evaporated to give the crude product as a white solid. Recrystallization from hexane, then methanol gave 9-(perfluorophenyl)anthracene (0.103 g, 6 %) as white crystals; MP 166 °C (hexanes); Anal. Calcd for $C_{20}H_9F_5$: C, 69.77; H, 2.63. Found: C, 69.79; H, 2.66; IR ν_{max} /cm^{-1} 2356, 1684, 1648, 1636, 1559, 1540, 1522; ^{1}H NMR (400 MHz, $CDCl_3$) δ 8.53 (1H, s, **10**), 7.99 (2H, d, *J* 8.0, **1/8**), 7.42 (6H, m, **2/3/4/5/6/7**); ^{19}F NMR (376 MHz, $CDCl_3$) δ -137.98 (2F, dd, $^{1}J_{CF}$ 22.9, $^{2}J_{CF}$ 7.9, **2'**), -153.59 (1F, t, $^{1}J_{CF}$ 20.9, **4'**), -161.21 – -161.47 (2F, m, **3'**); ^{13}C NMR (101 MHz, $CDCl_3$) δ 147.06 –138.06 (overlapping multiplets), 131.44, 130.74, 129.64, 129.09, 127.20, 125.65, 124.80; MS (ASAP$^+$) *m/z*: 344 (M^+, 100%).

1h, *9-(2,3,5,6-tetrafluoro-4-(trifluoromethyl)phenyl)anthracene*

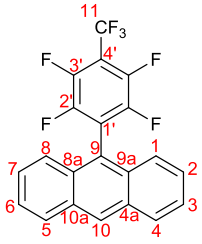

9-bromoanthracene (1.30 g, 5.0 mmol) in dry, degassed THF (30 ml) was cooled to -78 °C and ^{n}BuLi in hexanes (5.5 mmol) added dropwise over 15 min. After stirring at -78 °C for 2 h octafluorotoluene (2.36 g, 1.4 ml, 10 mmol) was added over 10 s and the resulting solution stirred overnight to room temperature, heated to 40 °C for 2 h then allowed to cool. Following quenching with water the organic portion extracted with DCM, washed with water and brine, dried ($MgSO_4$) and evaporated to give the crude product as a white solid. Recrystallization gave 9-(2,3,5,6-tetrafluoro-4-(trifluoromethyl)phenyl)anthracene (1.11 g, 56 %) as white crystals; MP 180-181 °C (hexane); Anal. Calcd for $C_{20}H_9F_7$: C, 63.97; H, 2.30. Found C, 63.76; H, 2.40; IR ν_{max} /cm^{-1} 3056, 1658, 1626, 16005, 15265, 1472; ^{1}H NMR (700 MHz, $CDCl_3$) δ 8.66 (1H, s, **10**), 8.14 – 8.10 (2H, d, *J* 7.9, **1/8**), 7.57 – 7.49 (6H, m, **2/3/4/5/6/7**); ^{13}C NMR (176 MHz, $CDCl_3$) δ 145.26 (ddt, $^1J_{CF}$ 249, $^2J_{CF}$ 13, $^3J_{CF}$ 3, **2'**), 144.53 (dd, *J* $^1J_{CF}$ 261, $^2J_{CF}$ 16, **3'**), 131.37 (**8a/9a**), 130.22 (**4a/10a**), 130.10 (**10**), 129.18 (**1/8**), 127.50 (**2/7**), 125.76 (**3/6**), 124.52 (**4/5**), 122.51 (t, *J* 20, **4'**), 121.14 (d, *J* 275, **1'**), 119.26 (**9**), 110.04 (dt, *J* $^1J_{CF}$ 35, $^3J_{CF}$ 13, **11**); ^{19}F NMR (658 MHz, $CDCl_3$) δ -63.12 (3F, t, $^1J_{CF}$ 22, **11**), -143.03 (2F, d, $^1J_{CF}$ 10, **2'**), -146.89 – -147.08 (2F, m, **3'**); MS (GCMS) *m/z*: 394 (M$^+$, 100%), 374 (77), 324 (75), 306 (69), 286 (25), 162 (47).

2a, *9,10-diphenylanthracene*

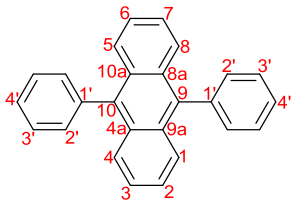

A solution of phenylboronic acid (0.306 g, 2.506 mmol), 9,10-dibromoanthracene (0.337 g, 1.003 mmol), and $PdCl_2$(dppf).DCM (0.0181 g, 0.025 mmol) in degassed dioxane (10 ml) and Bu_4NOH (5 ml 1M) were heated to reflux for 72 h. The solution was concentrated and filtered, the solid washed with H_2O then methanol. Recrystallizatopm gave 9,10-diphenylanthracene (0.110 g, 34%) as yellow crystals; MP 248-251 °C (acetonitrile, lit;[25] 245 – 247 °C); Anal. Calcd for $C_{26}H_{18}$: C, 94.51; H 5.49. Found: C, 94.38; H 5.69; IR ν_{max} /cm^{-1} 3065, 1444, 1388, 1162, 1073; ^{1}H NMR (700 MHz, $CDCl_3$) δ 7.72 (4H, dd, *J* 6.8,3.3, **1/4/5/8**), 7.62 (4H, d, *J* 14.7, **3'**), 7.57 (2H, t, *J* 7.5, **4'**), 7.51 (4H, d, *J* 6.8, **2'**), 7.35 (4H, dd, *J* 6.9,3.2, **2/3/6/7**); ^{13}C NMR (176 MHz, $CDCl_3$) δ 139.24 (**1'**), 137.26 (**9**), 131.47 (**2'**), 130.03 (**4a/8a/9a/10a**), 128.55 (**3'**), 127.60 (**4'**), 127.11 (**1/4/5/8**), 125.13 (**2/3/6/7**); MS (GCMS) *m/z*: 330 (M$^+$, 100%), 252 (71), 156 (60).

***2c**, 9,10-di(3-fluorophenyl)anthracene*

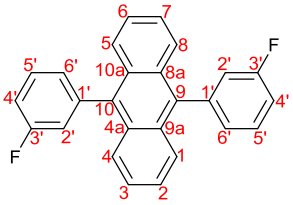

A solution of 3-fluorophenylboronic acid (0.183 g, 1.329 mmol), 9,10-dibromoanthracene (0.197 g, 0.585 mmol), and $PdCl_2$(dppf).DCM (0.0302 g, 0.0234 mmol) in degassed dioxane (10 ml) and Bu_4NOH (2 ml 1M) were microwave heated to 95 °C 2 hr. The solution was diluted with H_2O, extracted with toluene, and the organics washed, filtered through celite and through silica gel before evaporation to dryness. Recrystallization gave 9,10-di-(3-fluorophenyl)anthracene (0.116 g, 54 %) as yellow crystals; MP 247-248 °C (methanol, lit;[26] 240 °C); Anal. Calcd for $C_{26}H_{16}F_2$: C, 85.23; H, 4.40. Found: C, 85.13; H, 4.45; IR ν_{max} /cm^{-1} 2922, 2354, 1610, 1580, 1435, 1387, 1224; ^{1}H NMR (500 MHz, $CDCl_3$) δ 7.67 (4H, dd, *J* 6.8,3.3, **1/4/5/8**), 7.61 – 7.55 (2H, m, **5'**), 7.37 (4H, dd, *J* 6.9,3.2, **2/3/6/7**), 7.29 – 7.24 (5H, m, **4'/5'**), 7.21 (2H, d, *J* 9.4, **2'**); ^{13}C NMR (126 MHz, $CDCl_3$) δ 163.06 (d, $^1J_{CF}$ 247, **3'**), 141.35 (d, $^3J_{CF}$ 8, **1'**), 136.09 (**9**), 130.16 (dd, $^3J_{CF}$ 8, 2, **5'**), 129.78 (**4a/8a/9a/10a**), 127.25 (**6'**), 126.80 (**1/4/5/8**), 125.54 (**2/3/6/7**), 118.50 (dd, $^2J_{CF}$ 21, 3, **2'**), 114.74 (d, $^2J_{CF}$ 21, **4'**); ^{19}F NMR (658 MHz, $CDCl_3$) δ -113.27 (dtd, $^1J_{CF}$ 28, $^2J_{CF}$ 9, $^2J_{CF}$ 6, **3'**); MS (ASAP$^+$) *m/z*: 366 (M^+, 100%).

***2d**, 9,10-bis(4-fluorophenyl)anthracene*

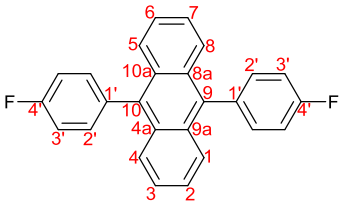

A solution of 4-fluorophenylboronic acid (0.385 g, 2.748 mmol), 9,10-dibromoanthracene (0.3618 g, 1.077 mmol), and $PdCl_2$(dppf).DCM (0.0230 g, 0.011 mmol) in degassed dioxane (8 ml) and Bu_4NOH (5 ml 1M) were heated to reflux for 72 h. The solution was concentrated and filtered, the solid washed with H_2O then methanol, and dissolved in toluene which was taken through a silica gel. The solution was evaporated to dryness to give 9,10-di-(4-fluorophenyl)anthracene (0.729 g, 73%) as a yellow solid; MP 305-306 °C (toluene, lit;[27] 303-304 °C); Anal. Calcd for $C_{26}H_{16}F_2$: C, 85.23; H, 4.40. Found: C, 85.50; H, 4.48; IR ν_{max} /cm^{-1} 2356, 1602, 1506, 1392, 1218; ^{1}H NMR (700 MHz, $CDCl_3$) δ 7.67 (4H, d, *J* 10.1, **1/4/5/8**), 7.44 (4H, dd, *J* 8.5,5.5, **2'**), 7.36 (4H, dd, *J* 6.9,3.2, **2/3/6/7**), 7.31 (4H, t, *J* 8.7, **3'**); ^{13}C NMR (176 MHz, $CDCl_3$) δ 162.56 (d, $^1J_{CF}$ 247, **4'**), 136.30 (**9**), 134.89 (d, *J* 3, **1'**), 133.00 (d, $^3J_{CF}$ 8, **2'**), 130.19 (**4a/8a/9a/10a**), 126.91 (**1/4/5/8**),

125.38 (**2/3/6/7**), 115.64 (d, $^{2}J_{CF}$ 21, **3'**); ^{19}F NMR (658 MHz, $CDCl_3$) δ -121.91 (tt, $^{1}J_{CF}$ 9, $^{2}J_{CF}$ 6, **4'**), MS (ASAP^{+}) *m/z*: 366 (M^{+}, 100%).

***2e**, 9,10-bis(3,4-difluorophenyl)anthracene*

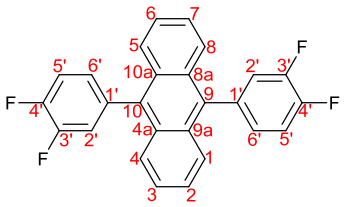

A solution of 3,4-difluorophenylboronic acid (0.403 g, 2.55 mmol), 9,10-dibromoanthracene (0.336 g, 1.00 mmol) and $PdCl_2$(dppf).DCM (0.022 g, 0.01 mmol) in degassed dioxane (10 ml) and Bu_4NOH (4 ml, 1M) were heated to reflux for 72 h. The solution was concentrated and filtered, the solid washed with H_2O then methanol. Recrystallization gave 9,10-bis(3,4-difluorophenyl)anthracene (0.0680 g, 17 %) as yellow crystals; MP 310-311 °C (acetonitrile); Anal. Calcd for $C_{26}H_{14}F_4$: C, 77.61; H, 3.51. Found: C, 77.94; H, 3.51; IR νmax /cm^{-1} 2981, 1601, 1516, 1421, 1271; ^{1}H NMR (700 MHz, $CDCl_3$) δ 7.66 (4H, dd, *J* 6.8, 3.3, **1/4/5/8**), 7.44 – 7.37 (6H, m, **5'/2/3/6/7**), 7.31 (2H, ddt, *J* 10.1,7.6,2.2, **2'**), 7.22 – 7.18 (2H, m, **6'**); ^{13}C NMR (176 MHz, $CDCl_3$) δ 151.10 (dd, $^{1}J_{CF}$ 59, $^{2}J_{CF}$ 13, **3'**), 149.68 (dd, $^{1}J_{CF}$ 58, $^{2}J_{CF}$ 13, **4'**), 135.80 (dd, $^{3}J_{CF}$ 6, $^{4}J_{CF}$ 5, **1'**), 135.37 (**9**), 129.93 (**4a/8a/9a/10a**), 127.60 (dd, $^{3}J_{CF}$ 9, $^{4}J_{CF}$ 6, **6'**), 126.63 (**1/4/5/8**), 125.79 (**2/3/6/7**), 120.47 (dd, $^{2}J_{CF}$ 17, $^{3}J_{CF}$ 5, **2'**), 117.64 (dd, $^{2}J_{CF}$ 17, $^{3}J_{CF}$ 3, **5'**); ^{19}F NMR (658 MHz, $CDCl_3$) δ -144.53 – -144.68 (1F, m, **4'**), -146.10 – -146.25 (1F, m, **3'**); MS (ASAP^{+}) *m/z*: 402 (M^{+}, 100%).

***2f**, 9,10-bis(3,4,5-trifluorophenyl)anthracene*

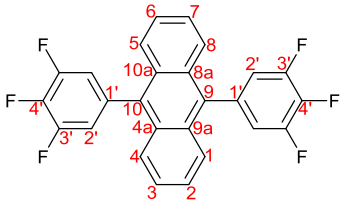

A solution of potassium trifluoroborate salt **6f** (0.513 g, 2.16 mmol), 9,10-dibromoanthracene (0.317 g, 0.943 mmol), Bu_4NBr (0.756 g, 2.34 mmol) and $PdCl_2$(dppf).DCM (0.145 g, 0.178 mmol) in degassed dioxane (8 ml) and NEt_3 (2 ml) were heated to reflux for 68 h. The solution was diluted with H_2O, and extracted with DCM. The organics were combined, washed and dried ($MgSO_4$), and filtered through celite. The solution was taken to dryness yielding a yellow solid, which was dissolved in Ethyl Acetate and the solution taken through silica gel. The product was purified by chromatography (silica, toluene) and recrystallized from methanol then acetonitrile to give 9,10-bis(3,4,5-trifluorophenyl)anthracene (0.0525 g, 13%) as yellow needles; MP 287-290 °C (acetonitrile); IR ν_{max} /cm^{-1} 3072, 2918, 2357, 1615, 1530, 1414; ^{1}H NMR (700 MHz, $CDCl_3$) δ

7.64 (4H, dd, *J* 6.7,3.2, **1/4/5/8**), 7.43 (4H, dd, *J* 6.9,3.1, **2/3/6/7**), 7.11 (4H, t, *J* 6.9, **2'**); ^{13}C NMR (176 MHz, $CDCl_3$) δ 151.53 (ddd, $^1J_{CF}$ 252, $^2J_{CF}$ 10, $^3J_{CF}$ 4, **4'**), 139.69 (dt, $^1J_{CF}$ 253, $^2J_{CF}$ 15, **3'**), 134.93 – 134.75 (m, **1'**), 134.64 (**9**), 129.65 (**4a/8a/9a/10a**), 126.36 (**1/4/5/8**), 126.19 (**2/3/6/7**), 115.69 (d, $^2J_{CF}$ 16, **2'**); ^{19}F NMR (658 MHz, $CDCl_3$) δ -134.07 (2F, dd, $^1J_{CF}$ 20, $^2J_{CF}$ 8, **3'**), -161.30 (1F, tt, $^1J_{CF}$ 20, $^2J_{CF}$ 6, **4'**); MS (ASAP$^+$) *m/z*: 438 (M$^+$, 100%). HRMS (TOF ASAP$^+$), Calcd for $[C_{26}H_{12}F_6]^+$: 438.0843. Found *m/z*: 438.0826.

2g, *9,10-bis(perfluorophenyl)anthracene*

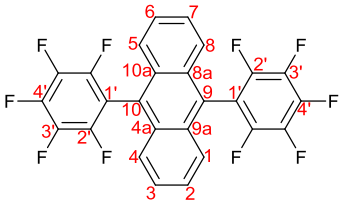

9,10-dibromoanthracene (1.728 g, 5.1 mmol) in dry, degassed THF (30 ml) was cooled to -78 °C and ^{n}BuLi in hexanes (12.0 mmol) added dropwise over 15 min. After stirring at -78 °C for 2 h hexafluorobenzene (3.721 g, 20.0 mmol 2.32 ml) was added over 10 s and the resulting solution stirred overnight to room temperature, heated to 40 °C for 2 h then allowed to cool. Following quenching with water the organic portion was extracted with DCM, washed with water and brine, dried ($MgSO_4$) and evaporated to dryness to give the crude product as a white solid. Recrystallization gave 9,10-bis(perfluorophenyl)anthracene (0.2845 g, 10 %) as white crystals; MP >250 °C (hexanes, lit;[28] 319.8 - 320.2 °C); ^{1}H NMR (400 MHz, $CDCl_3$) 7.80 – 7.50 (8 H, m). ^{19}F NMR (188 MHz, $CDCl_3$) δ -137.55 – -138.36 (4F, m, **2'**), -153.12 (2F, t, $^1J_{CF}$ 21.0, **4'**), -160.83 – -161.49 (4F, m, **3'**); ^{13}C NMR (101 MHz, $CDCl_3$) 160 – 140 (overlapping multiplets) 130.33, 128.73, 128.62, 127.22, 127.14, 125.45, 125.09; MS (ASAP$^+$) *m/z*: 610 (M$^+$, 100%).

2h, *9,10-bis(2,3,5,6-tetrafluoro-4-(trifluoromethyl)phenyl)anthracene*

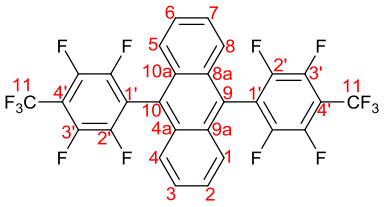

^{t}Butyl-lithium (1.7 M in hexane, 4 ml, 6.8 mmol) was added dropwise over 15 minutes to a stirring solution of 9,10-dibromoanthracene (0.704 g, 2.01 mmol) at −78 °C. Following 1 h stirring at −78 °C octafluorotoluene (1 ml, 1.66 g, 7.06 mmol) was added over 1 min. This solution was stirred to room temperature overnight, then heated at 60 °C for 3 h. Upon quenching with water the organics were extracted with toluene, washed with water and brine before drying with $MgSO_4$ and removal of the solvent under reduced pressure giving the crude product in 88% yield. This was purified by

column chromatography (hexane : acetone 9:1). Recrystallization gave 9,10-bis(2,3,5,6-tetrafluoro-4-(trifluoromethyl)phenyl)anthracene (0.120 g, 22%) as yellow crystals; MP = 270 °C (methanol / ethyl acetate); Anal. Calcd for $C_{28}H_8F_{14}$: C, 55.10; H, 1.32. Found: C, 55.108; H, 1.37; IR ν_{max} /cm^{-1} 1656(w), 1471(s), 1214(m), 1157(vs); ^{1}H NMR (700 MHz, $CDCl_3$) δ 7.61 (4H, m, **1/4/5/8**), 7.58 (4H, m, **2/3/6/7**); ^{13}C NMR (176 MHz, $CDCl_3$) δ 145.65 (dm, $^1J_{CF}$ 92), 144.17 (dm, $^1J_{CF}$ 95), 129.88, 127.69, 125.41, 122.99, 121.81 (t, $^2J_{CF}$ 20), 120.24, 110.51; ^{19}F NMR (658 MHz, $CDCl_3$) δ -63.15 (t, $^1J_{CF}$ 22), -142.59 (dd, $^1J_{CF}$ 21, $^2J_{CF}$ 11), -146.33 (m); MS (ASAP$^+$) m/z: 610 (60%, M$^+$), 611 (M$^+$+1, 100%), 612 (M$^+$+2, 55%,); HRMS (TOF ASAP$^+$), Calcd for $[C_{28}H_8F_{14}]^+$: 610.0402, found *m/z*: 610.0418.

6d, *Potassium (4-fluorophenyl) trifluoroborate*

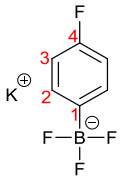

To a stirring solution of 4-fluorophenylboronic acid (1.99 g, 14.24 mmol) in methanol (30 ml) KHF_2 (3.27 g, 2.94 eq) in H_2O (2 ml) was added slowly and the resulting cloudy solution stirred at room temperature overnight. The reaction mixture was evaporated to dryness and acetone added. The resulting solution was heated at reflux then filtered, and the filtrate evaporated to dryness to give potassium (4-fluorophenyl) trifluoroborate (3.16 g, 99%) as a white solid; MP 275-280 °C (acetone, lit;[29] >260 °C); Found: C, 35.11; H, 1.91. $C_6H_4BF_4K$ requires C, 35.68; H, 2.00%; IR ν_{max} /cm^{-1} 1699, 1606, 1594, 1513, 1204; ^{1}H NMR (400 MHz, Acetone) δ 7.45 (2H, dd, *J* 8.1,6.7, **2**), 6.79 (2H, app t, **3**); ^{13}C NMR (101 MHz, Acetone) δ 133.03 – 131.59 (m, **4**), 112.20 (**3**), 112.01 (**2**); ^{19}F NMR (188 MHz, Acetone) δ -119.22 – -119.51 (**4**), -142.41 (**1**); ^{11}B NMR (128 MHz, Acetone) δ 3.70 (s, **1**).

6e, *Potassium (3,4-difluorophenyl)trifluoroborate*

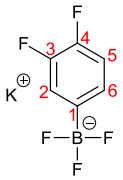

To a stirring solution of 3,4-difluorophenylboronic acid (1.01 g, 6.372 mmol) in methanol (20 ml) KHF_2 (2.0 g, 4 eq) in H_2O (2 ml) was added slowly and the resulting cloudy solution stirred at room temperature for 30 min. The white precipitate was collected by filtration, dried and then washed with hot acetone. The acetone filtrate was evaporated to dryness to give potassium (3,4-difluorophenyl)trifluoroborate (0.49 g, 35%) as a white solid; MP 259-262 °C (acetone); Found: C, 32.39; H, 1.37. $C_6H_3BF_5K$ requires C, 32.76; H, 1.37%; IR ν_{max} /cm^{-1} 2356, 1513, 1398, 1270,

1141; ^{1}H (400 MHz, Acetone) δ 7.31 – 7.16 (2H, m, **2/5**), 6.97 (1H, dtd, *J* 11.3,8.0,0.6, **6**); ^{13}C (101 MHz, Acetone) δ 204.52 (**1**), 149.04 (d, $^{1}J_{CF}$ 13, **4**), 146.64 (d, $^{1}J_{CF}$ 13, **3**), 126.66 – 126.46 (m, **2**), 118.53 (dd, $^{3}J_{CF}$ 13, $^{4}J_{CF}$ 2, **6**), 114.11 (d, $^{2}J_{CF}$ 16, **5**); ^{19}F (188 MHz, $CDCl_3$) δ -138.15 (3F, d, $^{1}J_{BF}$ 61, **B**), -139.61 (1F, ddd, $^{1}J_{CF}$ 20, $^{2}J_{CF}$ 11, $^{3}J_{CF}$ 9, **3**), -140.81 – -141.23 (1F, m, **4**); ^{11}B (128 MHz, Acetone) δ 3.14 (d, *J* 45.2, **1**).

6f, *Potassium (3,4,5-trifluorophenyl)trifluoroborate*

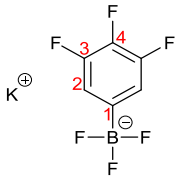

To a stirring solution of 3,4,5-trifluorophenylboronic acid (1.977 g, 11.24 mmol) in methanol (30 ml) KHF_2 (3.0 g, 3.4 eq) in H_2O (2 ml) was added slowly and the resulting cloudy solution stirred at room temperature for 1 hr. The reaction mixture was evaporated to dryness and acetone added. The resulting solution was heated at reflux then filtered, and the filtrate evaporated to dryness to give potassium (3,4,5-trifluorophenyl)trifluoroborate (2.8 g, 99%) as a white solid; MP 297-298 °C (acetone); IR ν_{max} /cm^{-1} 3364, 1608, 1594, 1514, 1396, 1208, 1160; Found: C, 29.91; H, 0.79. $C_6H_2BF_6K$ requires C, 30.28; H, 0.85%; ^{1}H (200 MHz, Acetone) δ 6.93 (t, *J* 8.2, **2**); ^{19}F (188 MHz, Acetone) δ -141.01 (2F, dd, *J* 19,9, **3**), -144.18 (3F, d, *J* 60, **B**), -169.40 (1F, tt, *J* 20,8, **4**), in agreement with literature.[30]

6g, *Potassium (pentafluorophenyl)Trifluoroborate*

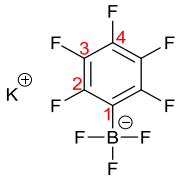

To a stirring solution of pentafluorophenylboronic acid (0.693 g, 3.27 mmol) in methanol (20 ml) KHF_2 (0.84 g, 3.29 eq) in H_2O (1 ml) was added slowly and the resulting cloudy solution stirred at room temperature overnight. The reaction mixture was evaporated to dryness and acetone added. The resulting solution was heated at reflux then filtered, and the filtrate taken to dryness yielding the product as a white solid (0.67 g, 75%). ^{19}F (188 MHz, Acetone) δ -135.19 (5F, m, **B/2**), -161.61 (t, *J* 19.6, **4**), -166.18 (m, **3**). In agreement with the literature.[30]

7a-b, *4-(pentafluorophenyl)toluene, 3-(pentafluorophenyl)toluene*

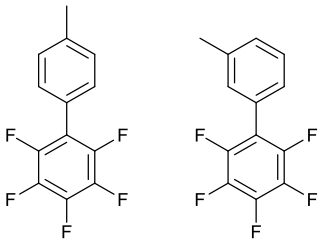

In radleys flask $Pd(OAc)_2$ (0.022 g, 10 mol%) and Ag_2CO_3 (0.289 g, 0.90 mmol) in 4 ml dry toluene (4 ml), $^{i}Pr_2S$ (0.09 ml, 0.6 mmol), HOAc (0.04 ml, 0.6 mmol) and pentafluorobenzene (0.07 ml, 0.6 mmol) under argon were heated to reflux for 48 hr. The solution was diluted with toluene (5 ml) and taken through a silica plug, the solution concentrated and purified by chromatography (petroleum ether /silica) yielding the product as a mix of isomers (0.0395 g, 0.153 mmol, 26%). ^{1}H NMR (700 MHz, $CDCl_3$) δ 7.31 (4H, m), 2.43 (3H, s). ^{13}C NMR (176 MHz, $cdcl_3$) δ 145.07 – 144.60 (m), 143.57 – 143.29 (m), 141.20 – 140.60 (m), 139.77 – 139.39 (m), 139.37, 138.45, 137.34 – 136.88 (m), 130.68, 130.03, 129.93, 129.41, 128.72, 128.55, 127.93, 127.85, 127.15, 126.76, 126.21, 125.74 – 125.48 (m), 124.23, 124.03, 123.33 (s). ^{19}F NMR (376 MHz, $CDCl_3$) δ -150.11 (2F, dd, $^{1}J_{CF}$ 23.0, $^{2}J_{CF}$ 8), -150.40 (2F, dd, $^{1}J_{CF}$ 23, $^{2}J_{CF}$ 8), -162.88 (2F, app t, $^{1}J_{CF}$ 21), -163.13 (2F, app t, $^{1}J_{CF}$ 21), -169.26 – -169.56 (m), in agreement with literature.[31]

(1) Merkel, P. B.; Dinnocenzo, J. P. Low-power green-to-blue and blue-to-UV upconversion in rigid polymer films. *J. Lumin.* **2009**, *129*, 303–306.

(2) Chen, H. C.; Hung, C. Y.; Wang, K. H.; September, W. S. F. D.; Chien, F. C.; Chen, P.; Chow, T. J.; Hsu, C. P.; Sun, S. S.; others White-light emission from an upconverted emission with an organic triplet sensitizer. *Chem. Commun.* **2009**, 4064–4066.

(3) Haefele, A.; Blumhoff, J.; Khnayzer, R. S.; Castellano, F. N. Getting to the (Square) Root of the Problem: How to Make Non-Coherent Pumped Upconversion Linear. *J. Phys. Chem. Lett.* **2012**, *3*, 299–303.

(4) Islangulov, R. R.; Kozlov, D. V.; Castellano, F. N. Low power upconversion using MLCT sensitizers. *Chem. Commun.* **2005**, *30*, 3776–3778.

(5) Islangulov, R. R.; Lott, J.; Weder, C.; Castellano, F. N. Noncoherent low-power upconversion in solid polymer films. *J. Am. Chem. Soc.* **2007**, *129*, 12652–12653.

(6) Baluschev, S.; Yakutkin, V.; Miteva, T.; Wegner, G.; Roberts, T.; Nelles, G.; Yasuda, A.; Chernov, S.; Aleshchenkov, S.; Cheprakov, A. A general approach for non-coherently excited annihilation up-conversion: transforming the solar-spectrum. *New J. Phys.* **2008**, *10*, 013007.

(7) Vingiello, F. A.; Spangler, M. O.; Bondurant, J. E. The Synthesis and Cyclization of Some 2'-Substituted 2-Benzylbenzophenones. *J. Org. Chem.* **1960**, *25*, 2091–2094.

(8) Smet, M.; Van Dijk, J.; Dehaen, W. An improved synthesis of substituted rubicenes providing access to heterocyclic rubicene analogues. *Synlett* **1999**, *4*, 495–497.

(9) Smet, M.; Van Dijk, J.; Dehaen, W. A novel acid-catalyzed rearrangement of 9, 10-diaryl-9, 10-dihydroanthracene-9, 10-diols affording 10, 10′-diaryl-9-anthrones. *Tetrahedron* **1999**, *55*, 7859–7874.

(10) Kuivila, H. G.; Reuwer Jr, J. F.; Mangravite, J. A. Electrophilic Displacement Reactions: XV. Kinetics and Mechanism of the Base-Catalyzed Protodeboronation of Areneboronic Acids. *Can. J. Chem.* **1963**, *41*, 3081–3090.

(11) Kuivila, H. G.; Reuwer, J. F.; Mangravite, J. A. Electrophilic Displacement Reactions. XVI. Metal Ion Catalysis in the Protodeboronation of Areneboronic Acids1-3. *J. Am. Chem. Soc.* **1964**, *86*, 2666–2670.

(12) Nahabedian, K.; Kuivila, H. G. Electrophilic Displacement Reactions. XII. Substituent Effects in the Protodeboronation of Areneboronic Acids1-3. *J. Am. Chem. Soc.* **1961**, *83*, 2167–2174.

(13) Kuivila, H. G.; Nahabedian, K. Electrophilic Displacement Reactions. X. General Acid Catalysis in the Protodeboronation of Areneboronic Acids1-3. *J. Am. Chem. Soc.* **1961**, *83*, 2159–2163.

(14) Kuivila, H. G.; Nahabedian, K. Electrophilic Displacement Reactions. XI. Solvent Isotope Effects in the Protodeboronation of Areneboronic Acids1-3. *J. Am. Chem. Soc.* **1961**, *83*, 2164–2166.

(15) Chambers, R.; Clark, H.; Willis, C. Some Salts of Trifluoromethylfluoroboric Acid. *J. Am. Chem. Soc.* **1960**, *82*, 5298–5301.

(16) Vedejs, E.; Chapman, R.; Fields, S.; Lin, S.; Schrimpf, M. Conversion of arylboronic acids into potassium aryltrifluoroborates: Convenient precursors of arylboron difluoride lewis acids. *J. Org. Chem.* **1995**, *60*, 3020–3027.

(17) Molander, G. A.; Ellis, N. Organotrifluoroborates: Protected boronic acids that expand the versatility of the Suzuki coupling reaction. *Acc. Chem. Res.* **2007**, *40*, 275–286.

(18) Corain, B.; Longato, B.; Favero, G.; Ajo, D.; Pilloni, G.; Russo, U.; Kreissl, F. Heteropolymetallic complexes of 1, 1'-bis (diphenylphosphino) ferrocene (dppf). III: Comparative physicochemical properties of (dppf) . *Inorg. Chim. Acta* **1989**, *157*, 259–266.

(19) Filthaus, M.; Oppel, I. M.; Bettinger, H. F. Supramolecular structures and spontaneous resolution: the case of ortho-substituted phenylboronic acids. *Org. Biomol. Chem.* **2008**, *6*, 1201–7.

(20) Li, Z. H.; Wong, M. S.; Tao, Y.; D'Iorio, M. Synthesis and functional properties of strongly luminescent diphenylamino end-capped oligophenylenes. *J. Org. Chem.* **2004**, *69*, 921–927.

(21) Li, H.; Liu, J.; Sun, C.-L.; Li, B.-J.; Shi, Z.-J. Palladium-Catalyzed Cross-Coupling of Polyfluoroarenes with Simple Arenes. *Org. Lett.* **2010**, *13*, 276–279.

(22) Pereira, R.; Cvengrovs, J. Tröger's Base Derived Phosphanes for Suzuki-Miyaura and Buchwald-Hartwig Cross-Coupling Reactions. *Eur. J. Org. Chem.* **2013**, *20*, 4233–4237.

(23) Vingiello, F. A.; Oot, J. G. V.; Hannabass, H. H. The Synthesis and Cyclization of Some o-Benzylphenones1, 2. *J. Am. Chem. Soc.* **1952**, *74*, 4546–4548.

(24) Bradsher, C. K.; Vingiello, F. A. Aromatic Cyclodehydration. XXII. 1 The Mechanism of the Cyclization of o-Benzylphenones. III. *J. Am. Chem. Soc.* **1949**, *71*, 1434–1436.

(25) Bradsher, C. K.; Smith, E. S. Aromatic Cyclodehydration. X. 1 9-Alkyl-and 9-Aryl-10-phenylanthracenes. *J. Am. Chem. Soc.* **1943**, *65*, 451–452.

(26) Nikitin, K.; Müller-Bunz, H.; Ortin, Y.; Muldoon, J.; McGlinchey, M. J. Restricted rotation in 9-phenyl-anthracenes: a prediction fulfilled. *Org. Lett.* **2011**, *13*, 256–259.

(27) Kotha, S.; Ghosh, A. K.; Deodhar, K. D. Synthesis of symmetrical and unsymmetrical 9, 10-diarylanthracene derivatives via bis-Suzuki-Miyaura cross-coupling reaction. *Synthesis* **2004**, *4*, 549–557.

(28) Matsubara, Y.; Kimura, A.; Yamaguchi, Y.; Yoshida, Z. Meso-Disubstituted Anthracenes with Fluorine-Containing Groups: Synthesis, Light-Emitting Characteristics, and Photostability. *Org. Lett.* **2008**, *10*, 5541–5544.

(29) Darses, S.; Genet, J.-P. Potassium organotrifluoroborates: new perspectives in organic synthesis. *Chem. Rev.* **2008**, *108*, 288–325.

(30) Frohn, H.-J.; Franke, H.; Fritzen, P.; Bardin, V. (Fluoroorgano) fluoroboranes and-fluoroborates I: synthesis and spectroscopic characterization of potassium fluoroaryltrifluoroborates and fluoroaryldifluoroboranes. *J. Organomet. Chem.* **2000**, *598*, 127–135.

(31) Lafrance, M.; Rowley, C. N.; Woo, T. K.; Fagnou, K. Catalytic intermolecular direct arylation of perfluorobenzenes. *J. Am. Chem. Soc.* **2006**, *128*, 8754–8756.

3. Fluorescence and up-conversion of phenylanthracene dyes

Molecules containing the anthracene core moiety were synthesised previously (Chapter 2). These emitters comprise two series of molecules with varying degrees of fluorination on their aryl periphery, based on 9-phenylanthracene and 9,10-diphenylanthracene (DPA). DPA is a common TTAUC emitter molecule, that has been commonly used in up-conversion investigations for converting green light into blue (Chapter 1).[1–5]

The photophysical properties of the emitter are dictated by the core emissive unit, here anthracene. While addition and modification of the aryl periphery will cause alterations in peak wavelength and shape the peak structures will have similarities. The normalised absorption and emission spectra of anthracene in dry toluene as measured by the author is shown (Figure 3.1) and is in agreement with the literature.[6]

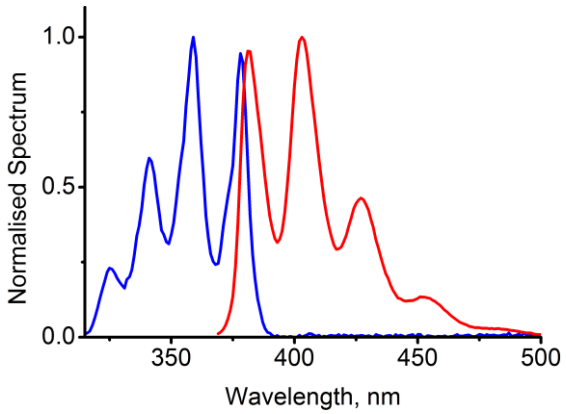

Figure 3.1 : Normalised absorption (blue) and emission spectra (red) of anthracene in dry toluene

The normalised absorption spectrum of anthracene has sharp distinct vibrational character due to the rigid nature of the PAH preventing a vibrational (as well as rotational) freedom. The absorption's vibrational bands are at 378 nm (0→0), 359 nm (0→1), 341 nm (0→2) and 325 nm (0→3). The transition (0→1) is the absorption maximum.

The normalised emission spectrum of anthracene is a classic "mirror image" of the absorption spectrum, with a very small Stokes shift, indicating that there is a very little non-radiative relaxation of the molecule between the absorption and emission events. The same sharp distinct vibrational character is seen, with vibrational bands at 381 nm (0→0), 403 nm (0→1), 427 nm (0→2) and 451 nm (0→3). The transition (0→2) is the emission maximum. Anthracene has been used as a blue emitter for TTAUCSs in the past,[7] but 9,10-diphenylanthracene is used more commonly (Chapter 1).

In this chapter we aim to show that fluorinated derivatives of 9-phenylanthracene and 9,10-phenylanthracene are competitive up-conversion emitters when compared to their non-fluorinated analogues. All fluorescence and up-conversion properties of the emitters were measured by the author, with the aid of our industrial sponsors, at Sony Deutschland GmbH, over a non-consecutive period of 11 weeks.

3.1. Fluorescence of 9-phenylanthracene dyes

A series of emitters **1a-h** (Figure 3.2) based on the structure 9-phenylanthracene was synthesised (Chapter 2) with a view to their use in up-converting systems.

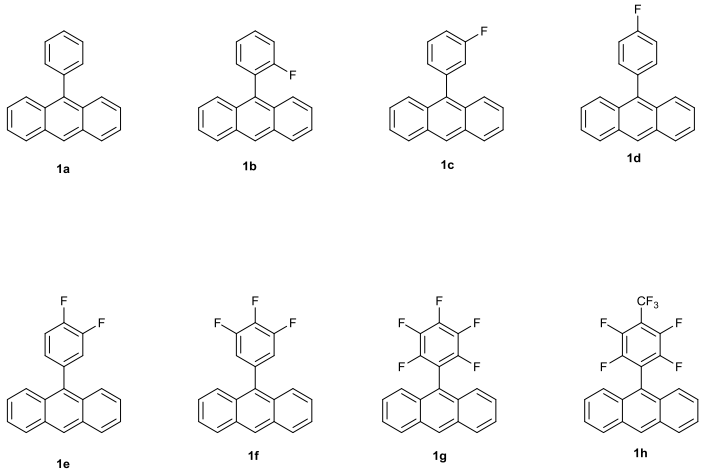

Figure 3.2 : 9-phenylanthracene analogues **1a-h**

The absorption spectra (Figure 3.3) of the emitters **1a-h** dissolved in dry toluene ($1x10^{-5}$ M) were recorded in 1 cm glass cuvettes using an Agilent Cary 50 UV/vis spectrometer. No attempt was made to exclude oxygen from the samples. The absorption spectra have similar vibrational structures to those of anthracene (Figure 3.1), with four distinct vibrational modes, of which the second is the strongest. For molecules **1a-f** the positions of the vibrational bands are similar, (0→1) at 386 nm, the absorption maximum (0→2) at 366 nm, (0→3) at 348 nm and (0→4) at 332 nm. These peaks are red shifted when compared to the absorption spectrum of anthracene, but their distribution is very similar. Emitters **1g-h** possess increased bathochromic shifts of 1 nm compared to the lesser fluorinated analogues, and have less sharp vibrational bands, due to greater rotational freedom allowed during the absorption caused by the presence of $–CF_3$ and perfluorophenyl groups. The relatively small shift in emission peak indicates that fluorinating the molecule does not cause a large shift in the S_1 level, this is desireable for the project as it conserves the energy output of the emitter. This rotational freedom causes a shoulder in the absorption spectrum of **1g**. When compared to the literature compound, non-fluorinated analogue, **1a**,[8] each of the emitters **1b-h** is consistent with the observation that replacing hydrogen with fluorine has little effect upon the

shape of the absorption spectrum of the 9-phenylanthracene emitters, and any line broadening is likely due to increased rotational freedom within the carbon framework.

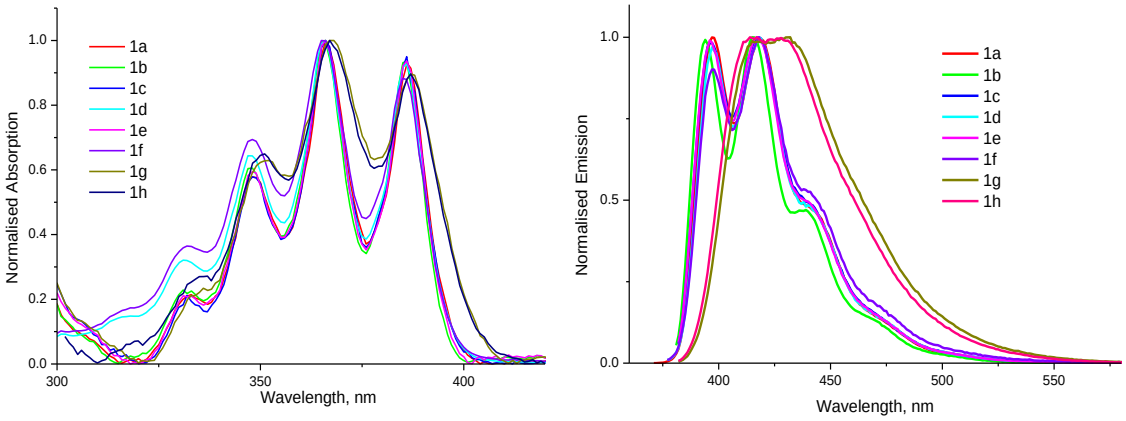

Figure 3.3 : Normalised absorption (left) and emission spectra (right) of emitters **1a-h** in dry toluene

The emission spectra of the emitters **1a-h** (Figure 3.3) dissolved in dry toluene ($1x10^{-5}$ M) were recorded in 1 cm glass cuvettes using an Horiba Fluoromax 4 spectrometer, no attempt was made to exclude oxygen from the samples. The emission spectra of the emitters **1a-h** (Figure 3.3) show a departure from the classic anthracene "mirror image" spectrum. The addition of the 9-phenyl moiety imparts a great deal of rotational freedom in the structure, allowing a bathochromic shift in the emission as well as a large degree of line broadening, which turns the (0→2) peak into a shoulder and almost obscures the (0→3) transition. In comparison to the non-fluorinated analogue **1a**, the substitution of a small number of hydrogen atoms with fluorine atoms causes little change, as seen for emitters **1b-f**. Emitters **1g-h** show a single, broad peak that is the (0→1) and (0→2) transitions at very close proximity merging due to the increased rotational freedom in these molecules. The highly electron withdrawing systems on emitter **1g-h** cause an increased bathochromic shift, as expected.

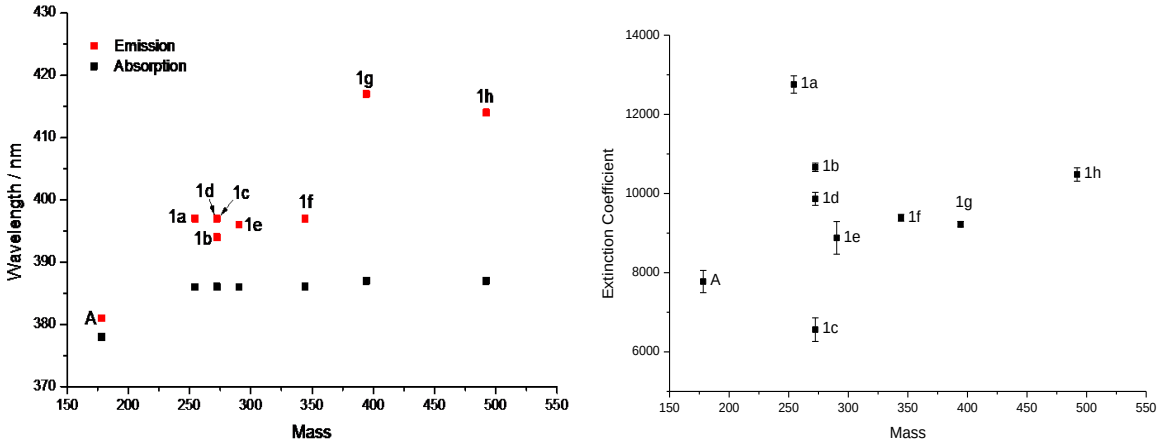

Figure 3.4 : Emission (0-0) (red) and absorption (0-0) (black) peaks of emitters **1a-h** and anthracene (**A**) in dry toluene (left) and extinction coefficients of emitters **1a-h** and anthracene (**A**) in dry toluene (right)

The Stokes shifts of the emitters (difference between black and red plots, Figure 3.4) show an increase with the addition of a phenyl moiety, as is the case for emitter **1a**, while the subsequent replacement of hydrogen with fluorine has little effect on the Stokes shifts of emitters **1b-f** compared to the non-fluorinated, literature compound, **1a**.[8] A small amount of site dependency is seen, with the ortho-fluorine **1b** showing the least Stokes shift. The trifluorophenylanthracene analogue **1f** has a similar Stokes shift to the non-fluorinated analogue **1a**. The highly fluorinated analogues **1g-h** have greatly increased Stokes shifts, indicating increased energy loss to non-radiative transitions.

Replacement of hydrogen with a single fluorine at varying points around the phenyl ring as is the case for emitters **1b-d**, shows a reduction of the extinction coefficient in comparison to non-fluorinated analogue **1a**, with the trend *ortho* < *para* < *meta* (Figure 3.4). This pattern indicates that the cause of the reduction is due to an electronic through bond effect, rather than steric or through space effect. Emitter **1e**, 3,4-difluorophenylanthacene, has a reduced extinction coefficient compared to **1d**, showing addition of a *meta* fluorine decreases the extinction coefficient, while **1f** indicates that the positive effect from *ortho* and *para* substitution can outweigh negative effects from *meta* fluorination. Since the absorption event requires a significant amount of electron character at the anthracene emissive unit, it would be expected that decreasing this through using inductive withdrawing groups decreases the extinction coefficient.

However, since fluorine atoms can both inductively withdraw electron character or donate electrons into π systems (Figure 3.5), fluorine atoms in *para* or *ortho* positions may donate electron character into the emissive anthracene unit, provided there is some conjugation between the phenyl and anthracene, allowing an increase in extinction coefficient. It is clear that there is a net decrease in extinction coefficient over these two effects (Figure 3.4).

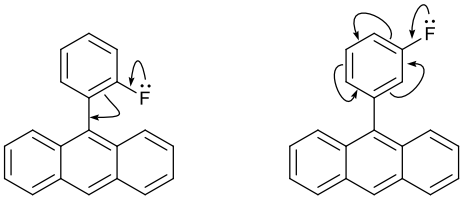

Figure 3.5 : π donating effects of ortho and meta fluorinated aromatic systems

The emitters **1g-h** have extinction coefficients in a similar region to that of the *ortho* and *para* monofluorinated analogues, indicating that further increases in fluorination have a very small effect upon the extinction coefficient.

Fluorescence quantum yields of the emitters **1a-h** were measured using a Horiba Fluoromax 4 spectrometer fitted with an integrating sphere.

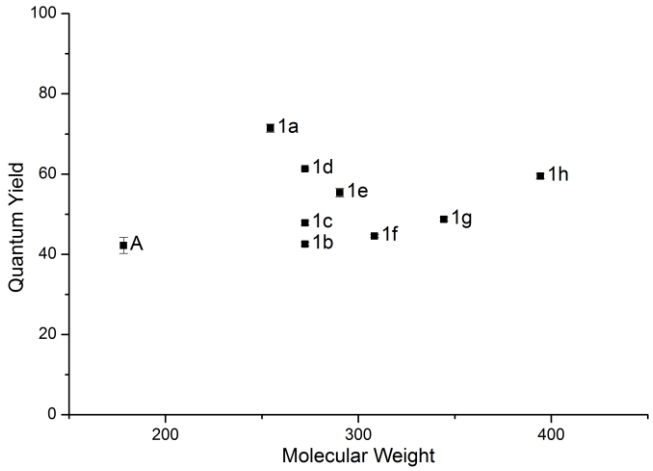

Figure 3.6 : Fluorescence quantum yields of emitters **1a-h** and anthracene (**A**) in dry toluene

The fluorescence quantum yields of 9-phenylanthracene molecules are extremely important to their potential as up-conversion emitter molecules, because a high fluorescence quantum yield is required for efficient up-conversion. It is clear that emitters **1a-h** do not reemit absorbed photons efficiently, but they are more efficient than anthracene (41%, lit 36% - in cyclohexane).[6] **1a** has the highest fluorescence quantum yield of 76% (lit 0.49 – in cyclohexane)[6], with **1d** and **1h** at around 60%. While all fluorinated analogues have decreased quantum yield compared to non-fluorinated **1a** it is clear that addition of an inductively electron withdrawing fluorine atom or trifluoromethyl group is the least harmful for the fluorescence quantum yield. This can be seen by the increase from **1c** to **1e** and **1g** to **1h.** Conversely addition of a *meta* fluorine atom causes decreasing quantum yield, with a clear downward trend from **1d** to **1e** and **1f**.

In summary, the fluorescent properties of the 9-phenylanthracene emitters indicate that **1a** has the highest potential as an TTAUC emitter, and that while mild fluorination of the peripheral phenyl group has little effect on the peak position the fluorescence quantum yields are reduced. Thus fluorination has decreased the up-conversion potential of the 9-phenylanthracene system.

Since 9-phenylanthracene has a higher quantum yield than anthracene alone, it might be expected that increasing phenyl substitution to 9,10-diphenylanthracene would have an increased fluorescence quantum yield again. A range of fluorinated 9,10-phenylanthracene (DPA) based dyes was investigated with a view to their capability as TTA up-conversion emitters.

3.2. Fluorescence of 9,10-bisphenylanthracene dyes

The synthesis of emitters **2a-h** based on the structure 9,10-diphenylanthracene was detailed in Chapter 2, and the fluorescence properties of samples **2a,c-f,h** were analysed in a similar manner to the 9-phenylanthracene series. Emitter **2a** is a known compound, and the spectra here are in agreement with the literature.[6]

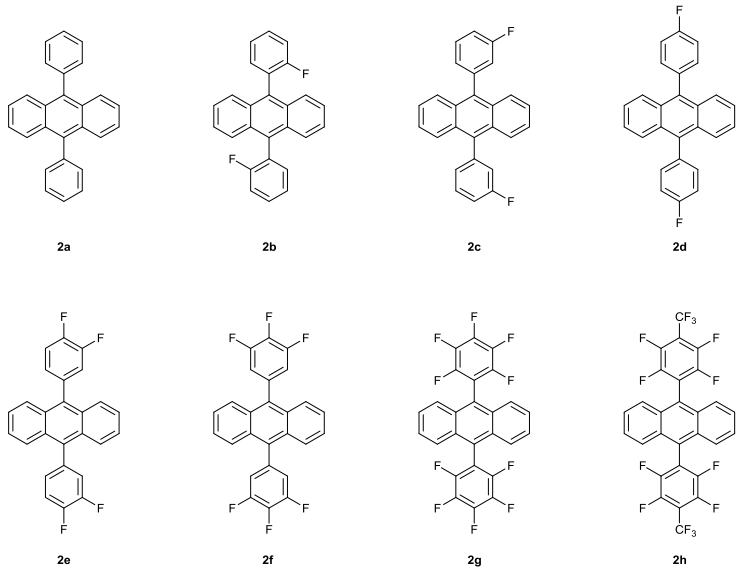

Figure 3.7 : 9,10-bisphenylanthracene emitters **2a-h** as planar molecules

The absorption spectra of the tested emitters **2a-h** (Figure 3.8) show the peak structures associated with diphenylanthracene based derivatives, with four distinct peaks, of which the second is the strongest. The spectra of the diphenylanthracenes are red shifted in comparison to anthracene itself, as would be expected from an increase in conjugation. The molecules **2a-d** have similar absorption spectra, while **2e** is blue-shifted compared to the non-fluorinated derivative. With increasing fluorination the 3,4,5-trifluoro derivative has a (0→0) bands in a similar position to the non-fluorinated diphenylanthracene, but the distance between the peak bands is widened, indicating slightly increased vibrational relaxation. The spectra of **2h** is broader, with less distinctive peaks, showing increased rotational and vibrational disorder in the molecule.

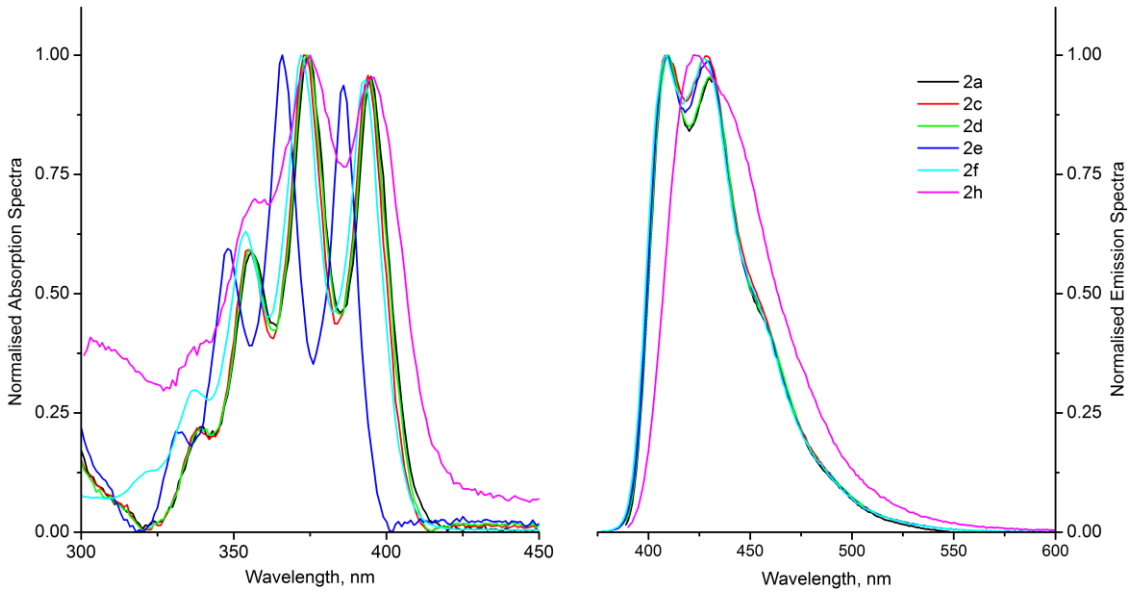

Figure 3.8 : Normalised absorption (left) and emission spectra (right) of 9,10-diphenylanthracene emitters **2a-h** in dry toluene

The emission spectra of emitters **2a-f** are very similar, while for **2h** the transition (0→1) is supressed to a shoulder, and higher order transitions not distinguishable.

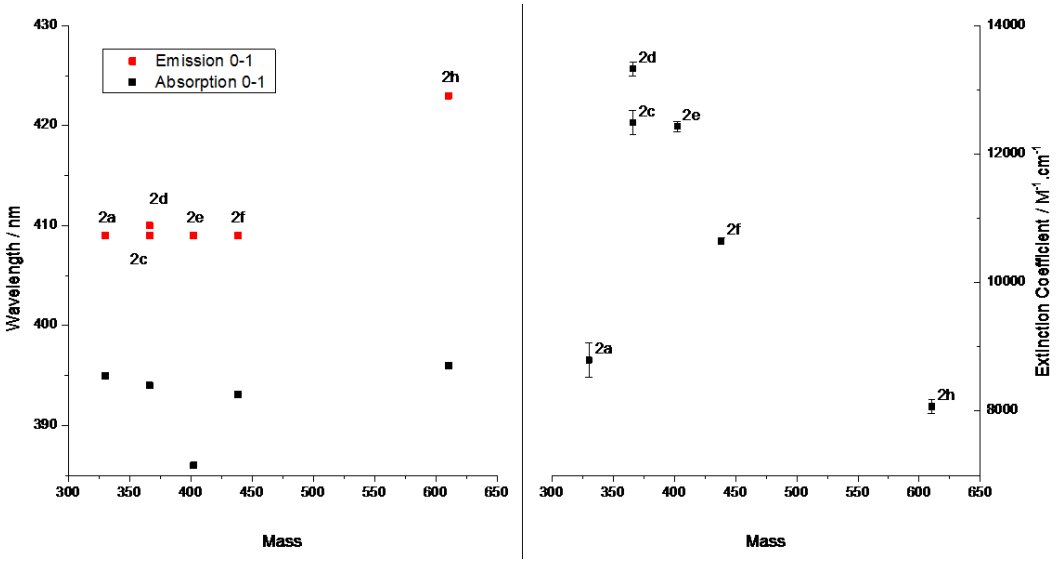

Figure 3.9 : Emission (0-0) (red) and absorption (0-0) (black) peaks (left) and Extinction coefficients (right) of emitters **2a-h** in toluene

The difference in absorption and emission wavelength (Stokes shift) of the emitters is shown Figure 3.9). The non-fluorinated analogue **2a** has the smallest Stokes shift of the series: increasing fluorination has a general effect of increasing Stokes shift. **2h** has the largest Stokes shift. Shifts are greatly increased compared to the 9-phenylanthracenes and anthracene (Figure 3.4).

The extinction coefficients of the 9,10-diphenylanthracene emitters **2a-h** (Figure 3.9) do not follow the same trend as 9-phenylanthracene emitters **1a-h** (Figure 3.4), where increasing fluorination generally had little effect. In the case of the diphenylanthracene emitters monofluorination at any site greatly increases the extinction coefficient of the chromaphore, while multiple fluorinations cause decreases in extinction coefficient to occur.

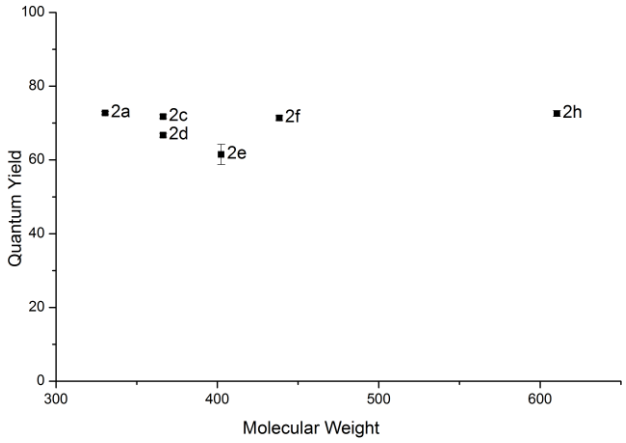

Figure 3.10 : Fluorescence Quantum Yields of emitters**2a-h**

The fluorescence quantum yields of the fluorinated emitters **2c-2h** are all similar to **2a** (73%, lit 100% in cyclohexane),[6] with **2h** and **2a** at parity. Since **2a** (DPA) has been used successfully in TTAUCSs (Chapter 1) **2h** has promise as an emitter with equal up-conversion capability but of increased stability to thermal and photodegradation. Consequently diphenylanthracene emitters **2a** and **2h** were selected for further stability investigation.

3.2.1.1. UV degradation of **2a** and **2h**

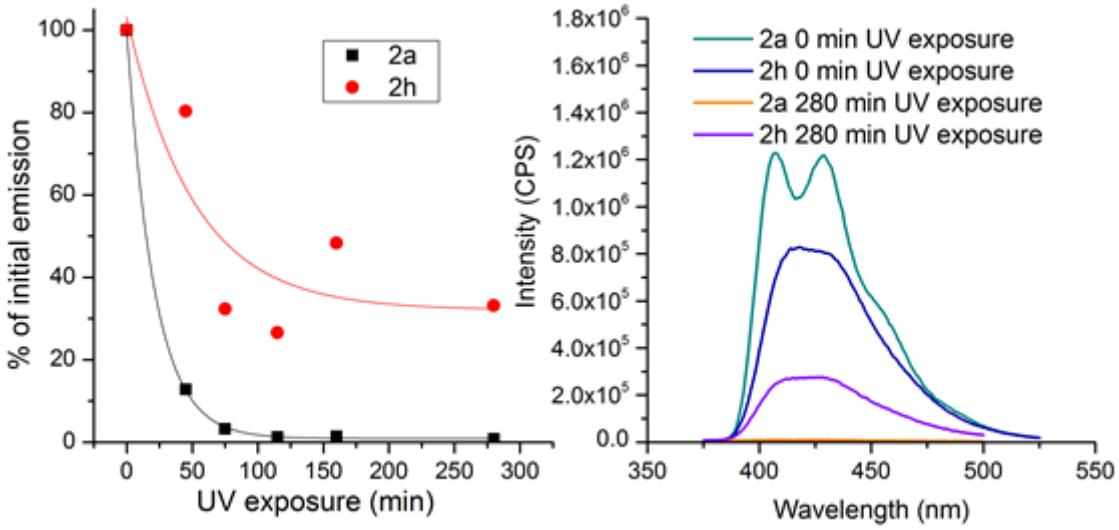

Figure 3.11 : Degradation of emission by films containing **2a** and **2h**, normalised peak emission (left) and emission spectra (right)

To test the stability of the two highest quantum yield emitters thin films (**2a**: 1.837 μm, **2h**: 1.791 μm) in PMMA (2% weight percent) were spin coated onto glass slides. Their stability to UV degradation was assessed by direct illumination with a UV lamp. No attempts at oxygen exclusion were made. Emission spectra measurements were taken using constant slit width and excitation wavelength and intensity.

As can be clearly seen from Figure 3.11, although diphenylanthracene is more emissive initially, and has a slightly higher quantum yield than the highly fluorinated **2h** analogue, it is nevertheless much more susceptible to degradation from UV light exposure. **2a** shows a more obvious initial decrease in emission, and after 100 min the emission is reduced to less than 1% of that initially recorded. In comparison emitter **2h** still gives obvious emission even after 280 minutes (almost 5 h) of intense UV illumination. This indicates that devices based on the fluorinated analogue would be likely to possess longer working lifetimes.

In summary the emitter **2h** shows potential as a novel up-conversion emitter molecule, due to a fluorescence quantum yield very close to the non-fluorinated analogue, but greatly improved photostability. Thus the emitters **1a, 1h, 2a** and **2h** were selected for detailed up-conversion study.

3.3. Upconversion measurements of anthracene based emitters

Up-conversion measurements of diphenylanthracene containing systems have, in the past, often used an octaethylporphyrin, complexing either a palladium or platinum ion as a sensitizing partner in both solution and solid state devices (Chapter 1).

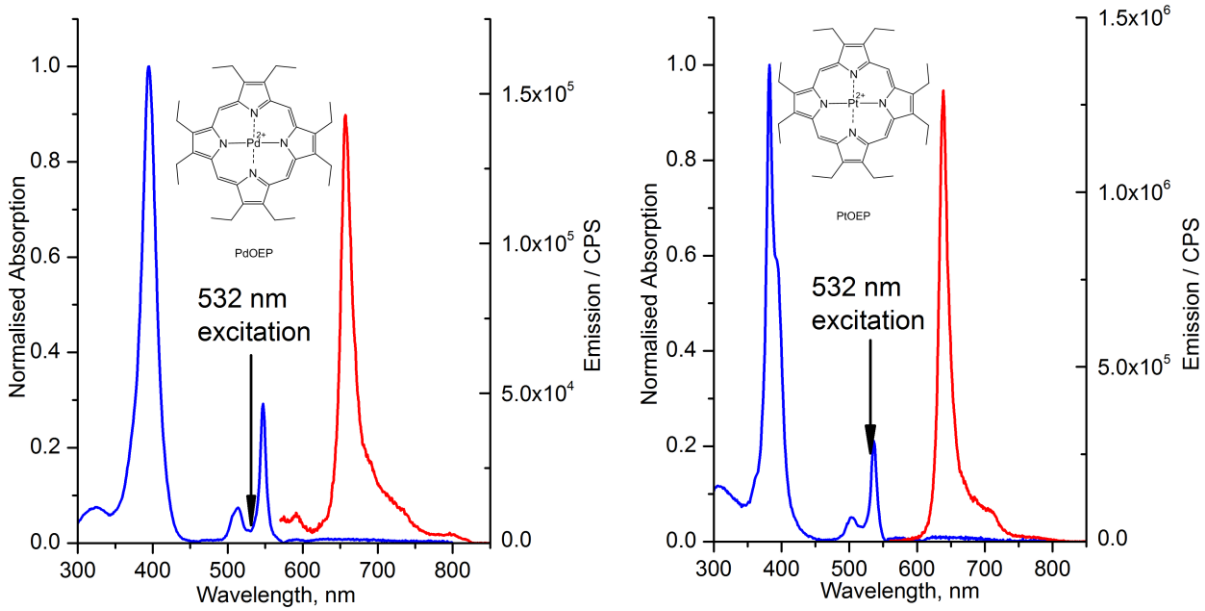

Figure 3.12 : Molecular structures and normalised absorption (blue) and emission spectra (red) of palladium(II) octaethylporphyrin **PdOEP** (left) and platinum(II) octaehtylporphyrin **PtOEP** (right)

Metal ion complexes **PdOEP** and **PtOEP** show characteristic bands in their measured absorption spectra (Figure 3.12), with obvious Soret (blue) bands at 394 and 382 nm, and Q-bands at 546 and 536 nm (Q-band I) and 514 and 503 nm (Q-band II) respectively, in agreement with the literature.[9,10] **PtOEP** shows better absorption at the laser excitation wavelength of 532 nm than **PdOEP**. The phosphorescent emissions are at 657 and 639 nm for **PdOEP** and **PtOEP** respectively. From these spectra we can assess that the approximate energy levels of the sensitizers, are as below.

	PdOEP	**PtOEP**
T_1	1.89 eV	1.94 eV
S_1	2.27 eV	2.31 eV
S_2	3.15 eV	3.25 eV

In general the S_1 of the TTAUC emitter should be no greater than twice the T_1 of the sensitizer molecule ($2 \times T_1 = 3.77$ (**PdOEP),** 3.88 (**PtOEP**) eV), in order to allow the TTA process to occur. Since the emitters **A, 1a-h** and **2a-h** have emissions in the range of 380-420 nm, corresponding to 3.25 – 2.93 eV, this requirement is satisfied.

Emitters **A, 1a, 1h, 2a** and **2h** were selected for up-conversion experiments, paired with the sensitizers **PdOEP** and **PtOEP**, since these anthracene systems have shown the highest fluorescence quantum yields.

Up-conversion measurements were made using flat walled tubes with mixtures of the emitter (6 $x10^{-4}$ M) and sensitiser (3 $x10^{-5}$ M) in dry, degassed, toluene, prepared in a glove box with <1 ppm oxygen, excited with 633 nm coherent photons.

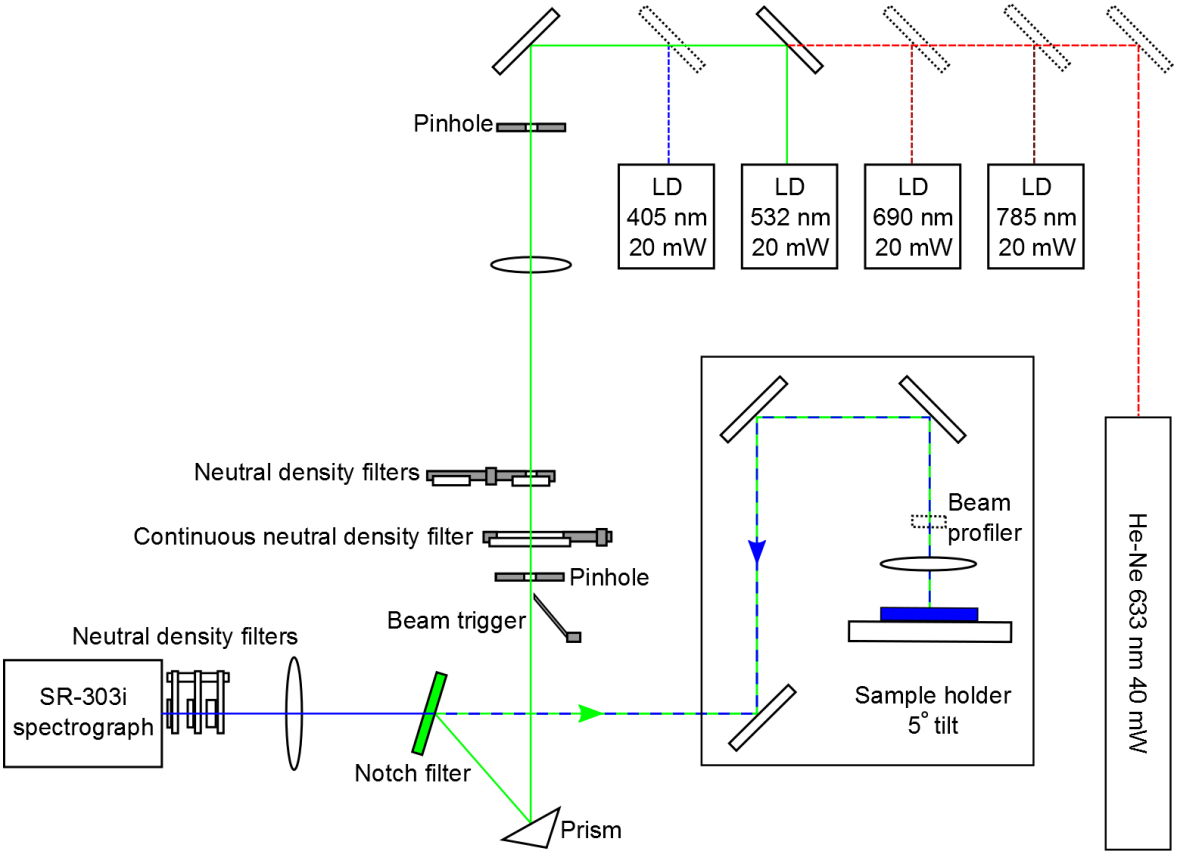

Figure 3.13 : Laser apparatus in Sony's Materials Science Laboratories for up-conversion measurements, with 532 nm laser diode in use. The beam paths of the other laser sources and mirrors not in use are shown by dashed lines.

A laser set-up, developed by the Materials Science Laboratories of Sony Deutschland was used (Figure 3.13): the wavelength of the excitation was selected by choice of laser source, while the intensity of the excitation was attenuated by use of neutral density filters to µW range. Once attenuated the beam is bounced off a prism and a notch filter to the sample holder apparatus (green path). The notch filter attenuates reflected light at the incident wavelength to prevent saturation of the photo sensor. The sample holder has a 5° lateral tilt to minimise incident beam reflection to the spectrometer (Figure 3.14). The emitted light travels directly back along the beam path (blue path), but passes through the notch filter allowing collection by the Andor SR-303i spectrograph. Neutral density filters attenuate the emitted light to prevent saturation of the spectrograph's photo sensor; these are corrected for in the emission spectra calculations.

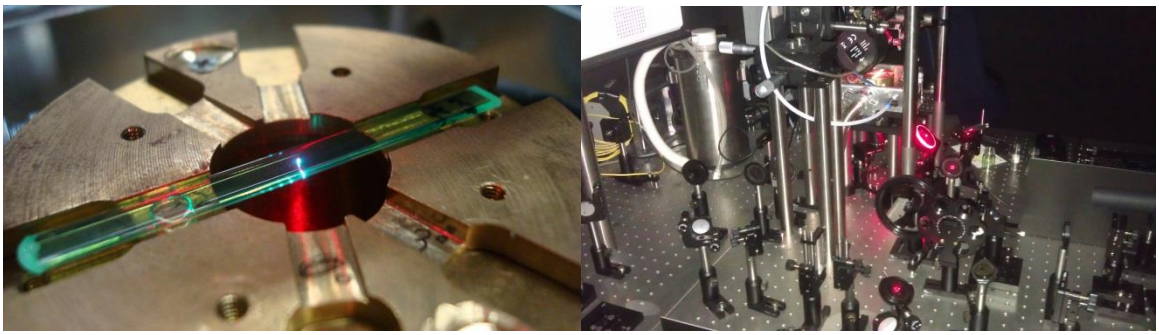

Figure 3.14 : Up-conversion tube in sample holder tilted at 5° (left) and sample holder apparatus and laser set up (right). Sample is **PdTBP** and **perylene**, illuminated with red light, emitting blue (see Chapter 5)

The emission spectra of the emitters when paired with the sensitizers are similar to when the emitter is directly excited, with less vibrational structure. The 9-phenylanthracenes show decreased up-conversion compared to the 9,10-bisphenylanthracenes. Each of the emitters can be seen to be quenching the phosphorescence of the sensitizer: compared to the sensitizer alone the peak at ~650 nm is reduced. However, while anthracene quenches the sensitizer it shows very low emission.

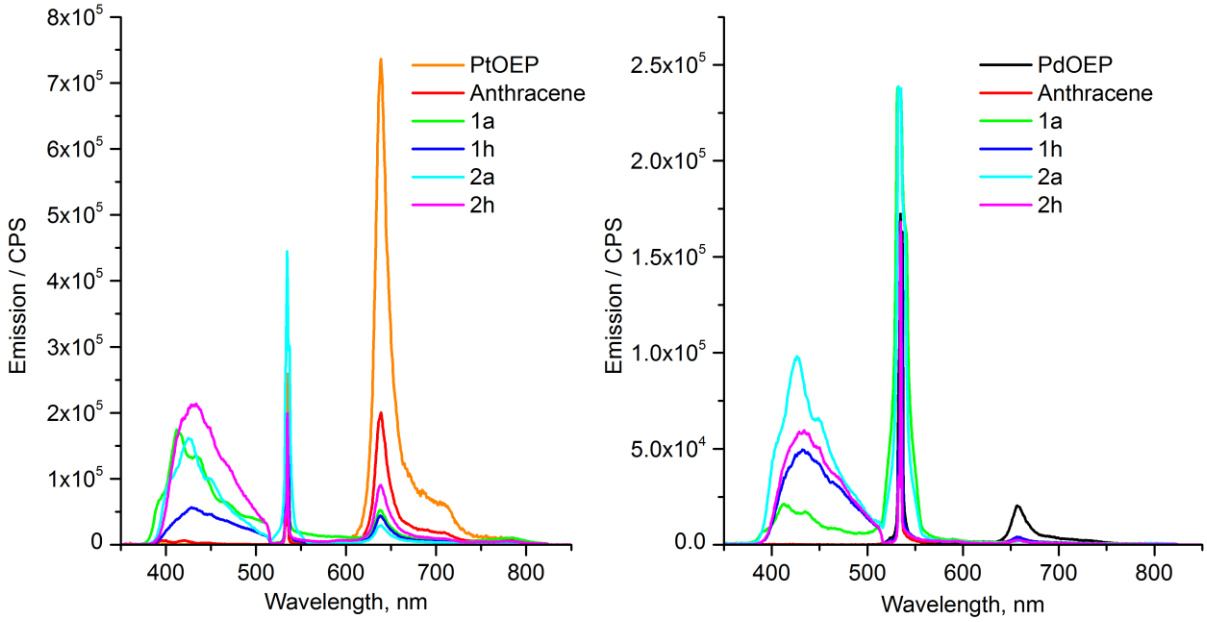

Figure 3.15 : Emission spectra of mixtures of each of emitters **A, 1a, 1h, 2a** and **2h** with **PtOEP** (left) and **PdOEP** (right) excited with 532 nm 1 mW coherent light. The excitation region ~520 – 570 nm is attenuated by a notch filter and is not integrated in quantum yield calculations.

A measurement of the unknown quantum yield may be taken by comparing a reference material of known quantum yield (Φ_r), provided the emission integral (F), light intensity at excitation wavelength (I), absorbance of the substrate at excitation wavelength (A), refractive index of the substrate (n) and energy of the excitation photons (hv) are known. Under most experimental procedures the intensity, refractive index and excitation energy is kept constant.

$$\Phi_x = \Phi_r \frac{F_x}{F_r} \times \frac{I_r}{I_x} \times \frac{A_r}{A_x} \times \frac{n_x^2}{n_r^2} \times \frac{h\upsilon_x}{h\upsilon_r} \qquad (3.1)$$

We will quote only external quantum yields in this thesis, without any multiplication factors, thus in this regime 50% is the maximum possible external quantum yield, as discussed in Chapter 1. For the emitters derived from anthracene, the reference emitter used for the up-conversion quantum yield calculation was the novel emitter molecule **4f**, 8-(perfluorophenyl)-3,5-di-(3,4,5-trifluoro) phenyldifluoroborondipyrrolemethene, (QY = 92.3%, Chapter 6).

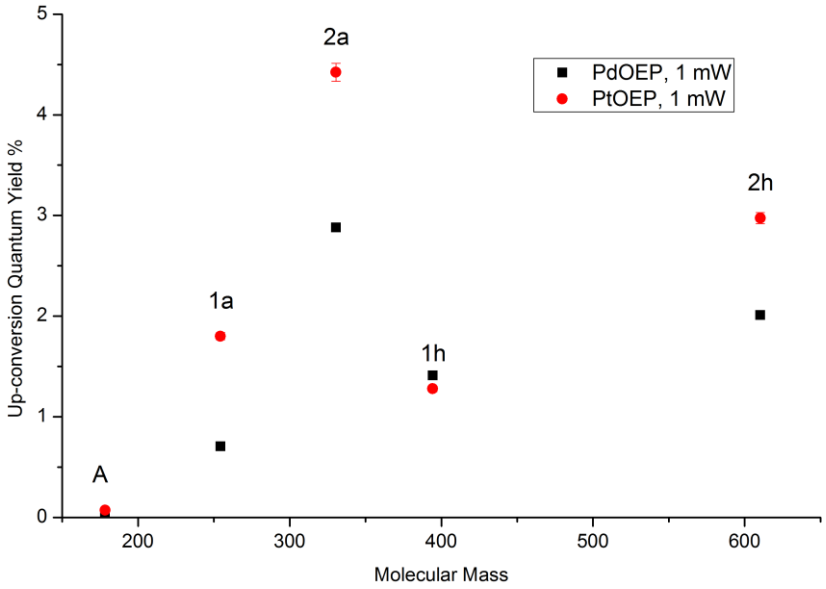

Figure 3.16 : Up-conversion quantum yields (%) of emitters **A**, **1a**, **1h**, **2a** and **2h** when sensitized by **PdOEP** (black) and **PtOEP** (red), excited with 532 nm 1 mW coherent light.

The up-conversion quantum yields of the emitters **A**, **1a**, **1h**, **2a** and **2h** paired with sensitizers **PdOEP** and **PtOEP** were calculated from the up-conversion emission spectra with comparison to emitter **4f**. It is clear that systems using **PtOEP** as a sensitizer have higher up-conversion quantum yields than with **PdOEP**. This is independent of the lower absorption by **PdOEP** since the up-conversion quantum yield comparison calculation takes this into account. Non-fluorinated emitter **2a** shows the greatest up-conversion yield, followed by **2h**, while the 9-phenylanthracenes are lower. Anthracene shows up-conversion quantum yield of less than 0.1% with both sensitizers, due to its low fluorescence quantum yield, and photochemical processes (Chapter 1).

The "up-conversion energy efficiency" parameter (Ξ) is calculated from the quantum yield of the emitter and the incident and emission photon energies.

$$\Xi = \frac{\Phi_x \times E_{obs}}{E_{exc}} \qquad (3.2)$$

This value is a measure of how much usable energy has been retained by the up-conversion system for possible use. The energy efficiency may be used to compare up-conversion systems composed of different types of emitter and sensitizer pairings.

Emitter	Φ_F %	**PdOEP**		**PtOEP**	
		Φ_{UC} %	Ξ %	Φ_{UC} %	Ξ %
A	42	0.01	0.01	0.07	0.1
1a	71	0.7	0.93	1.8	2.35
1h	60	1.4	1.78	1.3	1.60
2a	73	2.9	3.69	4.4	5.57
2h	73	2.0	2.54	3.0	3.71

Figure 3.17 : Table of fluorescence quantum yield (Φ_F), up-conversion quantum yield (Φ_{UC}) and up-conversion energy efficiency (Ξ) as percentages for anthracene based emitters sensitized by **PdOEP** and **PtOEP,** excited with 532 nm 1 mW coherent light.

It is clear that the up-conversion quantum yields are closely linked to the fluorescence quantum yield as expected. The most efficient emitter molecule in these systems is **2a** (DPA) which has been investigated in detail elsewhere (see Chapter 1). Therefore we chose to investigate the best performing fluorinated anthracene based emitter, **2h,** in more detail, as its up-conversion quantum yield and energy efficiency, paired with its high photostablity make it a good candidate for TTAUC devices.

3.3.1. Up-conversion of 9,10-di-((4-trifluoromethyl) perfluorophenyl)anthracene **(2h)** with varying concentration and intensity

Two series of up-conversion solutions were prepared, using the different sensitizsers **PdOEP and PtOEP** with varying concentrations of fluorinated emitter **2h**. Their up-conversion capabilities were measured with a view to comparing their response to increasing illumination intensity and to assess the efficiency of the TTT step using the laser set up described (Figure 3.13). When illuminated with 1 mW 532 nm coherent photons these clearly show that increasing the concentration of the emitter molecule causes increased quenching of the sensitizer's phosphorescence at 660 nm.

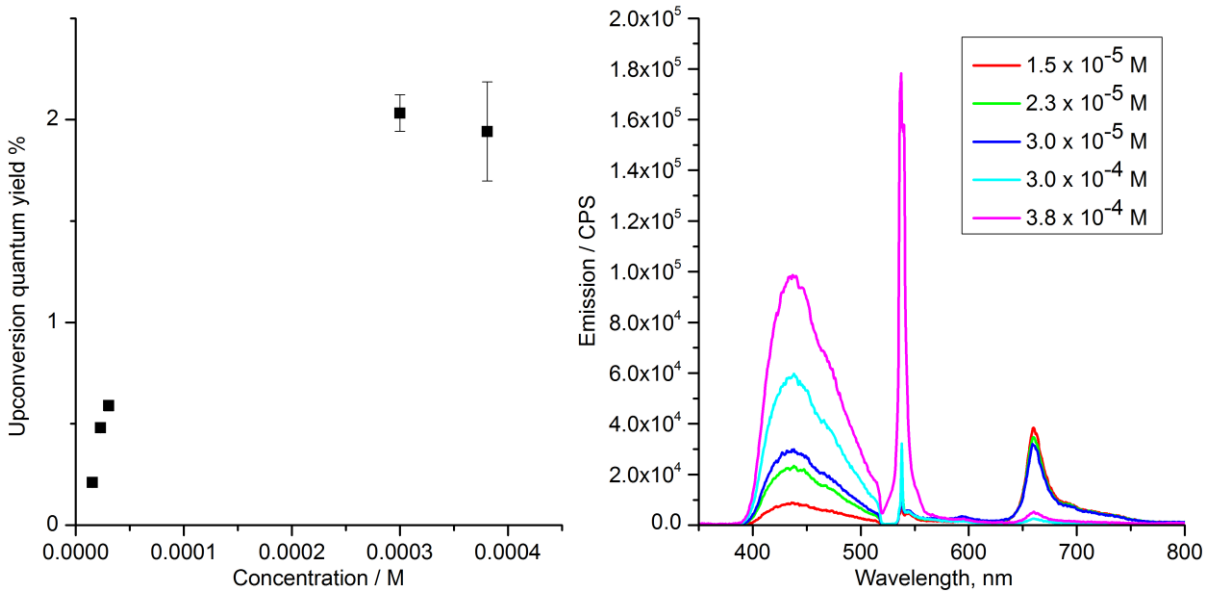

Figure 3.18 : Up-conversion quantum yields (left) and up-conversion emission spectra (right) of **2h** at varying concentrations with **PdOEP** (1.5 x 10^{-5} M), excited with 532 nm 1 mW coherent photons, 5.55 W/cm^2

The up-conversion quantum yield has a plateau at 2% once the concentration of the emitter reaches around 20 times that of the sensitizer. Each of the solutions was illuminated with varying intensities of 532 nm coherent light.

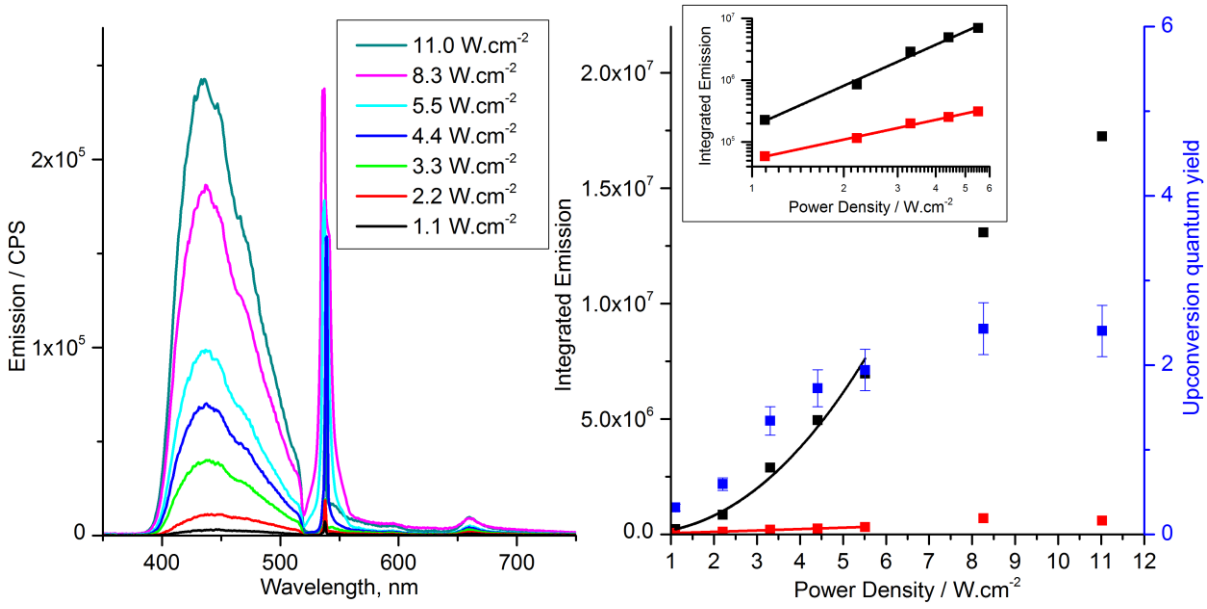

Figure 3.19 : Up-conversion emission spectra (left) and integrated emission of up-conversion emission (black) and unquenched sensitizer emission (red) with double log plot inset (right) of **2h** (3.8 x 10^{-4} M) and **PdOEP** (1.5 x 10^{-5} M) in dry, degassed toluene, excited with varying intensity 532 nm coherent light

Shown are representative graphs for the most concentrated (Figure 3.19) and least concentrated samples (Figure 3.20), 1.5x10^{-5} M and 3.8x10^{-5} M respectively. The spectra of the most concentrated sample shows both the up-conversion emission and the unquenched sensitizer emission increasing as the incident excitation intensity increases (Figure 3.19).

It is clear that the up-conversion emission increases exponentially with excitation intensity, while the unquenched phosphorescence increases linearly, this is a common indication of TTAUC (Chapter 1). This exponential relationship holds for low power intensities, however at higher power intensities a linear relationship is apparent, as is seen above 6 W.cm^{-2}. This transition is known as the difference between the weak up-conversion limit at low intensity and the strong up-conversion limit at high intensity illumination.

The exponential increase in up-conversion emission with increasing power density is confirmed by the double logarithm plot (Figure 3.19 inset), gradient 2.2, while the gradient of the unquenched sensitizer phosphorescence is 1.0, indicating a linear relationship. The up-conversion quantum yield increases to a plateau of 2.2 % as the excitation intensity increases.

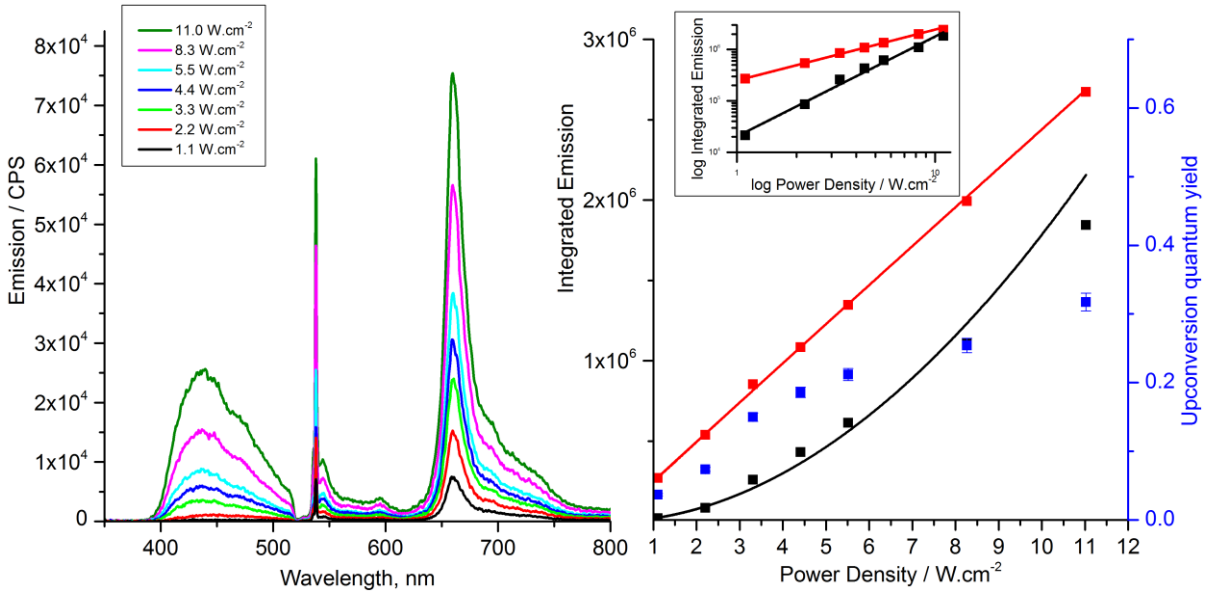

Figure 3.20 : Up-conversion emission spectra (left) and Emission - Intensity relationship of up-conversion emission (black) and unquenched sensitizer emission (red) with double log plot inset (right) of **2h** (1.5 x 10^{-5} M) and **PdOEP** (1.5 x 10^{-5} M) in dry, degassed toluene, excited with varying intensity 532 nm coherent light

At a lower concentration of emitter the phosphorescence of the sensitizer is quenched less effectively, and the up-conversion quantum yield is considerably reduced (Figure 3.20). This is due to both bi-molecular processes TTT and TTA being less efficient at a lower concentration of emitter molecules. While the up-conversion quantum yield plateaus for high concentrations with high excitation intensity (Figure 3.19), the quantum yield is still increasing with intensity >10 W.cm^{-2} at lower concentration. This is due to the later onset of the more efficient strong up-conversion limit, at > 10 W.cm^{-2} for the 1:1 mixture of sensitizer and emitter. The concentration of emitters in the first triplet state is the instrumental ratio in TTAUC, and the onset of the strong up-conversion limit can be made at lower excitation intensities provided this concentration is maximised by preventing oxygen quenching and ensuring effective quenching of the sensitizer phosphorescence.

The double logarithm plot for the lower concentration again shows the exponential relationship between up-conversion emission and excitation intensity (gradient 1.9), and the linear relationship between phosphorescence and excitation intensity (gradient 1.0). There is no clear deviation from the exponential relationship within the intensity range studied.

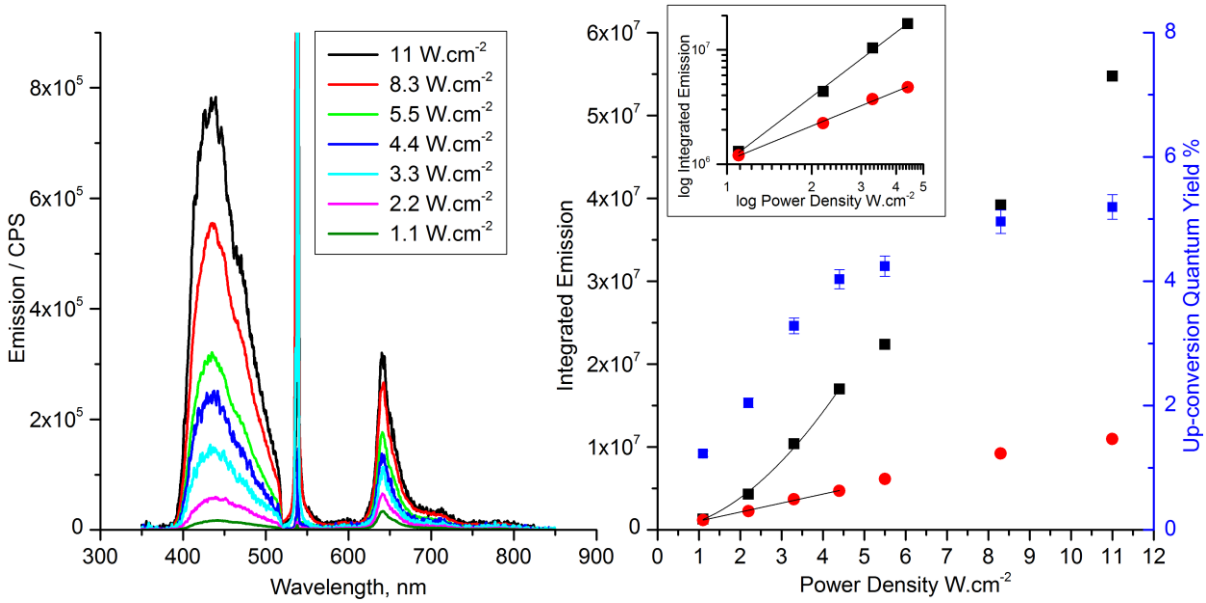

Figure 3.21 : Up-conversion emission spectra (left) and Integrated emission of up-conversion emission (black) and unquenched sensitizer emission (red) with double log plot inset (right) of **2h** (3.8 x 10^{-4} M) and **PtOEP** (1.5 x 10^{-5} M) in dry, degassed toluene, excited with varying intensity 532 nm coherent light

Using **PtOEP** instead of **PdOEP** gives a higher up-conversion quantum yield, in agreement with earlier results (Figure 3.15). At higher concentrations there is more effective quenching of the sensitizer phosphorescence, maximising the concentration of the emitter molecules in the first triplet state, causing earlier onset of the strong up-conversion limit.

For the highest concentration of emitter **2h** system (Figure 3.21), the double logarithm plot (inset) again shows the exponential relationship between up-conversion emission and excitation intensity but attenuated by the early onset of the strong up-conversion limit (gradient 1.2), and the linear relationship between phosphorescence and excitation intensity (gradient 0.9). The transition to the strong up-conversion limit is visible at around 4 W.cm^{-2} power density. By normalising the up-conversion emission with respect to the unquenched sensitizer emission (i.e. $F_{UC} \div F_S$) the transition between the weak and strong up-conversion limits can be more clearly seen, compensating for small fluxes in incident laser power and neutral density filter aberrations (Figure 3.22).

The normalised log plot of up-conversion emission against power density clearly shows that the transition from weak to strong up-conversion for the system composed of **2h** (3.8x10^{-4} M) and **PtOEP** (1.5x10^{-5} M) occurs at a power density of around 4 W.cm^{-2} when excited with 532 nm photons.

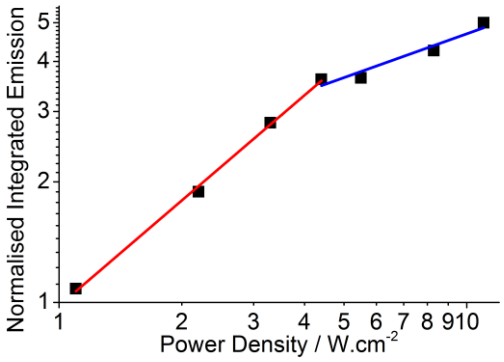

Figure 3.22 : Normalised integrated up-conversion emission against power density of **2h** and **PtOEP** (black) with linear fit lines of weak up-conversion limit (red) and strong up-conversion limit (blue).

The same system, **2h** and **PtOEP**, with the emitter at much lower concentration, was tested using the same experimental apparatus and the spectra and up-conversion quantum yields measured with varying illumination intensity (Figure 3.23).

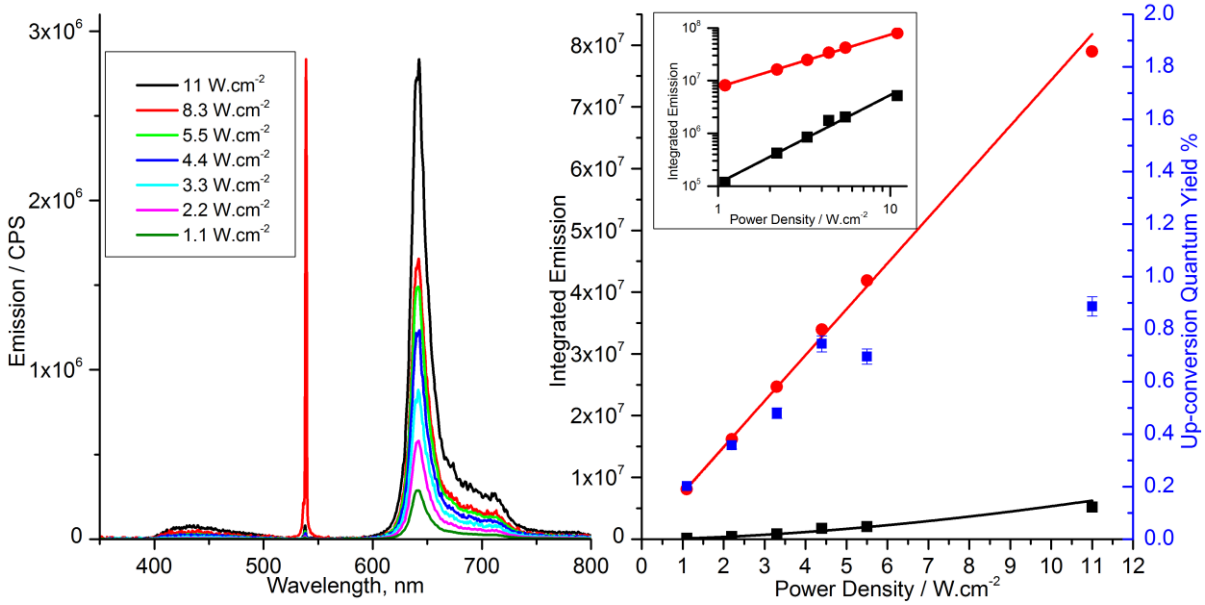

Figure 3.23 : Up-conversion emission spectra (left) and Integrated emission of up-conversion emission (black) and unquenched sensitizer emission (red) with double log plot inset (right) of **2h** (1.5×10^{-5} M) and **PtOEP** (1.5×10^{-5} M) in dry, degassed toluene, excited with varying intensity 532 nm coherent light

At lower concentration, with a 1:1 ratio of **2h** and **PtOEP** the phosphorescence is very poorly quenched, having a higher intensity emission that the associated up-conversion. Again the double logarithm plot shows the linear relationship between phosphorescence and excitation intensity (gradient 1.0), and the exponential relationship between up-conversion emission and excitation intensity is seen (Figure 3.23), attenuated to a lesser extent due to lower concentration by the early onset of the strong up-conversion limit (gradient 1.6). These measurements were taken towards the limit of the sensitivity of the spectrometer, therefore the weak up-conversion limit cannot be effectively probed in this case.

3.3.2. Stern-Vollmer quenching analysis of 9,10-di-((4-trifluoromethyl)perfluorophenyl)anthracene **(2h)**

By comparing the phosphorescent behaviour of the sensitizer both alone and in the presence of differing concentrations of the emitter (quencher) molecule the Stern-Vollmer quenching coefficient, and thus the bimolecular quenching coefficient, can be assessed. This allows a direct measurement of the efficiency of the TTT step in the TTAUC mechanism.

$$\tau_0/\tau = I_0/I = 1 + K_{SV}[Q] \qquad (3.3)$$

The data above can be used to access the Stern-Vollmer coefficient by a plot of sensitizer emission alone, divided by sensitizer emission in the presence of quencher, plotted against quencher concentration.

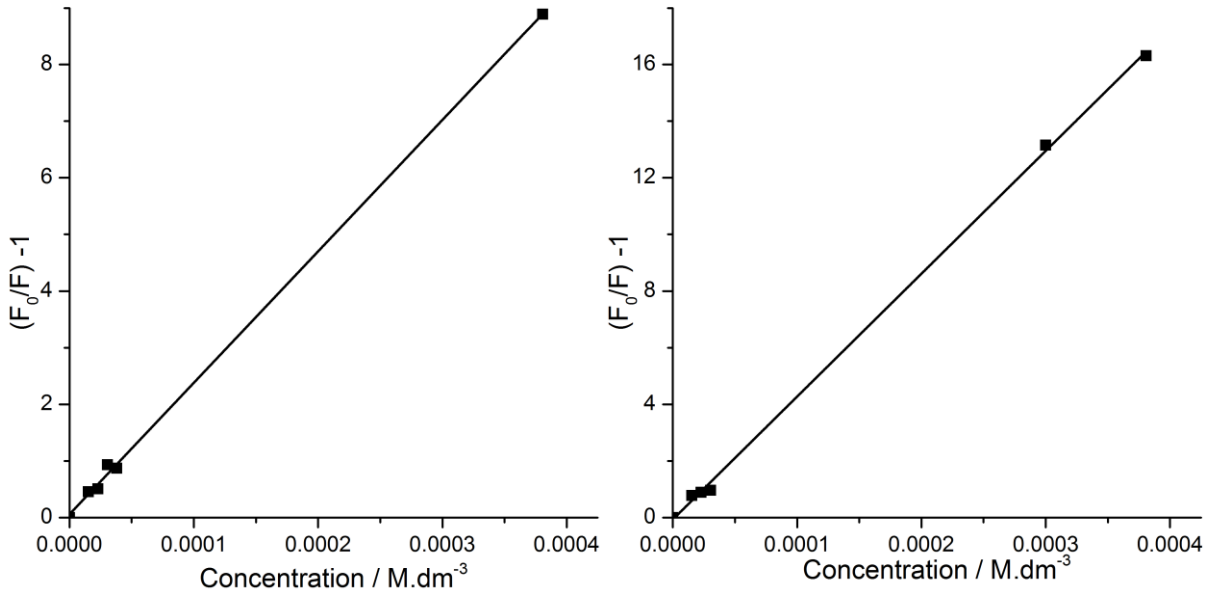

Figure 3.24 : Stern-Vollmer plots of **PdOEP** and **2h** (left) and **PtOEP** and **2h** (right) in dry, degassed toluene

The gradients and associated Stern-Vollmer coefficients for **2h** quenching **PdOEP and PtOEP** are 23200 M^{-1} and 43400 M^{-1} respectively.

$$K_{SV} = k_q \tau_0 \qquad (3.4)$$

Using literature values[9,10] of the lifetimes (**PdOEP** = 460 μs **, PtOEP** = 90 μs**)** the bimolecular quenching coefficients of 0.05 $x10^{-9}$ $M^{-1}.s^{-1}$ and 0.48 $x10^{-9}$ $M^{-1}.s^{-1}$ can be found, these are similar to literature values for DPA and the sensitizers $0.07x10^{-9}$ $M^{-1}.s^{-1}$ and 1.01 $x10^{-9}$ $M^{-1}.s^{-1}$ respectively.[9] It is clear that fluorinated emitter **2h** quenches the sensitizers to a lesser extent than the non-fluorinated analogue **2a** (DPA).

3.4. Conclusion

Emitters composed of fluorinated 9-phenylanthracenes and 9,10-bisphenylanthracenes were assessed for their photophysical properties – the 9,10-bisphenylanthracenes show higher fluorescence quantum yields, which is important for their associated up-conversion yields. The two emitter dyes with the highest fluorescence yields, non-fluorinated literature compound 9,10-diphenylanthracene (**2a**) and 9,10-di-((4-trifluoromethyl)perfluorophenyl)anthracene (**2h**) were spin coated onto glass slides and subjected to concentrated UV light – the highly fluorinated analogue was shown to be much more resilient to photodegradation. For each of the two series the up-conversion ability of the non-fluorinated literature compound was compared to the highly fluorinated analogue when paired with the common triplet sensitizers **PdOEP** and **PtOEP**. In both cases the non-fluorinated compound shows a higher up-conversion quantum yield, and the sensitizer **PtOEP** is more effective than **PdOEP**, **1a** and **2a** showed better up-conversion capabilities than **1h** and **2h** respectively.

The highly fluorinated compound **2h** was investigated more closely to assess its up-conversion ability with both **PdOEP** and **PtOEP**. The maximum external up-conversion quantum yield of **2h** (3.8×10^{-4} M) was 5.2%, when paired with **PtOEP** (1.5×10^{-5} M) and excited with 532 nm 11 $W.cm^{-2}$ coherent photons. A clear exponential relationship was seen for the up-conversion phenomenon, but the early onset of the strong up-conversion limit caused a deviation at power densities as low as 4 $W.cm^{-2}$.

The bimolecular quenching coefficient of **2h** is comparable to literature values of the **2a** with the same sensitizers, but it is clear that the TTT step is not carried out as efficiently by the fluorinated analogue.

It is clear that for green-blue up-conversion the **PtOEP** and DPA system has the highest up-conversion and overall energy efficiency, however for devices which require increased resistance to degradation the use of **2h** would be a viable alternative, with slightly decreased up-conversion capability, offset by significantly increased stability and device lifetime.

In the ideal up-conversion system, the deviation from an exponential to a linear relationship between emission and excitations intensities would occur as early as possible. The strong up-conversion limit shows that the system is operating at peak efficiency, indeed an extremely effective TTAUCS would be expected to have a peak up-conversion yield at an excitation intensity close to the transition between weak and strong up-conversion limits.

3.5. Experimental

Adsorption measurements were obtained with a Varian Cary 50 Scan UV-visable spectrometer, emission and excitation measurements were obtained with a Horiba Scientific Fluoromax 4 spectrometer. Fluorescence emission measurements were taken using a Fluoromax-4 spectrometer, and fluorescence quantum yields were obtained using an integrating quantum sphere accessory.

The up-conversion measurements were taken in flat walled tubes of dimensions 50×5×2.5 mm containing solutions of dry, degassed toluene and the dyes, excited by a laser diode with filters allowing 1 mW (10 $mW.cm^{-2}$) and 100 μW ($1mW.cm^{-2}$) incident light at the experiment area. Up-conversion emission was measured by a SR-303i Andor spectrograph.

Solutions of the dye compounds (1 $g.ml^{-1}$) were prepared in toluene and samples taken using pipettes and diluted to required concentrations. Samples that required degassing were prepared from freeze-pump-thaw degassed toluene in a glove box under nitrogen and sealed in flat walled tubes using UV activated glue.

The use of the laser set up is detailed in the text, and was developed by Sony MSL.

(1) Chen, H. C.; Hung, C. Y.; Wang, K. H.; September, W. S. F. D.; Chien, F. C.; Chen, P.; Chow, T. J.; Hsu, C. P.; Sun, S. S.; others White-light emission from an upconverted emission with an organic triplet sensitizer. *Chem. Commun.* **2009**, 4064–4066.

(2) Islangulov, R. R.; Kozlov, D. V.; Castellano, F. N. Low power upconversion using MLCT sensitizers. *Chem. Commun.* **2005**, *30*, 3776–3778.

(3) Khnayzer, R. S.; Blumhoff, J.; Harrington, J. A.; Haefele, A.; Deng, F.; Castellano, F. N. Upconversion-powered photoelectrochemistry. *Chem. Commun.* **2012**, *48*, 209–211.

(4) Monguzzi, A.; Frigoli, M.; Larpent, C.; Tubino, R.; Meinardi, F. Low-Power-Photon Up-Conversion in Dual-Dye-Loaded Polymer Nanoparticles. *Adv. Funct. Mater.* **2012**, *22*, 139–143.

(5) Liu, Q.; Yang, T.; Feng, W.; Li, F. Blue-emissive upconversion nanoparticles for low-power-excited bioimaging in vivo. *J. Am. Chem. Soc.* **2012**, *134*, 5390–5397.

(6) Berlman, I. B. *Handbook of Fluorescence Spectra of Aromatic Molecules*; ACS Publications, 1971.

(7) Islangulov, R. R.; Castellano, F. N. Photochemical Upconversion: Anthracene Dimerization Sensitized to Visible Light by a RuII Chromophore. *Angew. Chem. Int. Edit.* **2006**, *118*, 6103–6105.

(8) Hirshberg, Y. The absorption spectra of phenylated anthracenes. *Transactions of the Faraday Society* **1948**, *44*, 285–289.

(9) Penconi, M.; Ortica, F.; Elisei, F.; Gentili, P. L. New molecular pairs for low power non-coherent triplet-triplet annihilation based upconversion: dependence on the triplet energies

of sensitizer and emitter. *J. Lumin.* **2012**, *135*, 265–270.

(10) Bansal, A.-K.; Holzer, W.; Penzkofer, A.; Tsuboi, T. Absorption and emission spectroscopic characterization of platinum-octaethyl-porphyrin (PtOEP). *Chem. Phys.* **2006**, *330*, 118–129.

4. Synthesis of perylene based emitters

The previous investigation of the triplet-triplet annihilation up-conversion capabilities of phenylanthracenes (Chapter 3) showed that increasing the fluorination of the phenyl periphery produces different effects depending on the position of fluorination: TTAUCSs using di-phenylanthracene emitters produce up-converted blue light from incident green light. However, for a number of applications, including solar photovoltaic devices, a TTAUCS that could convert incident red light into higher energy light (e.g. green) could be highly beneficial. One emitter compound that has shown promise in such up-conversion applications is perylene (Chapter 1), which up-converts red light into blue.[1] Modification of the perylene core PAH unit by addition of fluorinated phenyl groups in a similar manner to that used by the author with anthracene (Chapter 2) could red shift the absorption and emission of the bisphenylperylene emitters into the green region of the visible spectrum, and provide improved stability to TTAUC systems for device fabrication.

Perylene is a widely used PAH structure commonly used in synthetic dyes due to its extremely high stability and quantum yield, low band gap, and low lying triplet level. Due to its flat hydrocarbon structure it is poorly soluble in organic solvents, thus many dyes use side chains added to the molecule such as diisobutyl perylene-3,9-dicarboxylate (Solvent Green) or extension of the π-system by amide groups in Rylene dyes.

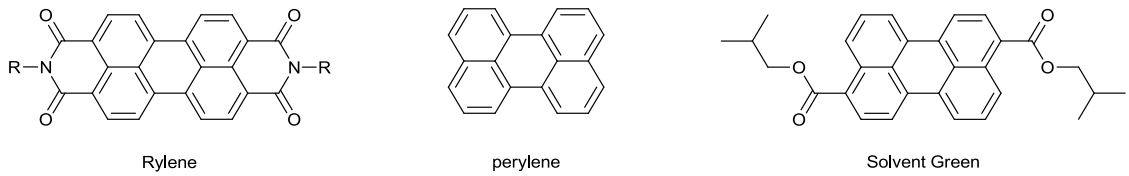

Figure 4.1 : Structure of perylene, as well as common dyes Rylene and Solvent Green

While functionalised perylenes may be synthesised from naphthalene compounds it is common to brominate perylene and then conduct normal cross-coupling and substitution reactions to produce perylene derivatives.[2]

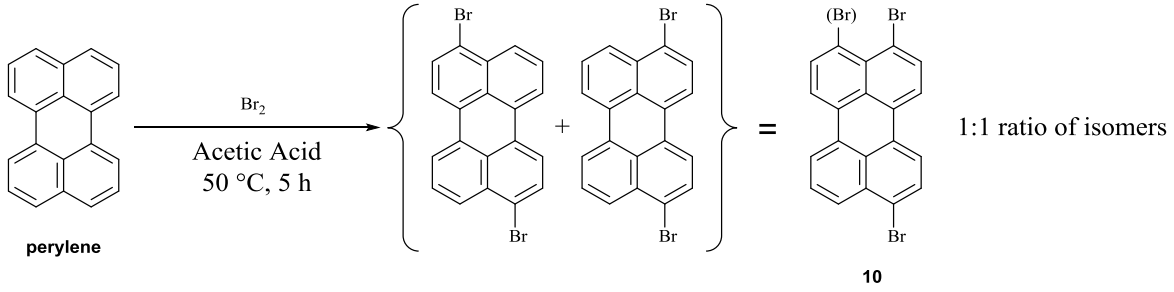

Figure 4.2 : Synthesis of dibromoperylene

4.1. Aims and Approach

In analogy to the phenylanthracene emitter molecules previously synthesised (Chapter 2) a range of diphenylperylene emitter molecules were chosen as synthetic targets (Figure 4.3) to assess their TTAUC properties for red to green up-conversion.

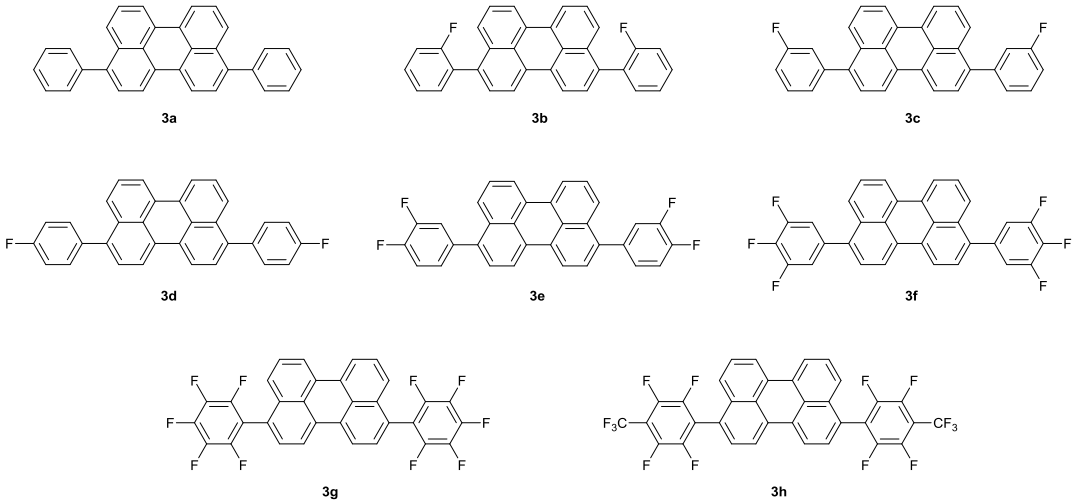

Figure 4.3 : Bisarylperylenes. The 3,9-disubstituted perylene isomers have been omitted for clarity.

Retrosynthetic analysis (Figure 4.4) for the preparation of bisfluoroarylperylene systems may be focussed on the functionalization of the complete perylene moiety, rather than by ring forming reactions, since perylene is readily available. The key aryl-perylene connection may be formed either by palladium catalysed Suzuki-Miyaura reactions involving coupling between either a perylene boronic acid and an appropriate fluoroaryl bromide or a bromo-perylene and a fluoroaryl boronic acid, palladium catalysed carbon-hydrogen bond activation of either the aryl or perylene fragment, or nucleophilic aromatic substitution (S_NAr) processes. The choice of method would depend upon the structure desired and level of fluorination of the fluoroaryl subunit.

Perylene boronic acids are not commercially available, while the boronic acids of the required fluorinated phenyl derivatives are widely available, so the Suzuki-Miyaura coupling route chosen involved reactions of dibromoperylene. The production of a perylene boronic acid system requires a halogenated precursor, thus using phenylboronic acids removes a synthesis step. Highly fluorinated phenylboronic acids are generally less reactive, and more susceptible to deboronation, while highly fluorinated aromatic systems may undergo S_NAr, making these two approaches complementary. While CH activation processes could theoretically be used to produce the perylene phenyl C-C bond, due to their lack of utility for anthracene substrates (Chapter 2) these were not investigated in detail for bisphenylperylene synthesis.

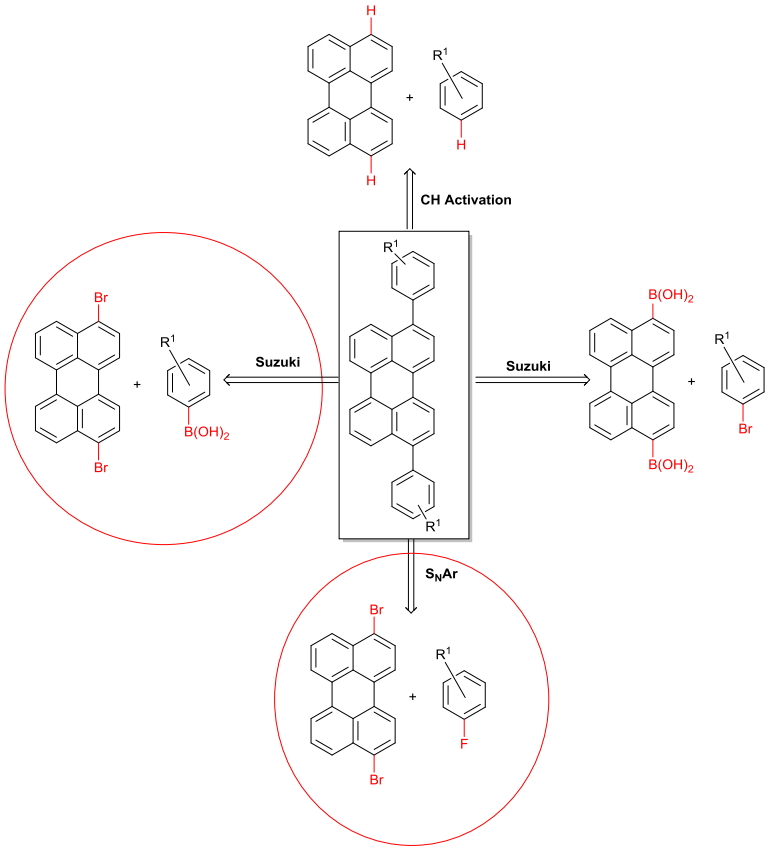

Figure 4.4 : Retrosynthetic analysis of bis-phenylperylene analogue synthesis

4.2. Synthesis of bisphenylperylenes

Perylene was brominated by elemental bromine in acetic acid, affording an inseparable mixture of 3,9-dibromoperylene and 3,10-dibromoperylene, generally denoted as 3,9(10)-dibromoperylene, in 98% yield (Figure 4.5), in agreement with literature data.[2] Since the separation of these two isomers is arduous and associated with extremely large yield losses, the mixture of isomers was used as obtained in all subsequent reactions.[3]

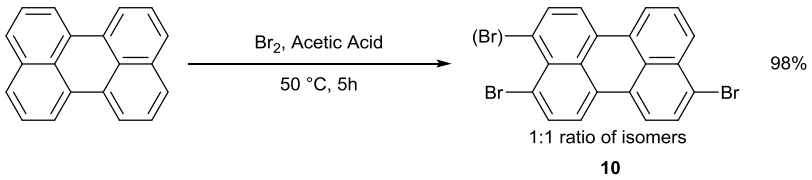

Figure 4.5 : Synthesis of dibromoperylene starting material

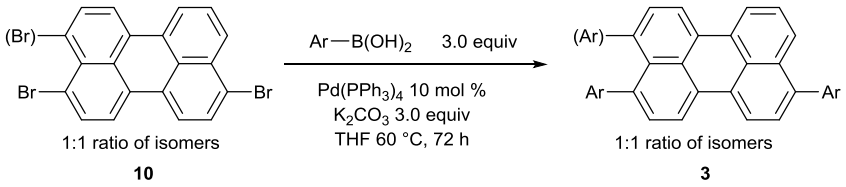

Boronic Acid	Bisphenylperylene product	Yield
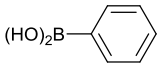	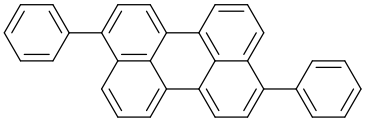	**3a**, 21%
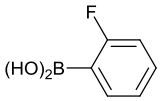	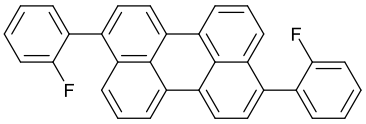	**3b**, 26%
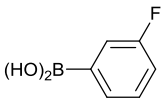	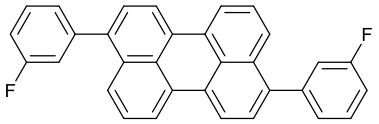	**3c**, 57%
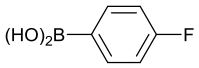	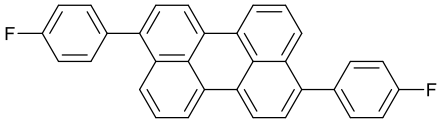	**3d**, 20%
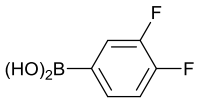	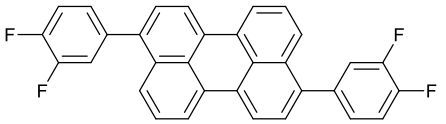	**3e**, 18%
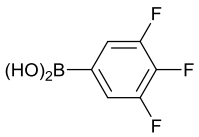	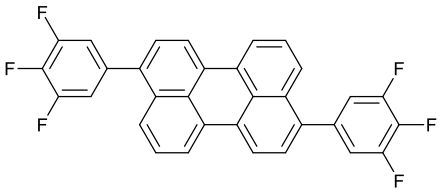	**3f**, 52%
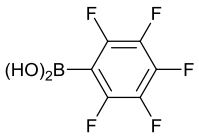	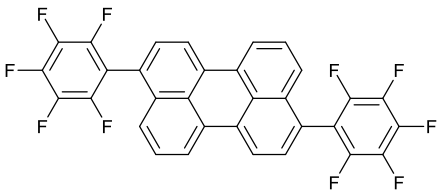	**3g**, 0%

Figure 4.6 : Suzuki-Miyaura synthesis of *bis*-phenylperylenes

The 3,9(10)-dibromoperylene starting material **10** reacted with an excess of phenyl boronic acid derivative, catalysed by $Pd(PPh_3)_4$. The reactions were monitored by TLC and ^{19}F NMR and extraction and recrystallization from toluene gave the pure products **3a-f**.

Due to competing protodeboronation of highly fluorinated boronic acids, attempts to synthesise 3,9(10)-*bis*(perfluorophenyl)perylene (**3g**) by analogous Suzuki-Miyaura processes were unsuccessful. Consequently, S_NAr processes were assessed (Scheme 1) in the same manner as for diphenylanthracene emitters (Chapter 2). Reaction of butyllithium with dibromoperylene gave

carbanionic perylene nucleophiles which gave **3g-h** upon addition of hexafluorobenzene and octafluorotoluene respectively. Hexafluorobenzene gave significant quantities of polymeric material leading to a low yield of **3g**, while substitution reaction of octafluorotoluene gave **3h** arising from substitution at the site *para* to the trifluoromethyl group only, consistent with well established principles.

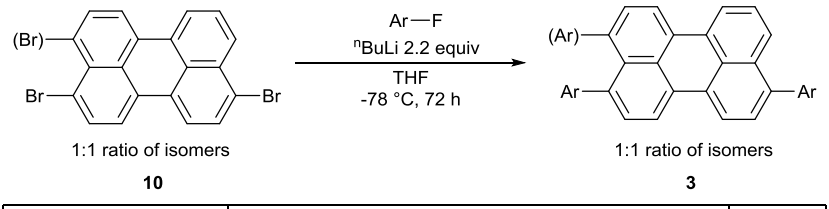

Arylfluoride derivative	Bisphenylperylene product	Yield
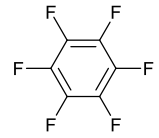	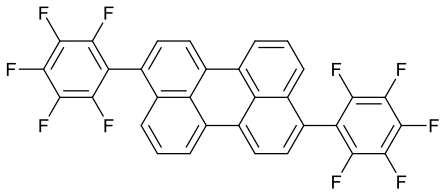	**3g**, 7%
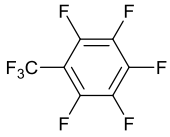	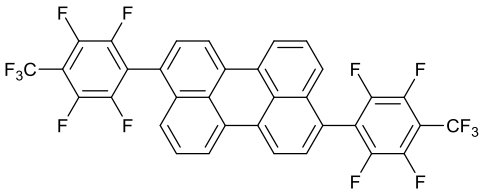	**3h**, 16%

Figure 4.7 : S_NAr synthesis of highly fluorinated *bis*-phenylperylenes

Each of the products **3a-h** were characterised by ^{1}H, ^{13}C and ^{19}F NMR, low resolution mass spectrometry (ASAP^{+}), high resolution mass spectrometry (HRMS-ASAP^{+}), IR, and thermogravimetric analysis.

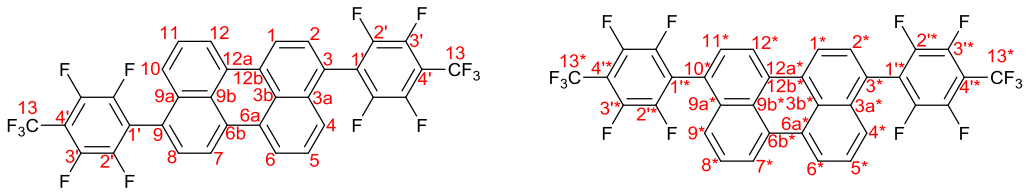

Figure 4.8 : **3h** with atomic numbering

The characterisation of compounds **3a-h** by NMR techniques is non-trivial, since necessarily from the synthesis there is a mixture of structural isomers which give peaks that overlap significantly making unambiguous assignments by ^{1}H and ^{13}C NMR very difficult. The numbering of both 3,9-*bis*-((4-trifluoromethyl)perfluorophenyl)perylene and 3,10-*bis*-((4-trifluoromethyl)perfluorophenyl) perylene is shown (Figure 4.8).

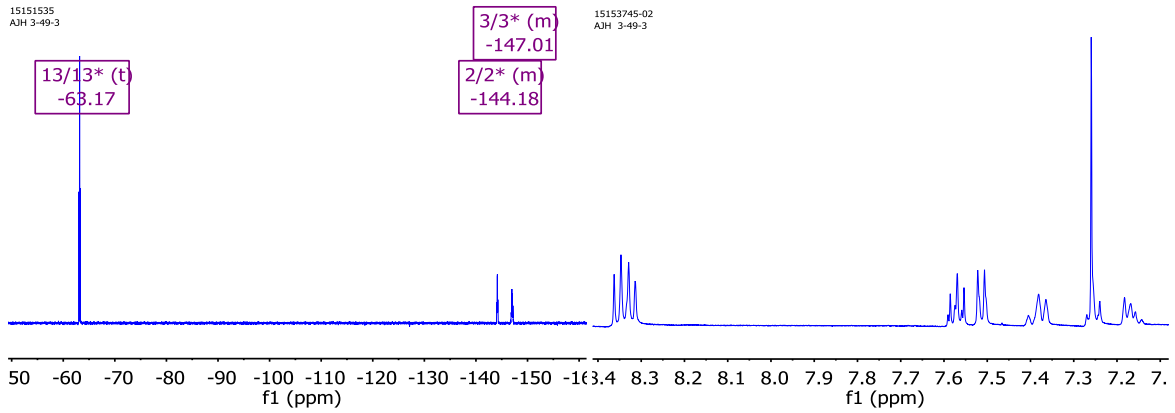

Figure 4.9 : ^{19}F (left) and ^{1}H (right) NMR Spectra of **3h**

The proton, ^{13}C NMR and COSY spectra show considerable overlap between peaks originating from both isomers of **3h**. The ^{19}F NMR spectrum has clear peaks attributable to the fluorine environments.

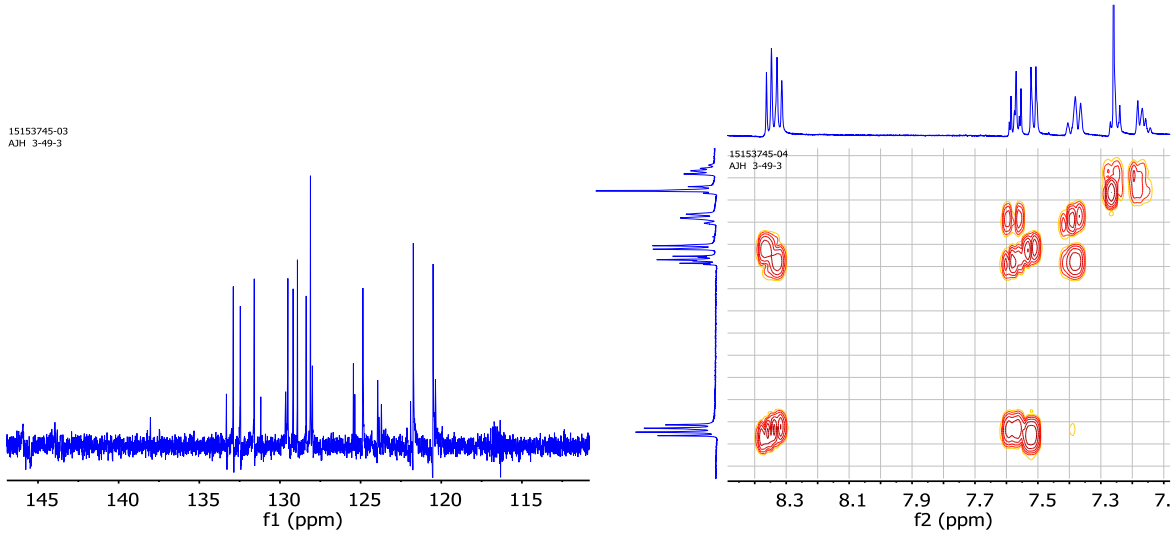

Figure 4.10 : 13C (left) and COSY (right) NMR spectra of **3h**

As well as the difficulties in NMR assignment sublimation is also apparent when taking melting points, making these less informative than thermogravimetric analysis. Atmospheric solids analysis probe (ASAP) mass spectrometry and High Resolution Mass Spectrometry (HRMS) was instrumental in the analysis of these compounds.

Single crystals of **3b** were obtained by slow evaporation of a bi-phase solution of water and DCM and the structure was confirmed by X-ray crystallography. The structure contains two independent molecules of the 3,9-*bis*-(2-fluoro)phenylperylene isomer, differing by orientation of terminal aryl rings where one is located at the centre of symmetry, this combination was found in each crystal tested. Crystals of the 3,10-*bis*-(2-fluoro)phenylperylene isomer were not obtained or measured by X-ray crystallography: the 3,9-*bis*-(2-fluoro)phenylperylene and 3,10-*bis*-(2-fluoro)phenylperylene

isomers were, in this case, separated by crystallization but in very low yield, in agreement with precedent for separation of isomers of dibromoperylene.[3]

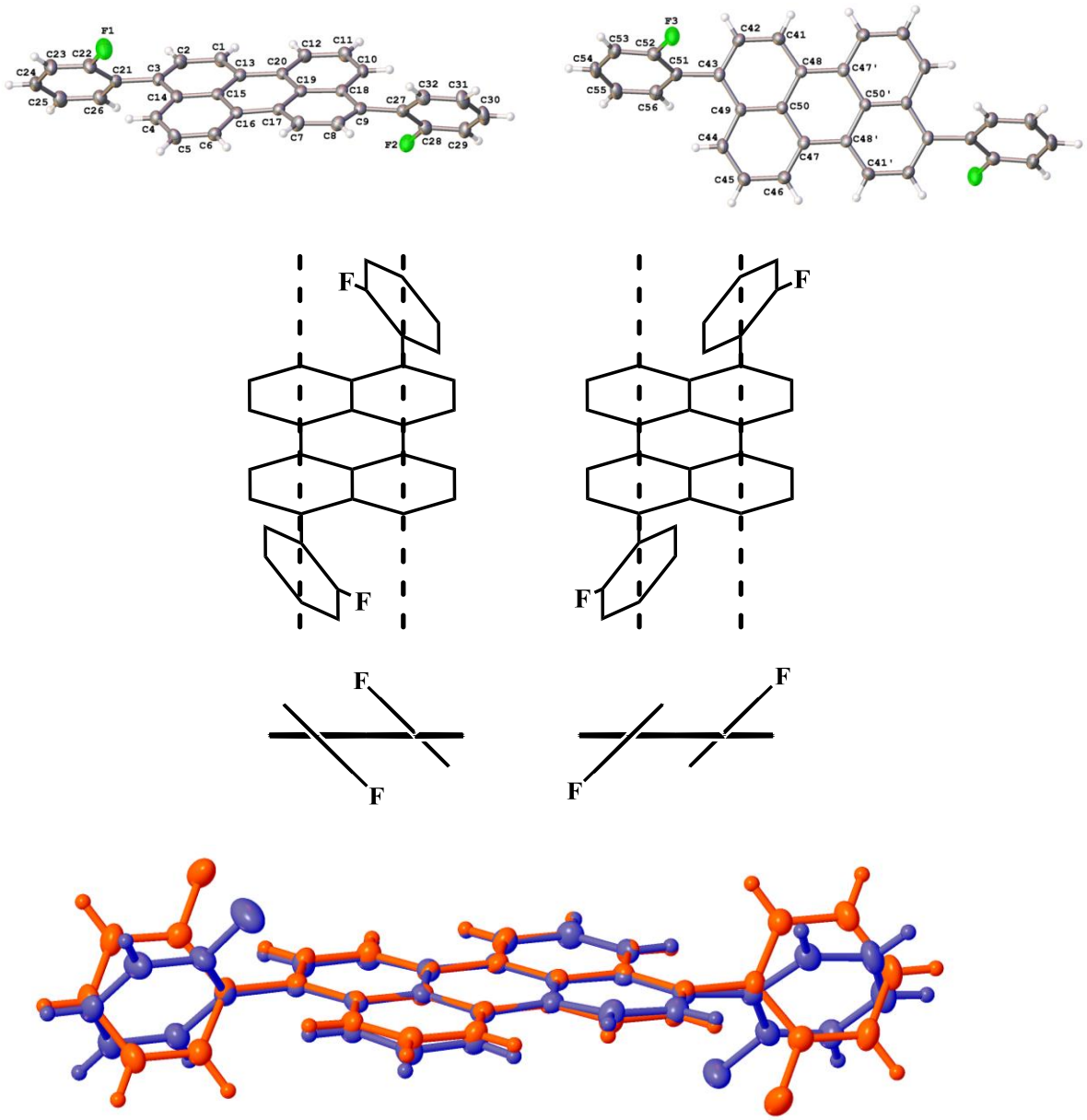

Figure 4.11 : Molecular structures of isomers of 3,9-di-(2-fluorophenyl)perylene (top), cartoons indicating the orientation of the phenyl rings – double bonds have been omitted for clarity, and overlap projection of figures showing restricted rotation of the isomers (bottom)

The cartoons in Figure 4.11 indicate the restricted rotation of the phenyl periphery present in compound **3b**, with one isomer having both fluorine atoms on a central plane (left), and the other with both fluorine atoms pointing towards the exterior of the molecule (right). This is further illustrated by the overlap projection (Figure 4.11, bottom) of the two constricted isomers - inward pointing fluorine atoms isomer (blue) and outward pointing fluorine atoms isomer (orange). It may be assumed that the restricted rotation of other emitters with *ortho* fluorine atoms **3g-h** is occurring,

but since both *ortho* positions are equivalent (containing fluorine atoms) there would be no different isomers formed by the constricted rotation.

4.3. Conclusion

A series of bis-phenylperylene emitter molecules have been synthesised with a view to their use in TTAUCSs. While phenyl groups possessing between 0-3 fluorine atoms could be coupled with the dibromoperylene using Suzuki-Miyaura protocols, these failed when applied to more highly fluorinated boronic acids. This effect had been seen before in the production of fluorinated bisphenylanthracene emitters, and so S_NAr routes were applied to produce the emitters with highly fluorinated periphery **3g-h**.

4.4. Experimental

***10**, 3,9(10)-dibromoperylene*

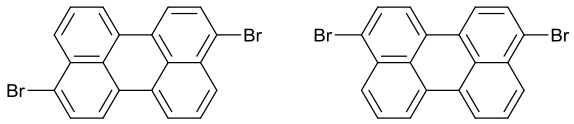

Bromine (1.32 g, 8.2 mmol, 0.43 ml) was added to a solution of perylene (1.05 g, 4.0 mmol) in conc. Acetic acid (30 ml) at 40 °C over 15 min. The reaction mixture was stirred at 50 °C for 5 h. After cooling to room temperature the dibromoperylene was collected by filtration, washed first with water and then with aqueous sodium bisulfite solution. Recrystallization gave 3,9(10)-dibromoperylene (1.87 g, 98 %) as an ochre powder; TGA: sublimation onset 309.58 °C; Anal. Calcd for $C_{20}H_{10}Br_2$: C, 58.57; H, 2.46. Found: C, 58.52; H, 2.44; IR ν_{max} /cm^{-1} 3050(w), 1493(m), 1377(m), 1194 (m); ^{1}H NMR (600 MHz, $CDCl_3$) δ 8.18 – 8.28 (2H, 2 d, *J* 7.0), 8.09 – 8.14 (2H, 2 dd, *J* 8.4, 2.5), 7.94 – 8.03 (2H, 2 d, *J* 8.1), 7.75 – 7.79 (2H, 2 d, *J* 7.0), 7.56 – 7.62 (2H, 2 t, *J* 7.5); ^{13}C NMR (151 MHz, $CDCl_3$) δ 133.17, 131.27, 131.09, 130.97, 130.92, 130.81, 130.63, 129.58, 128.02, 127.96, 127.60, 127.54, 123.16, 123.13, 121.73, 121.48, 121.18, 120.91; MS (ASAP+) m/z: 410 (M^+, 100%); 412 (50); 408 (40); 413 (20). Data in agreement with the literature.[3]

***3a,** 3,9(10)-bisphenylperylene*

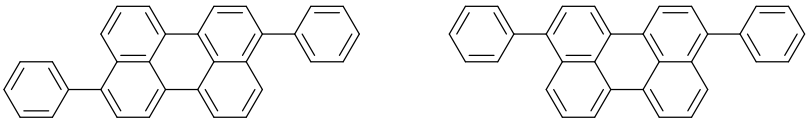

A solution of **(10)** (0.128 g, 0.312 mmol), phenylboronic acid (0.083 g, 0.68 mmol), potassium carbonate (0.091 g, 0.66 mmol) and $Pd(PPh_3)_4$ (18 mg, 0.016 mmol) in degassed THF (10 ml) were heated to reflux under an atmosphere of argon for 72 h. A second portion of phenylboronic acid (0.500 g, 4.10 mmol) was added, and the heating continued for a further 24 h. The solution was

diluted with H_2O, extracted with toluene, and the organics washed, dried and filtered through celite and evaporated to dryness. Recrystallization gave the mixture of isomers 3,9(10)-bisphenylperylene (0.027 g, 21%) as an ochre solid; TGA: sublimation onset 306.99 °C; Anal. Calcd for $C_{32}H_{20}$: C, 95.02; H, 4.98. Found: C, 94.11; H, 4.98; IR ν_{max} /cm^{-1} 3052(vw), 14910(vw), 1393(vw); ^{1}H NMR (600 MHz, $CDCl_3$) δ 8.30 – 8.22 (4H, m), 7.78 (2H, d, $^3J_{HH}$ 8.4), 7.57 – 7.50 (8H, m), 7.48 – 7.42 (6H, m); ^{13}C NMR (151 MHz, $CDCl_3$) δ 140.91 (d, $^2J_{CH}$ 1.9), 140.09 (d, $^2J_{CH}$ 6.0), 133.06, 131.74, 131.57, 130.98, 130.81, 130.12, 129.10, 128.55, 127.97 (m), 127.53, 126.74, 126.22, 126.19, 120.64, 120.41, 120.21, 119.99; MS (ASAP+) *m/z*: 404.1 (M^+, 100%).

***3b**, 3,9(10)-bis(2-fluorophenyl)perylene*

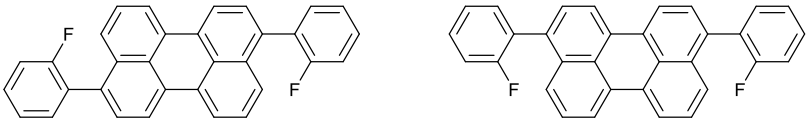

A solution of **(10)** (0.507 g, 1.24 mmol), 2-fluorophenylboronic acid (0.544 g, 3.89 mmol), potassium carbonate (0.580 g, 4.20 mmol) and $Pd(PPh_3)_4$ (0.204 g, 0.173 mmol) in degassed THF (20 ml) and H_2O (1 ml) were heated to 55 °C under an atmosphere of argon for 72 h. A second portion of 2-fluorophenylboronic acid (0.188 g, 1.34 mmol), and the heating continued for a further 24 h. The solution was diluted with H_2O, extracted with toluene, and the organics washed, dried and filtered through celite and evaporated to dryness. Recrystallization gave the mixture of isomers 3,9(10)-bis(2-fluorophenyl)perylene (0.139 g, 26%) as an ochre solid; TGA: sublimation onset 313.70 °C; IR νmax /cm^{-1} 3206(w), 1584(vw), 1488(m), 1450(s), 1394(m), 1206(s; ^{1}H NMR (700 MHz, $CDCl_3$) δ 8.28 (4H, dd, $^3J_{HH}$ 9.0, $^3J_{HH}$ 7.3), 7.57 – 7.52 (2H, m), 7.51 – 7.41 (8H, m), 7.31 (2H, dd, $^3J_{HH}$ 7.4, $^4J_{HH}$ 1.3), 7.26 – 7.21 (2H, m); ^{13}C NMR (176 MHz, $CDCl_3$) δ 160.10 (d, $^1J_{CF}$ 246), 133.55 , 133.02 , 132.28 (d, $^3J_{CF}$ 3), 131.36 (d, $^2J_{CF}$ 33), 129.52 (d, $^2J_{CF}$ 8), 128.70 , 128.50 , 127.95 (d, $^2J_{CF}$ 16.2), 126.77 , 126.75 , 125.95 , 124.17 , 120.88 – 119.54 (m), 115.80 (d, $^2J_{CF}$ 22); ^{19}F NMR (376 MHz, $CDCl_3$) δ -113.69 (d, $^1J_{CF}$ 40); HRMS (TOF ASAP$^+$), Calcd for $[C_{32}H_{18}F_2+H]^+$: 441.1455. Found *m/z*: 441.1443.

***3c**, 3,9(10)-bis(3-fluorophenyl)perylene*

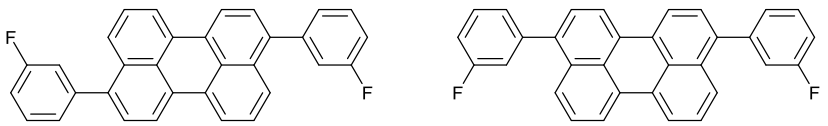

A solution of **(2)** (0.498 g, 1.22 mmol), 3-fluorophenylboronic acid (0.512 g, 3.66 mmol), potassium carbonate (0.505 g, 3.66 mmol) and $Pd(PPh_3)_4$ (225 mg, 0.194 mmol) in degassed THF (20 ml) and H_2O (1 ml) were heated to 55 °C under an atmosphere of argon for 72 h. A second portion of 3-fluorophenylboronic acid (0.207 g, 1.48 mmol), and the heating continued for a further 24 h. The solution was diluted with H_2O, extracted with toluene, and the organics washed, dried

and filtered through celite and evaporated to dryness. Recrystallization gave the mixture of isomers 3,9(10)-bis(3-fluorophenyl)perylene (0.305 g, 57%) as an ochre solid; TGA: sublimation onset 283.36 °C; IR νmax /cm^{-1} 3184(w), 1610(vw), 1574(w), 1484(m), 1436(m), 1392(m), 1202(m); ^{1}H NMR (600 MHz, CD_2Cl_2) δ 8.31 – 8.24 (4H, m), 7.77 (2H, d, $^{3}J_{HH}$ 8.3), 7.51 – 7.44 (6H, m), 7.35 – 7.32 (2H, m), 7.26 (2H, d, $^{3}J_{HH}$ 9.7), 7.20 – 7.14 (2H, m); ^{13}C NMR (151 MHz, CD_2Cl_2) δ 163.48 (d, $^{1}J_{CF}$ 246), 143.56 (d, $^{2}J_{CF}$ 8), 139.38 (d, $^{3}J_{CF}$ 2), 139.34 (d, $^{3}J_{CF}$ 2), 135.78 (t, $^{2}J_{CF}$ 6), 135.06 (d, $^{2}J_{CF}$ 10), 133.33, 132.65 (d, $^{2}J_{CF}$ 10), 132.57 (d, $^{4}J_{CF}$ 3), 132.14, 131.92, 131.75, 131.53, 131.40, 131.32, 131.13, 130.70, 130.65, 129.52, 129.17 (d, $^{3}J_{CF}$ 12), 128.52, 127.57, 127.56, 126.51, 126.48, 126.46, 126.46, 121.04 (d, $^{1}J_{CF}$ 118), 121.04 (d, $^{2}J_{CF}$ 67), 117.49 (d, $^{3}J_{CF}$ 22), 114.92 (d, $^{2}J_{CF}$ 21); ^{19}F NMR (564 MHz, CD_2Cl_2) δ -120.26 (2F, td, $^{1}J_{CF}$ 9, $^{2}J_{CF}$ 6); HRMS (TOF ASAP^{+}), Calcd for $[C_{32}H_{18}F_2]^{+}$: 440.1377. Found *m/z*: 440.1373.

4d, *3,9(10)-bis(4-fluorophenyl)perylene*

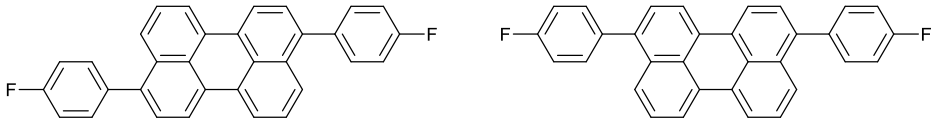

A solution of **(10)** (0.501 g, 1.22 mmol), 4-fluorophenylboronic acid (0.512 g, 3.66 mmol), potassium carbonate (0.506 g, 3.67 mmol) and $Pd(PPh_3)_4$ (212 mg, 0.183 mmol) in degassed THF (20 ml) and H_2O (1 ml) were heated to 55 °C under an atmosphere of argon for 72 h. A second portion of 4-fluorophenylboronic acid (0.170 g, 1.22 mmol), and the heating continued for a further 24 h. The solution was diluted with H_2O, extracted with toluene, and the organics washed, dried and filtered through celite and evaporated to dryness. Recrystallization gave the mixture of isomers 3,9(10)-bis(4-fluorophenyl)perylene (0.108 g, 20%) as a dark brown solid; TGA: sublimation onset >350 °C; IR νmax /cm^{-1} 3190(w), 1481(m), 1436(m), 1193(m); ^{1}H NMR (700 MHz, CD_2Cl_2) δ 8.23 (2H, d, $^{3}J_{HH}$ 7.8 Hz), 7.69 (2H, d, $^{3}J_{HH}$ 8.4), 7.57 (2H, m), 7.44 (6H, m), 7.18 (2H, t, $^{3}J_{HH}$ 8.7); ^{13}C NMR (176 MHz, CD_2Cl_2) δ 138.89, 134.34 (m), 131.51 (d, $^{2}J_{CF}$ 8), 131.28, 130.74 (m), 128.84, 127.89, 126.72, 125.80, 120.23 (d, $^{2}J_{CF}$ 52), 115.26 (d, $^{2}J_{CF}$ 21); ^{19}F NMR (188 MHz, CD_2Cl_2) δ -122.07 (m); HRMS (TOF ASAP^{+}), Calcd for $[C_{32}H_{18}F_2]^{+}$: 440.1377. Found *m/z*: 440.1364

3e, *3,9(10)-bis(3,4-difluorophenyl)perylene*

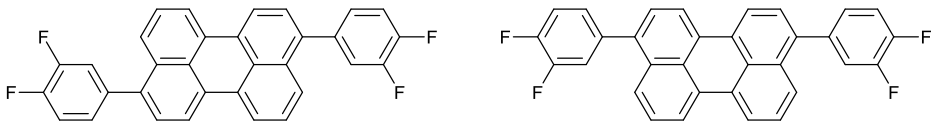

A solution of **(2)** (0.499 g, 1.22 mmol), 3,4-difluorophenylboronic acid (0.589 g, 3.73 mmol), potassium carbonate (0.515 g, 3.73 mmol) and $Pd(PPh_3)_4$ (225 g, 0.194 mmol) in degassed THF (20 ml) and H_2O (1 ml) were heated to 55 °C under an atmosphere of argon for 72 h. A second portion of 3,4-difluorophenylboronic acid (0.190 g, 1.20 mmol), and the heating continued for a

further 24 h. The solution was diluted with H_2O, extracted with toluene, and the organics washed, dried and filtered through celite and evaporated to dryness. Recrystallization gave the mixture of isomers 3,9(10)-bis(3,4-difluorophenyl)perylene (0.105 g, 18%) as a green/brown solid; TGA: sublimation onset 319.06 °C; IR ν_{max} /cm^{-1} 3190(m), 1605(w), 1518(s), 1423(s), 1391(s), 1263(s); ^{1}H NMR (700 MHz, CD_2Cl_2) δ 8.23 (4H, t, $^3J_{HH}$ 7.4), 7.68 (2H, dd, $^3J_{HH}$ 8.4, $^4J_{HH}$ 1.0 Hz), 7.45 (2H, m), 7.39 (2H, d, $^3J_{HH}$ 7.6), 7.32 (2H, m), 7.28 (2H, m), 7.22 (2H, d, $^3J_{HH}$ 10.7); ^{13}C NMR (176 MHz, CD_2Cl_2) δ 134.31 (d, $^3J_{CF}$ 10), 132.59, 131.12 (m), 130.66, 128.76, 127.89, 126.92, 126.09, 125.58, 120.61, 120.07, 118.74, 117.21 (d, $^3J_{CF}$ 17); ^{19}F NMR (188 MHz, CD_2Cl_2) δ -144.91 (1F, m), -146.80 (1F, s); HRMS (TOF ASAP$^+$), Calcd for $[C_{32}H_{16}F_4]^+$: 476.1188. Found *m/z*: 476.1180

3f, *3,9(10)-bis(3,4,5-trifluorophenyl)perylene*

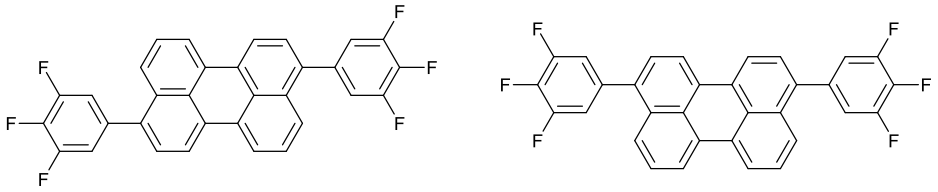

A solution of **(2)** (0.500 g, 1.22 mmol), 3,4,5-trifluorophenylboronic acid (0.650 g, 3.71 mmol), potassium carbonate (0.508 g, 3.68 mmol) and $Pd(PPh_3)_4$ (211 mg, 0.183 mmol) in degassed THF (20 ml) and H_2O (1 ml) were heated to 55 °C under an atmosphere of argon for 72 h. A second portion of 3,4,5-trifluorophenylboronic acid (0.210 g, 1.20 mmol), and the heating continued for a further 24 h. The solution was diluted with H_2O, extracted with toluene, and the organics washed, dried and filtered through celite and evaporated to dryness. Recrystallization gave the mixture of isomers 3,9(10)-bis(3,4,5-trifluorophenyl)perylene (0.420 g, 52%) as a yellow/brown solid; TGA: sublimation onset 227.21 °C; IR ν_{max} /cm^{-1} 3196(w), 1615(m), 1590(w), 1526(s), 1422(s), 1360(s), 1248(m), 1216(m); ^{1}H NMR (500 MHz, CD_2Cl_2) δ 8.24 (2H, d, $^3J_{HF}$ 7.4), 8.22 (2H, d, $^3J_{HF}$ 7.8), 7.66 (2H, d, $^3J_{HF}$ 8.0), 7.47 (2H, t, $^3J_{HF}$ 8.0), 7.38 (2H, d, $^3J_{HF}$ 7.7), 7.13 (4H, dd, $^3J_{HF}$ 8.3, $^4J_{HF}$ 6.6); ^{13}C NMR (126 MHz, CD_2Cl_2) δ 151.29 (d, $^1J_{CF}$ 250), 140.79 – 138.40 (m), 137.23, 135.33 (t, $^3J_{CF}$ 6), 132.59, 131.66, 131.41, 128.13 (14), 127.49 (8), 125.55 (7), 121.29 (13), 120.28 (9), 117.88 (d, $^4J_{CF}$ 4), 117.77 (d, $^4J_{CF}$ 4), 114.45 (d, $^4J_{CF}$ 5), 114.32 (d, $^4J_{CF}$ 5); ^{19}F NMR (564 MHz, $CDCl_3$) δ -141.33 (dd, *J* 20, 8), -168.91 (tt, $^1J_{CF}$ 20, $^2J_{CF}$ 6); HRMS (TOF ASAP$^+$), Calcd for $[C_{32}H_{14}F_6]^+$: 512.1000. Found *m/z*: 512.0999.

3g, *3,9(10)-bis(perfluorophenyl)perylene*

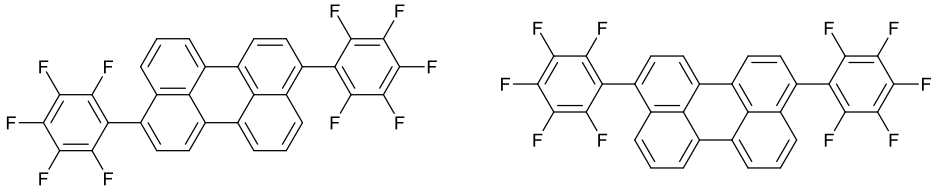

A solution of **8** (0.500 g, 1.22 mmol) in dry, degassed THF (30 ml) was cooled to -78 °C and ^{n}BuLi in hexanes (2.7 mmol) added dropwise over 15 min. After stirring at -78 °C for 2 h hexafluorobenzene (2.23 g, 12.0 mmol, 1.39 ml) was added over 10 s and the resulting solution stirred overnight to room temperature, heated to 40 °C for 2 h then allowed to cool. Following quenching with water the organic portion extracted with DCM, washed with water and brine, dried ($MgSO_4$) and evaporated to give the crude product. Recrystallization gave the mixture of isomers 3,9(10)-bis(perfluorophenyl)perylene (0.0499 g, 7 %) as a yellow/orange solid; TGA: sublimation onset 306.68 °C. Anal. Calcd for $C_{32}H_{10}F_{10}$: C, 65.71; H, 1.72. Found C, 65.71; H, 1.81; IR ν_{max} /cm^{-1} 1654(w), 1602(vw), 1522(s), 1488(vs), 1431(w), 1388(m); ^{1}H NMR (600 MHz, $CDCl_3$) δ 8.30 – 8.35 (4H, 2 d, *J* 8.0), 7.53 – 7.57 (2H, 2 t, *J* 7.9), 7.46 – 7.51 (2H, d, *J* 7.7), 3.37 – 7.41 (2H, d, *J* 8.6); ^{13}C NMR (151 MHz, $CDCl_3$) δ 132.81, 132.77, 131.09, 129.79, 128.79, 127.57, 125.19, 121.43, 120.15; ^{19}F NMR (564 MHz, $CDCl_3$) δ -146.14 (4F, dd, *J* 23, 8), -161.27 (2F, t, *J* 21), -168.49 – -168.62 (4F, m); HRMS (TOF ASAP^{+}), Calcd for $[C_{32}H_{10}F_{10}]^{+}$: 584.0623. Found *m/z*: 584.0633

3h, *3,9(10)-bis(2,3,5,6-tetrafluoro-4-(trifluoromethyl)phenyl)perylene*

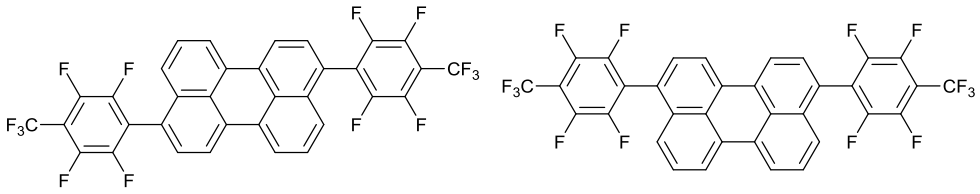

A solution of **8** (0.525 g, 1.28 mmol) in dry, degassed THF (30 ml) was cooled to -78 °C and ^{n}BuLi in hexanes (2.7 mmol) added dropwise over 15 min. After stirring at -78 °C for 2 h octafluorotoluene (1.4 g, 6.0 mmol, 0.85 ml) was added over 10 s and the resulting solution stirred overnight to room temperature, heated to 40 °C for 2 h then allowed to cool. Following quenching with water the organic portion extracted with DCM, washed with water and brine, dried ($MgSO_4$) and evaporated to give the crude product as a white solid. Recrystallization gave the mixture of isomers 3,9(10)-bis(2,3,5,6-tetrafluoro-4-(trifluoromethyl)phenyl)perylene (0.138 g, 16 %) as a yellow solid; TGA: sublimation onset 273.81 °C; IR ν_{max} /cm^{-1} 1659(w), 1600(vw), 1471(s), 1337(s), 1254(m); ^{1}H NMR (500 MHz, $CDCl_3$) δ 8.35 (2H, d, *J* 7.9), 8.32 (2H, d, *J* 7.8), 7.55 – 7.59 (2H, 2 t, *J* 7.9), 7.49 – 7.53 (2H, 2 d, *J* 7.8), 7.35 – 7.41 (2H, 2 d, *J* 8.8); ^{13}C NMR (126 MHz, $CDCl_3$) δ 146.14 – 145.29 (m), 144.35 – 142.95 (m), 132.90, 132.46, 131.60, 131.19, 129.65, 129.52, 129.19, 128.92, 128.38, 128.11, 127.99, 125.45, 125.36, 124.86, 123.94, 123.71, 121.90, 121.73, 120.50, 120.36, 118.26 – 114.92 (m); ^{19}F NMR (188 MHz, $CDCl_3$) δ -56.58 (6F, t, *J* 21.7), -137.23 – -137.87 (4F, m), -140.11 – -140.75 (4F, m); HRMS (TOF ASAP^{+}), Calcd for $[C_{34}H_{10}F_{14}]^{+}$: 684.0559. Found *m/z*: 684.0551.

(1) Singh-Rachford, T. N.; Castellano, F. N. Triplet Sensitized Red-to-Blue Photon Upconversion. *J. Phys. Chem. Lett.* **2009**, *1*, 195–200.

(2) Schlichting, P.; Rohr, U.; Mullen, K. New synthetic routes to alkyl-substituted and functionalized perylenes. *Liebigs. Ann. Chem.* **1997**, *2*, 395–407.

(3) Uchida, T.; Kozawa, K.; Nagao, Y.; Misonoo, T. Crystal and Molecular-Structure of an Isomer of Dibromoperylenes. *B. Chem. Soc. Jpn.* **1979**, *52*, 1547–1548.

5. Fluorescence and up-conversion of bisphenylperylene dyes

Perylene is a polyaromatic hydrocarbon (PAH) that is constructed by the pairing of two naphthalene molecules. This produces a flat raft structure, with 5 rings of sp^2 hybridized carbon atoms. Due to its large flat structure, perylene shows a high degree of π- π interactions, making it sparingly soluble in most organic solvents and insoluble in water.

Perylene has a fluorescence quantum yield 0.94,[1] and shows mirror image absorption and emission spectra, with the peak emission maximum at 450 nm, in the blue visible region. Perylene would be expected to be a suitable molecule for TTAUCSs, since it possesses a large triplet – singlet gap of around 1.23 eV.[2,3] When tested by Castellano *et al.* the external quantum yield of perylene was 6.5%: up-conversion was perturbed by a competing annihilation to the second triplet level and clear excimer excitation (~560 nm).[3]

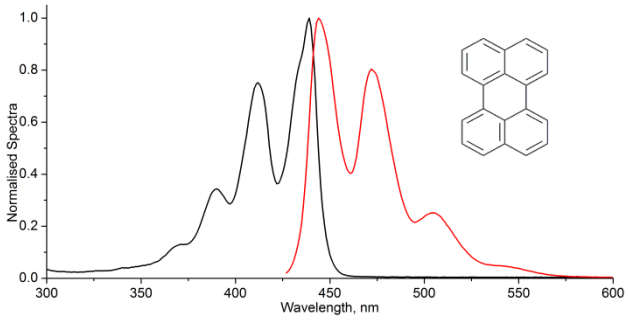

Figure 5.1 : Normalised absorption (black) and emission (red) spectra of perylene (toluene)

By functionalising the perylene structure with aromatic groups it may be possible to change the energy of the T_2 level to prevent this pathway, and prevent excimer emission (Chapter 1).

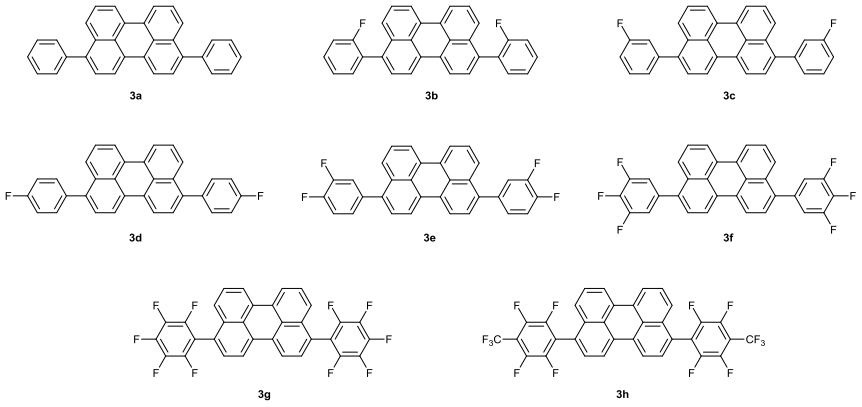

Figure 5.2 : Emitters **3a-h**, the 3,9-bisphenylperylene isomers are omitted for clarity

The emitters **3a-h** were synthesised by palladium cross coupling and nucleophilic aromatic substitution techniques, with a view to producing emitters suitable for efficient red to green up-conversion (Chapter 4). The fluorescence and up-conversion capabilities of these novel emitter molecules were tested by the author at Materials Science Laboratories in collaboration with Sony Deutschland, to ascertain their potential for uses in TTA up-conversion devices.

5.1. Fluorescence Measurements

The fluorescence properties of the bisphenylperylene dyes **3a-h** were tested in a similar manner to the anthracene based dyes (Chapter 3).

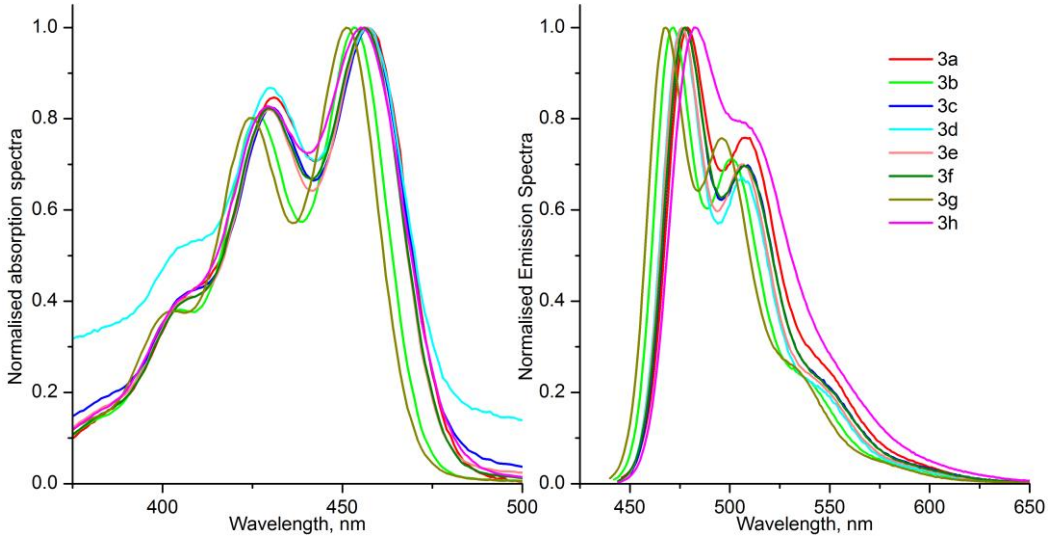

Figure 5.3 : Absorption (left) and emission (right) spectra of emitters **3a-h** in toluene

The adsorption and emission profiles of the synthesised *bis*-phenylperylene compounds **3a-h** (Figure 5.3) are similar to perylene (Figure 5.1), although the vibronic structure of the peaks is increasingly dampened with increasing fluorination. The aryl derivatives have a similar maximum emission wavelength (475 ± 10 nm), red shifted as expected when compared to perylene due to an increase in π conjugation with **3h** showing the greatest effect. Increasing the fluorination of the emitters causes a modulation in the Stokes shifts of the dyes (Figure 5.4), the highest Stokes shifts are for non-fluorinated emitter **3a** and highly fluorinated emitter **3h**.

The fluorescence quantum yields of the bisphenylperylene analogues (Figure 5.4) are in the same region as perylene itself. The highest fluorescence quantum yield is shown by the most fluorinated analogue (**3h** Φ_F = 98.2±0.8%), followed by the non-fluorinated bisphenylperylene (**3a** Φ_F = 96.8±1.2%). Interestingly the analogue bearing the perfluorophenyl periphery is among the lowest quantum yields (**3g** Φ_F = 80.6±0.3%), possibly due to increased dye-solvent π-π interactions.

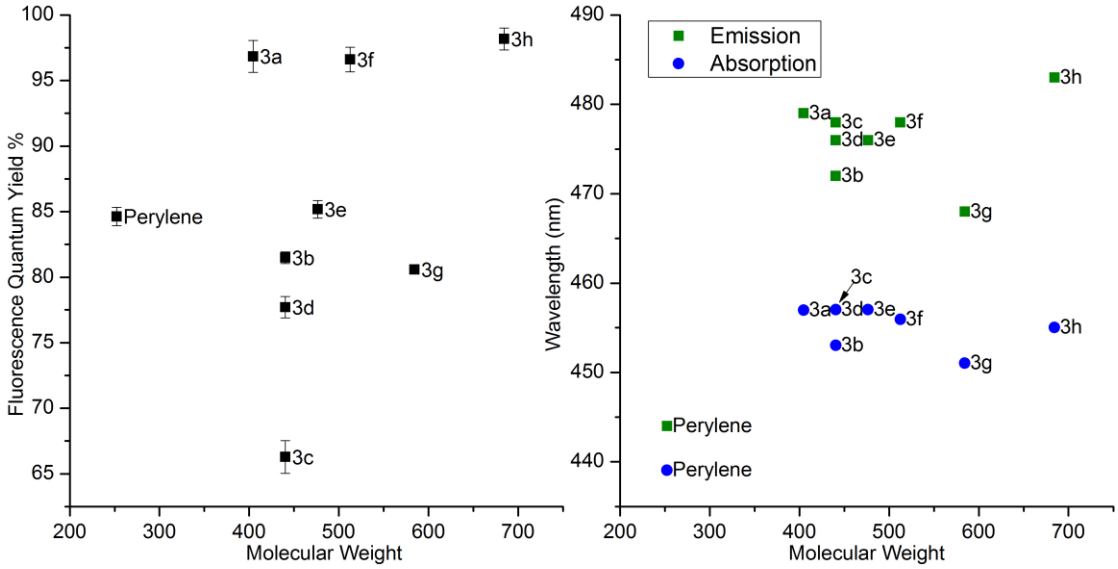

Figure 5.4 : Fluorescence quantum yield (left), and absorption (blue) and emission (green) peaks (right) of bisphenylperylenes and perylene in dry toluene. No attempt was made to exclude oxygen from the samples.

The extinction coefficient (Figure 5.5) varies considerably over the series, the two most fluorinated compounds **3g-h** giving the greatest extinction coefficient.

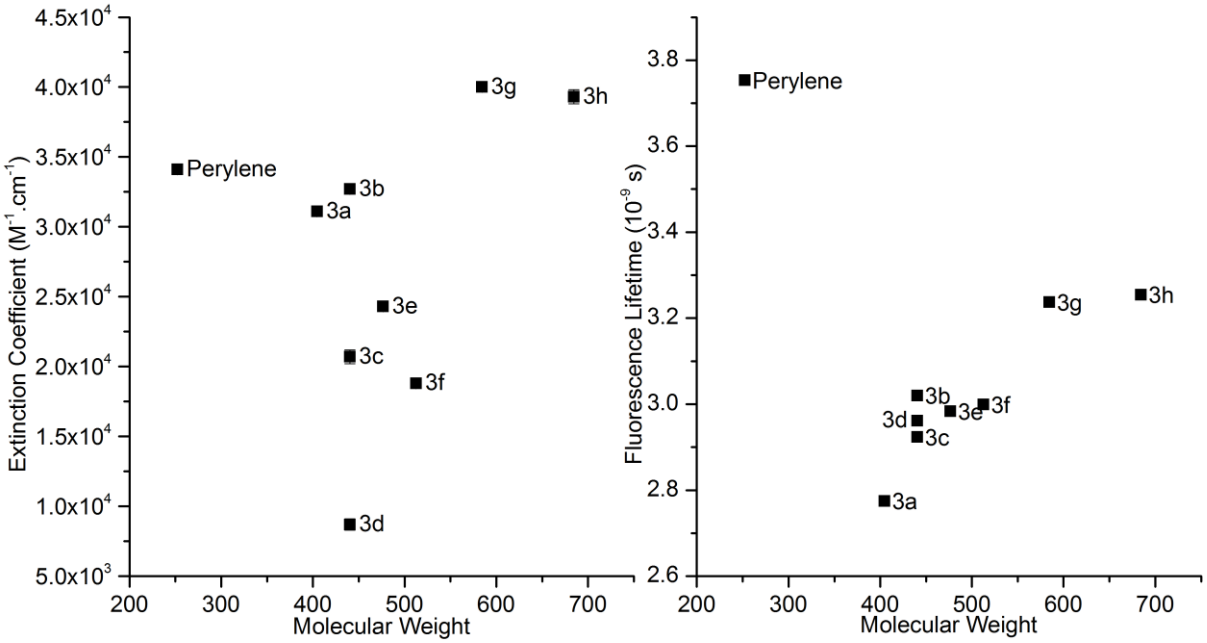

Figure 5.5 : Extinction coefficient (left) and fluorescence lifetime (right) of bisphenylperylene emitters and perylene

There appears to be a clear correlation between increasing fluorination and fluorescence lifetime of the *bis*-phenylperylene derivatives. While the degree of the fluorination on the periphery is important, the site of fluorination also has an effect and this is most clearly seen in the difference in extinction coefficient between *ortho* **(3b)**, *meta* **(3c)** and *para* **(3d)** fluorinated aryl derivatives. **3b** has an extinction coefficient similar to that of perylene itself, whilst **3d** is 20% lower. It can also be seen from the three mono-fluorinated derivatives that the site of fluorination effects the spectral

properties. In general the fluorescence lifetime increases with fluorination of the bisphenylperylene emitters (Figure 5.5).

The emitters with highest fluorescence quantum yield, **3a** and **3h,** were selected for investigation of their stability to UV light, with a view to their effectiveness in emissive devices.

5.1.1. UV degradation of bisphenylperylene emitters

Thin films of the emitters (**3a**: 1.639 μm, **3h**: 1.617 μm) in PMMA (2% weight percent) were spin coated onto glass slides, and the emitters' stability to UV degradation assessed in a similar manner to the anthracene based dyes (Chapter 3). No attempts at oxygen exclusion were made.

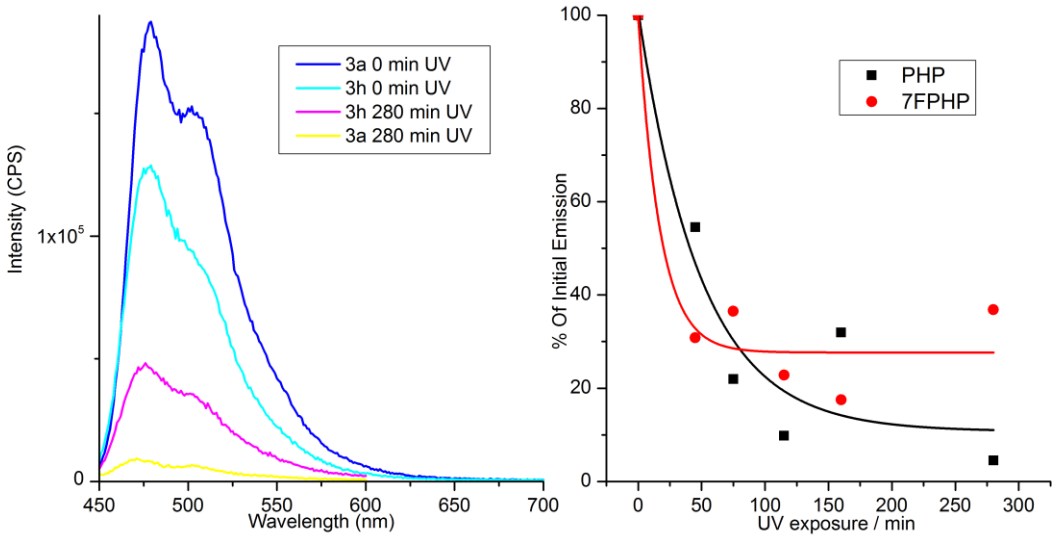

Figure 5.6 : Degradation of emission, emission spectra (left) and normalised peak emission (right)

Similarly to the anthracene based analogues (Chapter 3) initially the nonfluorinated bisphenylperylene emitter, **3a**, is more emissive, however following UV irradiation the fluorinated bisphenylperylene analogue, **3h**, is a more effective emitter. Replacing fluorine for hydrogen in the molecules aromatic periphery has increased its photostability, making the fluorinated emitter more attractive for device applications than bisphenylperylene or perylene itself.

5.2. Up-conversion measurement of *bis*-phenylperylene emitters

---

Up-conversion requires that the MLCT sensitizer compound possess a long-lived triplet making the employment of a nitrogen filled glove box during the preparation and sealing of the tubes essential for the exclusion of oxygen which is known to quench phosphorescence.[4]

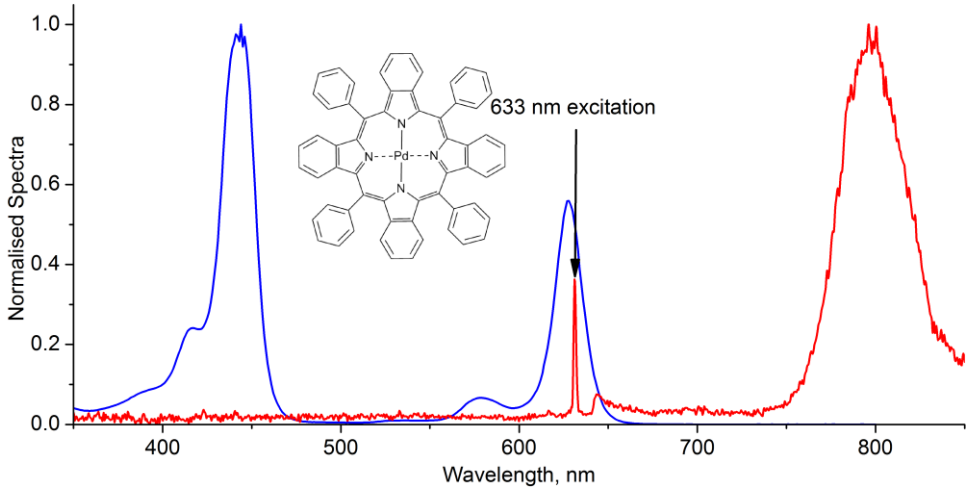

Figure 5.7 : Absorption (blue) and emission (red, 1 mW 633 nm coherent excitation) spectra and structure of **PdTBP** in dry, degassed toluene

The bisphenylperylene emitters are paired with the sensitiser palladium(II) tetraphenyl benzoporphyrin (**PdTBP**). **PdTBP** absorbs in the red region of the visible spectrum, and has a high ISC yield, producing phosphorescence in the outer red region (Figure 5.7). It has an extremely high extinction coefficient, ISC yield of ~1 and good solubility in organic solvents, and these properties, as well as its long lived triplet state, allows its use as a common TTAUC sensitizer. The measured absorption spectra of **PdTBP** (Figure 5.7) shows the expected absorption bands of a metal coordinated porphyrin compound,[5] with the Soret (B) band at 444 nm and the Q-band with α peak at 578 nm and β peak at 628 nm. The Q band corresponds to the $\pi \rightarrow \pi^*$ transition. The emission spectrum of **PdTBP** shows a wide phosporescence peak at 796 nm, corresponding to a triplet level of 1.56 eV. Prompt fluorescence is not distinguishable, indicating a very high intersystem crossing yield.

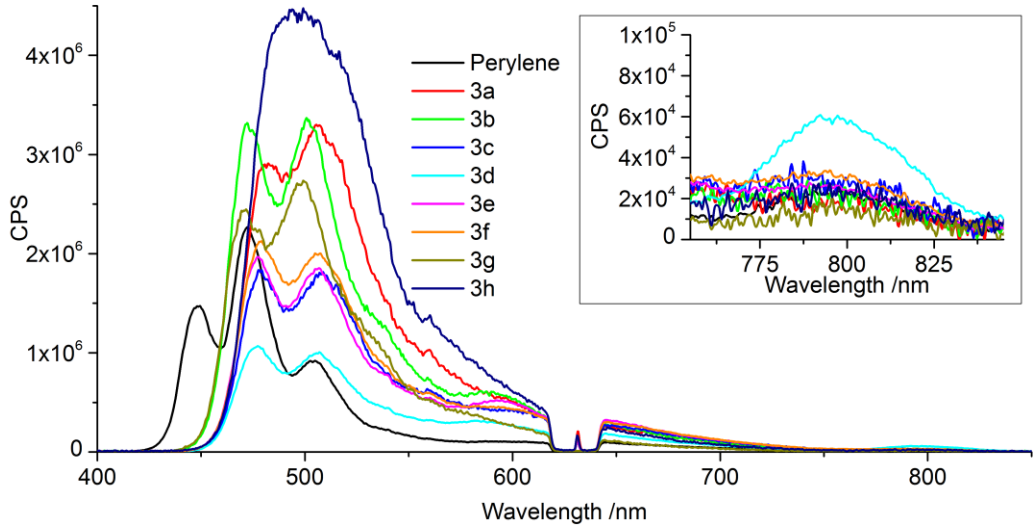

Figure 5.8 : Emitters **3a-h** sensitised by **PdTBP**, 1 mW (5.55 W.cm^{-2}) 633 nm coherent excitation

Using the same experimental equipment as used for up-conversion analysis of the anthracene dyes (Chapter 3) the up-conversion capabilities of the bisphenylperylene dyes **3a-h** were assessed. Upconversion measurements were made using flat walled tubes with emitters **3a-h** (6 x10^{-4} M) and sensitiser PdTBP (3 x10^{-5} M) in dry toluene, prepared in a glove box with <1 ppm oxygen, excited with 633 nm coherent photons attenuated to 1 mW and 0.1 mW.

The up-conversion emission spectra of tubes containing **3a-h** when irradiated with 633 nm 1 mW light clearly show that **3h** produces the greatest number of emitted photons. The phosphorescence of the sensitizer is almost completely quenched in each case, except **3d** the *para*-fluorophenyl derivative. The quantum yields of emitters **3a-h** show a range from 0.04, lower than perylene, to 0.16 which is the highest experimentally recorded for perylene systems, and on a par with the highest measured TTA up-conversion external quantum yield (Rubrene emitter)[6]. As with the UV/vis spectroscopy, the vibronic structure in the emission profile is greatly reduced with increased fluorination, an effect that is desired to improve the homogenous nature of output light. The emission wavelengths in the up-conversion tube are equal or lower than observed in the cuvettes by direct excitation due to the increased concentration of the emitters. An excimer emission is clearly evident at ~600 nm for **3b**, **3d** and perylene, as has been reported previously.[3] While this excimer causes some anti-Stokes emission it decreases the up-conversion quantum yield, and also the up-conversion energy efficiency due to the deacreased anti-Stokes shift. Excimer emission is not evident for **3h**.

At lower excitation intensities the sensitizer peak in the perylene system is more visible at ~800 nm, indicating decreased quenching efficiency at lower intensity.

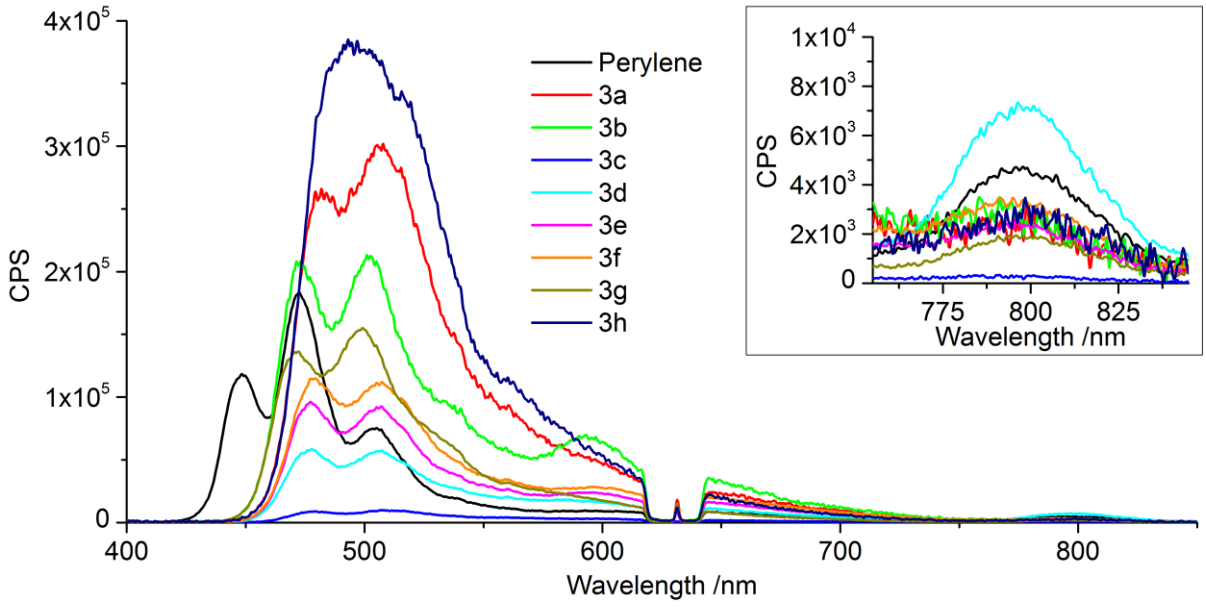

Figure 5.9 : Emitters 3a-h sensitised by PdTBP, 0.1 mW (0.55 W.cm^{-2}) 633 nm coherent excitation

A measurement of the unknown quantum yield (Φ_x) may be taken by comparison to a reference of known quantum yield (Φ_r), provided the emission integral (*F*), light intensity at excitation wavelength (*I*), absorbance of the substrate at excitation wavelength (*A*), refractive index of the substrate (*n*) and energy of the excitation photons ($h\upsilon$) are known. Under most experimental procedures the refractive index is kept constant.

$$\Phi_x = \Phi_r \frac{F_x}{F_r} \times \frac{I_r}{I_x} \times \frac{A_r}{A_x} \times \frac{n_x^2}{n_r^2} \times \frac{h\upsilon_x}{h\upsilon_r} \qquad (5.1)$$

The results of the up-conversion measurements are shown in Table 2, as can be seen the fluorinated emitters **3a-h** possess higher quantum yields than has previously been reported for related non-fluorinated systems (Chapter 1). It is important to note that not only are the quantum yields high, the Stokes shift also remains comparatively high, producing extremely high energy efficiencies.

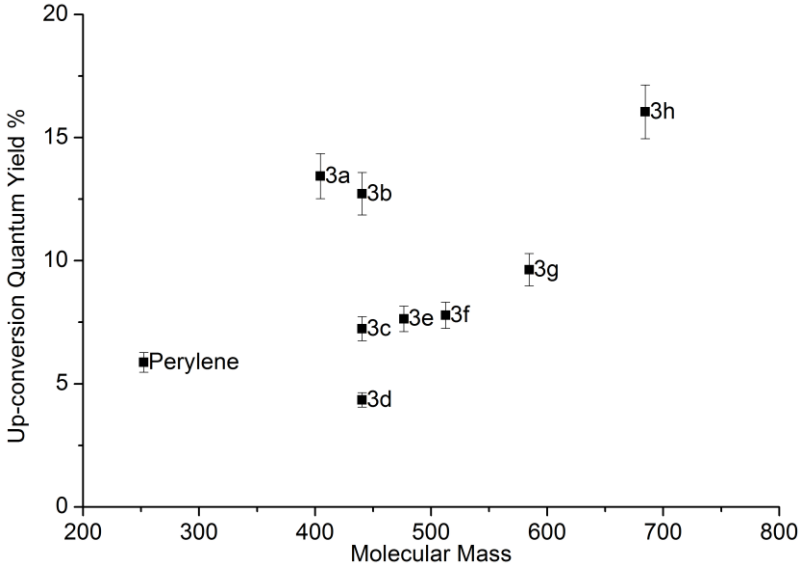

Figure 5.10 : Up-conversion quantum yield of emitters 3a-h, excited with 532 nm 1 mW coherent photons

Emitter	$\lambda_{(ex)}$ (nm)	$\lambda_{(obs)}$ (nm)	$E_{(obs)} - E_{(ex)}$ (eV)	Φ_x %	Ξ %
3h	633	489	0.58	16.0	20.7
3a	633	482	0.61	13.4	17.6
3b	633	474	0.66	12.7	17.0
3g	633	472	0.67	9.6	12.9
3f	633	480	0.62	7.8	10.2
3e	633	479	0.63	7.6	10.1
3c	633	480	0.62	7.2	9.5
Perylene	633	450	0.80	5.9	8.3
3d	633	476	0.65	4.3	5.8

Figure 5.11 : Up-conversion spectral properties of emitters **3a-h**, 1 mW irradiation

The "up-conversion energy efficiency" parameter (Ξ) is calculated from the quantum yield of the emitter and the incident and emission photon energies.

$$\Xi = \frac{\Phi_x \times E_{obs}}{E_{exc}} \qquad (5.2)$$

This value is a measure of how much usable energy has been retained by the up-conversion system for possible use. For example, if no energy is lost in the transitions and the external quantum yield is 50% the energy efficiency would be 100%. The energy efficiency may be used to compare up-conversion systems composed of different types of emitter and sensitizer pairings. As emitter **3h** showed the best up-conversion response further in-depth investigation of its properties were investigated.

5.2.1. Up-conversion measurements of 3,9(10)-bis-((4-trifluoromethyl)perfluorophenyl)perylene **3h**

The concentration dependence of the up-conversion by emitter **3h** when paired with sensitizer **PdOEP** was assessed.

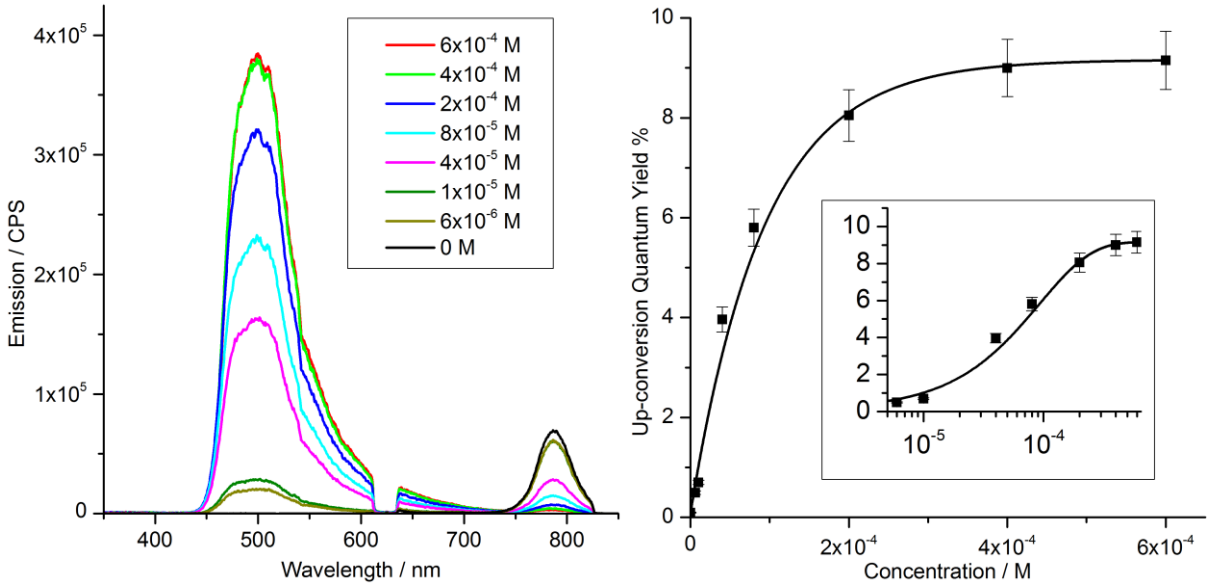

Figure 5.12 : Emission spectra (left) and up-conversion quantum yield of **3h** at varying concentrations, sensitized by **PdOEP** (1.5×10^{-5} M) in dry, degassed toluene, excited by 532 nm 100 µW (0.55 W.cm^{-2}) coherent photons

In agreement with previous up-conversion measurements (Chapter 3) the effectiveness of the up-conversion increases to saturation with emitter concentration, indicating more effective quenching of the sensitizer triplets and rapid TTA. With a 20 fold excess of emitter the sensitizer is quenched almost completely, and the up-conversion quantum yield is ~9%.

Common proof of TTA up-conversion is the exponential increase of up-conversion with incident power until high power (around 1 W), when a linear relationship is found.[7] This work uses a range of excitation intensities from below 0.01 W.cm^{-2} to above 30 W.cm^{-2}: below this range the emission peak becomes indistinguishable from the baseline, above it the heating effect of the laser begins to cause increased likelihood of unreliable results.

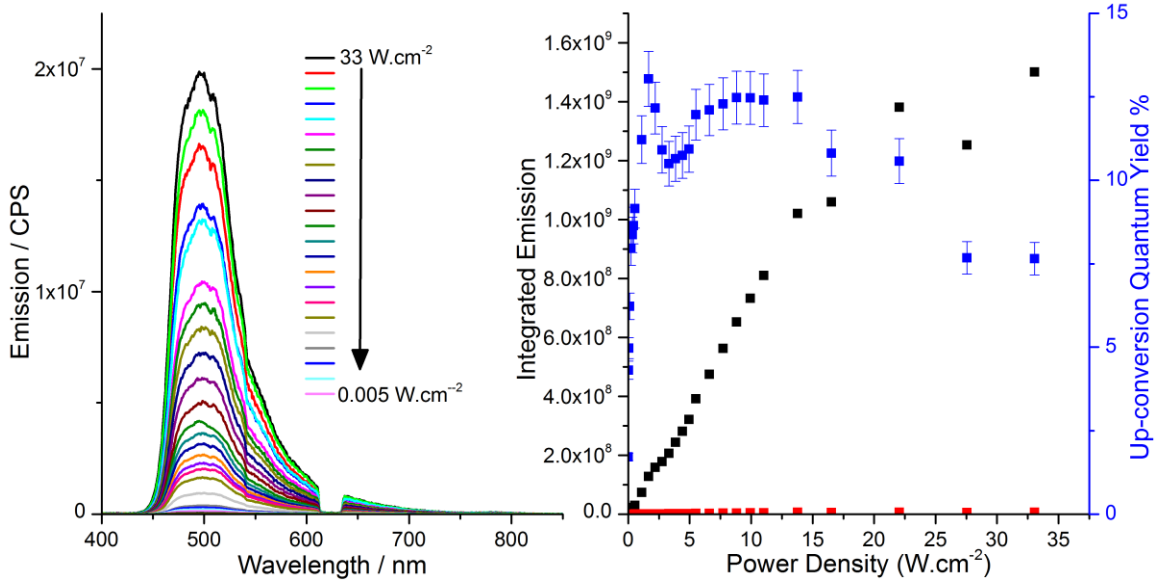

Figure 5.13 : Emission spectra (left) and integrated up-conversion (black) and sensitizer (red) emission, with up-conversion quantum yield (blue) of emitter **3h** (6x10^{-4} M) and **PdTBP** (1.5x10^{-5} M), excited by 633 nm varying intensity coherent photons

The emission spectra collected show a clear intesity response (Figure 5.13), increasing the intensity causes an increased up-conversion emission. However, the normal exponential relationship is not clear from a graph of emission integral against power density, instead showing a linear response, beginning to deviate before saturation at 15 W.cm^{-2}. The up-conversion quantum yield is intensity dependant, as before, peaking and then decreasing, then increasing to saturation.

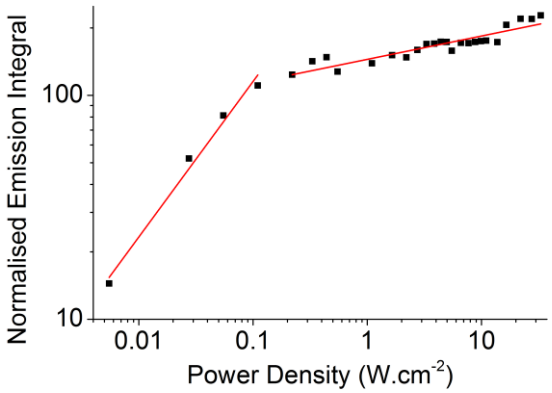

Figure 5.14 : Normalised up-conversion emission integral (black) against power density, with linear fits (red) in weak and strong up-conversion limits

The "onset" of up-conversion, i.e. the lowest incident power where the up-conversion becomes linear is often a region of high up-conversion quantum yield. The onset of the strong up-conversion limit is very low, so that there is no clear weak up-conversion limit visible upon the graph of integrated emission against power density, saturation is visible at higher power densities (Figure 5.13).

Due to the large range of power densities tested, a plot of the log of the normalised up-conversion integral against log of the power density was used to ensure that aberations in the experimental setup, for example changing neutral density filters, does not affect the results (Figure 5.14).

The normalised up-conversion emission plot allows us to ascertain that the onset of the strong up-conversion limit is at 0.1 W.cm^{-2}, much lower than the similar diphenylanthracene analogue (**2h**, 4 W.cm^{-2}). Emitter **3h** is an extremely efficient up-conversion emitter, and this system has a low strong annihilation onset power densities, as well as extremely high up-conversion quantum yield and energy efficiency.

TTA up-conversion requires that two distinct bimolecular processes occur quickly for efficient emission and these are generally accepted to require collision of the components. The first is triplet-triplet transfer (TTT) from the sensitizer triplet state to the emitter triplet state ($T_1^S \rightarrow T_1^E$). Since the TTT process is in essence an example of bimolecular quenching of the phorphyrin triplet, a measure of how efficiently energy is passed from the sensitizer to the emitter may be assessed by the bimolecular quenching constant (k_q). This is found by calculation of the Stern-Volmer quenching constant (K_{SV}) from concentration of the quencher ($[Q]$) the photoluminescence lifetime in the absence of the quencher (τ_0) and the lifetime in the presence of the quencher (τ). These may be compared to the diffusion limit.

$$\frac{\tau_0}{\tau} = \frac{F_0}{F} = 1 + K_{SV}[Q] \qquad (5.3)$$

$$K_{SV} = k_q \tau_0 \qquad (5.4)$$

The TTT step of **3h** and **PdTBP** TTAUCS was analysed using a Stern-Volmer plot of the intensity of the unquenched sensitizer phorphorescence compared to concentration of quencher (Figure 5.15). We can see that in contrast to the Stern-Volmer analysis of the anthracene dye (Chapter 3) the plot saturates for the highly fluorinated bisphenylperylene emitter **3h** - above 0.0001 M of emitter the plot is not linear. Below this threshold the gradient, and thus the Stern-Volmer coefficient, is 41700 M^{-1}, since the **PdTBP** lifetime has been measured as 195 μs (Rogers *et al*),[5] this corresponds to a quenching coefficient of **PdTBP** by **3h** of 0.21 x10^9 M^{-1}.s^{-1}, this is in the region expected for a porphyrin sensitized system.

The origin of the non-linearality of the Stern-Volmer plot is due to the presence of both accessible and inaccessible fluorophores. This commonly occurs for protein fluorescence, where fluorescent units are protected from quenching species by the folding of the protein. Here this indicates that an aggregation effect is preventing the full quenching of the **PdTBP** sensitizer. This could be producing sensitizer molecules that are not quenched at all, or complexes that are less emissive are formed, ie. quenched sensitizer molecules with a non-zero quantum yield. That this may occur indicates that oxygen has been successfully excluded from the solution.

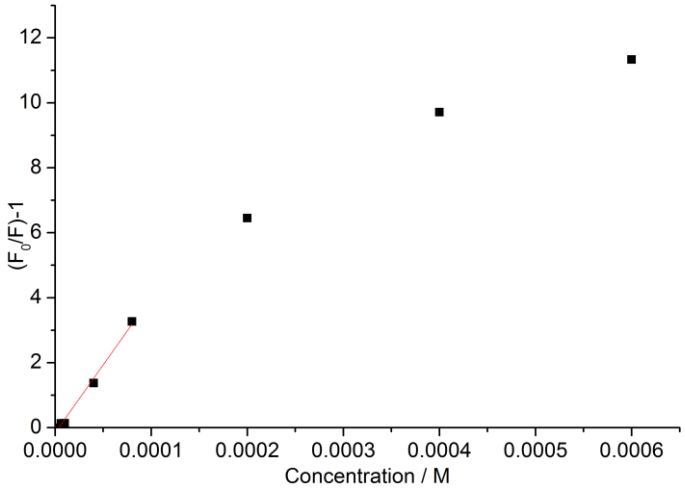

Figure 5.15 : Stern-Volmer plot of the phosphorescence of sensitizer **PdTBP** quenched by varying concentration of emitter **3h**

The stability of the prepared up-conversion tubes can be assessed by comparing a composition of **3h** and PdTBP when freshly prepared and after 14 months. There is no significant change in the emission profile or up-conversion quantum yield.

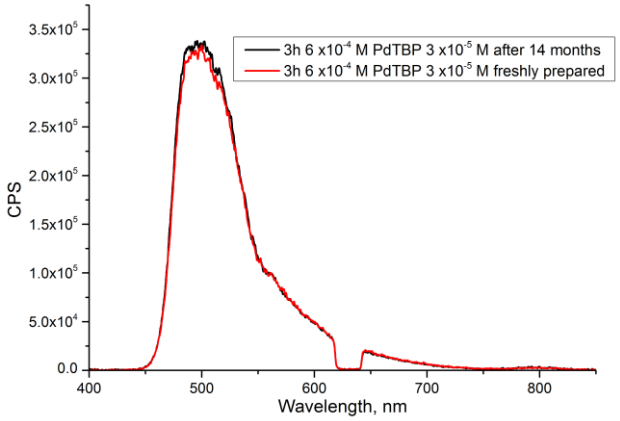

Figure 5.16 : Stability of up-conversion tube composed of 3h and PdTBP

As outlined above the stages of TTA up-conversion (adsorption, intersystem crossing, triplet-triplet transfer, triplet-triplet annihilation and emission) must be maximised to provide the greatest

quantum yield and therefore performance, while processes that retard or reduce these stages must be prevented. (Chapter 1)

Oxygen is notorious for its negative effects in these systems, both upon the organometallic sensitizer and the organic emitter. The clearest example of this is the formation of endoperoxides, forming a quenching pathway from the emitter in an excited triplet state that can irreversibly degrade the emitter molecule.[8,9] Fluorinated PAHs are known to be less affected by oxygen degradation, this could be one of the reasons that the highly-fluorinated *bis*-phenylperylenes **3g-h** in this report show an improved performance compared to other less fluorinated analogues.

Another deleterious effect in these systems is aggregation of the raft like molecules, decreasing diffusion which is required for the bi-molecular processes. Since aggregation is encouraged by pi stacking and perylene is a planar raft-like molecule it may form aggregates easily, and excimer emission from PAHs is well known.[3,10] It would be expected that with added phenyl groups this aggregation could be prevented, thus increasing the quantum yield. However the excimer emission associated with aggregation at around 600 nm is more pronounced with some of the fluorinated systems than seen for perylene alone. Since electron deficient and electron rich rings prefer to sequentially π stack this may increase the aggregation, however excimer excitation is not seen in the case of **3g-h.** However, the negative curvature of the Stern-Volmer plot of **PdTBP** phosphorescence quenched by **3h** indicates that some aggregation is occurring, preventing full quenching.

While a decrease in the harmful influences of oxygen and excimer emission is very encouraging the influence of fluorine to tune the energy levels of the emitter is the most exciting possibility. If the T_1 level is ideally located at half the S_1 level while significantly less than the half T_2 energy level the TTA process would produce only singlet emitter dimers. This would make external up-conversion quantum yields of 50% and external energy efficiencies of 100% theoretically feasible (Chapter 1).

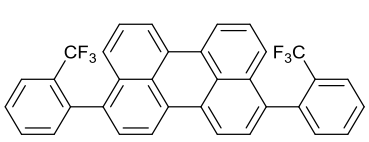

3i

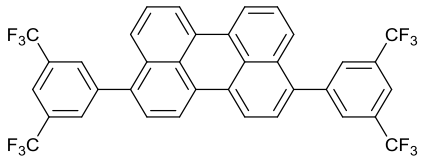

3j

Figure 5.17 : Structures of emitter 3i-j

The addition of the CF_3 group in emitter **3h** causes a large difference in both the fluorescence and up-conversion capability when compared to fluorinated emitter **3g**. This could be due to the bulk of the CF_3 group preventing π-stacking effects, as well as the extreme electron withdrawing character of the functional group. To investigate the effect that addition of CF_3 groups can the emitters **3i-j**

were synthesised. The synthesis was analogous to that of other bisphenylperylene emitters (Chapter 4).

The fluorescence and up-conversion properties of the emitters **3i-j** were assessed as described above (Chapter 3). Absorption and emission measurements in dry toluene indicate that the addition of trifluoromethyl groups causes a decrease in the vibrational structure of the spectra, and an increase in the Stokes shift.

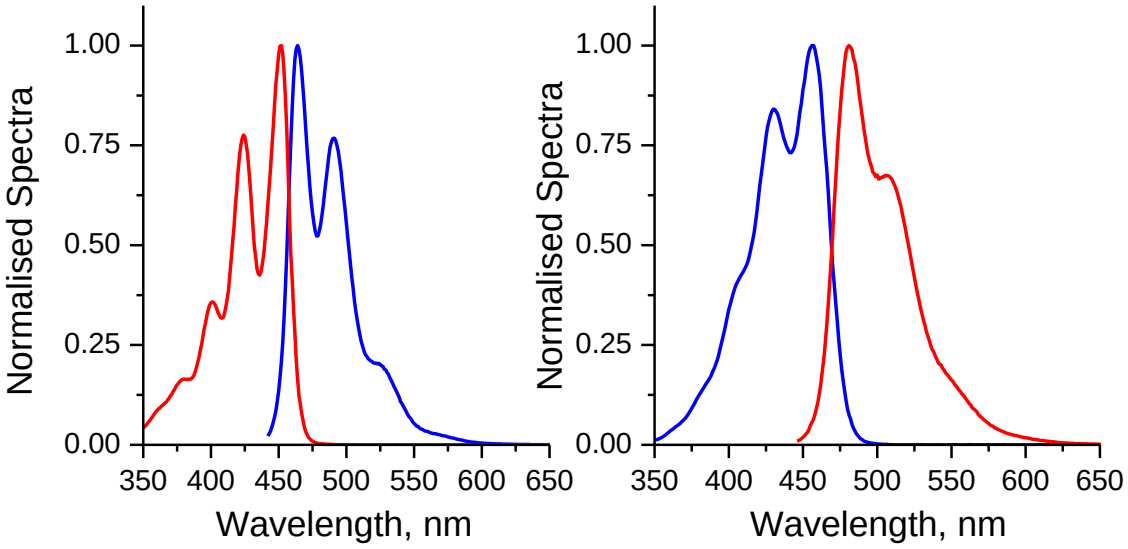

Figure 5.18 : Normalised absorption (blue) and emission (red) spectra of **3i** (left) and **3j** (right)

The fluorescence quantum yields of **3i** and **3j** were found to be 75.3 ± 0.5 % and 88.5 ± 0.5 % respectively, with extinction coefficients of 32700 ± 300 $M^{-1}.cm^{-1}$ and 28900 ± 100 $M^{-1}.cm^{-1}$ respectively. Since molecules of similar structure and properties generally show different up-conversion quantum yields in line with their fluorescence quantum yields it would be expected that **3j** would have increased up-conversion when compared to **3i**, but less than **3h**.

The up-conversion emission of **3i** is much lower than that of **3j**, when the external up-conversion quantum yield is calculated they are 2.2% and 6.8% respectively (Figure 5.19). The addition of the extremely electron withdrawing CF_3 groups in the *meta* positions has reduced the up-conversion effectiveness of the system, and addition of the group in the *ortho* position has greatly decreased the up-conversion capability when compared to **3a**. The trifluoromethyl group has a similar steric bulk to isopropanol, it is likely the decreased freedom to rotation of the phenyl groups of emitter **3i** is also lowering the emission efficiency.

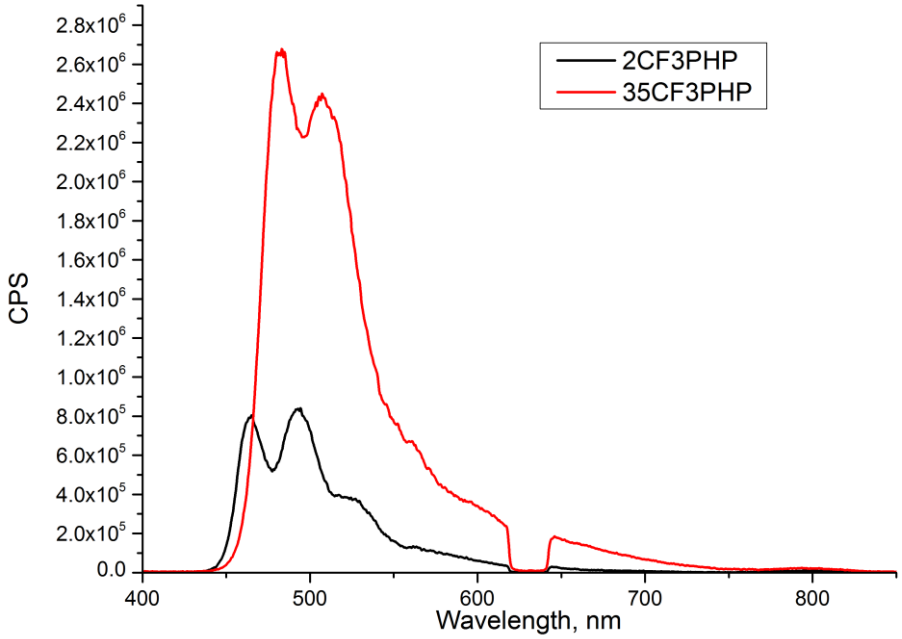

Figure 5.19 : Up-conversion emission of **3i-j**, paired with **PdTBP** excited with 633 nm 1 mW coherent light

In the up-conversion emission spectra the maximum emission is at 492 and 482 nm for **3i** and **3j**, making the up-conversion energy efficiency (Ξ) 2.8% and 8.9% respectively. Both of these are far lower than the highly fluorinated **3h** and also the non-fluorinated **3a**; the up-conversion anti-Stokes shifts are similar to those of other bisphenylperylene emitters, but the comparatively low up-conversion quantum yields show that energy is being lost in the up-conversion process. This is to be expected, as emitters **3i-j** have decreased fluorescence quantum yields, indicating that even if the system reaches the emitter S_1 efficiently the following fluorescence is perturbed by a non-radiative relaxation pathway.

5.3. Up-converting Nanoparticles of 3,9(10)-di-((4-trifluoromethyl)perfluorophenyl)perylene **(3h)** and **PdTBP**

One interesting adaption of TTAUC media is the use of dye-loaded nanoparticles .[11–13] These allow simple delivery of dye molecules, and the nanoparticles may be functionalised to encourage accumulation in specific cells, such as tumors, allowing fluorescence aided diagnosis and surgery (Chapter 1). TTAUC nanoparticles have also been investigated for photovoltaic applications.[13]

The upconversion quantum yields necessarily fall as a result of their use in solids, including nanoparticles, due to the decreased molecular mobility, since the TTAUC mechanism requires sequential molecular collisions that are often diffusion limited. The best quantum yield reported in a solid matrix is around 1000 times less than the best in solution.[14]

5.3.1. TTAUC Nanoparticle fabrication

The method used in this work was developed by Materials Science Laboratory (Sony Deutschland) to produce well characterised nanoparticles of tight size distribution.

One batch of nanoparticles was prepared containing the **PdTBP** and **3h** sensitized up-conversion system.

	NP1
Average Size / nm	126 ± 1
PDI	0.20 ± 0.01
Zeta Potential / mv (neutral pH)	-51.5 ± 0.7
Conductivity (μS/cm)	11.3 ± 2.4
Mobility (μmcm/Vs)	-4.0 ± -0.1

For the nanoparticle batch the PDI is around 0.2, which is standard for this preparation method. Zeta potential is a measure of colloidal stability, in general values of a magnitude greater than 40 mV indicate a stable colloid, with those above 60 mW showing excellent stability. Since for this batch the value is ~-50 mV this indicated that these colloidal solutions are not likely to aggregate due to the repulsive slipping plane charges the particles possess. The Zeta potential is calculated from the measured conductivity of the solution, and the mobility of the particles.

The nanoparticles were measured for size distribution following storage for 5 days to check their stability and degree of aggregation.

	Average size difference / nm	**PDI difference**
NP1	4.68 ± 3.00	0.0288 ± 0.0212

Any change in particle size or PDI is in the region of the error of the measurement.

5.3.2. Photophysical investigation of TTAUC nanoparticles

The absorption and emission spectra of dilute suspensions of the nanoparticles NP in water were taken in plastic walled cuvettes (Figure 5.20), the peaks due to emitter **3h** (~450 nm) and sensitizer **PdTBP** (~630 nm) are visible over the absorption of the PMMA. The dilute suspensions of nanoparticles were used to measure the emission of **3h** within nanoparticles.

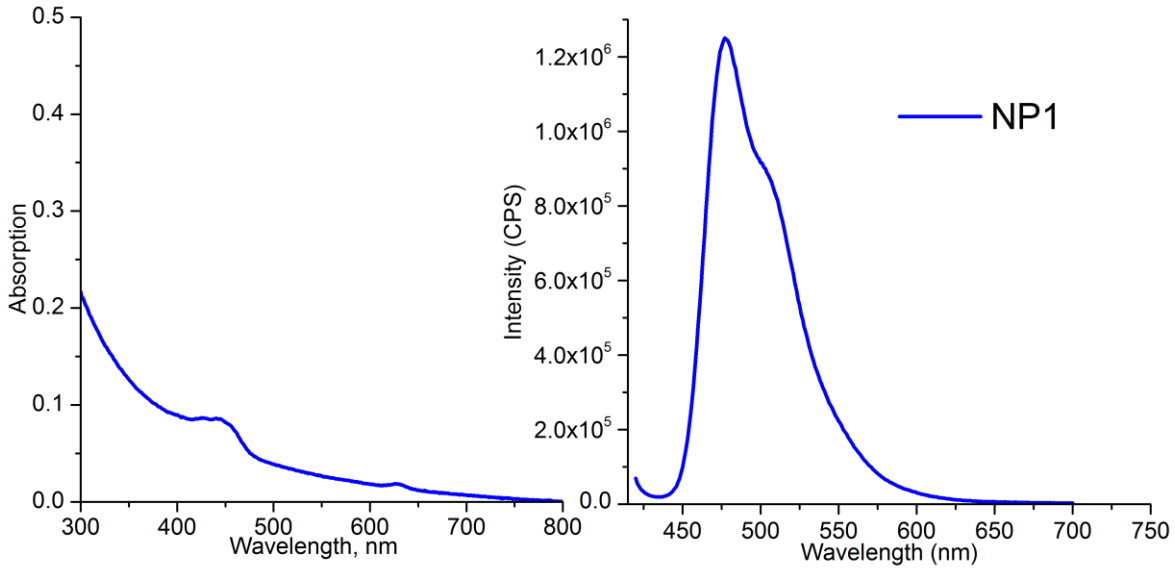

Figure 5.20 : Absorption (a) and emission (405 nm excitation) (b) spectra of nanoparticles dispersed in water

Solutions of the nanoparticles NP1 were degassed by stirring in a glovebox, and injected into flat walled tubes for up-conversion capability assessment.

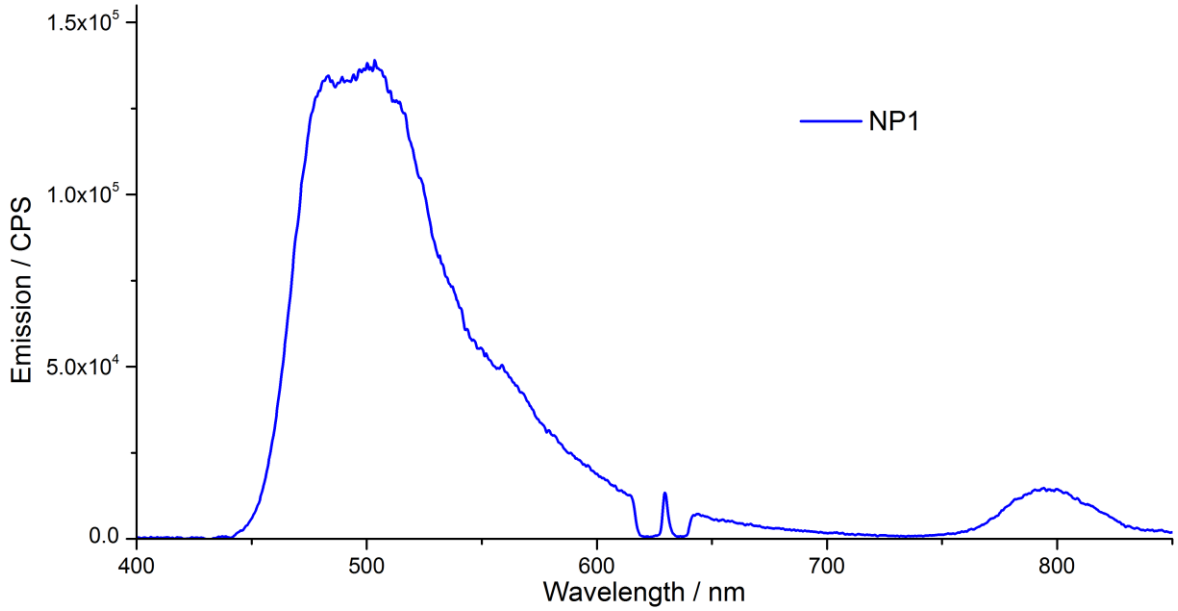

Figure 5.21 : Emission spectra (left) and associated up-conversion quantum yield (right) of nanoparticles NP1 irradiated with 2.5 mW 633 nm coherent light

The quantum yields of the nanoparticles were assessed using the same method as measurements of free dyes in toluene (Chapter 3). The external quantum yield of 0.9 could be increased by increasing the concentration of dye molecules used - not all of the sensitizer emission is being quenched in this mixture. These TTAUC nanoparticles have a higher up-conversion quantum yield than the highest external up-conversion quantum yield for rare earth up-conversion nanoparticles, reported to be 0.3% for 100 nm NaYF4:Yb,Er nanocrystals.[15]

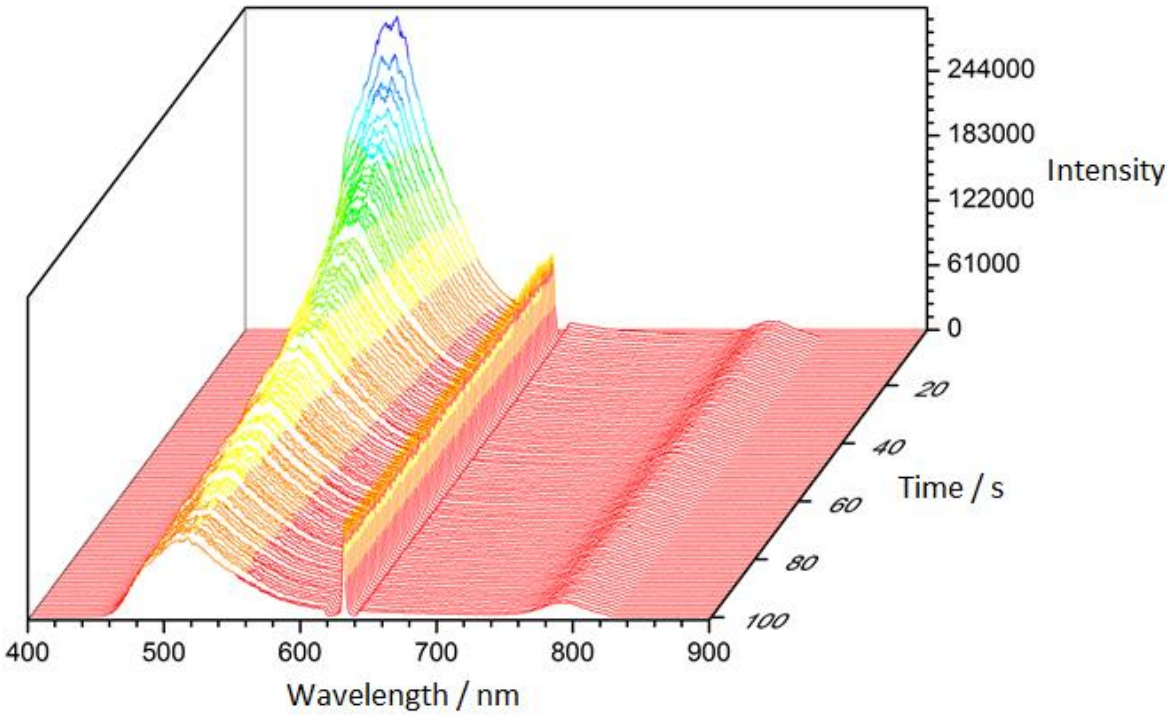

Figure 5.22 : 3h and PdTBP nanoparticles, dispersed in water, measurement over 100 s

The stability of the emission of the nanoparticles was assessed by taking measurements during continuous excitation.

5.4. Conclusions

Current solar cells do not use the sun's energy as efficiently as they might – if "lost" photons can be frequency up-converted they could be harnessed for the power generation. This thesis shows that tailoring the design of emitters in UCSs can greatly improve up-conversion quantum yield and energy efficiency. By making a range of fluorinated *bis*-phenylperylene analogues the relationship between their structure and up-conversion efficiency was probed, the most striking example being 3,9(10)-di-((4-trifluoromethyl)perfluorophenyl)perylene (**3h**) which, when coupled with **PdTBP,** possesses;

- An external up-conversion quantum yield of 16%
- A high anti-Stokes shift, allowing 21% energy efficiency
- An extremely low onset of the linear strong up-conversion limit of 0.1 $W.cm^{-2}$
- Excellent resistance to photodegradation

This system, when incorporated into nanoparticles, shows up-conversion clearly in water suspensions, with an up-conversion quantum yield of 0.9%, higher than that seen for the best rare-earth up-conversion system.[15]

5.5. Experimental

Fluorescence measurements were taken using the same apparatus as before (Chapter 3). Up-conversion measurements were taken using the same apparatus as before (Chapter 3) making use of ZnPc (fluorescence quantum yield 26% in toluene, absorption 0.1, measured by the authors, lit 0.3).[16] Zeta potentials were measured in MilliQ water at 25 °C n=4 using electrophoresis and the Henry equation, (Smoluchowski approximation) in a folded capillary cell.

$$U_E = \frac{2\varepsilon z f(ka)}{3\eta}$$

Where z = zeta potential, U_E = Electrophoretic mobility, ε = dielectric constant, η = viscosity and f(ka) = Henry's function, (1.5).

3i, *3,9(10)-bis(2-trifluoromethylphenyl)perylene*

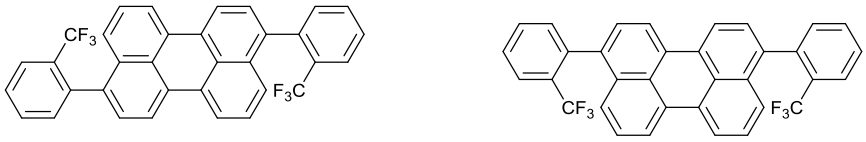

A solution of 3,9(10)dibromoperylene (0.498 g, 1.21 mmol), 2-(trifluoromethyl)benzene boronic acid (0.697 g, 3.67 mmol), potassium carbonate (0.500 g, 3.62 mmol) and $Pd(PPh_3)_4$ (214 mg, 0.182 mmol) in degassed THF (20 ml) and H_2O (1 ml) were heated to 55 °C under an atmosphere of argon for 48 h. A second portion of 2-(trifluoromethyl)benzene boronic acid (0.616 g, 3.24 mmol), and the heating continued for a further 4 days. The solution was diluted with H_2O, extracted with toluene, and the organics washed, dried and filtered through celite and evaporated to dryness. Recrystallization gave the mixture of isomers 3,9(10)-bis(2-trifluoromethylphenyl)perylene (0.218, 33%) as a green/brown solid; MP (hexane/toluene): 200 °C (apparent); IR ν_{max} /cm^{-1} 3057(w), 1574(w), 1384(m), 1318(s), 1262(w), 1173(s), 1122(s) 1110(s); δ_H (600 MHz, Chloroform-*d*) 8.25 (11 H, ddt, *J* 37.2, 22.2, 7.5), 8.12 (3 H, dd, *J* 8.4, 2.4), 8.09 – 8.05 (1 H, m), 8.04 (2 H, d, *J* 8.1), 7.86 (4 H, d, *J* 8.0), 7.80 (3 H, dd, *J* 8.1, 6.1), 7.75 – 7.68 (7 H, m), 7.68 – 7.55 (12 H, m), 7.46 – 7.35 (22 H, m), 7.23 – 7.17 (4 H, m); δ_C (151 MHz, Chloroform-*d*) 135.31 , 132.76 , 131.53 , 130.91 , 128.06 , 128.02 , 127.29 , 126.79 , 121.32 , 120.90 , 120.70 , 119.91; MS ($ASAP^+$) 541.1 (M^+, 100%); HRMS (TOF $ASAP^+$), Calcd for $C_{34}H_{19}F_6$: 541.1391. Found *m/z*: 541.1382.

3j*, 3,9(10)-bis(3,5-di(trifluoromethyl)phenyl)perylene*

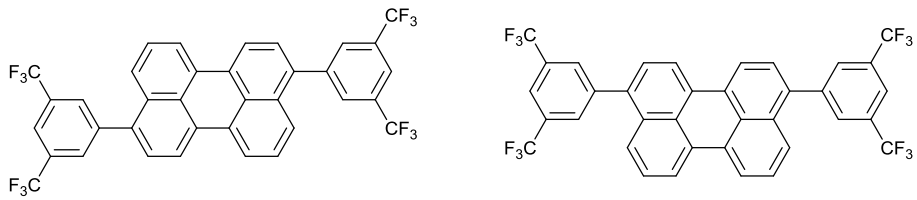

A solution of 3,9(10)dibromoperylene (0.294 g, 0.720 mmol), 3,5-di(trifluoromethyl)benzene boronic acid (0.420 g, 1.63 mmol), potassium carbonate (0.212 g, 1.54 mmol) and $Pd(PPh_3)_4$ (214 mg, 0.043 mmol) in degassed dry toluene were heated to 55 °C under an atmosphere of argon for 48 h. The solution was diluted with H_2O, extracted with toluene, and the organics washed, dried and filtered through celite and evaporated to dryness. Recrystallization gave the mixture of isomers 3,9(10)-bis(3,5-di(trifluoromethyl)phenyl)perylene (0.190, 39%) as a green/brown solid; MP (hexane/toluene): 178 °C (apparent); MS ($ASAP^+$) 676.1 (M^+, 100%); HRMS (TOF $ASAP^+$), Calcd for $C_{36}H_{16}F_{12}$: 676.1044. Found *m/z*: 676.1060; IR ν_{max} /cm^{-1} 2920(w), 1369 (s), 1350 (m), 1274(s), 1176(s), 1120(s); ^1H NMR (700 MHz, Methylene Chloride-d_2) δ 8.30 – 8.24 (3H, m), 8.04 – 8.02 (1H, m), 7.99 – 7.96 (5H, m), 7.60 – 7.54 (1H, m), 7.51 – 7.47 (2H, m), 7.46 – 7.42 (2H, m); ^{13}C NMR (176 MHz, CD_2Cl_2) δ 142.68 , 140.37 , 136.89 , 136.70 , 132.65 (d, *J* 34), 132.09 (d, *J* 81), 131.79 – 131.06 (m), 130.09 , 128.81 , 128.28 , 127.87 (d, *J* 127), 127.45 , 125.20 , 125.00 , 124.19 , 123.86 , 122.64 , 121.30 – 120.09 (m); ^{19}F NMR (188 MHz, Methylene Chloride-d_2) δ -69.43 . MS ($ASAP^+$) 676.1 (M^+, 100%); HRMS (TOF $ASAP^+$), Calcd for $C_{36}H_{16}F_{12}$: 676.1044. Found *m/z*: 676.1060.

(1) Berlman, I. B. *Handbook of Fluorescence Spectra of Aromatic Molecules*; ACS Publications, 1971.

(2) Wu, W.; Zhao, J.; Sun, J.; Guo, S. Light Harvesting Fullerene Dyads as Organic Triplet Photosensitizers for Triplet-triplet Annihilation Upconversions. *J. Org. Chem.* **2012**, *77*, 5305–5312.

(3) Singh-Rachford, T. N.; Castellano, F. N. Triplet Sensitized Red-to-Blue Photon Upconversion. *J. Phys. Chem. Lett.* **2009**, *1*, 195–200.

(4) Baluschev, S.; Miteva, T.; Yakutkin, V.; Nelles, G.; Yasuda, A.; Wegner, G. Up-conversion fluorescence: Noncoherent excitation by sunlight. *Phys. Rev. Lett.* **2006**, *97*, 143903.

(5) Rogers, J. E.; Nguyen, K. A.; Hufnagle, D. C.; McLean, D. G.; Su, W.; Gossett, K. M.; Burke, A. R.; Vinogradov, S. A.; Pachter, R.; Fleitz, P. A. Observation and Interpretation of Annulated Porphyrins: Studies on the Photophysical Properties of m eso-Tetraphenylmetalloporphyrins. *J. Phys. Chem. A* **2003**, *107*, 11331–11339.

(6) Cheng, Y. Y.; Khoury, T.; Clady, R. G. C. R.; Tayebjee, M. J. Y.; Ekins-Daukes, N.; Crossley, M. J.; Schmidt, T. W. On the efficiency limit of triplet-triplet annihilation for photochemical upconversion. *Phys. Chem. Chem. Phys.* **2009**, *12*, 66–71.

(7) Haefele, A.; Blumhoff, J.; Khnayzer, R. S.; Castellano, F. N. Getting to the (Square) Root of the Problem: How to Make Non-Coherent Pumped Upconversion Linear. *J. Phys. Chem. Lett.* **2012**, *3*, 299–303.

(8) Piper, R.; Yoshida, M.; Ekins-Daukes, N.; Haque, S.; Cheng, Y. Y.; Fuckel, B.; Khoury, T.; Clady, R. G. C. R.; Tayebjee, M. J. Y.; Crossley, M. J.; others In *Photovoltaic Specialists Conference (PVSC), 2011 37th IEEE*; 2011; pp. 003632–003635.

(9) Islangulov, R. R.; Castellano, F. N. Photochemical Upconversion: Anthracene Dimerization Sensitized to Visible Light by a RuII Chromophore. *Angew. Chem. Int. Edit.* **2006**, *118*,

6103–6105.

(10) Bohne, C.; Abuin, E.; Scaiano, J. Characterization of the triplet-triplet annihilation process of pyrene and several derivatives under laser excitation. *J. Am. Chem. Soc.* **1990**, *112*, 4226–4231.

(11) Liu, Q.; Yang, T.; Feng, W.; Li, F. Blue-emissive upconversion nanoparticles for low-power-excited bioimaging in vivo. *J. Am. Chem. Soc.* **2012**, *134*, 5390–5397.

(12) Zou, W.; Visser, C.; Maduro, J. A.; Pshenichnikov, M. S.; Hummelen, J. C. Broadband dye-sensitized upconversion of near-infrared light. *Nat. Photonics* **2012**, *6*, 560–564.

(13) Monguzzi, A.; Frigoli, M.; Larpent, C.; Tubino, R.; Meinardi, F. Low-Power-Photon Up-Conversion in Dual-Dye-Loaded Polymer Nanoparticles. *Adv. Funct. Mater.* **2012**, *22*, 139–143.

(14) Monguzzi, A. In *SPIE Photonics Europe*; 2012; pp. 843511–843511.

(15) Zhou, J.; Liu, Z.; Li, F. Upconversion nanophosphors for small-animal imaging. *Chem. Soc. Rev.* **2012**, *41*, 1323–1349.

(16) Seybold, P. G.; Gouterman, M.; Callis, J. Calorimetric, Photometric and Lifetime Determinations of Fluoresnce Yields of Fluorescein Dyes. *Photochem. Photobiol.* **1969**, *9*, 229–242.

6. Synthesis, fluorescence and up-conversion of fluorinated 3,5,8-triarylBODIPY dyes

Having shown that fluorinated diphenylanthracene and diphenylperylene dyes are competitive emitters in TTAUC systems for the production of blue and green light respectively, an emitter molecule for red emission was required. An emitter that could be paired with sensitizers that absorb in the far red or NIR regions would be invaluable for up-converting photons for solar photovoltaic applications. One possible core structure for addition of fluorinated periphery is the tricyclic BODIPY moiety.

6.1. Fluorescent properties of BODIPY dyes

4,4-Difluoro-4-bora-3a,4a-diaza-s-indacene (BODIPY: difluoro***bo***ron ***dipy***rromethene) based dyes have been the subject of much research interest over the last twenty years due to their potential as fluorescent molecules for a wide range of applications.[1,2] It is a heterocyclic fluorophore with structural similarities to both s-indacene and porphyrin, and has been called "porphyrin's little sister" due to its structure and excellent photophysical properties.[2]

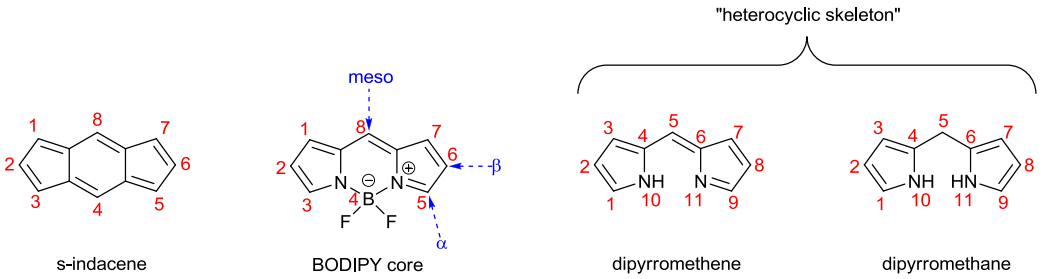

Figure 6.1 : The BODIPY core

The central BODIPY "core" is structurally similar to the tricyclic PAH s-indacene, and the numbering of any substituents is analogous, while the parent "heterocyclic skeleton" uses slightly different IUPAC based numbering.[2] The parent heterocyclic structures are also fluorescent, but the complexation of the BF_2 unit improves the fluorescent properties, as well as the chemical and photo stability of the molecule.[1,3]

BODIPY derivatives can be described as rigid cross-conjugated cyanines, with improved properties such as increased lipophilicty and slight water solubility due to its zwitterionic structure. Since

BODIPY emitters commonly have aryl phenyl groups these are structurally similar to fluorescein and Rhodamine, and have comparable fluorescent properties.[3]

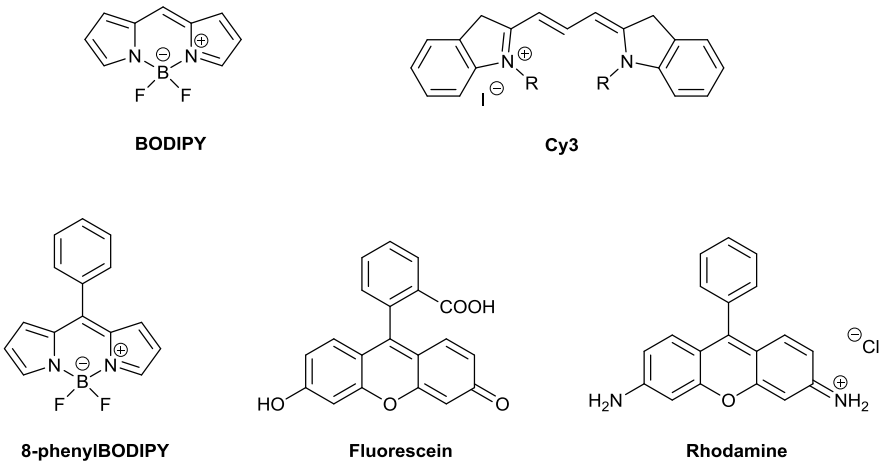

Figure 6.2 : Common BODIPY like emitters

The BODIPY structure is used widely as a chromaphore due to its good chemical and photo stability; excellent fluorescent properties including high molar extinction coefficients and fluorescence quantum yields; sharp excitation and emission peaks with high intensities within the visible spectrum; nanosecond range fluorescence lifetimes; and good solubility and low aggregation in solution.[1,4] The BODIPY core molecule's crystallographic structure has been found to contain no double bond structure on N-B bonds as well as, different B-F distances and the boron atom is not coplanar with the aromatic raft, instead it is at ~5° angle.[5–7] They are zwitterionic: the negative charge is centred on the boron atom, while the positive charge is delocalized through the heterocyclic conjugated system, making them neutral overall. This allows them good solubility in organic solvents and high polarity and pH tolerance.[1,4,8,9] The spectroscopic, photophysical and physical properties of these dyes may be tuned by functionalization on various sites of the BODIPY core, leading to a wide range of synthesis paths to various chromaphores.[10]

In addition to increasing interest in BODIPY dyes an offshoot of investigation into modified versions of the BODIPY core have also been fruitful. These include replacing the C-8 with a nitrogen atom, [11–13] giving aza-BODIPYs, which possess increased red-shift due to HOMO-LUMO gap stabilization by the introduced nitrogen lone pair.[2] The replacement of the fluorine atoms on the central boron atom with aryl,[14] ethynyl,[15] or alkoxide groups,[16] named C-, E- and O- BODIPYs respectively, gives emitters with greatly increased Stokes shift that make use of intramolecular through-space energy-transfer to allow multiple UV-photon collectors to pass energy to BODIPY as the single emissive portion.[17] Aromatic ring fusion produces a raft which acts as a steric block, increases conjugation so causes a red-shift in the spectral maxima, and acts as a platform for further functionalization – the emissive properties of such molecules when compared to their more flexible analogues is greatly improved.[18]

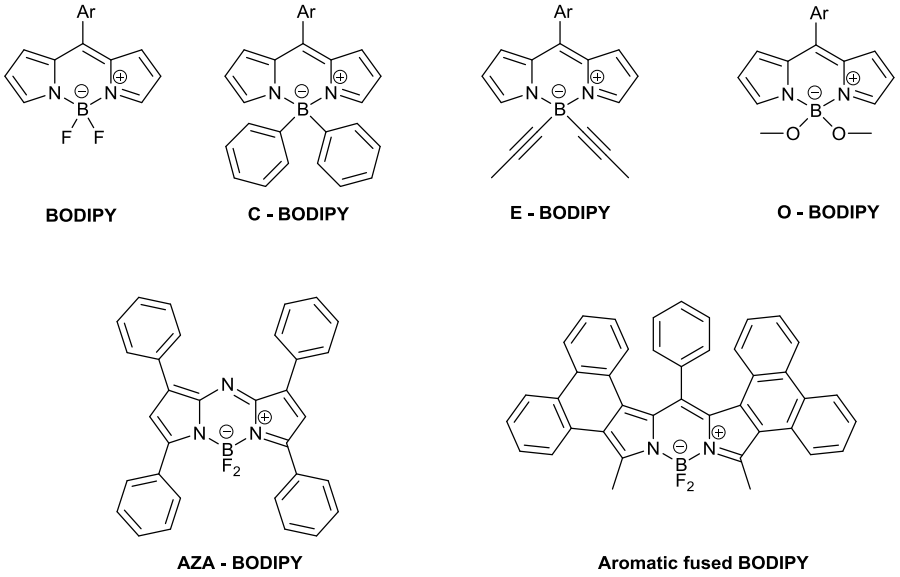

Figure 6.3 : Modified BODIPY structures

BODIPYs have been the focus of a renewed effort on organic chromaphores, and have been used for pH sensing,[19] bioimaging and biomolecule sensing,[20,21] metal ion sensing,[22–24] molecular electronics,[25] molecular viscosity probes,[10] light harvesting crystalline chromaphores,[10] oxygen species sensors,[10] drug delivery agents,[26] OLEDs,[27–29] laser dyes,[30,31] and for photosensitizers,[10,32–35] including solar cells.[36] Commercially available BODIPY molecules allow emission across the visible spectrum.

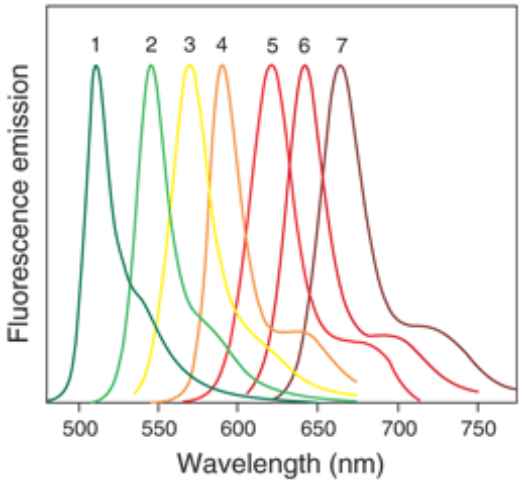

Figure 6.4 : Normalised fluorescence emission spectra of BODIPY chromaphores available from Life Technologies Corporation

Molecules based on the BODIPY often have photophysical properties comparable to fluorescein, rhodamine and perylene dyes. They normally absorb and fluoresce in the visible region, with molar

absorption coefficients in the range 4-8 x10^5 $M^{-1}.cm^{-1}$, very small Stokes shifts, nanosecond range fluorescence lifetimes and reasonable to excellent fluorescence quantum yields.[2]

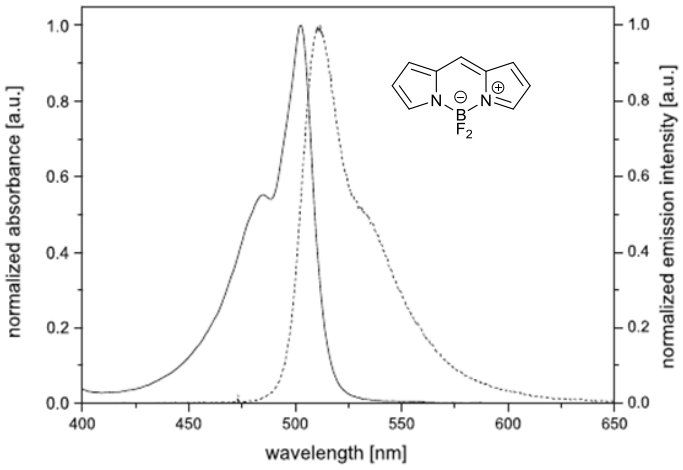

Figure 6.5 : Absorption (solid line) and fluorescence emission (dashled line) spectra of "naked" BODIPY in DCM(adapeted from Schmitt *et al.* [6])

The "naked" BODIPY core, without functionalization, has absorption and emission spectra characteristic of the series: the absorption spectra has the $S_0 \rightarrow S_1$ (π-π^*) transition at ~500 nm, with the vibrational transition 0→1 at ~470 nm, and a $S_0 \rightarrow S_2$ transition at ~375 nm. Mirror image emission spectra with a Stokes shift of around 10 nm are standard for these molecules[37]

BODIPY dyes have very low intersystem crossing yields, giving a double benefit of increasing fluorescence quantum yields and also preventing the formation of singlet oxygen species that cause chromaphore degradation.[2] Thus it is not common for BODIPY dyes to phosphoresce. Iodine functionalized BODIPYs show intersystem crossing due to the heavy atom effect, these are used as photosensitizers in biological systems,[35] as well as TTAUC.[32–34] Iodine containing BODIPY sensitizers can have high ISC yields, rather than high fluorescence quantum yields, these are mutually exclusive.

The BODIPY core is highly tunable with respect to the position of the absorption and emission bands, by altering the number, position and type of substituents, due to both electronic and steric interactions.[1,38]

The great majority of suggested applications for BODIPY dyes make use of their excellent emissive properties so it is natural that the effect of functionalization upon these chromaphores has been investigated in detail.[1] Since altering the *meso* functionalisation is the most facile route to producing diverse BODIPY analogues Boens *et al*. have reviewed the effect of electron donating and electron withdrawing aryl groups in this position.[1,19]

Compared to the completely unfunctionalised BODIPY addition of a phenyl group at the *meso* 8 position causes a large decrease in fluorescence quantum yield, due to rotation allowing a non-

radiative relaxation mechanism.[4] The insertion of steric blocks preventing this pushes the quantum yield back up.[38]

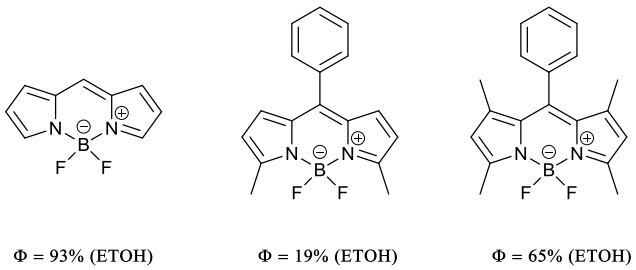

Figure 6.6 : Effect upon the quantum yield of BODIPY emitters due to the addition of unconstrained and constrained meso phenyl groups

However once the phenyl group is in place, its alteration by carbon skeleton extension through the *para* position or by additional withdrawing groups does not produce large changes in the fluorescent properties of the BODIPY dye, with little change to peak position, Stokes shift, extinction coefficient or fluorescence quantum yield. This is likely due to the perpendicular geometry of the 8-aryl group, which does not have strong π conjugation with the emissive BODIPY core. Again, preserving the orthogonal nature of the 8-aryl by introduction of 8-aryl ortho substituents, to prevent rotational relaxation has been shown to increase the fluorescence quantum yield significantly.[38]

While groups on a *meso*-phenyl generally do not have large effects on the emissive properties due to the orthogonal position of the pi systems, increasing the amount of electron donating groups on the phenyl increases the quantum yield, and can cause a bathochromic shift.[39]

In addition to the steric blocking effect, the presence of a pentafluorophenyl in the 8- position has been shown to red-shift the spectral maxima by ~20 nm, due to stabilization of the HOMO-LUMO energy gap. The presence of the pentafluorophenyl group causes a solvent effect, with fluorescence quenching in polar solvents such as methanol, and greatly improved fluorescence quantum yields in apolar solvents such as toluene. Substitution in the 3,5- positions often has a greater effect on the fluorescent properties of the BODIPY dye, and can cause large red-shifts of absorption and emission maxima. In general more constrained BODIPYs are better emitters, since less energy is lost as a function of rotation and vibration in the molecule.[38,40]

Substitution in 2,6- positions has little steric effect upon the BODIPY core, while substitution in 1,7- positions can have a large effect on the emissive properties due to steric effects. Substitution in the 3,5- positions often has a greater effect on the fluorescent properties of the BODIPY dye, and can cause large red-shifts of absorption and emission maxima.

6.1.1. BODIPY emitters in TTAUC

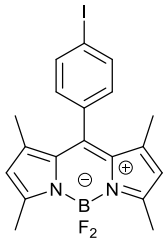

BD-1

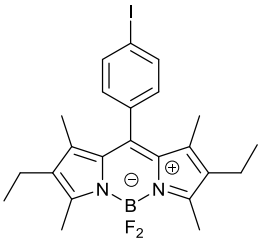

BD-2

Figure 6.7 : BODIPY chromaphores used for TTAUC emission

Within the TTAUC arena BODIPY based molecules have been used as the sensitiser,[32–34] and also the emitter dye.[41,42] Bodipy class emitters are a departure from the emitters that have been commonly used it the past, as they are not based on polyaromatic hydrocarbons, but are rather based on boron dipyrromethene heterocyclic structures. They have reasonable to very high fluorescence quantum yields and are stable under emissive conditions.

The compounds selected, BD-1 and BD-2, possessed fluorescence quantum yields of 69% and 78% and produced external up-conversion quantum yields of 3% and 8% respectively.

BODIPYs provide a range of selectable emission peaks by their well investigated structures, however they do not provide a high up-conversion quantum yield – they do not navigate the up-conversion gauntlet as efficiently as PAH based dyes. This may be due to a mismatch between the energy level of the porphyrin sensitizer and BODIPY emitter, preventing efficient TTT, or inefficient TTA due to either an extremely low lying T_1 level, or very accessible higher energy levels. The triplet energy of BODIPY systems is relatively low, ~780 nm (~1.6 eV), [10] but is not so low as to preclude TTA to S_1 in the region of ~450 nm (~2.8 eV). As with all TTA systems oxygen should be rigorously excluded, since BODIPY molecles may break down under high laser intensities in the presence of oxygen, similar to other PAH.[39]

6.2. Synthesis Aims and Approach

Target molecules with structural similarities to the previously synthesised diphenylanthracenes (Chapter 2) and diphenylperylenes (Chapter 4) were chosen. As our investigations had showed that the most effective emitter molecules were the non-fluorinated and most highly fluorinated derivatives (Chapters 3,5) these derivatives were selected for study of BODIPY up-converting dyes.

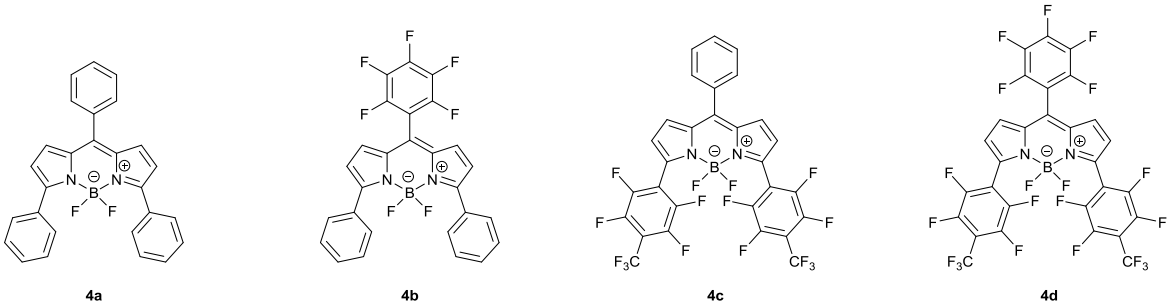

Figure 6.8 : BODIPY emitter targets

The emitters **4a-d** are 3,5,8-triphenylBODIPY dyes that are expected to have high fluorescence quantum yields, and therefore be good up-conversion emitter candidates. To produce a retrosynthetic analysis of the BODIPY emitters a short survey of literature preparations is required.

6.2.1. Synthesis of the first and "naked" BODIPYs

The first BODIPY structure, reported in 1968 by Treibs and Kreuzer, was produced adventitiously by condensation of 2,4-dimethylpyrrole with acetic acid in the presence of boron trifluoride etherate.[43]

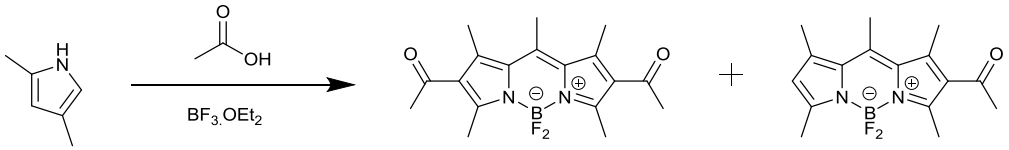

Figure 6.9 : The original BODIPY

The formation of the BODIPY heterocyclic skeleton is based on condensation reactions between pyrroles and carbonyl compounds forming dipyrromethane analogues, which draws on the wealth of knowledge from related porphyrins.[2]

Despite the increasing interest in BODIPY dyes over the last 30 years the "naked" (i.e. no substitution on the core moiety) BODIPY structure was not isolated until 2008, when three groups released their syntheses in quick succession. The difficulty in its preparation is the instability of the dipyrromethene precursor, decomposing even at -40 °C.[5]

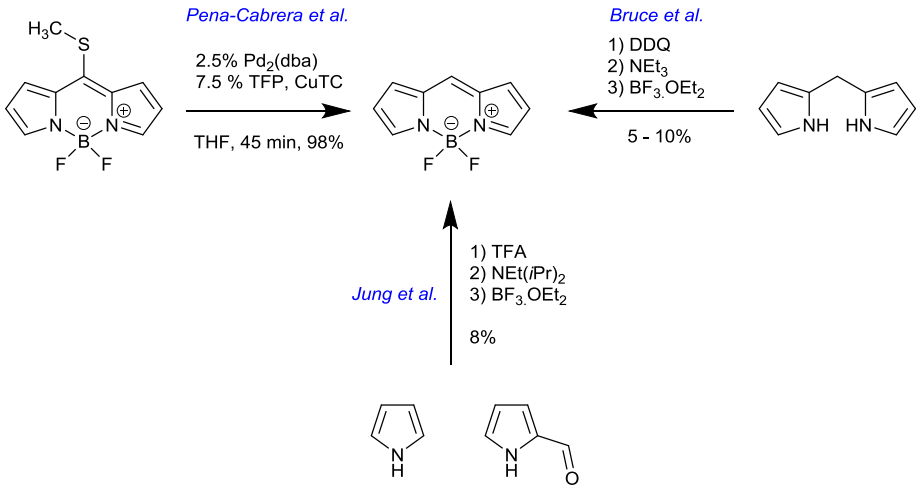

Figure 6.10 : Syntheses of the "naked" BODIPY core compound

The first synthesis by Jung *et al.* used an acid catalyzed condensation of pyrrole-2-carbaldehyde and pyrrole, followed by complexation in one pot allowing the title compound in 8% yield. They also provided extensive spectral and crystallographic data.[6] This was followed by Bruce *et al*, who showed that the heterocyclic skeleton could be produced by oxidation of the parent dipyrromethane with DDQ at low temperature under inert conditions. This was then complexed with boron trifluoride etherate in the presence of DBU to form BODIPY in 5-10% yield, sufficient quality and quantity for analysis and x-ray crystallography.[7] Finally Pena-Cabrera et al simply produced a 8-thiomethyl protected BODIPY and removed the extra functionality with catalytic palladium and stoichiometric copper(I) thienyl-2-carboxylate (CuTc), allowing the product in quantitative yield.[5]

Following the successful synthesis of the naked BODIPY core it was shown to possess a high quantum yield of up to 93% in non-polar and polar solvents, a high photostability (τ = 7.2 ns) and absorption and emission peaks at 503 and 512 nm, respectively. However, it has poor thermal stability and decomposes above 50 °C.[5–7] Nearly every addition to the naked BODIPY core cause red-shifts, to varying degrees.[4]

6.2.2. Routes to structurally diverse BODIPY dyes

The BODIPY core molecule, while an efficient emissive molecule, has a number of draw backs, not least its low thermal stability. This means that routes to other BODIPY dyes, with differing properties, such as linkers for biomolecule binding,[20] or iodine incorporation to produce heavy atom effect ISC, are desired.[32–34] In general there are three main portions to the synthesis of BODIPYs: formation of the heterocyclic skeleton, complexation of the boron trifluoride, and functionalization of the organic structure.

6.2.2.1. Heterocyclic skeleton formation

Synthetic routes to the dipyrromethene heterocyclic skeleton makes use of the wealth of knowledge already available from porphyrin syntheses.

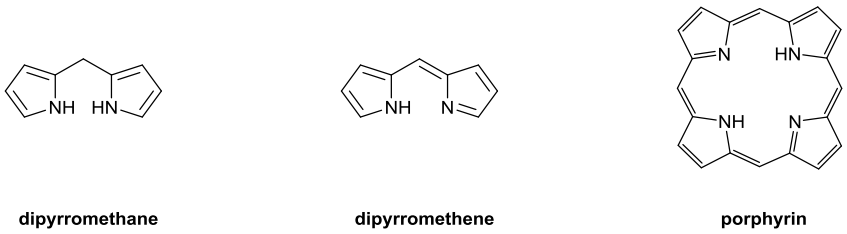

Figure 6.11 : BODIPY heterocyclic core and porphyrin heterocyclic structure

Acid catalyzed condensation of two or more equivalents of a pyrrole with an acid chloride, anhydride or aldehyde allows a symmetrical heterocyclic skeleton, with substitution in the 8-position easily added by modulating the carbonyl partner.[44] To promote the production of a dipyrromethene rather than porphyrin either a large excess of pyrrole derivative is used, or a substrate with substitution at the pyrrole 2- position, commonly a methyl group is used.

Aldehydes form light, air and acid sensitive dipyyromethanes, which are best oxidized to dipyrromethenes and complexed with BF_3 soon after preparation. Oxidation is generally carried out with DDQ (2,3-dichloro-5,6-dicyano-p-benzoquinone) or, for more mild reaction conditions, p-chloranil (2,3,5,6-tetrachloro-p-benzoquinone). Acid chlorides and anhydrides form dipyrromethenes *in situ*. Formation of the heterocyclic core and oxidation then complexation with boron trifluoride etherate may be carried out in a one pot procedure.[1]

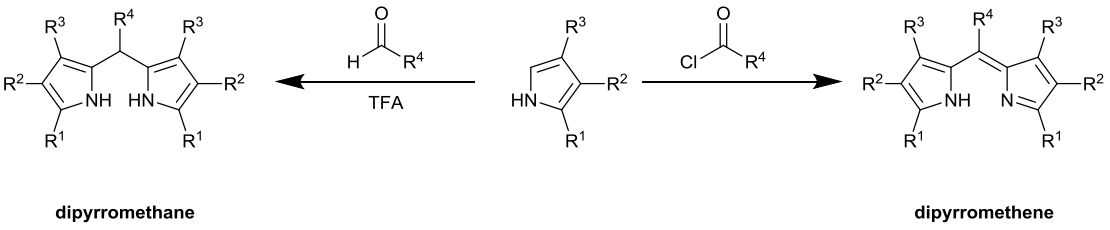

Figure 6.12 : Condensation to produce heterocyclic core

Formation of the simple BODIPY emitter with no pyrrole functionality and a *meso*-phenyl group is carried out using benzaldehyde, since the acid chloride is too reactive, and a large excess of pyrrole to prevent formation of porphyrin byproducts.[45]

This Lindsey type chemistry is the most common approach to the BODIPY heterocyclic skeleton.[46,47] Heterocyclic skeletons that are not functionalized in the 8- position, while being generally less stable than their substituted analogues,[48] have been synthesized by either acid catalyzed self-condensation of a pyrrole carbonyl cation,[49] or self-condensation of pyrrole-2-carbaldehyde in the presence of phosphorus oxychloride.[50]

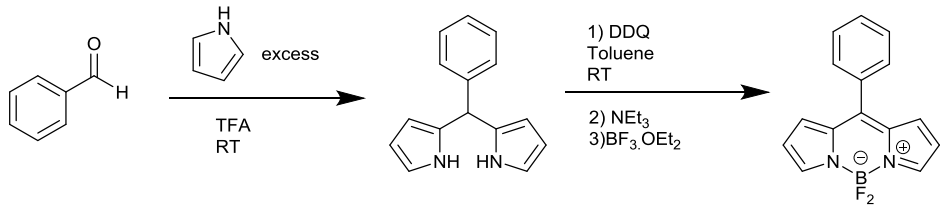

Figure 6.13 : Synthesis of simple BODIPY emitter

Assymetric BODIPYs are formed by one-pot two-step condensations of a pyrrole with one equivalent of acid chloride,[51] acid anhydride,[52] or ester,[53] followed by addition of a second, different pyrrole allowing an asymmetric dipyrromethene.[54]

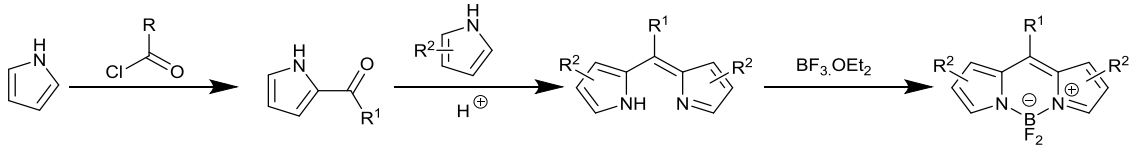

Figure 6.14 : Synthesis of assymetric BODIPY emitters

6.2.2.2. Boron trifluoride complexation

Once formed, the heterocyclic skeleton is subjected to treatment with boron trifluoride etherate in the presence of a tertiary amine base (commonly NEt_3 although Hünig's base is also used), giving the BODIPY dye in typically ~50% yield. This may be done *in situ*, although it has been reported that isolation of the dipyrromethene/dipyrromethane and then complexation improves the overall yields, possibly due to more facile purification of the final product.

This reaction is a two step mechanism, first the dipyrromethene (H-DPM) electron donor forms a stable donor-acceptor complex with the boron trifluoride acceptor, by donation of electrons into the vacant boron p-orbital, forcing a change in geometry from trigonal planar to tetrahedral. This puts a fluorine atom very close to the opposite N-H group of the dippyrromethene. Hydrogen bonding through [N-H ---- F-B] stabilizes this structure allowing fluorine – hydrogen bond formation and elimination of HF to form the BODIPY core.[55]

$$\text{H-DPM} + BF_3 \rightleftharpoons [\text{H-DPM}.BF_3] \qquad (6.1)$$

$$[\text{H-DPM}.BF_3] \rightarrow [BF_2.\text{DPM}] + \text{HF} \qquad (6.2)$$

These complexation reactions are carried out in moderately polar solvent mixtures, such as toluene and DCM, to allow slight solvation of the BF_3 molecule, more polar solvents form stable complexes with BF_3.

6.2.2.3. Functionalisation of the *meso* position

The functionalization of BODIPY dyes in the meso (C-8) position is normally a matter of altering the carbonyl condensation partner when forming the heterocyclic skeleton. As the dyes are chemically robust, further modifications to the *meso* substituent may be made following the formation of the BODIPY core. These include oxidation, reduction, nucleophilic aromatic substitution.[1]

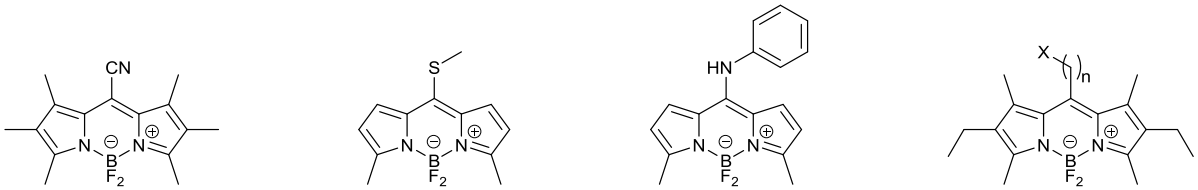

Figure 6.15 : Alternative meta functionality of BODIPY emitters

While halo alkyl, nitrogen, and sulfur containing moieties have been attached to the *meso* site of the BODIPY structure, the most common substituent is an aryl group.[4] This is incorporated during the condensation reaction, with the appropriate benzaldehyde or benzoyl chloride.

6.2.2.4. Functionalisation of the pyrrole periphery

Routes to effective functionalization of the pyrrole periphery are myriad, and may be conducted in varying order. In general, there are two main routes to functionalised BODIPY emitters, since functionalization of the periphery may be carried out before,[56] or after the formation of the heterocyclic skeleton.[19,33,57] Reactions functionalizing the heterocyclic core or complexed BODIPY form symmetrical dyes, normally with substitution in the 2,6- or 3,5- positions.

6.2.2.4.1. BODIPY core: 2,6- functionalization

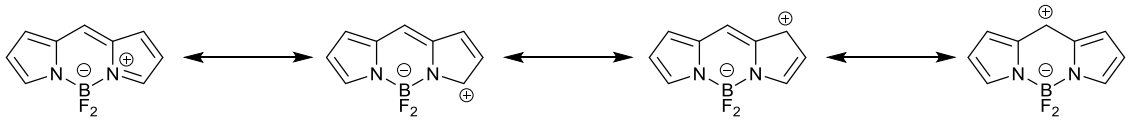

Figure 6.16 : Positions of electrophilic attack on a BODIPY core

Electrophilic substitution reactions on the BODIPY core occur at the 2 and 6 positions and these include halogenation,[58] nitration,[59] sulfonation,[60] and formylation.[44] Each of these substitutions causes a decrease in quantum yield, and halogenation, especially bromination and iodination, causes a large decrease due to the heavy atom effect.[61] These halogenated BODIPYs may be used as transition metal catalyzed coupling partners, and both Sonogashira and Suzuki-Miyaura

reactions have been carried out on these systems to form conjugated emissive polymers and supramolecular assemblies.[62,63]

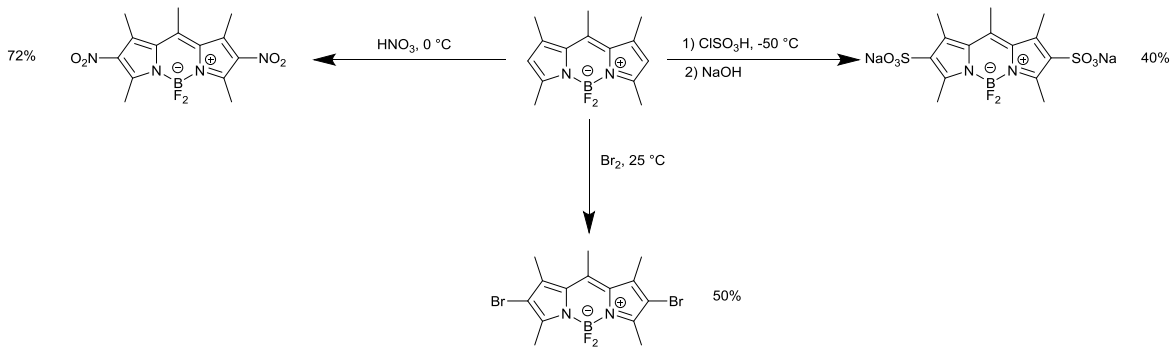

Figure 6.17 : Electrophilic substitution reactions on the BODIPY core, adapted from[4]

In addition to electrophilic substitution, the 2,6- positions allow C-H activation reactions and functionalisations to be carried out, producing substituted analogues in one step.[9]

6.2.2.4.2. BODIPY core: 3,5- functionalization

Due to the risk of polymerization during the heterocyclic skeleton forming condensation step, it is rare to use unfunctionalised pyrrole, and instead 2-methylpyrrole is commonly used. This introduces a methyl group to the 3,5- position of the BODIPY core, which may undergo Knoevenagel-type condensations with carbonyl compounds, commonly aromatic aldehydes, as the methyl groups possess reasonably acidic protons.[14] This introduces styryl moieties at the 3,5-positions in a more convenient method than for example a Stille coupling, but in low yields.[64]

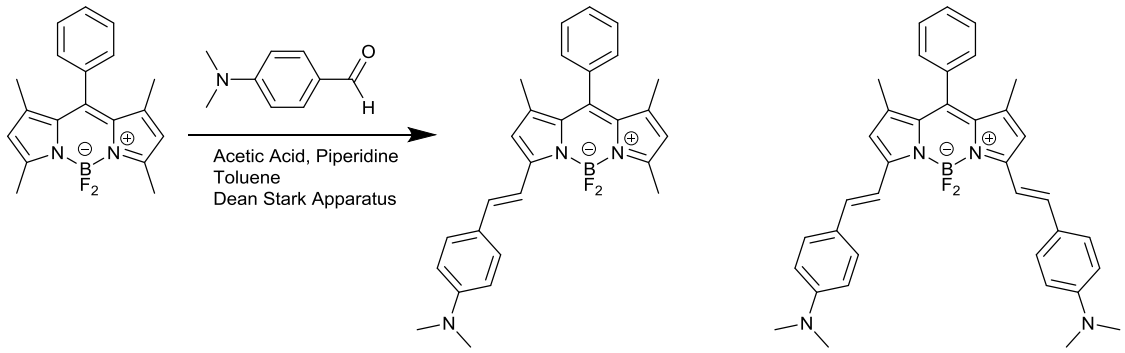

Figure 6.18 : Knoevenagel Reaction

The Knoevenagel reaction is an aldol-like reaction, where a stabilized carbanion attacks the partner carbonyl, followed by an overall dehydration giving the styryl derivative.

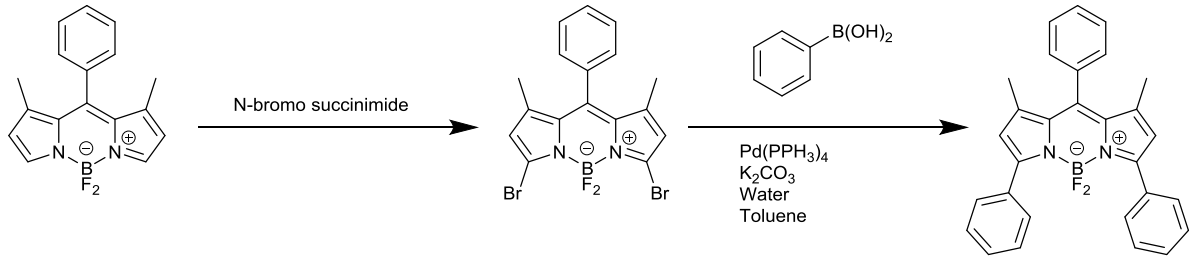

Figure 6.19 : Halogenation and functionalisation in the 3,5-positions of a BODIPY emitter

Incorporation of halogens in the 3,5- positions of the BODIPY core using electrophilic halogenating agents including NIS, NBS, NCS, etc, allows these halogenated BODIPY dyes to be used as coupling partners in Heck, Ullman, Sonogashira, Stille and Suzuki-Miyaura reactions, as well S_NAr processes.[8,57,65–67] Recently a preparation using CH activated coupling of a BODIPY core with bromo-aryl derivatives has been reported, working best with electron rich bromo-aryl compounds.[68] While this is a useful procedure it is unlikely to be successful with highly fluorinated substituents.

6.2.2.4.3. Reactions on pyrrole substituents

Rather than altering the BODIPY emitter following coordination, the functionalisation of the pyrrole before condensation can give access to a wide range of BODIPY dyes and 2-aryl pyrroles prepared by Suzuki-Miyaura reactions are common precursors.

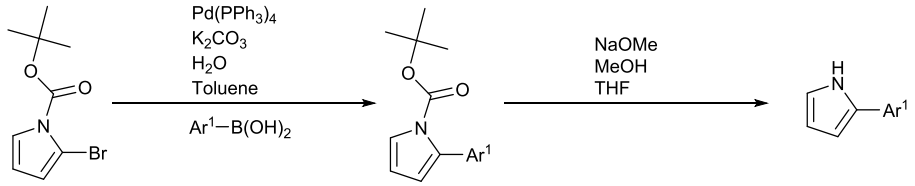

Figure 6.20 : 2-aryl pyrrole synthesis

6.3. Practical Synthesis Results and Discussion

With these literature preparations in hand, a retrosynthetic analysis of the desired fluorinated BODIPY products can be produced (Figure 6.21).

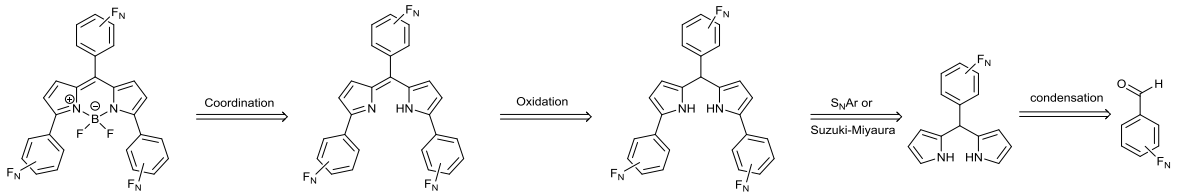

Figure 6.21 : Retrosynthetic analysis to BODIPY emitters

An initial target molecule, with highly fluorinated aryl rings in the 3,5 positions of the BODIPY core, with a phenyl group in the *meso* position, was selected. Condensation of the heterocyclic skeleton precursor is known in the literature, and the octafluorotoluene should undergo ready nucleophilic substitution, whereas for addition of non-fluorinated periphery, a Suzuki-Miyaura reaction may be used. Following functionalization the core can be oxidised and the boron trifluoride coordinated to provide the completed emitter.

The non-fluorinated BODIPY was synthesised by a literature procedure; benzaldehyde with 25 equivalents of freshly distilled pyrrole as solvent and a drop of trifluoroacetic acid was stirred for 15 min.

Aldehyde	Dipyrromethane Product	Yield
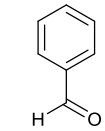	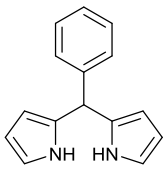	**11a,** 24%
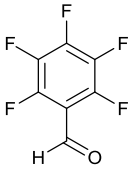	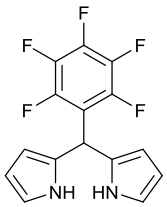	**11b,** 35%

Figure 6.22 : Synthesis of Dipyrromethane

This slightly exothermic condensation reaction produces the desired product, as well as a large amount of polypyrrole by-products.[69] Purification by sublimation followed by recrystalisation from ethanol gives the dipyrromethane.

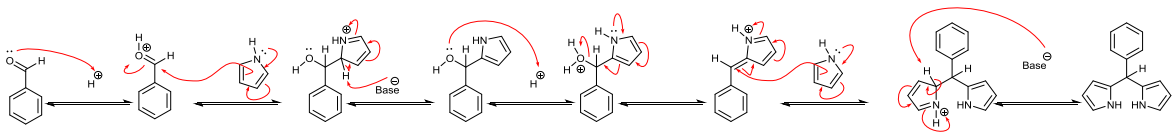

Figure 6.23 : Acid catalysed condensation of pyrrole and benzaldehyde

While the dipyrromethane product is of sufficient purity following a sublimation and recrystalisation for subsequent reactions, however, a second sublimation allowed x-ray crystallography quality crystals to be collected.

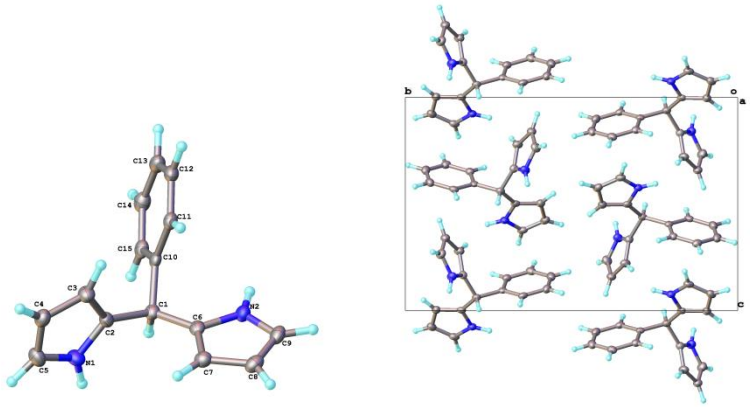

Figure 6.24 : Molecular (left) and crystal (right) structures for dipyrromethane **11a**

The perfluorophenyl dipyrromethane analogue was synthesised in the same manner, and the structure was characterised by x-ray crystallography.

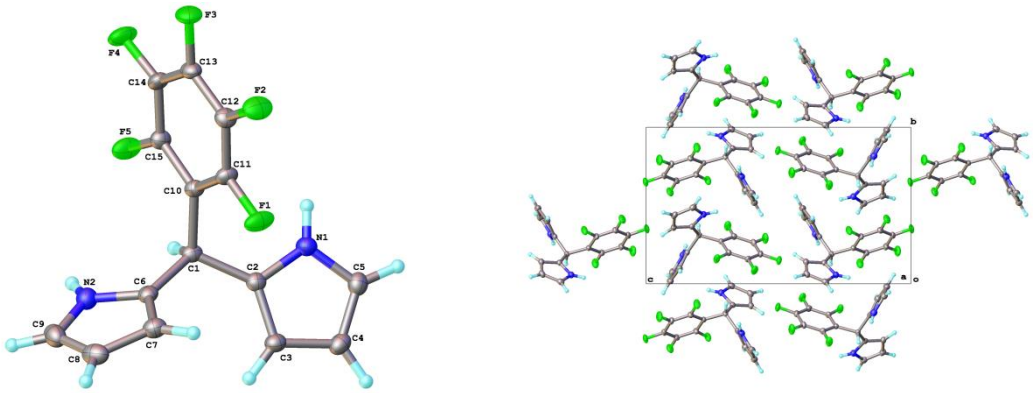

Figure 6.25 : Molecular (left) and crystal (right) structures of perfluorophenyldipyrromethane **11b**

The heterocyclic core **11a** was protected with Boc, using 2.1 equivalents of Boc_2O in acetonitrile using DMAP as an initiator. Washing with basic solution and extraction of organic material with ether gave the N-Boc protected molecule in high yield.

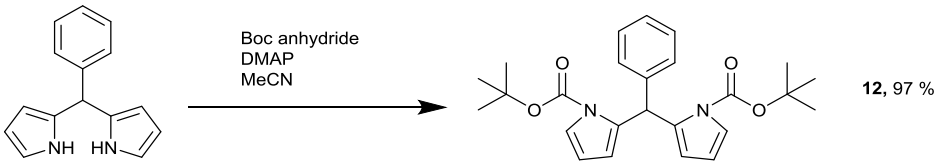

Figure 6.26 : Protection of Dipyrromethane

Following isolation of the purified protected intermediate, S_NAr reaction with octafluorotoluene was attempted. This made use of LDA at low temperature to produce a carbanion capable of nucleophilically attacking the activated aromatic ring, potentially leading to highly fluorinated functionalization in the dipyyromethane 1,9 positions.

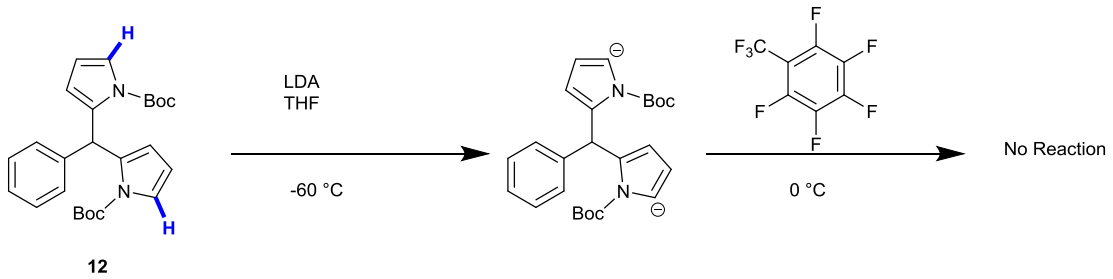

Figure 6.27 : Nucleophilic substitution reaction

Addition of LDA under inert conditions causes the development of a vivid purple colour. Following stirring for 1 h octafluorotoluene was added dropwise and the reaction stirred to room temperature over 72 h. Following isolation by a dilution with dilute HCl and extraction with ether the products were analysed by mass spectrometry, and showed a mixture of products, but the desired compound was not detected. Since octafluorotoluene is highly activated to nucleophilic attack it can be assumed that other less fluorinated analogues would not be successful for this synthesis route.

Another route was required for the production of fluorinated 3,5,8-triarylBODIPY dyes and by functionalising the pyrrole moiety before the condensation reaction the S_NAr reaction could be encouraged, and so the target intermediate produced.

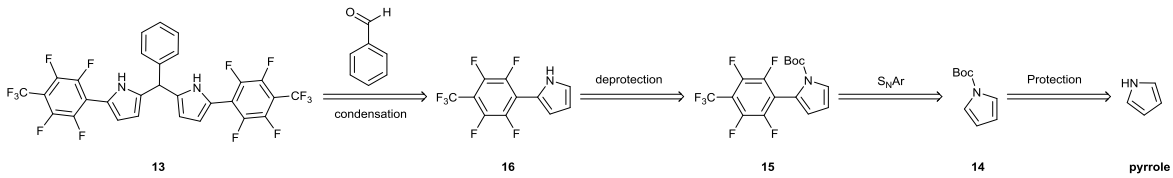

Figure 6.28 : Retrosynthetic analysis of target intermediate

The first step in this new route is the Boc protection of pyrrole. This was carried out in quantitative yield in dry MeCN using DMAP as an initiator. The N-Boc protected pyrrole was then subjected to LDA at low temperature, followed by dropwise addition of octafluorotoluene.

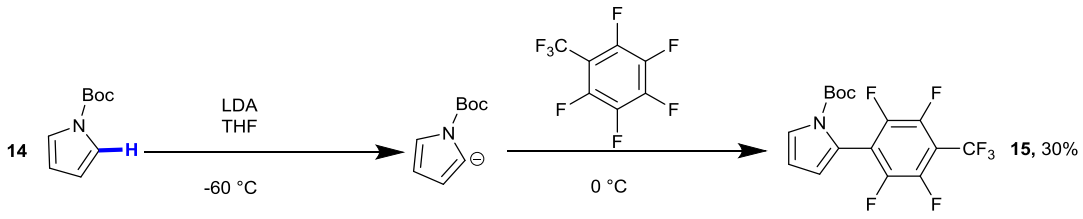

Figure 6.29 : Synthesis of fluorinated n-boc pyrrole intermediate

Impurities include the disubstituted 2,5-di-((4-trifluoromethyl)perfluorophenyl)pyrrole molecule, and the product was purified by short path distillation at 150 °C and 15 mbar using Kugelrohr apparatus giving 30% yield. Analysis by NMR showed the distinct CF_3 and aryl fluorine

functionality, while mass spectrometry showed the molecular ion, as well as the loss of the MS sensitive Boc group.

Removal of the Boc protecting group from the 2-arylpyrrole intermediate **15** was carried out using TFA in DCM (10% v/v), stirring for 72 h at room temperature. The resulting solid was recrystallized from water and methanol to give 2-((4-trifluoromethyl)perfluorophenyl)pyrrole molecule, which easily sublimed. Following collection of the unprotected intermediate condensation reactions with benzaldehyde were attempted on multiple occasions; however the desired condensation product with the BODIPY heterocyclic skeleton could not be isolated after various attempts. It is likely that the extremely strong electron withdrawing character of the 4-trifluoromethylperfluoroaryl group greatly deactivates the pyrrole moiety, preventing the condensation reaction from occurring even at elevated temperatures for prolonged periods. Under the same conditions the unfunctionalised 2-phenylpyrrole condensation with benzaldehyde is completed in 15 min at room temperature.

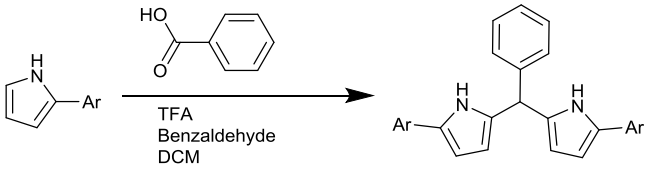

2-Arylpyrrole	Dipyrromethane Product	Yield
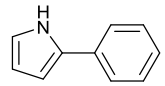	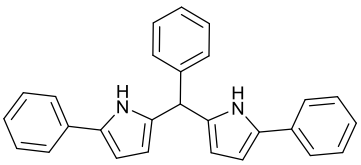	46%
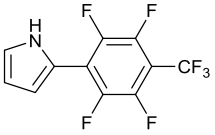	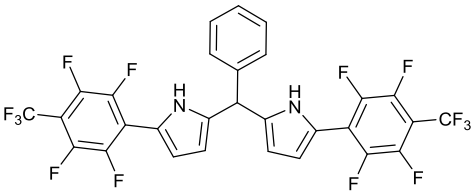	0%

Figure 6.30 : Attempted condensation of highly fluorinated arylpyrrole analogue with benzaldehyde

Clearly a less deactivated aryl-pyrrole analogue is required to allow the condensation reaction to proceed. This would necessarily require a less fluorinated aryl moiety, which would therefore be less activated to S_NAr – another method is required to functionalise the pyrrole portion with an aryl partner. Since the Suzuki-Miyaura reaction has been employed with successfully previously in the project to produce aryl-aryl bonds (Chapters 2,4) it was rational to revisit it.

Other groups have used Suzuki-Miyaura couplings in the production of BODIPY molecules, both before and after condensation to produce the heterocyclic core. The target BODIPY emitters

(Figure 6.31) were chosen to show the effects of fluorination, without significantly retarding the crucial condensation reaction.

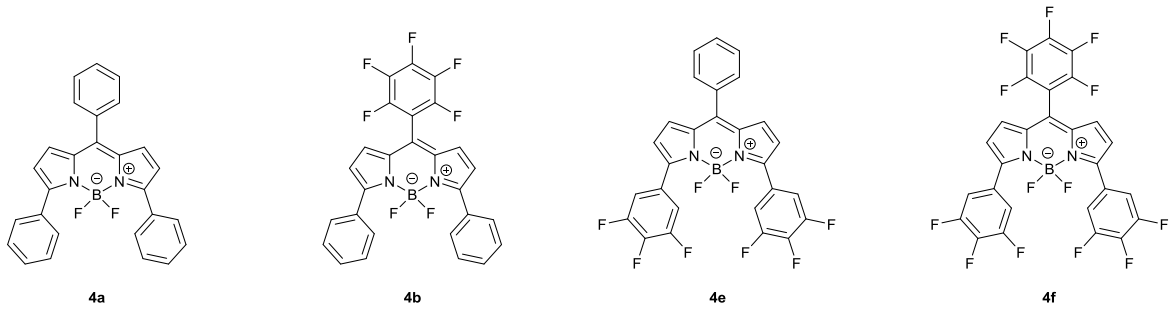

Figure 6.31 : BODIPY emitter targets

Each of these targets use a combination of aryl substitution at the 3,5 and 8 positions, being non-fluorinated or partially fluorinated at the 3,5 positions and non-fluorinated or perfluorinated at the *meso* position. A retrosynthetic analysis of the required aryl-pyrrole intermediate shows the Suzuki-Miyaura coupling of a N-boc protected 2-brominated pyrrole, which may be produced from the pyrrole starting material.

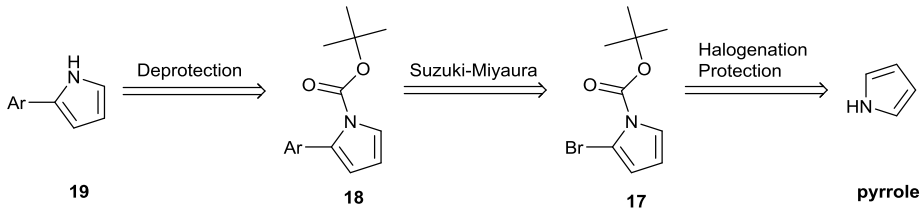

Figure 6.32 : Retrosynthetic analysis of Suzuki-Miyaura coupling route

The initial reaction uses the *N*-bromo halogenating agent 1,3-dibromo-5,5-dimethylhydantoin (DMBMH), initiated by AIBN at -78 °C, the intermediate 2-bromopyrrole is kept cold and the Boc anhydride, DMAP and amine are added. Following a standard work up and short path silica chromatohraphy this literature procedure gives the product in excellent yield. The oil is stored at -10 °C and is stable under these conditions for months as a solid.

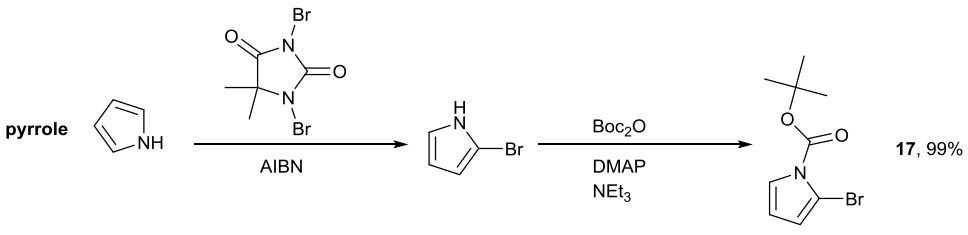

Figure 6.33 : Bromination and protection of pyrrole

The Suzuki-Miyaura halogenated substrate was used to produce two aryl-pyrrole analogues, in high yields. The reagents and solvents were subjected to three freeze-pump-thaw cycles to completely

exclude oxygen. Filtration of the reaction solvent through a pad of silica on a bed of celite gave the intermediate protected aryl-pyrrole in sufficient purity for continuation, in > 90% yield.

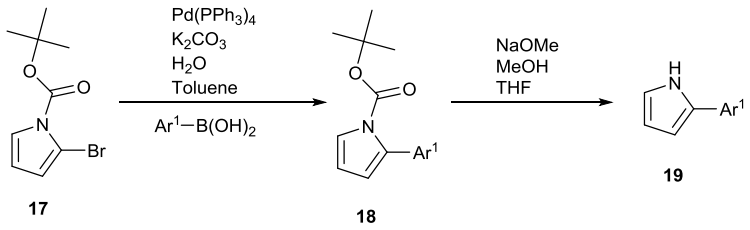

Boronic Acid	2-Arylpyrrole Product	Yield
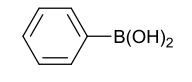	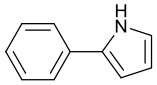	**19a,** 50 %
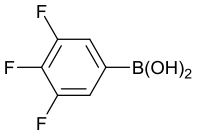	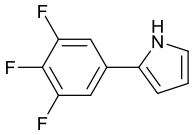	**19b**, 39 %

Figure 6.34 : One-pot Suzuki-Miyaura reactions and subsequent deprotection allowing aryl-pyrrole analogues

Deprotection was accomplished using a suspension of sodium methoxide in THF and methanol, rather than TFA as had been used previously. This gives a cleaner reaction. The majority of yield losses occurred during the deprotection step. There was evidence of *in situ* deprotection of the intermediate *N*-Boc-2-arylpyrrole under Suzuki-Miyaura reaction conditions for the 3,4,5-fluorinated analogue, these were not separated, but carried through to the following deprotection step, allowing a yield over the two steps of 39%. Following a standard workup the aryl-pyrroles were purified by recrystallization (hexane). The aryl-pyrrole analogues should be stored cold to prevent autocondensation occurring.

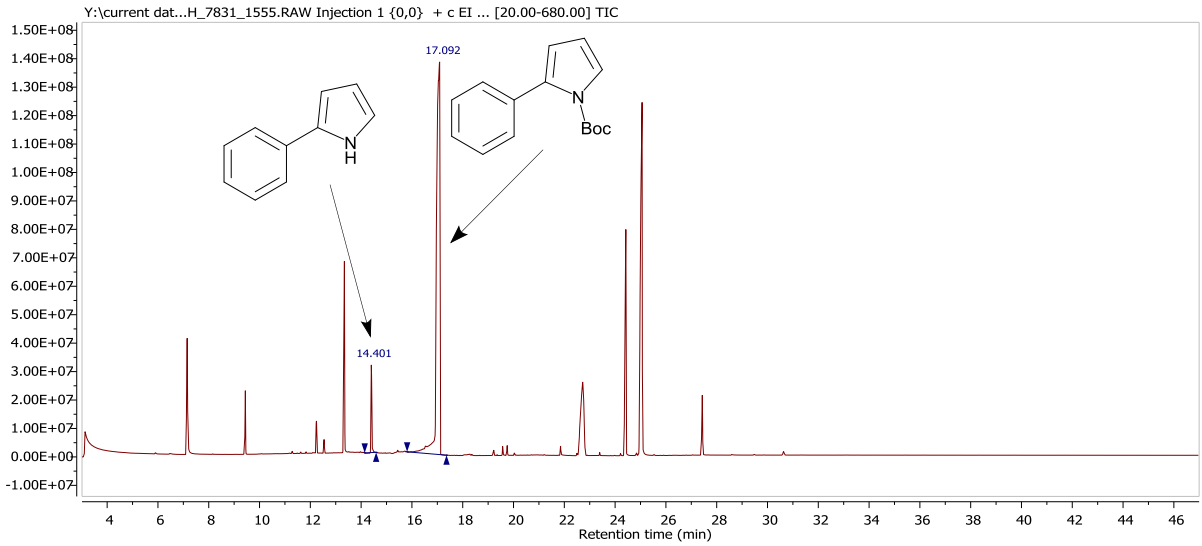

Figure 6.35 : GC trace of attempted one pot synthesis of **19a**

The synthesis of **19a** was repeated with the intention of creating a one-pot procedure, where, following the Suzuki-Miyaura coupling, excess NaOMe was added to the cooled reaction mixture and the suspension stirred for 48 h. However under these conditions the deprotection step did not proceed to completion, a ratio of 20:1 for *N*-Boc protected intermediate : deprotected product was detected by GCMS, along with a number of impurity peaks (Figure 6.35). Deprotection of the nonfluorinated analogue required stirring with excess sodium methoxide for three days, after which the unreacted boc-protected intermediate was removed by column chromatography (silica, eluted hexane: ethyl acetate 1:1) and the product recrystallized to give the desired 2-arylpyrrole.

Condensation of aryl-pyrroles with benzoyl chlorides rather than benzaldehydes was selected as this produces the dipyrromethene heterocyclic BODIPY core in one step, without the need for additional oxidising reagents. These condensation reactions were carried out at 85 °C and often required a number of days to proceed to completion, and when isolated and purified by column chromatography gave the desired intermediate in low to very poor yields, although sufficient material for photophysical investigation was obtained.

The coordination reaction used boron trifluoride etherate, the addition of which to the stirring solution of heterocyclic intermediate with triethylamine and toluene produces a dark green colour, typically turning orange and blood red upon heating. Illumination with UV light after 5 minutes showed a vivid fluorescence associated with BODIPY molecules. The targets were purified by direct application of the reaction solvent to a short basic alumina column and chromatographic separation without any additional pressure.

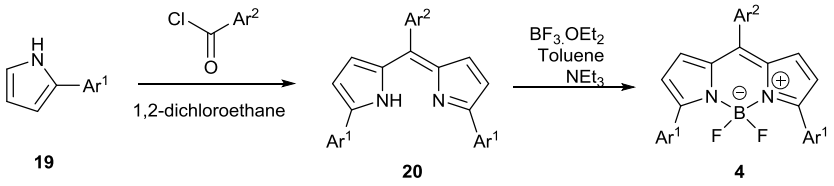

2-Arylpyrrole	Benzoyl Chloride	3,5,8-triarylBODIPY Product	Yield
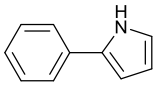	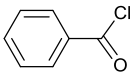	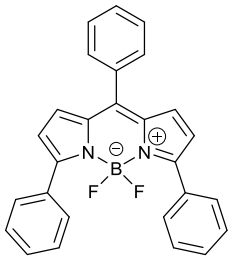	**4a,** 2%
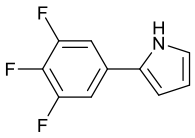	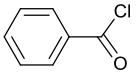	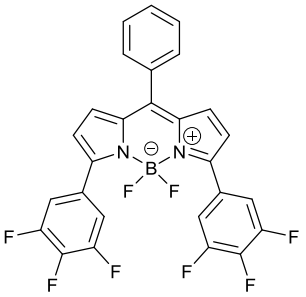	**4b,** 0.6%
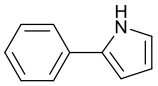	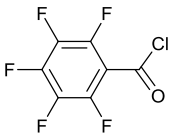	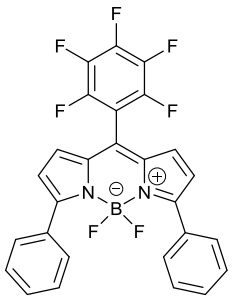	**4e,** 7%
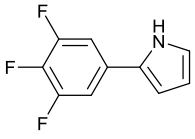	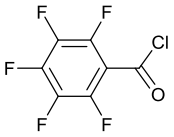	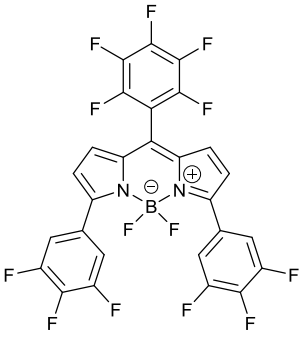	**4f,** 0.3%

Figure 6.36 : Condensation of aryl-pyrroles and boron trifluoride coordination giving the target BODIPY emitters

When the condensation reaction to form **20f** was allowed to continue for only 4 days at reflux the product, when analysed, was instead the ketone intermediate, **20f***. Crystals of the intermediate were isolated and the structure verified by x-ray crystallography. Within the crystal are four

crystallographically independent molecules, with virtually identical geometry, forming loose columns.

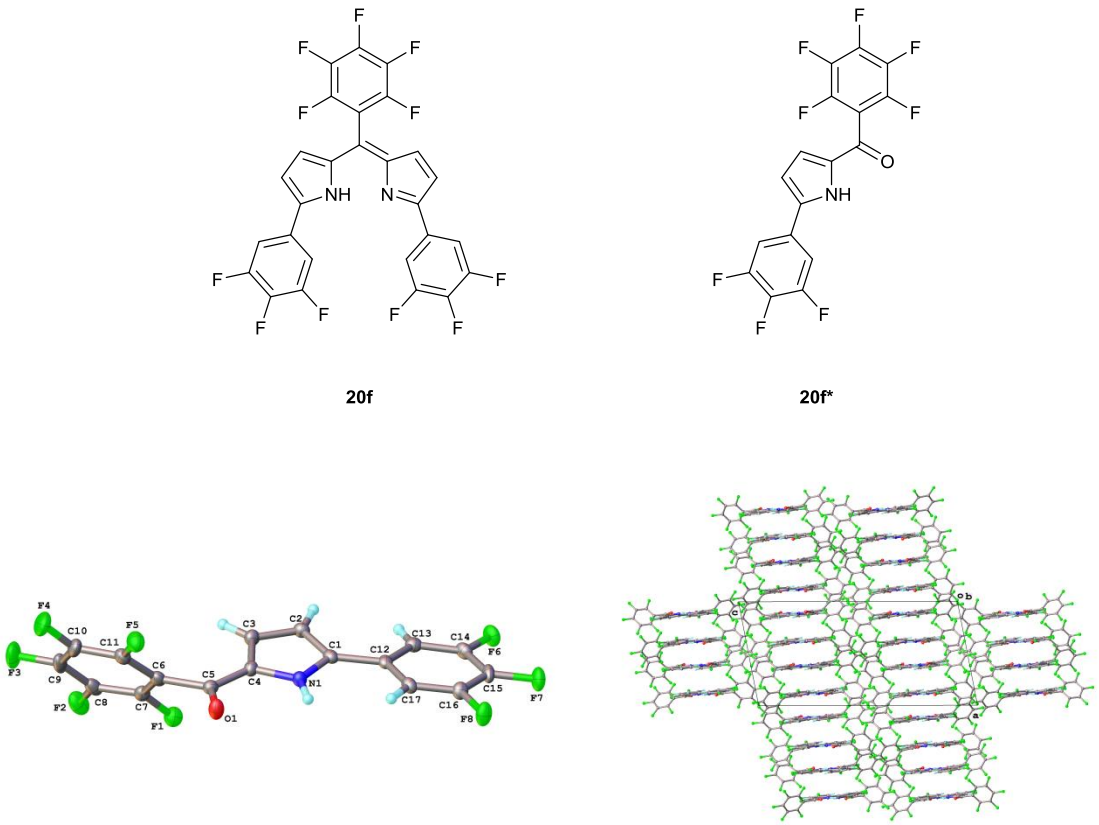

Figure 6.37 : Molecular and crystal structure of intermediate **20f***

Synthesis of **4f** was repeated in a one pot reaction from the relevant aryl-pyrrole without isolation. The condensation reaction was allowed to continue for 5 days and the coordination reaction for 3 days, before application of the reaction mixture to a basic alumina column, eluted with hexane, gradually increasing the polarity with ethyl acetate, until 100% ethyl acetate, allowing the product in 12% yield. It was clear that the preparation of these samples could be improved, both in yield and speed of synthesis.

The synthesis of **4b** was repeated, however following condensation in 1,2-dichloroethane at 80 °C overnight the solvent was removed, and hexane added. The resultant dark purple solution was heated at 80 °C for 3 days, before removal of the solvent, yielding a blue solid. This was analysed by ASAP MS but not purified. Complexation was carried out by addition of dry DCM, dry toluene and dry triethylamine, stirring for five minutes and then addition of excess boron trifluoride etherate. The resulting pink solution was heated at 80 °C overnight. Analysis by ASAP MS indicated that the condensation reaction had completed, but the complexation had not been successful.

A sample of **4a** was recrystallized with hexane / DCM allowing crystals in sufficient quality for x-ray crystallography, allowing its structure to be elucidated. The BODIPY core structure is not a flat raft, rather two flat pyrrole rings joined by a twisted six membered ring. This twisting is caused by the 1.57 Å single N-B bonds, causing the central ring to flare out by 0.1 Å towards the tetrahedral boron complex. The bond distances in the pi conjugated BODIPY core are all ~1.4 Å, while the connections to the phenyl groups are ~1.5 Å, and rotated from the perpendicular position by ~45°.

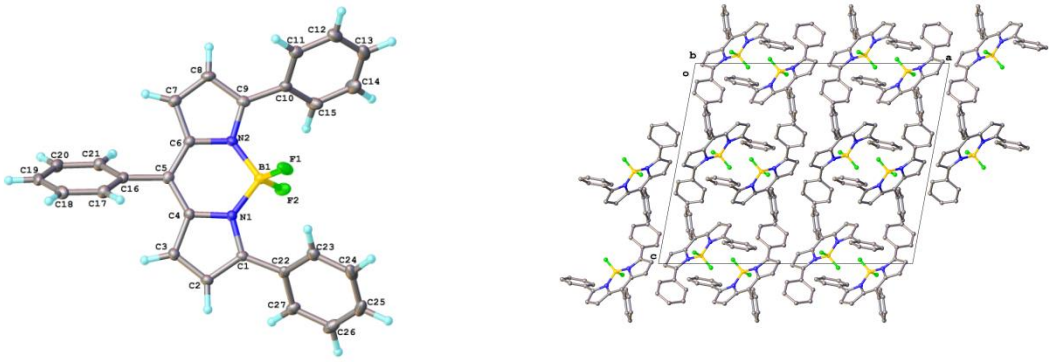

Figure 6.38 : Molecular structure and unit cell structure of **4a**

The twisting is caused by the 1.57 Å single N-B bonds, causing the central ring to flare out by 0.1 A towards the tetrahedral boron complex. The bond distances in the pi conjugated BODIPY core are all ~1.4 Å, while the connections to the phenyl groups are ~1.5 Å, and rotated from the perpendicular position by ~45°. This twisted structure is contrast to the "saddle" like BODIPY core seen for the "naked" BODIPY – it is likely the extra functionality causes a packing structure that influences the internal configuration of the molecule. All attempts to recrystallize the other BODIPY products synthesised were unsuccessful.

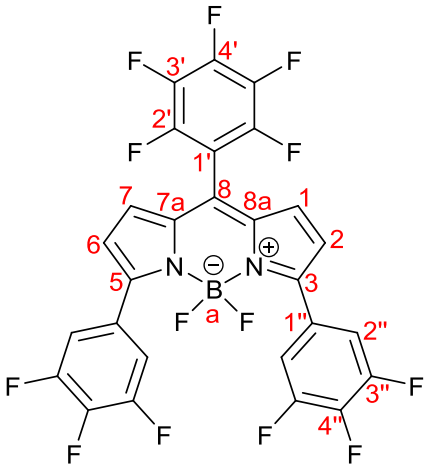

Figure 6.39 : Emitter **4f** with atoms numbered for NMR analysis

Assignment of the NMR specrum of the final products may be accomplished in a similar manner to other emitters synthesised in this project (Chapters 2,4). The carbon atoms are numbered in analogy

with the indacene IUPAC numbering, while the boron atom is labelled **a** rather than **4**. Fluorine and hydrogen atoms are labelled after their parent atom.

First the proton spectrum is assessed. This has three peaks, corresponding to protons at positions 2'', 1 and 2. Proton 2'' couples to its surrounding fluorine atoms, forming a doublet of doublets, while protons 1 and 2 couple to each other. Proton 1 is shifted to a greater extent due to its proximity to the highly electron withdrawing perfluorophenyl group. The fluorine spectrum is assigned initially by integral: position 3'' has 4 equivalent fluorine atoms, while position 4' has only 1. The inequivalent boron bonded fluorines (a) are the least shifted. Fluorine 4'' is a doublet, and fluorines at the 3' and 2' positions are assigned by their integral and the peak structure.

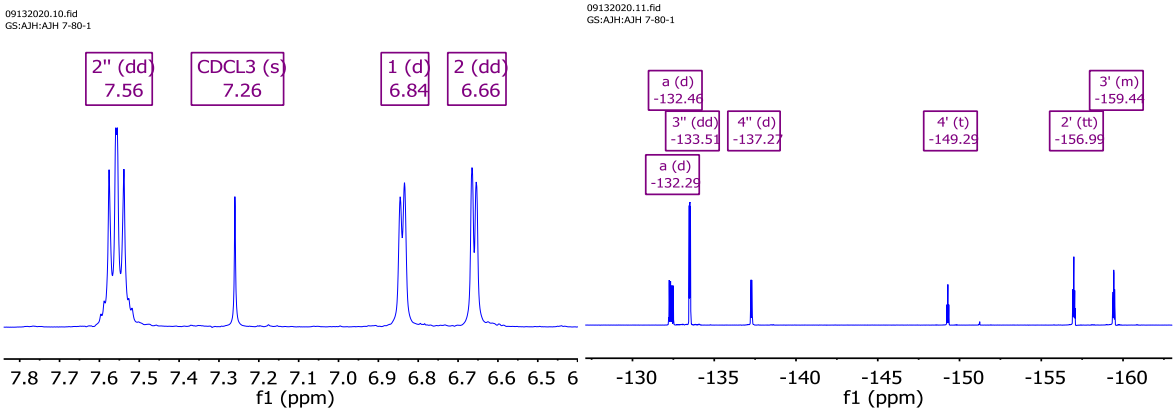

Figure 6.40 : Proton and fluorine NMR spectra of emitter **4f**

The boron NMR spectrum has a triplet for the central BODIPY boron atom, as well as the internal standard boron trifluoride etherate at 0 ppm. The carbon NMR spectrum of BODIPY **6f** is more complicated, with 13 distinct environments.

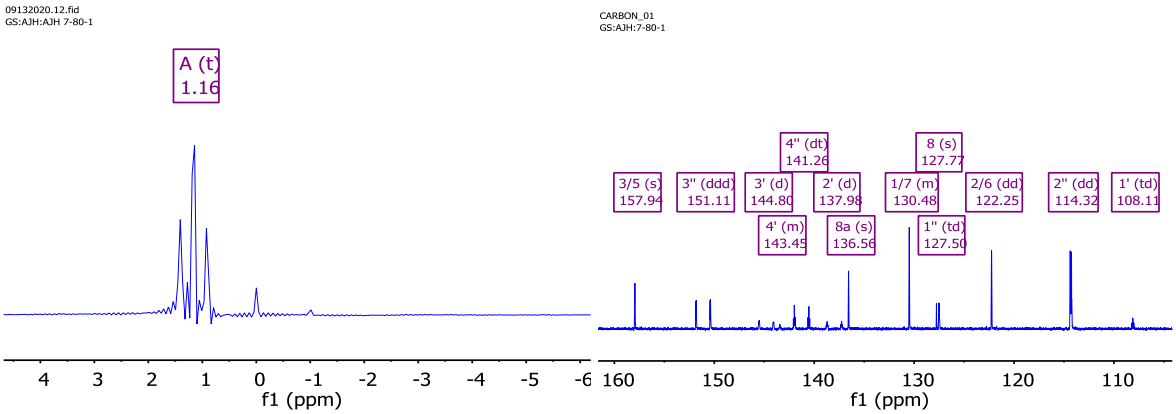

Figure 6.41 : Boron and carbon NMR spectra of emitter **4f**

The HSQC and HMBC 2D NMR spectra can be used to correlate the protons with their bonded carbons, 1,2 and 2''. Carbon environment 2'' also shows 2 bond fluorine coupling, ~ 20Hz, and 3 bond fluorine coupling ~ 5Hz. Carbons with directly bonded fluorines show couplings of ~ 250 Hz, there are 5 of these environments, five wide peaks in the region 155 – 136 ppm. Two of these

overlap each other. The strongest signal of these fluorine coupled carbons environments is 3'', having 4 carbons, while the next strongest is 4'', having 2 carbons. This is correlated by HMBC coupling to proton 11. The weakest of these strongly coupled carbon environments is carbon 4', overlapping with the carbon 4'' environment, while the other two environments are 3' and 2'. Environments 2', 3' and 4' do not show any HMBC coupling to protons, as is expected. Carbon environment 1' shows two bond and three bond fluorine coupling and no HMBC coupling. Carbon environment 1'' shows long distance fluorine coupling, and is very short, with HMBC to proton environment 2''. Carbon environment 3 shows coupling to proton environments 1, 2 and 2', without fluorine coupling. Equivalent carbons 7a/8a HMBC couple strongly to both BODIPY proton environments, while carbon environment 8 couples to them weakly, and shows some long range fluorine coupling. NMR assignments are collated in Figure 6.40 and Figure 6.41.

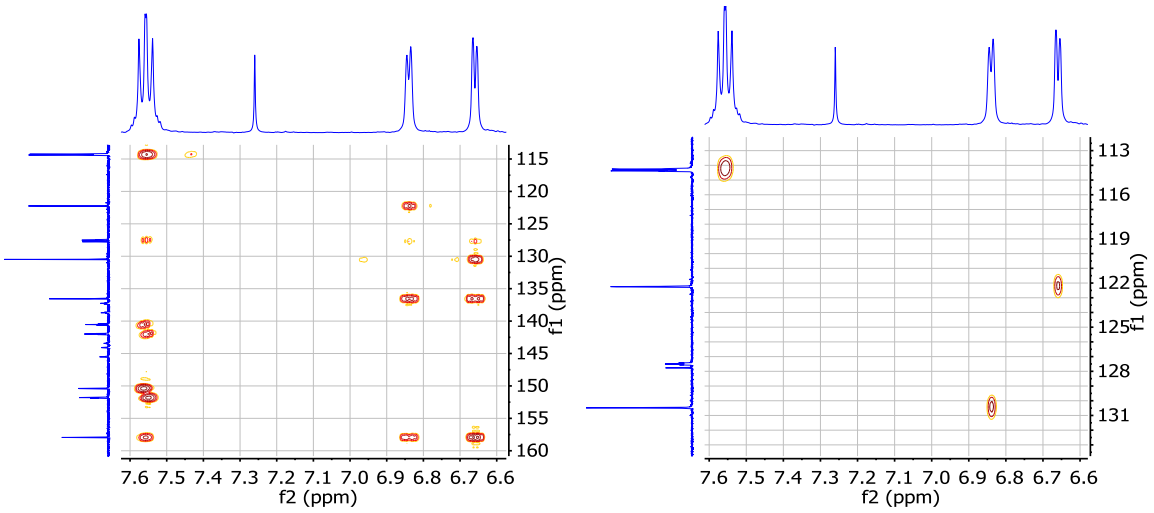

Figure 6.42 : HMBC and HSQC 2D NMR spectra of emitter **4f**

The synthesis of a range of 3,5,8-triarylBODIPY emitter dyes of varying fluorination was achieved in several steps and isolated and purified in quantities required for further testing.

6.4. Fluorescence Measurements of BODIPY dyes

Having synthesised the BODIPY target molecules **4a-b** and **4e-f** their potential as up-conversion emitters was assessed. As before (Chapters 3 and 5) the fluorescence properties of the dyes were measured initially, and then the most promising candidates taken forward to up-conversion measurement.

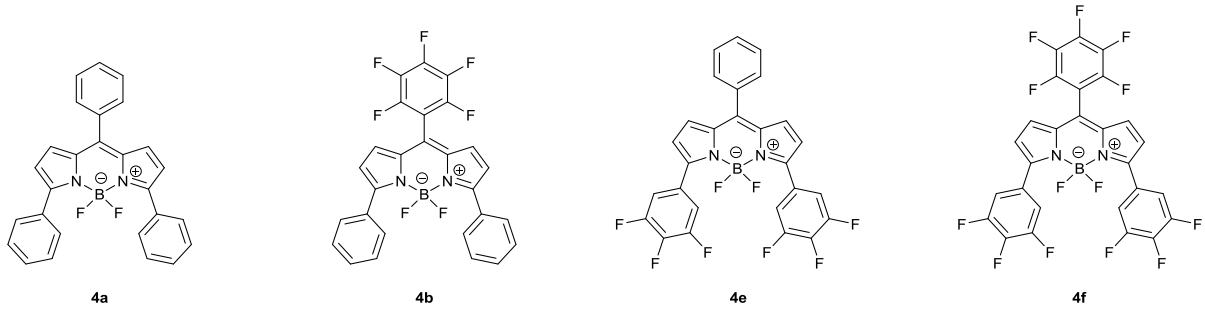

Figure 6.43 : Tested BODIPY emitter dyes

The BODIPY emitters **4a-b,e-f** were synthesised and their fluorescence properties assessed. Each of these dyes have extended conjugation through phenyl groups producing red shifted spectra when compared non-arylated standard BODIPY molecules.

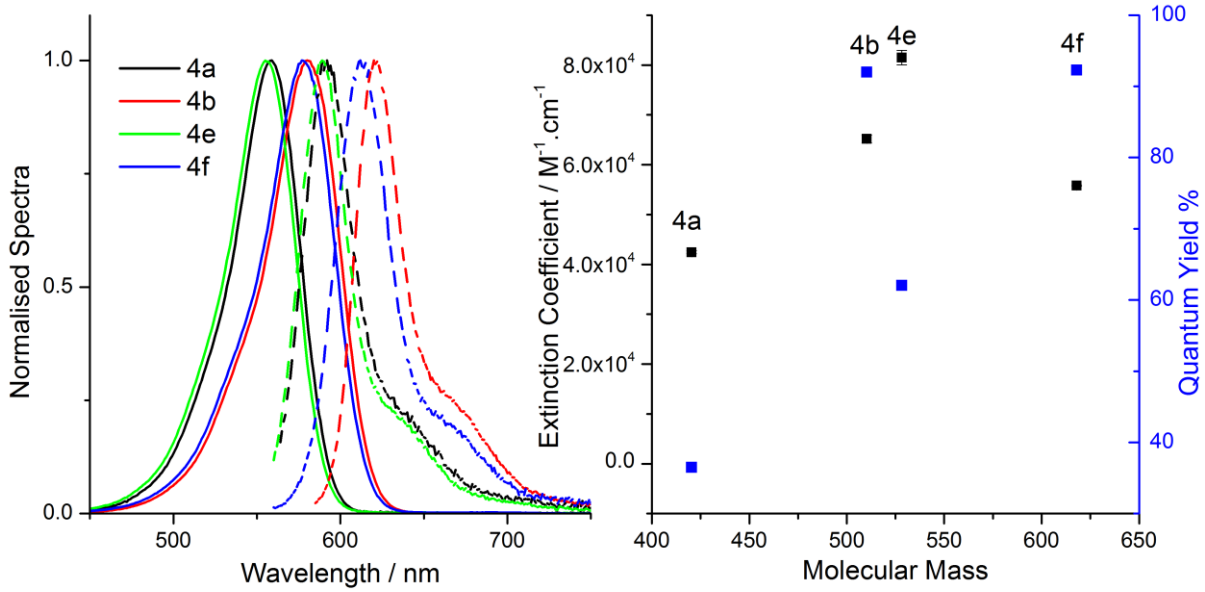

Figure 6.44 : Normalised absorption (solid line) and emission (dashed line) spectra (left); and fluorescence quantum yield (blue squares) and extinction coefficient (black squares) against molecular mass (right) of BODIPY emitters in dry toluene.

The effect of fluorinating the aryl periphery of the BODIPY chromaphores on their fluorescence properties is clearly site specific – while fluorination of the 3,5-phenyl groups has little effect on the wavelength of the absorption or emission peaks, fluorination in the *meso* position causes a large red shift of both absorption and emission.

An increase in fluorescence quantum yield is seen for each of the fluorinated analogues when compared to non-fluorinated **4a.** Surprisingly, while both **4b** and **4e** show an increase in fluorescence quantum yield the effect is not cumulative – **4f** is higher than **4e** but not significantly. However **4f** shows a blue shift in emission peak compared to **4b**, giving it a higher potential anti-Stokes shift, and thus could have a higher up-conversion energy efficiency.

Compound	$\lambda_{(0-0)}^{Em}$	$\lambda_{(0-0)}^{Abs}$	Extinction coefficient $M^{-1}.cm^{-1}$	Fluorescence QY %
4a	594	558	42400±300	36.5±0.6
4b	620	580	65200±800	92.0±0.6
4e	596	554	81500±1500	62.1±0.6
4f	612	578	55800±100	92.3±0.8

Figure 6.45 : Table of photophysical data, BODIPY emitters

The quantum yield results could be rationalised for the *meso* position by the increase in steric hindrance to rotation, preventing non-radiative rotational relaxation pathways. However as fluorine atoms are of comparable size to hydrogen it is more like that an electronic effect is dominating. The extinction coefficient seems to follow the presence of a molecular dipole, as those with fluorination only at one end (**4b** and **4e**) have higher extinction coefficients than the non-fluorinated **4a** and the doubly fluorinated **4f**.

From this data we can conclude that **4f** should be the best candidate for TTA upconversion since it possesses a high fluorescence quantum yield, which is essential for efficient upconversion, and also has a higher energy emission than its closest competitor **4e**. As absorption by the emitter is not required for the up-conversion process the comparitively low extinction coefficient of **4f** is not a problem.

6.4.1. Upconversion measurements of BODIPY dyes

The dyes **4b** and **4f** were selected for up-conversion measurements as these BODIPY dyes had the highest fluorescence quantum yields as described above. Initially they were paired with the sensitizer **PdTBP** (Chapter 5) and excited with 633 nm coherent photons.

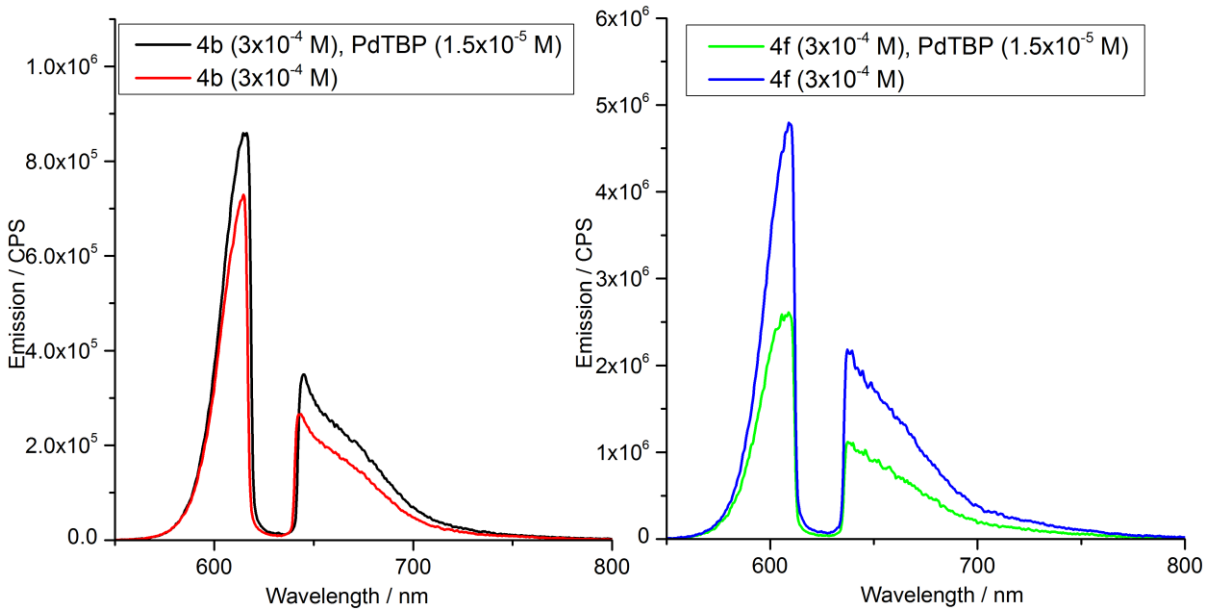

Figure 6.46 : Emission spectra of 4b (left) and 4d (right) alone and paired with PdTBP sensitizer, illuminated with 633 nm 0.1 mW coherent photons

Up-conversion emission of the BODIPY dyes **4b** and **4d** when paired with the **PdTBP** sensitizer cannot be measured accurately, since the emission of these dyes is too close to the excitation wavelength of 633 nm. The notch filter in place to ameliorate the excitation peak is within the emission peak. The unsensitized BODIPY dyes show clear emission, indicating direct excitation of the BODIPY in its absorption region. A different sensitizer was required, with absorption further in the red region.

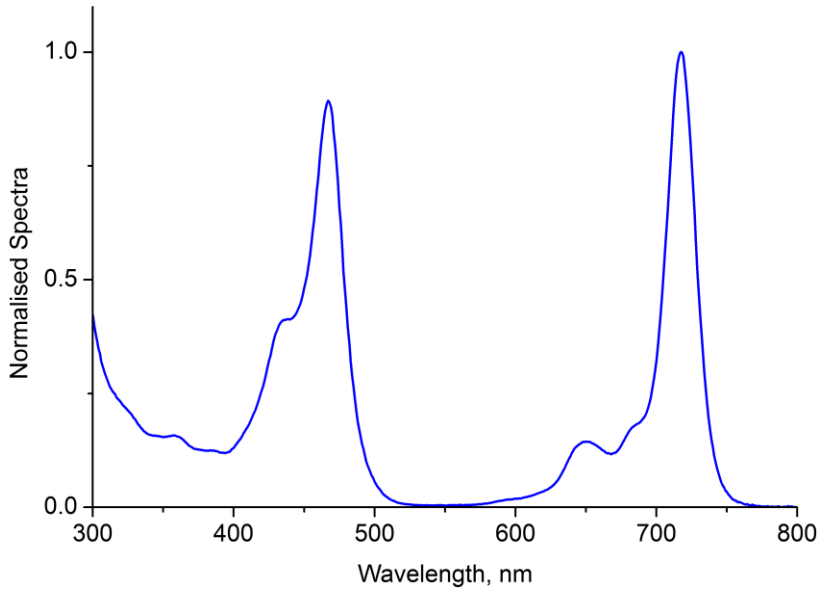

Figure 6.47 : Normalised absorption (blue) and structure of PdTNP

PdTNP absorbs in the low energy red region ($\lambda_{(max)}^{Abs}$ = 718 nm) and has a phosphorescence peak sufficiently high in energy to be able to pass energy via TTT to the BODIPY emitters. This sensitizer has been used previously by MSL for TTAUC systems.[70,71]

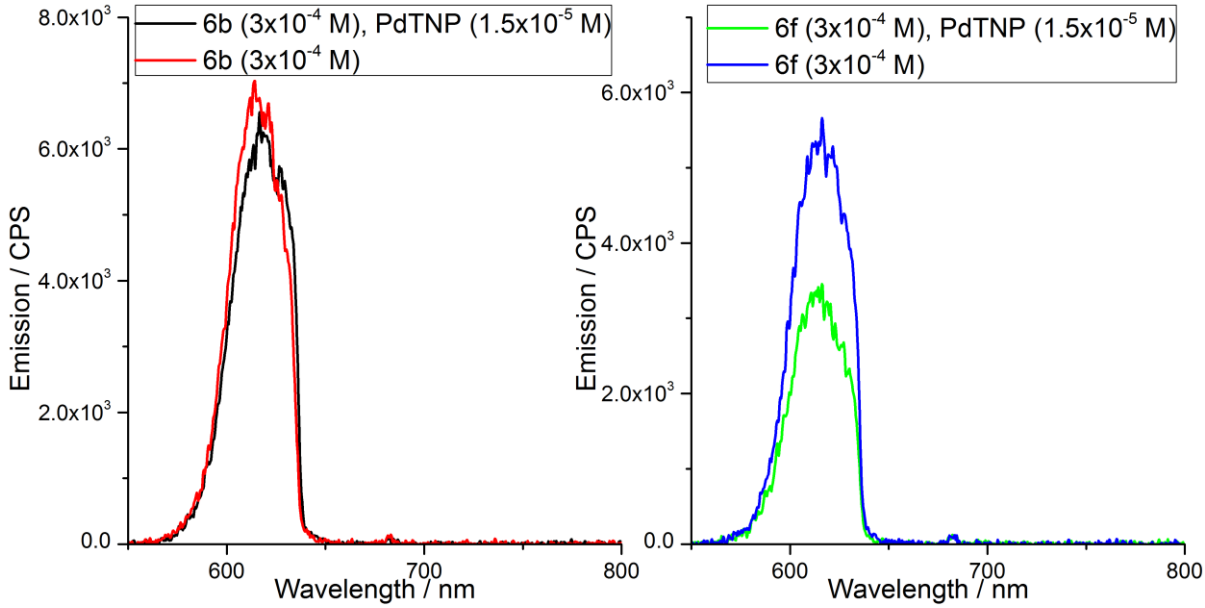

Figure 6.48 : Emission spectra of 4b (left) and 4d (right) alone and paired with PdTNP sensitizer, illuminated with 682 nm 1 mW coherent photons

When **4b** and **4f** are sensitized by **PdTNP** and illuminated with 682 nm photons there is again indication of direct excitation of the emitter. It was expected that 682 nm would be sufficiently distant from the dye absorption maxima to prevent this phenomenon ($\lambda_{(max)}^{Abs}$ ~ 580 nm), however since BODIPY molecules have structural features related to porphyrins the similarities in the spectral properties cannot be discounted. In analogy with a porphyrin dye, the BODIPY dyes have multiple absorption bands distinguishable when graphed on a log scale.

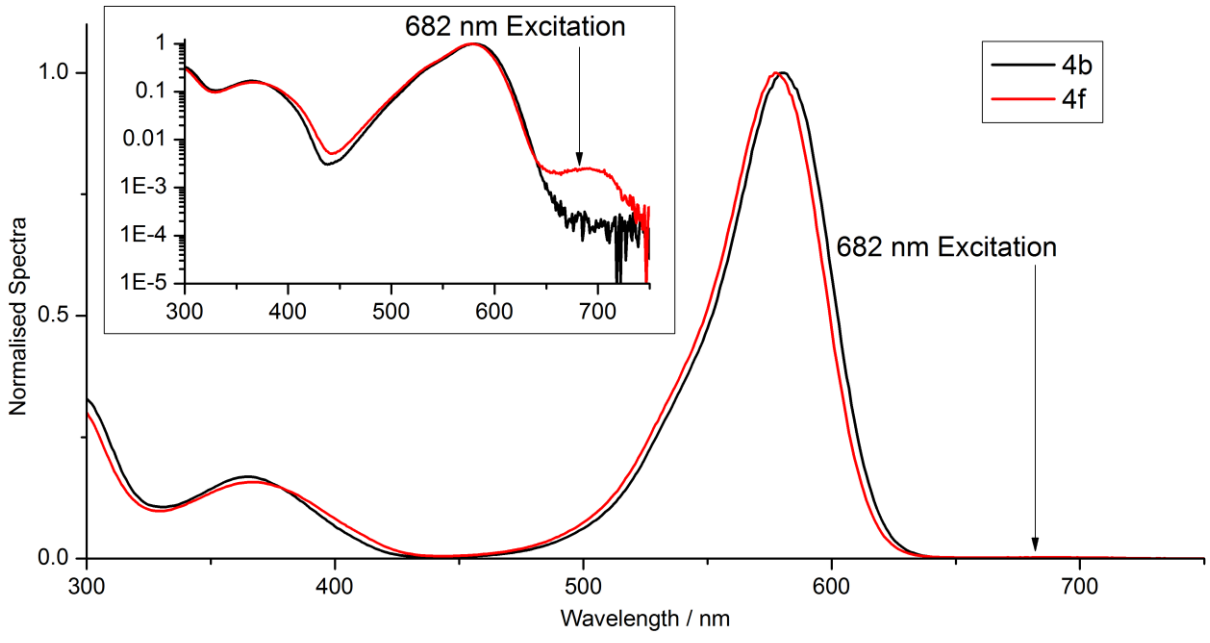

Figure 6.49 : Normalised absorption spectra of 4b (black) and 4d (red) with log scale (inset)

While there is a very low absorption in this region, it is sufficient to allow the associated emission to swamp any true sensitized up-conversion, since these BODIPY emitters have extremely high quantum yields of fluorescence. The "up-conversion" seen is actually a thermal contribution allowing a small degree of anti-Stokes emission.

Another possible mechanism for emission of the BODIPY dye when excited with 682 nm could be auto-TTA up-conversion – if the dye undergoes ISC and then meets another dye molecule in the T_1 state TTA could occur, allowing emission from a single S_1. This is unlikely since the high fluorescence quantum yields of these dyes precludes a high ISC yield. The hypothesis was tested by using BODIPY dye **4f** as a sensitizer with diphenylanthracene and bisphenylperylene emitter **3h**.

Since there are no emission peaks associated with DPA (Chapter 3) or **3h** (Chapter 5), we can conclude that **4f** does not act as a sensitizer for these molecules.

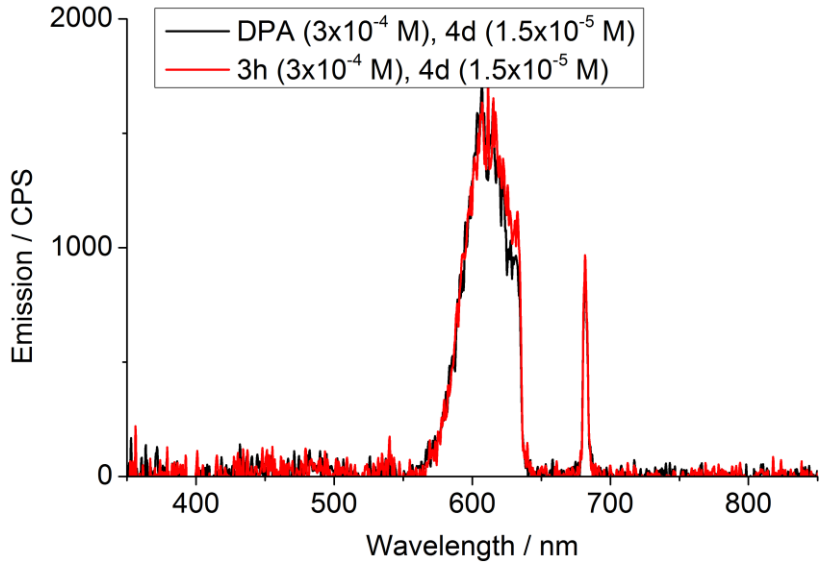

Figure 6.50 : Emitters DPA and 3h paired with sensitizer **4f,** illuminated with 682 nm 1 mW coherent photons

Due to the direct excitation of the BODIPY dyes occurring with 682 nm coherent photons, another sensitizer molecule with absorption further into the NIR region was required. **PdTAP** is a sensitizer that has been used in the past for TTAUC emission, and adsorbs strongly in the NIR region. This sensitizer has been previously used in TTAUC systems by Sony MSL.[72]

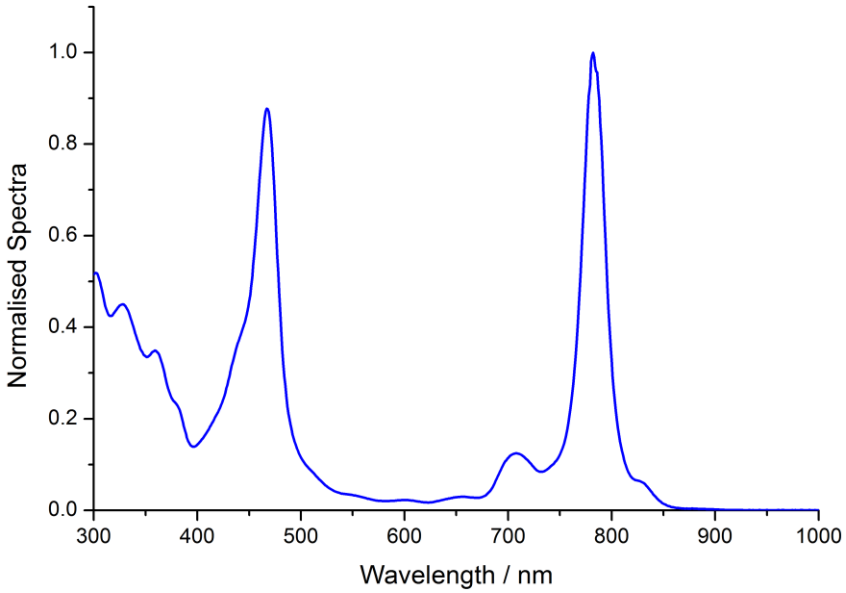

Figure 6.51 : Absorption (blue) and spectra of **PdTAP** (dry, degassed toluene)

A sample of the emitter **4f** and sensitizer **PdTAP** in dry, degassed toluene was prepared in a glove box (<1 ppm oxygen). When excited with 782 nm coherent photons no emission of **4f** is detected at all: the absorption is far enough from the excitation to prevent direct excitation, but the emitter triplet is likely too far above the sensitizer triplet for the TTT step to progress.

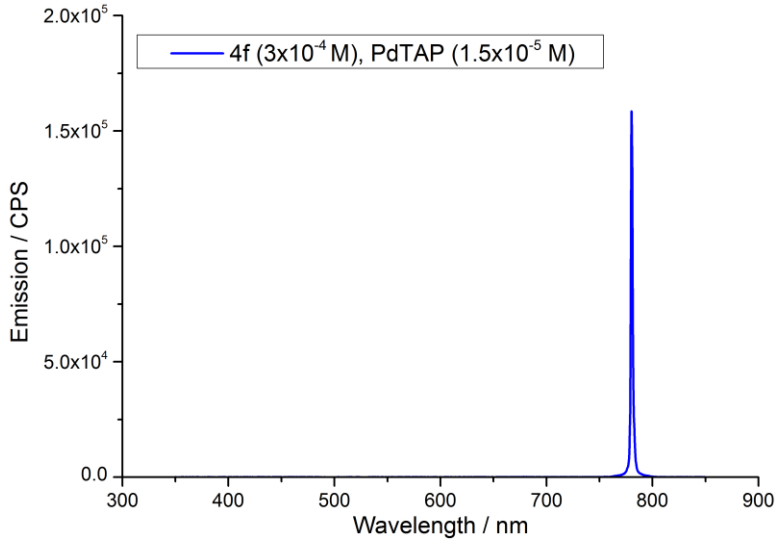

Figure 6.52 : BODIPY dye **4d** sensitized with PdTAP, illuminated with 782 nm 3 mW coherent photons

No successful up-conversion could be detected that was significantly higher than the direct excitation fluorescence produced by one of these emitter sensitizer pairings. While these BODIPY dyes are excellent fluorescent compounds, with high solubility, extinction coefficient, fluorescent quantum yield and stability they are unsuitable for up-conversion applications until a suitable sensitizer is found for them.

6.5. Conclusions

Fluorinated 3,5,8-triarylBODIPY dyes were synthesised and their fluorescence and up-conversion capabilities tested to probe their ability in TTAUCSs. Highly fluorinated BODIPY **4f** shows the highest fluorescence quantum yield of 92% and is an effective orange emissive dye. When tested for up-conversion ability BODIPY dye **4f** proves to be a poor candidate for TTAUCSs with sensitizers **PdTBP**, **PdTNP** and **PdTAP** when tested under the previously used experimental parameters (Chapters 3,5).

6.6. Experimental

17, *Tert-butyl-2-bromo-1H-pyrrole-1-carboxylate*

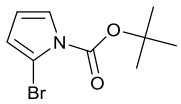

Pyrrole (4.675 ml, 4.5 g, 67 mmol), 2,2′-azobis(2-methylpropionitrile) (0.1 g, 0.01 eq) in 180 ml dry THF was cooled to -78 C and 1,3-dibromo-5,5-dimethylhydantoin (9.6 g, 33 mmol) added over 20 min. The solution was stirred for 10 min then allowed to stand at -78 °C for 2 h, before filtration into a flask (pre-cooled to -78 °C). Following the addition of NEt_3 (3.75 ml), 4-dimethylaminopyridine (0.1 g, 0.01 eq) and di-tert-butyl dicarbonate (21 g, 95 mmol) the solution was stirred to room temperature overnight, then stirred at room temperature for an additional 2 h. The solvent was evaporated en vacuo and hexane (100 ml), then water (100 ml) added. The organic portion was extracted with hexane (3 x 100 ml) dried over $NaSO_4$, filtered, and the solvent removed *en vacuo* to yield the crude product as an oil. Chromatographic purification (silica, pretreated with 5% NEt_3 in hexane, eluted 100% hexane) gave *tert*-butyl-2-bromo-1H-pyrrole-1-carboxylate (16.4 g, 99%) as a colourless oil. ^{1}H NMR (400 MHz, Chloroform-*d*) δ 7.29 (1H, dd, *J* 3.6, 2.0 Hz), 6.27 (1H, dd, *J* 3.5, 2.0), 6.13 (1H, t, *J* 3.5), 1.59 (9H, s); ^{13}C NMR (101 MHz, $CDCl_3$) δ 146.80, 123.04, 117.27, 111.62, 100.30, 84.81, 28.01; MS (GCMS) *m/z*: 247 (M^+, 16%), 245 (15), 147 (51), 146 (32), 145 (52), 144 (32), 57(100), in agreement with the literature.[73]

19a, *2-phenyl-1H-pyrrole*

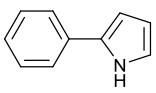

Protected bromopyrrole **17** (4.80 g, 19.4 mmol), phenylboronic acid (2.37 g, 19.4 mmol), $Pd(PPh_3)_4$ (0.488 g, 0.423 mmol, 2%), K_2CO_3 (19.4 ml 2 M aq solution), MeOH (17 ml), toluene (80 ml) were combined in a flask and the solution degassed by three freeze-pump-thaw cycles before heating at 85 °C under inert atmosphere overnight. Following cooling to room temperature the

solution was filtered through a bed of celite on a short silica pad and the solid washed with 1:1 hexane:ethyl acetate. The resulting organic solution was evaporated to give crude *tert*-butyl-2-phenyl-1H-pyrrole-1-carboxylate (**18a**) as an oil (4.62 g, 98%). MS (GCMS) *m/z*: 243 (M^+, 17%), 187 (49), 143 (100), 115 (61), 57(99), 41 (40). Crude **18a** was deprotected with NaOMe (1 g) by stirring in a suspension of dry THF (30 ml) and dry MeOH (35 ml) at room temperature overnight. Water (20 ml) is added, the organic solvents removed *en vacuo*, and then dilute HCl added to produce pH 5. The aqueous layer is extracted with ether (3 x 20 ml), the organic washings combined, dried over $NaSO_4$, filtered, and evaporated *en vacuo*. Recrystallization gave 2-phenyl-1H-pyrrole (1.5782g, 57%) as white flakes; ^{1}H NMR (600 MHz, $CDCl_3$) δ 8.43 (1H, s), 7.49 (1H, d, *J* 1.5), 7.48 (1H, d, *J* 1.2), 7.38 (2H, t, *J* 7.8), 7.22 (1H, tt, *J* 7.3, 1.2), 6.87 (1H, td, *J* 2.7, 1.5), 6.54 (1H, ddd, *J* 3.9, 2.7, 1.5), 6.32 (1H, dt, *J* 3.6, 2.6); ^{13}C NMR (151 MHz, $CDCl_3$) δ 132.91, 132.26, 129.02, 126.33, 123.98, 118.96, 110.25, 106.08; MS (GCMS) *m/z*: 143 (M^+, 100%), 115 (79), in agreement with the literature.[74]

19b, *2-(3,4,5-trifluorophenyl)-1H-pyrrole*

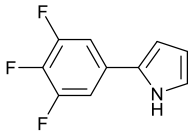

Protected bromopyrrole **17** (3.94 g, 16.0 mmol), 3,4,5-trifluorophenylboronic acid (3.09 g, 17.6 mmol), $Pd(PPh_3)_4$ (0.40 g, 0.35 mmol, 2%), K_2CO_3 (19.4 ml 2M aq solution), MeOH (17 ml), toluene (80 ml) were combined in a flask and the solution degassed by three freeze-pump-thaw cycles before heating at 85 °C under inert atmosphere overnight. Following cooling to room temperature the solution was filtered through a bed of celite on a short silica pad and the solids washed with 1:1 hexane:ethyl acetate. The resulting organic solution was evaporated to give the product as an oil (4.25 g, 90%). MS (GCMS) *m/z*: 297 (M^+, 9%), 241 (22), 197 (76), 169(47), 57(100) 41(45). The crude (**3b**) was deprotected with NaOMe (3 eq) by stirring in a suspension of dry THF (30 ml) and dry MeOH (35 ml) at room temperature overnight. Water (20 ml) is added, the organic solvents removed *en vacuo*, and then dilute HCl added to produce pH 5. The aqueous layer is extracted with ether (3 x 20 ml), the organics combined, dried over $NaSO_4$, filtered, and evaporated *en vacuo*. Recrystallization gave 2-(3,4,5-trifluorophenyl)-1H-pyrrole (1.22 g, 39% over two steps) as white flakes; ^{1}H NMR (600 MHz, Chloroform-*d*) δ 8.43 (1H, s), 7.49 (1H, d, *J* 1.5), 7.48 (1H, d, *J* 1.2), 7.38 (2H, t, *J* 7.8), 7.22 (1H, tt, *J* 7.3, 1.2), 6.87 (1H, td, *J* 2.7, 1.5), 6.54 (1H, ddd, *J* 3.9, 2.7, 1.5), 6.32 (1H, dt, *J* 3.6, 2.6); ^{13}C NMR (151 MHz, $CDCl_3$) δ 132.91, 132.26, 129.02, 126.33, 123.98, 118.96, 110.25, 106.08; MS (GCMS) *m/z*: 143 (M^+, 100%), 115 (79).

***4a**, 5,5-difluoro-3,7,10-triphenyl-5H-dipyrrolo[1,2-c:1',2'-f][1,3,2]diazaborinin-4-ium-5-uide (3,5,8-triphenylBODIPY)*

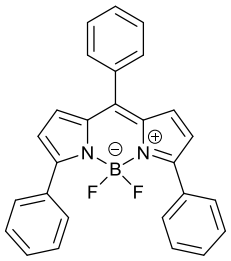

To a solution of **19a** (0.299 g, 2.10 mmol) in 1,2-dichloroethane (10 ml) benzoyl chloride (115 µl, 0.14 g, 1 mmol) was added, causing an immediate purple colour to appear. The solution was stirred for 6 days at reflux, allowed to cool, diluted with water (10 ml) and the aqueous layer brought to pH 7 by addition of saturated $NaHCO_3$ solution. The solution was extracted with DCM (3 x 10 ml) and reduced *en vacuo* before purification of the intermediate by chromatography (silica, pretreated with 5% NEt_3 in hexane, eluted hexane: ethyl acetate 8:2) to give the phenyldi-(2-phenylpyrromethene intermediate as a purple solid (0.171 g, 0.460 mmol, 46%). HRMS (TOF ASAP$^+$), Calcd for $[C_{27}H_{21}N_2+H]^+$: 373.1705, found *m/z*: 373.1695. ^{1}H NMR (400 MHz, Chloroform-*d*) δ 7.95 (4H, m), 7.57 (2H, m), 7.51 (7H, m), 7.41 (3H, m), 6.86 (2H, d, *J* 4.2), 6.73 (2H, d, *J* 4.2); ^{13}C NMR (101 MHz, $CDCl_3$) δ 154.23, 142.10, 139.80, 137.26, 133.33, 131.00, 130.06, 129.12, 128.96, 128.91, 127.96, 127.85, 127.33, 126.29, 123.84, 115.71, 112.29. To a stirring solution of the intermediate in dry toluene (20 ml) under inert atmosphere NEt_3 (0.64 ml, 4.6 mmol) then boron trifluoride etherate (0.87 ml, 6.9 mmol) were added dropwise over 10 minutes. The fuming solution was stirred at room temperature for 10 min then heated at 80 °C for 3 h before cooling to room temperature and the solvent evaporated *en vacuo*. The reduced solution was purified by chromatography (alumina, activated, Brockmann basic, eluted hexane:$CHCl_3$ 1:1 graduation to 100% $CHCl_3$), and then recrystallized (hexane/dcm) giving 5,5-difluoro-3,7,10-triphenyl-5H-dipyrrolo[1,2-c:1',2'-f][1,3,2]diazaborinin-4-ium-5-uide as a green – purple solid (0.0946 g, 49%); MS (ASAP) *m/z*: 420.1 (M^+, 60%), 401.1 ([M^+ − F], 100); HRMS (TOF ASAP$^+$), Calcd for $[C_{27}H_{19}BF_2N_2]^+$: 420.1610, found *m/z*: 420.1646.

***4b**, 5,5-difluoro-10-(perfluorophenyl)-3,7-diphenyl-5H-dipyrrolo[1,2-c:1',2'-f][1,3,2] diazaborinin-4-ium-5-uide (3,5-diphenyl-8-(perfluorophenyl)BODIPY)*

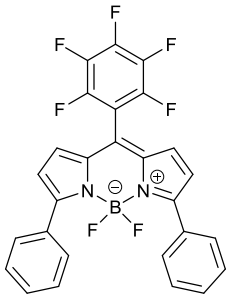

To a solution of **19a** (0.42 g, 2.93 mmol) in 1,2-dichloroethane (10 ml), pentafluorobenzoyl chloride (200 µl, 0.322 g, 1.397 mmol) was added, causing an immediate strong purple colour to appear. The solution was stirred for 12 h at reflux, allowed to cool, diluted with water (10 ml) and the aqueous layer brought to pH 7 by addition of saturated $NaHCO_3$ solution. The solution was extracted with DCM (3 x 10 ml) and reduced *en vacuo* before purification by chromatography (silica, pretreated with 5% NEt_3 in hexane, eluted hexane: ethyl acetate 8:2) to give the intermediate perfluorophenyldi-(2-phenyl)pyrromethene as a purple solid as a mix of isomers (0.0374 g, 2%). To a stirring solution of the intermediate under inert atmosphere in dry toluene (20 ml) NEt_3 (112 µl, 0.805 mmol) then boron trifluoride etherate (0.152 ml, 1.21 mmol) are added dropwise over 10 minutes. The fuming solution is stirred at room temperature for 10 min then heated at 80 °C for 3 h before cooling and the solvent evaporated *en vacuo*. The reduced solution was purified by chromatography (alumina, activated, Brockmann basic, eluted hexane:$CHCl_3$ 1:1 graduation to 100% $CHCl_3$), and then recrystallized (hexane/dcm) giving 5,5-difluoro-10-(perfluorophenyl)-3,7-diphenyl-5H-dipyrrolo[1,2-c:1',2'-f][1,3,2] diazaborinin-4-ium-5-uide as a green – purple solid (0.0191 g, 47%); MS (ASAP) *m/z*: 510.1 (M^+, 88%), 491.1 ([M^+ − F], 100%), 429.1 (11), 355.1 (10); HRMS (TOF ASAP$^+$), Calcd for $[C_{27}H_{14}BF_7N_2]^+$: 510.1138, found *m/z*: 510.1180.

4e, *5,5-difluoro-10-phenyl-3,7-bis(3,4,5-trifluorophenyl)-5H-dipyrrolo[1,2-c:1',2'-f][1,3,2]diazaborinin-4-ium-5-uide (3,5-di-(3,4,5-trifluorophenyl)-8-(phenyl)BODIPY)*

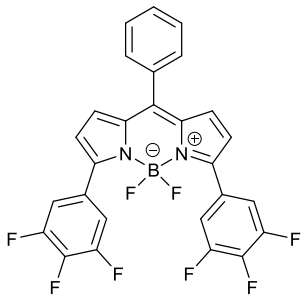

To a solution of **19b** (0.396 g, 2.01mmol) in 1,2-dichloroethane (10 ml), benzoyl chloride (111 µl, 0.957 mmol) was added, causing an immediate strong purple colour to appear. The solution was stirred for 3 days at reflux, allowed to cool, diluted with water (10 ml) and the aqueous layer brought to pH 7 by addition of saturated $NaHCO_3$ solution. The solution was extracted with DCM (3 x 10 ml) and reduced *en vacuo* before purification by chromatography (silica, pretreated with 5% NEt_3 in hexane, eluted hexane: ethyl acetate 8:2) to give the product as a purple solid as a mix of isomers (0.19 g, 20%). ^{19}F NMR (376 MHz, $CDCl_3$) δ -133.90 (2F, dd, *J* 20.5, 8.4), -162.98 (1F tt, *J* 20.6, 6.2). To a stirring solution of the intermediate in dry toluene under inert atmosphere (20 ml) NEt_3 (0.55 ml, 3.96 mmol) then boron trifluoride etherate (0.75 ml 5.94 mmol) are added dropwise over 10 minutes. The fuming solution is stirred at room temperature for 10 min then

heated at 80 °C for 3 h before cooling and the solvent evaporated *en vacuo*. The reduced solution was purified by chromatography (alumina, activated, Brockmann basic, eluted hexane:$CHCl_3$ 1:1 graduation to 100% $CHCl_3$), and then recrystallized (hexane/dcm) giving 5,5-difluoro-10-phenyl-3,7-bis(3,4,5-trifluorophenyl)-5H-dipyrrolo[1,2-c:1',2'-f][1,3,2]diazaborinin-4-ium-5-uide as a green – purple solid (0.0363 g, 17%); ^{1}H NMR (600 MHz, Chloroform-*d*) δ 7.64 – 7.60 (1H m), 7.57 (2H, dd, *J* 7.6, 1.5), 7.52 (2H, dd, *J* 8.3, 6.5), 6.96 – 6.93 (1H, m), 6.61 (1H, dd, *J* 4.3, 1.2); ^{19}F NMR (564 MHz, $CDCl_3$) δ -131.96 (2F, dd, *J* 64.4, 32.1), -133.65 (4F, dd, *J* 20.6, 8.3), -157.94 (2F, ddt, *J* 20.6, 14.1, 6.6); MS (ASAP) *m/z*: 528.1 (M^+, 70%), 509.1 ([M^+ − F], 100%), 492.1 ([M^+ − 2F], 10%), 473.1 (30).

***4f**, 5,5-difluoro-10-(perfluorophenyl)-3,7-bis(3,4,5-trifluorophenyl)-5H-dipyrrolo[1,2-c:1',2'-f][1,3,2]diazaborinin-4-ium-5-uide (3,5-di-(3,4,5-trifluorophenyl)-8-(perfluorophenyl)BODIPY)*

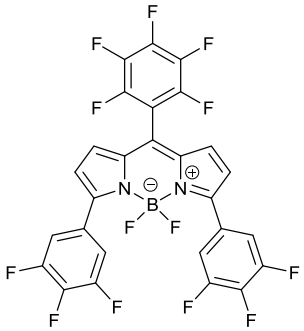

To a solution of **19b** (0.406 g, 2.06 mmol) in 1,2-dichloroethane (10 ml), perfluorobenzoyl chloride (140 µl, 0.972 mmol) was added. The solution was stirred for 5 days at reflux, allowed to cool, and stirred for a further 3 days at room temperature. Dry toluene (10 ml), dry triethylamine (2 ml) and boron trifluoride etherate (2.0 ml) were added and the resulting green solution stirred at 80 °C for 3 days before cooling. The reaction solution was applied directly to an alumina pad (activated, Brockmann basic, eluted hexane:$CHCl_3$ 1:1 graduation to 100% $CHCl_3$) allowing 5,5-difluoro-10-(perfluorophenyl)-3,7-bis(3,4,5-trifluorophenyl)-5H-dipyrrolo[1,2-c:1',2'-f][1,3,2]diazaborinin-4-ium-5-uide (0.071 g, 12%) as a purple solid; MP = 226 °C (hexane / $CHCl_3$); IR νmax /cm^{-1} 2918(w), 2849(w), 1652(vw), 1617(w), 1563(s), 1537(s), 1478(vs), 1260(s); ^{1}H NMR (400 MHz, $CDCl_3$) δ 7.56 (2H, dd, *J* 8.2, 6.4), 6.84 (1H, d, *J* 4.4), 6.66 (1H, dd, *J* 4.4, 1.3); ^{13}C NMR (176 MHz, $CDCl_3$) δ 157.94 , 151.11 (ddd, *J* = 250, 10, 4), 144.80 (d, *J* 253), 143.59 – 143.27 (m), 141.26 (dt, *J* 258, 15), 137.98 (d, *J* 255), 136.56 , 130.73 – 130.26 (m), 127.77 , 127.50 (td, *J* 9, 5), 122.25 (dd, *J* = 5.0, 2.3 Hz), 114.32 (dd, *J* 18, 5), 108.11 (td, *J* 18, 4); ^{19}F NMR (376 MHz, $CDCl_3$) δ -132.29 (d, *J* 31.7), -132.46 (d, *J* 31.6), -133.51 (dd, *J* 20.5, 8.2), -137.27 (d, *J* 16.5), -149.29 (t, *J* 20.9), -156.99 (tt, *J* 20.5, 6.5), -159.32 – -159.55 (m); ^{11}B NMR (128 MHz, $CDCl_3$) δ 1.16 (t, *J* 31.6); MS (ASAP) *m/z*: 618 (M^+, 50%), 599 ([M^+ − F], 100%), 580 ([M^+ − 2F], 40), 552 (60), 524 (30); HRMS (TOF ASAP$^+$), Calcd for $[C_{27}H_8BF_{13}N_2]^+$: 617.0609, found *m/z*: 617.0592.

(1) Boens, N.; Leen, V.; Dehaen, W. Fluorescent indicators based on BODIPY. *Chem. Soc. Rev.* **2012**, *41*, 1130–1172.

(2) Ulrich, G.; Ziessel, R.; Harriman, A. The chemistry of fluorescent bodipy dyes: versatility unsurpassed. *Angew. Chem. Int. Ed. Engl.* **2008**, *47*, 1184–201.

(3) Wang, Y.-W.; Descalzo, A. B.; Shen, Z.; You, X.-Z.; Rurack, K. Dihydronaphthalene-fused boron-dipyrromethene (BODIPY) dyes: insight into the electronic and conformational tuning modes of BODIPY fluorophores. *Chemistry* **2012**, *18*, 7306–9.

(4) Loudet, A.; Burgess, K. BODIPY dyes and their derivatives: syntheses and spectroscopic properties. *Chem. Rev.* **2007**, *107*, 4891–932.

(5) Arroyo, I. J.; Hu, R.; Merino, G.; Tang, B. Z.; Peña-Cabrera, E. The smallest and one of the brightest. Efficient preparation and optical description of the parent borondipyrromethene system. *J. Org. Chem.* **2009**, *74*, 5719–5722.

(6) Schmitt, A.; Hinkeldey, B.; Wild, M.; Jung, G. Synthesis of the core compound of the BODIPY dye class: 4,4'-difluoro-4-bora-(3a,4a)-diaza-s-indacene. *J Fluoresc* **2009**, *19*, 755–758.

(7) Tram, K.; Yan, H.; Jenkins, H. A.; Vassiliev, S.; Bruce, D. The synthesis and crystal structure of unsubstituted 4, 4-difluoro-4-bora-3a, 4a-diaza-s-indacene (BODIPY). *Dyes and Pigments* **2009**, *82*, 392–395.

(8) Li, L.; Nguyen, B.; Burgess, K. Functionalization of the 4, 4-difluoro-4-bora-3a, 4a-diaza-s-indacene (BODIPY) core. *Bioorgan. Med. Chem.* **2008**, *18*, 3112–3116.

(9) Thivierge, C.; Bandichhor, R.; Burgess, K. Spectral dispersion and water solubilization of BODIPY dyes via palladium-catalyzed C-H functionalization. *Org. Lett.* **2007**, *9*, 2135–2138.

(10) Benniston, A. C.; Copley, G. Lighting the way ahead with boron dipyrromethene (Bodipy) dyes. *Phys Chem Chem Phys* **2009**, *11*, 4124–31.

(11) Loudet, A.; Bandichhor, R.; Burgess, K.; Palma, A.; McDonnell, S. O.; Hall, M. J.; O'Shea, D. F. B,O-chelated azadipyrromethenes as near-IR probes. *Org. Lett.* **2008**, *10*, 4771–4774.

(12) Li, Y.; Dolphin, D.; Patrick, B. O. Synthesis of a BF complex of indol-2-yl-isoindol-1-ylidene-amine: a fully conjugated azadipyrromethene. *Tetrahedon Lett.* **2010**, *51*, 811–814.

(13) Zhao, W.; Carreira, E. M. Conformationally restricted aza-BODIPY: highly fluorescent, stable near-infrared absorbing dyes. *Chemistry* **2006**, *12*, 7254–7263.

(14) Ziessel, R.; Ulrich, G.; Harriman, A. The chemistry of Bodipy: A new El Dorado for fluorescence tools. *New J. Chem.* **2007**, *31*, 496–501.

(15) Ulrich, G.; Goze, C.; Guardigli, M.; Roda, A.; Ziessel, R. Pyrromethene dialkynyl borane complexes for "cascatelle" energy transfer and protein labeling. *Angew. Chem. Int. Ed. Engl.* **2005**, *44*, 3694–3698.

(16) Tahtaoui, C.; Thomas, C.; Rohmer, F.; Klotz, P.; Duportail, G.; Mély, Y.; Bonnet, D.; Hibert, M. Convenient method to access new 4, 4-dialkoxy-and 4, 4-diaryloxy-diaza-s-indacene dyes: Synthesis and spectroscopic evaluation. *J. Org. Chem.* **2007**, *72*, 269–272.

(17) Harriman, A.; Izzet, G.; Ziessel, R. Rapid energy transfer in cascade-type bodipy dyes. *J. Am. Chem. Soc.* **2006**, *128*, 10868–10875.

(18) Descalzo, A. B.; Xu, H.-J.; Xue, Z.-L.; Hoffmann, K.; Shen, Z.; Weller, M. G.; You, X.-Z.; Rurack, K. Phenanthrene-fused boron-dipyrromethenes as bright long-wavelength fluorophores. *Org. Lett.* **2008**, *10*, 1581–1584.

(19) Baruah, M.; Qin, W.; Basaric, N.; De Borggraeve, W. M.; Boens, N. BODIPY-based hydroxyaryl derivatives as fluorescent pH probes. *J. Org. Chem.* **2005**, *70*, 4152–4157.

(20) Wang, L.; Xiao, Y.; Tian, W.; Deng, L. Activable Rotor for Quantifying Lysosomal Viscosity in Living Cells. *J. Am. Chem. Soc.* **2013**, *135*, 2903–2906.

(21) Niu, L. Y.; Guan, Y. S.; Chen, Y. Z.; Wu, L. Z.; Tung, C. H.; Yang, Q. Z. BODIPY Based Ratiometric Fluorescent Sensor for Highly Selective Detection of Glutathione over Cysteine and Homocysteine. *J. Am. Chem. Soc.* **2012**, *134*, 18928–18931.

(22) Coskun, A.; Akkaya, E. U. Ion sensing coupled to resonance energy transfer: a highly selective and sensitive ratiometric fluorescent chemosensor for Ag(I) by a modular approach. *J. Am. Chem. Soc.* **2005**, *127*, 10464–5.

(23) Zeng, L.; Miller, E. W.; Pralle, A.; Isacoff, E. Y.; Chang, C. J. A selective turn-on fluorescent sensor for imaging copper in living cells. *J. Am. Chem. Soc.* **2006**, *128*, 10–1.

(24) Peng, X.; Du, J.; Fan, J.; Wang, J.; Wu, Y.; Zhao, J.; Sun, S.; Xu, T. A selective fluorescent sensor for imaging Cd2+ in living cells. *J. Am. Chem. Soc.* **2007**, *129*, 1500–1.

(25) Yuan, M.; Zhou, W.; Liu, X.; Zhu, M.; Li, J.; Yin, X.; Zheng, H.; Zuo, Z.; Ouyang, C.; Liu, H.; Li, Y.; Zhu, D. A multianalyte chemosensor on a single molecule: promising structure for an integrated logic gate. *J. Org. Chem.* **2008**, *73*, 5008–14.

(26) Erbas, S.; Gorgulu, A.; Kocakusakogullari, M.; Akkaya, E. U. Non-covalent functionalized SWNTs as delivery agents for novel Bodipy-based potential PDT sensitizers. *Chem. Commun. (Camb.)* **2009**, 4956–8.

(27) Li, F.; Yang, S. I.; Ciringh, Y.; Seth, J.; Martin, C. H.; Singh, D. L.; Kim, D.; Birge, R. R.; Bocian, D. F.; Holten, D.; others Design, synthesis, and photodynamics of light-harvesting arrays comprised of a porphyrin and one, two, or eight boron-dipyrrin accessory pigments. *J. Am. Chem. Soc.* **1998**, *120*, 10001–10017.

(28) Lammi, R. K.; Ambroise, A.; Balasubramanian, T.; Wagner, R. W.; Bocian, D. F.; Holten, D.; Lindsey, J. S. Structural control of photoinduced energy transfer between adjacent and distant sites in multiporphyrin arrays. *J. Am. Chem. Soc.* **2000**, *122*, 7579–7591.

(29) Ambroise, A.; Kirmaier, C.; Wagner, R. W.; Loewe, R. S.; Bocian, D. F.; Holten, D.; Lindsey, J. S. Weakly coupled molecular photonic wires: synthesis and excited-state energy-transfer dynamics. *J. Org. Chem.* **2002**, *67*, 3811–26.

(30) Mula, S.; Ray, A. K.; Banerjee, M.; Chaudhuri, T.; Dasgupta, K.; Chattopadhyay, S. Design and development of a new pyrromethene dye with improved photostability and lasing efficiency: theoretical rationalization of photophysical and photochemical properties. *J. Org. Chem.* **2008**, *73*, 2146–2154.

(31) Chen, T.; Boyer, J. H.; Trudell, M. L. Synthesis of 2, 6-diethyl-3-methacroyloxymethyl-1, 5, 7, 8-tetramethylpyrromethene-BF2 for the preparation of new solid-state laser dyes. *Heteroatom Chem.* **1997**, *8*, 51–54.

(32) Zhang, C.; Zhao, J.; Wu, S.; Wang, Z.; Wu, W.; Ma, J.; Guo, S.; Huang, L. Intramolecular RET Enhanced Visible light-Absorbing Bodipy Organic Triplet Photosensitizers and Application in Photooxidation and Triplet-triplet-annihilation Upconversion. *J. Am. Chem. Soc.* **2013**, *135*, 10566–10578.

(33) Wu, W.; Guo, H.; Wu, W.; Ji, S.; Zhao, J. Organic Triplet Sensitizer Library Derived from a Single Chromophore (BODIPY) with Long-Lived Triplet Excited State for Triplet-Triplet Annihilation Based Upconversion. *J. Org. Chem* **2011**, *76*, 7056–7064.

(34) Wu, W.; Zhao, J.; Sun, J.; Guo, S. Light Harvesting Fullerene Dyads as Organic Triplet Photosensitizers for Triplet-triplet Annihilation Upconversions. *J. Org. Chem.* **2012**, *77*, 5305–5312.

(35) Yogo, T.; Urano, Y.; Ishitsuka, Y.; Maniwa, F.; Nagano, T. Highly efficient and photostable photosensitizer based on BODIPY chromophore. *J. Am. Chem. Soc.* **2005**, *127*, 12162–3.

(36) Kim, B.; Ma, B.; Donuru, V. R.; Liu, H.; Fréchet, J. M. J. Bodipy-backboned polymers as electron donor in bulk heterojunction solar cells. *Chem. Commun. (Camb.)* **2010**, *46*, 4148–50.

(37) Shen, Z.; Röhr, H.; Rurack, K.; Uno, H.; Spieles, M.; Schulz, B.; Reck, G.; Ono, N. Boron-diindomethene (BDI) dyes and their tetrahydrobicyclo precursors-en route to a new class of highly emissive fluorophores for the red spectral range. *Chemistry* **2004**, *10*, 4853–71.

(38) Hu, R.; Lager, E.; Aguilar-Aguilar, A.; Liu, J.; Lam, J. W.; Sung, H. H.; Williams, I. D.; Zhong, Y.; Wong, K. S.; Peña-Cabrera, E.; others Twisted intramolecular charge transfer and aggregation-induced emission of BODIPY derivatives. *J. Phys. Chem. C* **2009**, *113*, 15845–15853.

(39) Mula, S.; Ray, A. K.; Banerjee, M.; Chaudhuri, T.; Dasgupta, K.; Chattopadhyay, S. Design and development of a new pyrromethene dye with improved photostability and lasing efficiency: theoretical rationalization of photophysical and photochemical properties. *J. Org. Chem.* **2008**, *73*, 2146–54.

(40) Jiao, L.; Yu, C.; Liu, M.; Wu, Y.; Cong, K.; Meng, T.; Wang, Y.; Hao, E. Synthesis and functionalization of asymmetrical benzo-fused BODIPY dyes. *J. Org. Chem.* **2010**, *75*, 6035–8.

(41) Singh-Rachford, T. N.; Haefele, A.; Ziessel, R.; Castellano, F. N. Boron Dipyrromethene Chromophores: Next Generation Triplet Acceptors/Annihilators for Low Power Upconversion Schemes. *J. Am. Chem. Soc.* **2008**, *130*, 16164–16165.

(42) Turshatov, A.; Busko, D.; Avlasevich, Y.; Miteva, T.; Landfester, K.; Baluschev, S. Synergetic Effect in Triplet-Triplet Annihilation Upconversion: Highly Efficient Multi-Chromophore Emitter. *ChemPhysChem* **2012**, *13*, 3112–3115.

(43) Treibs, A.; Kreuzer, F.-H. Difluorboryl-Komplexe von Di-und Tripyrrylmethenen. *Liebigs Ann. Chem.* **1968**, *718*, 208–223.

(44) Jiao, L.; Yu, C.; Li, J.; Wang, Z.; Wu, M.; Hao, E. Beta-formyl-BODIPYs from the Vilsmeier-Haack reaction. *J. Org. Chem.* **2009**, *74*, 7525–8.

(45) Goud, T. V.; Tutar, A.; Biellmann, J.-F. Synthesis of 8-heteroatom-substituted 4, 4-difluoro-4-bora-3a, 4a-diaza-s-indacene dyes (BODIPY). *Tetrahedron* **2006**, *62*, 5084–5091.

(46) Escobedo, J. O.; Rusin, O.; Lim, S.; Strongin, R. M. NIR dyes for bioimaging applications. *Curr. Opin. Chem. Biol.* **2010**, *14*, 64–70.

(47) Ntziachristos, V.; Bremer, C.; Weissleder, R. Fluorescence imaging with near-infrared light: new technological advances that enable in vivo molecular imaging. *Eur Radiol* **2003**, *13*, 195–208.

(48) Wood, T. E.; Thompson, A. Advances in the chemistry of dipyrrins and their complexes. *Chem. Rev.* **2007**, *107*, 1831–61.

(49) Jackson, A. H.; Pandey, R. K.; Nagaraja Rao, K.; Roberts, E. Reactions on solid supports part II: a convenient method for synthesis of pyrromethanes using a montmorillonite clay as catalyst. *Tetrahedron Lett.* **1985**, *26*, 793–796.

(50) Wu, L.; Burgess, K. A new synthesis of symmetric boraindacene (BODIPY) dyes. *Chem. Commun. (Camb.)* **2008**, 4933–5.

(51) Boyer, J. H.; Haag, A. M.; Sathyamoorthi, G.; Soong, M.-L.; Thangaraj, K.; Pavlopoulos, T. G. Pyrromethene-BF2 complexes as laser dyes: 2. *Heteroatom Chem.* **1993**, *4*, 39–49.

(52) Li, Z.; Mintzer, E.; Bittman, R. First synthesis of free cholesterol-BODIPY conjugates. *J. Org. Chem.* **2006**, *71*, 1718–21.

(53) Yakubovskyi, V. P.; Shandura, M. P.; Kovtun, Y. P. Boradipyrromethenecyanines. *Eur. J. Org. Chem.* **2009**, *2009*, 3237–3243.

(54) Boens, N.; Leen, V.; Dehaen, W. Fluorescent indicators based on BODIPY. *Chem Soc Rev* **2012**, *41*, 1130–72.

(55) Rumyantsev, E.; Marfin, Y. S.; Antina, E. Donor-acceptor complexes of dipyrrolylmethenes with boron trifluoride as intermediates in the synthesis of Bodipy. *Russ. Chem. B+* **2010**, *59*, 1890–1895.

(56) Aleško̧vić, M.; Basarić, N.; Milinarić-Majerski, K. Optimization of the Suzuki coupling reaction in the synthesis of 2-[(2-substituted) phenyl] pyrrole derivatives. *J. Heterocyclic Chem.* **2011**, *48*, 1329–1335.

(57) Domaille, D. W.; Zeng, L.; Chang, C. J. Visualizing ascorbate-triggered release of labile copper within living cells using a ratiometric fluorescent sensor. *J. Am. Chem. Soc.* **2010**, *132*, 1194–1195.

(58) Johnson, I. D.; Kang, H. C.; Haugland, R. P. Fluorescent membrane probes incorporating dipyrrometheneboron difluoride fluorophores. *Anal. Biochem.* **1991**, *198*, 228–37.

(59) Pavlopoulos, T. G.; Boyer, J. H.; Shah, M.; Thangaraj, K.; Soong, M.-L. Laser action from 2, 6, 8-position trisubstituted 1, 3, 5, 7-tetramethylpyrromethene-BF2 complexes: part 1. *Appl. Optics* **1990**, *29*, 3885–3886.

(60) Wories, H.; Koek, J.; Lodder, G.; Lugtenburg, J.; Fokkens, R.; Driessen, O.; Mohn, G. A novel water-soluble fluorescent probe: Synthesis, luminescence and biological properties of the sodium salt of the 4-sulfonato-3, 3′, 5, 5′-tetramethyl-2, 2′-pyrromethen-1, 1′-BF2 complex. *Recl. Trav. Chim. Pay-B* **1985**, *104*, 288–291.

(61) Zhou, C.; Nagy, G.; Walker, A. V. Toward molecular electronic circuitry: selective deposition of metals on patterned self-assembled monolayer surfaces. *J. Am. Chem. Soc.* **2005**, *127*, 12160–12161.

(62) Cakmak, Y.; Akkaya, E. U. Phenylethynyl-BODIPY oligomers: bright dyes and fluorescent building blocks. *Org. Lett.* **2009**, *11*, 85–8.

(63) Thivierge, C.; Loudet, A.; Burgess, K. Brilliant BODIPY-fluorene Copolymers With Dispersed Absorption and Emission Maxima. *Macromolecules* **2011**, *44*, 4012–4015.

(64) Niu, S. L.; Massif, C.; Ulrich, G.; Ziessel, R.; Renard, P.-Y.; Romieu, A. Water-solubilisation and bio-conjugation of a red-emitting BODIPY marker. *Org. Biomol. Chem.* **2011**, *9*, 66–9.

(65) Móczár, I.; Huszthy, P.; Maidics, Z.; Kádár, M.; Tóth, K. Synthesis and optical characterization of novel enantiopure BODIPY linked azacrown ethers as potential fluorescent chemosensors. *Tetrahedron* **2009**, *65*, 8250–8258.

(66) Yin, S.; Leen, V.; Van Snick, S.; Boens, N.; Dehaen, W. A highly sensitive, selective, colorimetric and near-infrared fluorescent turn-on chemosensor for Cu2+ based on BODIPY. *Chem. Commun. (Camb.)* **2010**, *46*, 6329–31.

(67) Rohand, T.; Baruah, M.; Qin, W.; Boens, N.; Dehaen, W. Functionalisation of fluorescent BODIPY dyes by nucleophilic substitution. *Chem. Commun. (Camb.)* **2006**, 266–8.

(68) Verbelen, B.; Leen, V.; Wang, L.; Boens, N.; Dehaen, W. Direct palladium-catalysed C-H arylation of BODIPY dyes at the 3- and 3,5-positions. *Chem. Commun. (Camb.)* **2012**, *48*, 9129–31.

(69) Littler, B. J.; Miller, M. A.; Hung, C. H.; Wagner, R. W.; O'SHEA, D. F.; Boyle, P. D.; Lindsey, J. S. Refined synthesis of 5-substituted dipyrromethanes. *J. Org. Chem.* **1999**, *64*, 1391–1396.

(70) Baluschev, S.; Yakutkin, V.; Wegner, G.; Miteva, T.; Nelles, G.; Yasuda, A.; Chernov, S.; Aleshchenkov, S.; Cheprakov, A. Upconversion with ultrabroad excitation band: Simultaneous use of two sensitizers. *Appl. Phys. Lett.* **2007**, *90*, 181103.

(71) Baluschev, S.; Yakutkin, V.; Miteva, T.; Wegner, G.; Roberts, T.; Nelles, G.; Yasuda, A.; Chernov, S.; Aleshchenkov, S.; Cheprakov, A. A general approach for non-coherently excited annihilation up-conversion: transforming the solar-spectrum. *New J. Phys.* **2008**, *10*, 013007.

(72) Yakutkin, V.; Aleshchenkov, S.; Chernov, S.; Miteva, T.; Nelles, G.; Cheprakov, A.; Baluschev, S. Towards the IR Limit of the Triplet-Triplet Annihilation-Supported Up-Conversion: Tetraanthraporphyrin. *Chem. Eur. J.* **2008**, *14*, 9846–9850.

(73) Chen, W.; Stephenson, E.; Cava, M.; Jackson, Y. 2-Substituted pyrroles from N-tert-butoxycarbonyl-2-bromopyrrole: N-tert-Butoxy-2-trimethylsilylpyrrole. *Org. Synth.* **1991**, *70*, 151.

(74) Burghart, A.; Kim, H.; Welch, M. B.; Thoresen, L. H.; Reibenspies, J.; Burgess, K.; Bergström, F.; Johansson, L. B.-Å. 3, 5-Diaryl-4, 4-difluoro-4-bora-3a, 4a-diaza-s-indacene (BODIPY) dyes: synthesis, spectroscopic, electrochemical, and structural properties. *J. Org. Chem.* **1999**, *64*, 7813–7819.

7. Synthetic Approaches to related fluorinated TTAUC systems

During the investigation of fluorinated emitters for TTA up-conversion media, a number of other fluorinated aromatic systems were studied. These include products arising from direct fluorination of anthracene.

Fluorination of the core moiety of the up-conversion emitter will likely have a different effect to fluorination of the periphery, most notably a major shift in the emissive properties of the chromaphore. Similarly to fluorination of the periphery, core fluorination is also likely to increase solubility and the photostability of the emitter.

Due to our previous experience with anthracene (Chapter 2) this core moiety was chosen for fluorination investigations.

7.1. Fluorination of anthracene, aided by design of experiments

Using microwave synthesis techniques we aimed to produce 9-fluoroanthracene and 9,10-difluoroanthracene by reaction of Selectfluor, an electrophilic fluorinating agent (Chapter 1), with anthracene. These emitters are closely related to systems synthesised previously (Chapter 2).

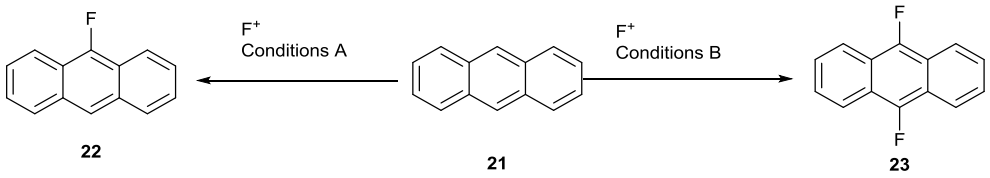

Figure 7.1 : Fluorination of anthracene using F+ reagents

By altering the reaction conditions we hoped that the selective production of 9-fluoroanthracene **22** or 9,10-difluoroanthracene **23** from anthracene **21** could be achieved.

A mixture of anthracene and Selectfluor was suspended in acetonitrile and heated in a microwave at 100 °C for 20 minutes. A sample was analysed by GCMS to evaluate the proportion of products. The analysis showed a mixture with the components anthracene (**21**, 0.8%) 9-fluoroanthracene (**22**, 7.5%), 9,10-difluoroanthracene (**23**, 20.6%) and 9,9,10,10-tetrafluoro-9,10-dihydroanthracene (**24**, 71.2%). As the proportion of anthracene that is unreacted is 0.8% the conversion is 99.2%.

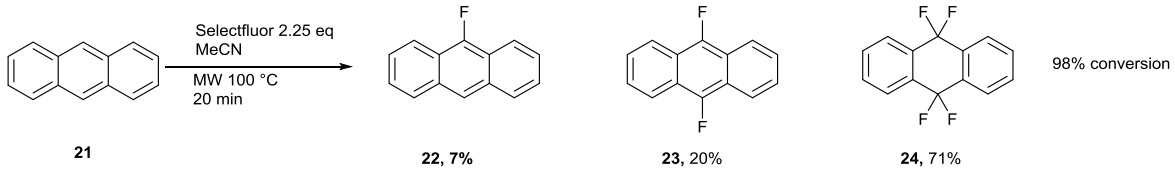

Figure 7.2 : Initial microwave reaction of anthracene and Selectfluor in acetonitrile

The expected major product, **23**, was produced in much lower yield than the unexpected tetrafluoro-deoxyanthraquinone, **24**. A design of experiments (DOE) method was employed to find conditions where each of the products **22-24** may be formed selectively with high purity and conversion as assessed by GCMS analysis.

Design of experiments (DOE) is widely used in industrial chemistry to improve chemical processes in a quantitative and rational manner,[1,2] and, by using similar methods, laboratory scale syntheses may be improved and rationalised by careful alteration of reaction conditions. A DOE approach to investigations allows fewer reactions to be carried out than sequentially adjusting one factor at a time, while providing more information about how each factor (e.g. Temperature, Time, Equivalents) affects the outcome, both individually and jointly. Using the information obtained from the experimental procedures and computations this allows a rational and systematic approach to the problem by constructing a model of the design space.

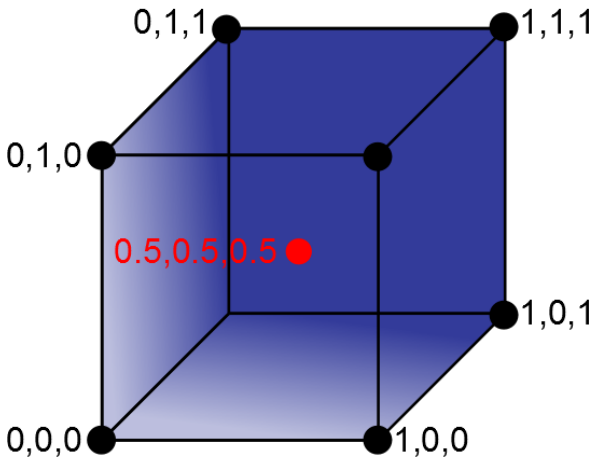

Figure 7.3 : DOE design space

The general method of experimental design is to define the goal of the investigation, identify what factors can affect the process; choose an experimental design; perform the experiments; and finally analyse the results.

7.1.1. Selection of DoE factors and screening

The microwave reactor employed may be used to vary the temperature and duration of the reaction. By virtue of an IR sensor, the temperature of the microwave vessel is measured and the machine then increases or decreases the wattage to achieve the desired temperature. The amounts of reagents and solvents within the vial may also be varied with accurate measurement. The microwave has the capacity for a single reaction vessel at a time, but the solutions may be prepared ahead of time and loaded into the cavity by an automated robot.

While temperature, time and equivalents of reagents are obvious factors to investigate, others must be kept in mind, to ensure random variance does not influence the results. For example, if the fluorination reaction occurs at room temperature, or reagents decompose once the samples have been prepared, the amount of time between the submission and insertion into the microwave cavity, reaction initialisation and quenching will have an effect. This uncertainty may be removed by the randomisation of the trial experiments, and can also be tested by a room temperature reaction in a round bottom flask.

The amount of solvent in the reaction can also play a part, most likely in this case due to solubility effects, so this should be measured. The presence of water and oxygen in the reaction may also affect the results.

Commonly when measuring the influence of time upon a reaction, samples are taken periodically by syringe from a round bottom flask. Due to the necessarily closed nature of the microwave cavity this is not possible, and the heating ramp and cooling time make multiple sampling of a single experiment in this way inaccurate.

Having selected the factors that may influence the results: temperature; heating time; equivalents of Selectfluor; amount of solvent, presence of water and oxygen, a screening matrix was devised (Figure 7.1).

	Pattern	Temperature	Time	Equivalents Selectfluor	Amount of Solvent	Water excluded	Oxygen excluded
1	−−−−++	-1	-1	-1	-1	L2	L2
2	−−++−−	-1	-1	1	1	L1	L1
3	−+−+−+	-1	1	-1	1	L1	L2
4	−++−+−	-1	1	1	-1	L2	L1
5	+−−++−	1	-1	-1	1	L2	L1
6	+−+−−+	1	-1	1	-1	L1	L2
7	++−−−−	1	1	-1	-1	L1	L1

8	++++++	1	1	1	1	L2	L2
9	000011	0	0	0	0	L1	L1

Figure 7.4 : Screening Matrix

By using the initial reaction's conditions (Figure 7.2) as a guide point, the design space around this was investigated: the minimum time that the microwave machine can heat the sample for is 1 second (this does not include the ramp up and cool down time), the time maximum was 10 min for the +1 variable. The minimum temperature that the microwave machine can operate at 60 °C, while for the +1 variable 100 °C was chosen. Finally as it would be expected one equivalent of "F^+" is required for a mono-fluorinated product and a tetra-fluorinated product requires 4, a minimum of 0.9 and maximum of 4.1 equivalents of Selectfluor was selected to ensure the optimised points were within the measured reaction space. The effect of air, water and concentration was assessed by degasing or drying the acetonitrile solvent. The mass of anthracene was kept constant throughout the experiments at 0.050 g. The results were assessed by taking a 0.5 ml sample which was quenched with water and extracted with DCM. After drying ($MgSO_4$) the organic layer was analysed by GCMS to evaluate the proportion of products. All peaks were included in the calculation except solvent peaks, to give an indication of other by-products that were formed.

Run	**Temperature**	**Time /s**	**Eq SF**	**Solvent**	**Water Excluded**	**Oxygen excluded**	**Conversion**	**Yield of Product**		
								22	**23**	**24**
1	60	1	0.94	2.5	y	y	65.81	38.6	14.66	2.18
2	60	1	4.12	5	n	n	100	8.95	2.21	62.59
3	100	1	0.90	5	y	n	70.97	37.31	14.3	2.37
4	100	600	0.90	2.5	n	n	69.3	36.5	12.73	1.26
5	60	600	4.13	2.5	y	n	98.51	3.9	1.39	78.45
6	60	600	0.97	5	n	y	56.44	26.22	1.65	0
7	80	300	2.57	3.75	n	n	100	13.6	26.23	51.88
8	100	1	4.11	2.5	n	y	98.4	0.95	0.89	59.17
9	100	600	4.21	5	y	y	100	0	0	80.89

Figure 7.5 : Screening plan and results

Software based analysis of the screening responses can indicate factors that are having an effect upon the measured outcome, including the cross products, and their significance. The Pseudo t-Ratio (Figure 7.6) indicates that the only factor that has a significant effect on the conversion and yield of products is the number of equivalents of Selectfluor, within the measured experimental volume. Time, temperature, concentration and the exclusion of water and oxygen did not have a statistically significant impact.

It is clear from these reactions that the saturated tetrafluoro product **24** is preferentially formed above 2.5 equivalents of SF. This indicates that this product is not made solely by the electrophilic attack by "F^+" upon the anthracene system.

Using less than 4 equivalents of Selectfluor allows the formation of **24**. This could be because the fluorinated intermediate difluoroanthracene is more activated to electrophilic attack by the "F^+" provided by the Selectfluor, however this would be unexpected as fluorine is sufficiently electron withdrawing to produce centres deactivated to electrophilic attack. Another possibility is that the counterion of the Selectfluor, BF_4^- is providing a source of nucleophilic fluorine. It is likely that using a different counterion would prevent the formation of **24**.

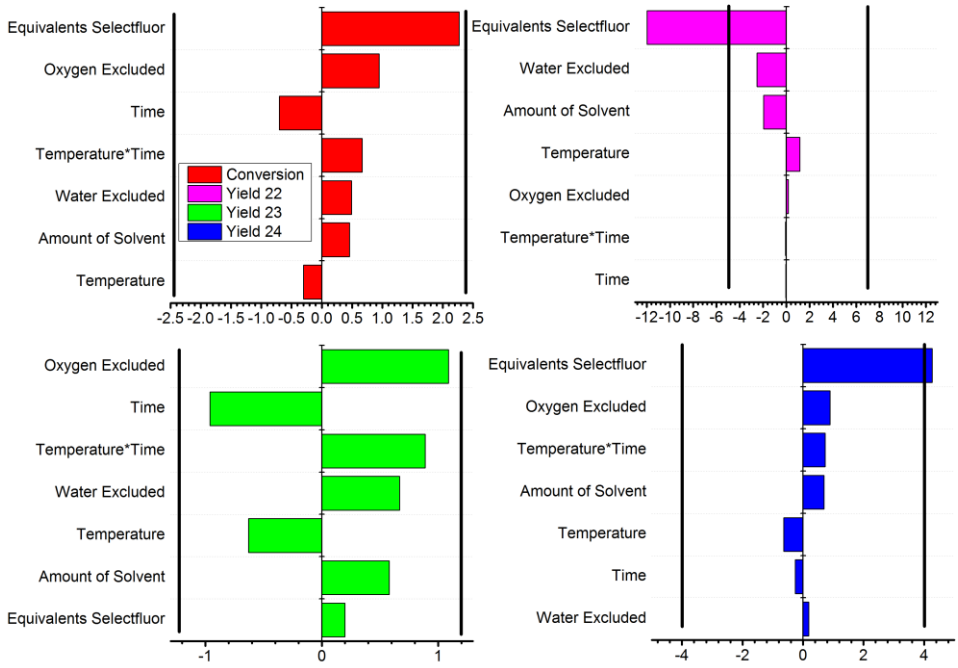

Figure 7.6 : Pseudo t-ratios of factors influencing the conversion and yields of products, with significance bars

Given the DOE data it is not possible to tune the reaction to selectively produce **22** or **23** without the presence of **24**. Since the time and temperature have no effect upon the yield of **24,** a reaction using 3.5 equivalents of Selectfluor, at 60 °C for 1 second in the microwave is sufficient to produce 99% conversion and 54% isolated yield.

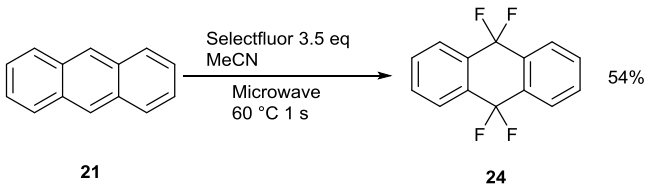

Figure 7.7 : Synthesis of **24**, tetrafluoro-deoxyanthraquinone

The same reaction in a round bottom flask at 60 °C overnight produces a similar result. The solid was recrystallized from acetone to give crystals of sufficient quality for crystallographic analysis. The molecule is in a special position with the mirror plane passing through C1, C2 and all fluorine atoms.

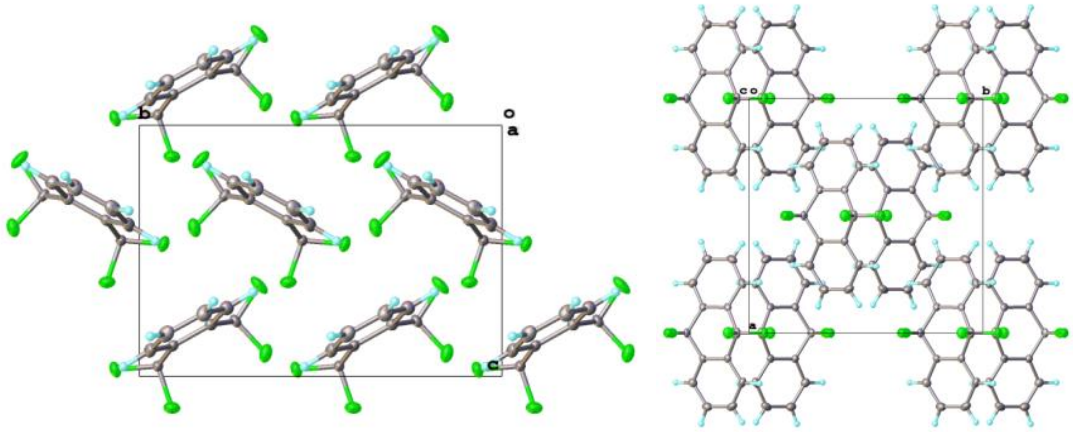

Figure 7.8 : X-ray crystallography of **24**

Attempts were made to produce **22** by the reduction and rearomatisation of **24** using a range of reagents. The tetrafluorinated molecule is highly stable to defluorination, resisting all attempts including refluxing with zinc powder in ammonia or TDAE (Figure 7.9).

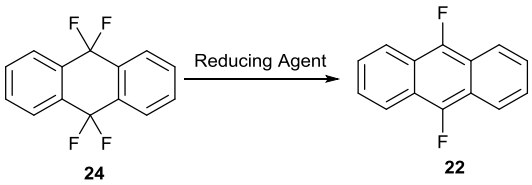

Reducing Agent	Solvent	Temperature	Time /m	Conversion
TDAE	DMF	0 °C	10	No Reaction
Zinc Powder	DMF	80 °C	120	No reaction
Magnesium	Propan-2-ol	80 °C	300	No reaction
^{t}BuLi	THF	80 °C	300	No Reaction
Zinc Powder	Ammonia	100 °C	150	No Reaction

Figure 7.9 : Reduction of **24**

It is possible that rather than using Selectfluor to produce **24** from anthracene, 9,10-difluoroanthracene **22** may be synthesised by using a fluorinating agent that does not contain a BF_4^- counter ion. Other NF reagents (Figure 7.10) that may be more suitable to the production of fluorinated anthracene structures were tested (Figure 7.11).

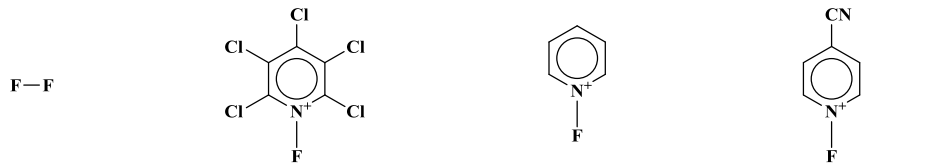

Figure 7.10 : Fluorinating reagents, the N-fluoro reagents have triflate counter ions

Attempts were made to fluorinate anthracene to difluoroanthracene using elemental fluorine.

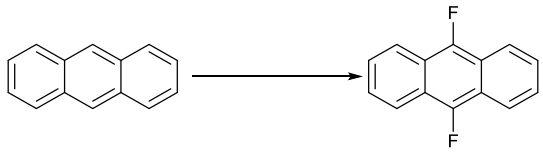

Solvent	Additive	Temperature	Time /h	Conversion
MeCN	n/a	RT	6	No Reaction
Sulfuric Acid	n/a	RT	2	Tar
MeCN	Triflic Acid 1%	RT	2	No Reaction

Figure 7.11 : Fluorination of anthracene by F_2

Bubbling 10% elemental fluorine gas through a suspension of anthracene in acetonitrile (5 mmol/h F_2) for 6 h, and quenched with aqueous sodium bicarbonate and extracted with chloroform. Analysis by GCMS showed that no reaction had occurred. The reaction was repeated using sulfuric acid, which produced black tar, and acetonitrile with 1% triflic acid, whereupon no reaction occurred.

N-fluoropyridinium salts with triflate counter ions were investigated with a view to their ability to fluorinate anthracene. Pentachloro-N-fluoropyridine produces a multiply fluorinated anthracene, indicating that the tetrafluoro borate counterion is required for the formation of **24**, in agreement with previous conclusions above.

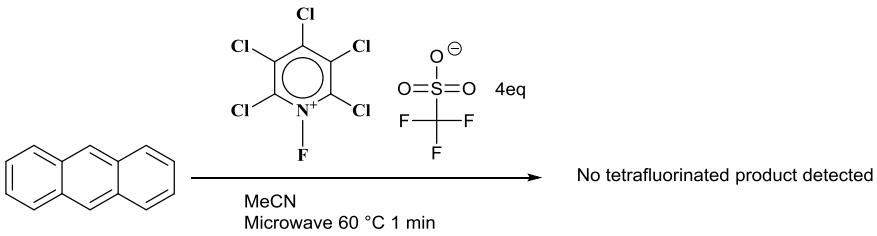

Figure 7.12 : Fluorination of anthracene by pentachloro-n-fluoropyridine

Two equivalents of 4-cyano-N-fluoropyridinium triflate salt when reacted with anthracene produces a mixture of unreacted anthracene, **22** and **23**, (10:4:1) and but **24** is detected.

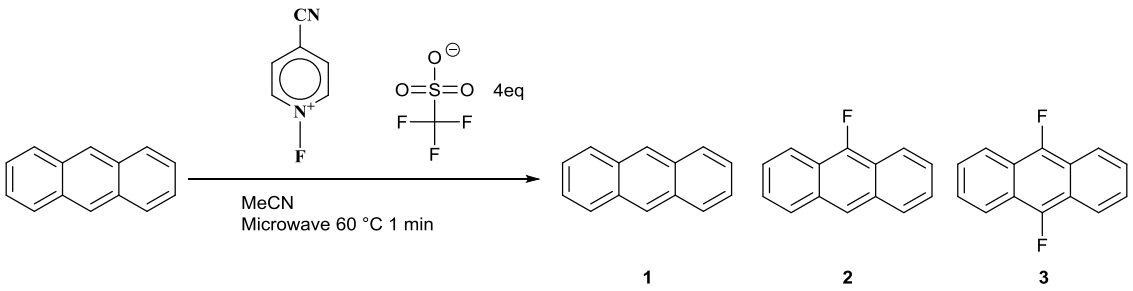

Figure 7.13 : Fluorination of anthracene by cyano-n-fluoropyridine

Related anthracene substrates were reacted with Selectfluor under similar conditions, to investigate the effect of functional groups on the fluorination process.

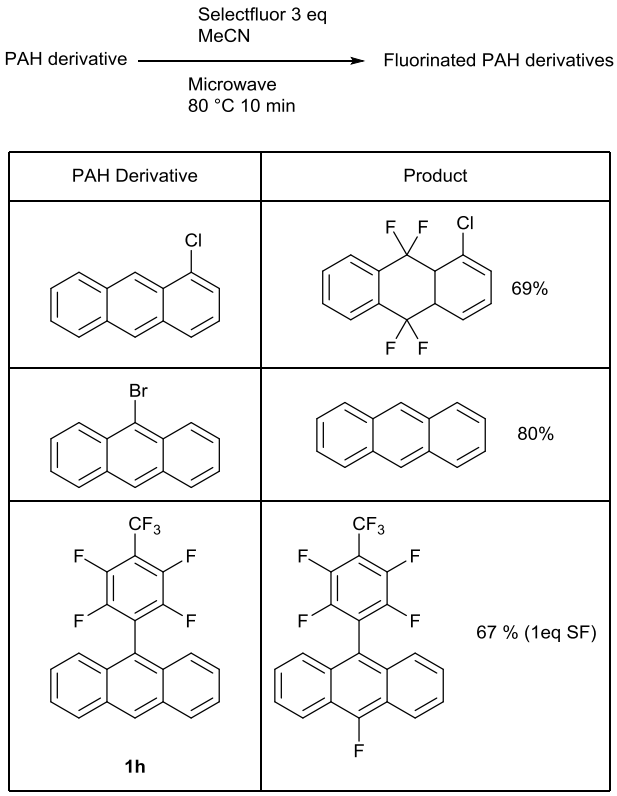

Figure 7.14 : Fluorination of PAH derivatives with Selectfluor, isolated yields

9-((4-Trifluoromethyl)perfluorophenyl)anthracene **1h** was fluorinated using Selectfluor using a microwave in 67% yield. No more highly fluorinated products were detected, and the aromaticity of the anthracene unit is not disturbed. The presence of a unit in the 9 position blocks the polyfluorination. 9-bromoanthracene did not undergo fluorination, but only formed debrominated anthracene. When substrates without a unit in the 9 position were tested these reacted in a similar manner to anthracene.

7.2. Perfluorodiphenylanthracene synthesis

A retrosynthetic analysis of the production of perfluorinated diphenylanthracene systems shows two schematic pathways – fluorination of the finished molecular scaffold, or construction using fluorinated building blocks. Previously explored methods for production of the DPA analogues (Chapter 2) may be utilized in the production of highly core fluorinated emitters, including aromatic nucleophilic substitution and Suzuki-Miyaura cross coupling reactions.

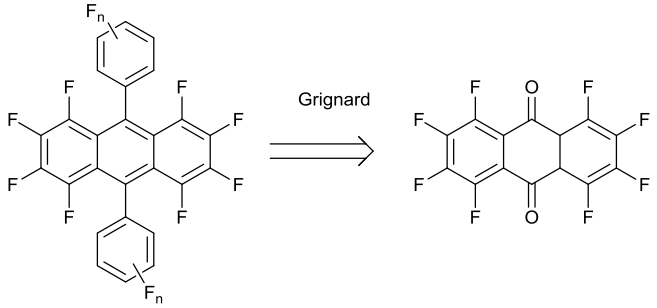

Figure 7.15 : Retrosynthetic analysis of diphenylanthracene emitters with perfluorinated cores

The synthetic route via an anthraquinone moiety was selected. First the production of a non-fluorinated core diphenylanthracene by nucleophilic attack upon the anthraquinone was tested, to ensure that this reaction was feasible, before the production of a fluorinated analogue.

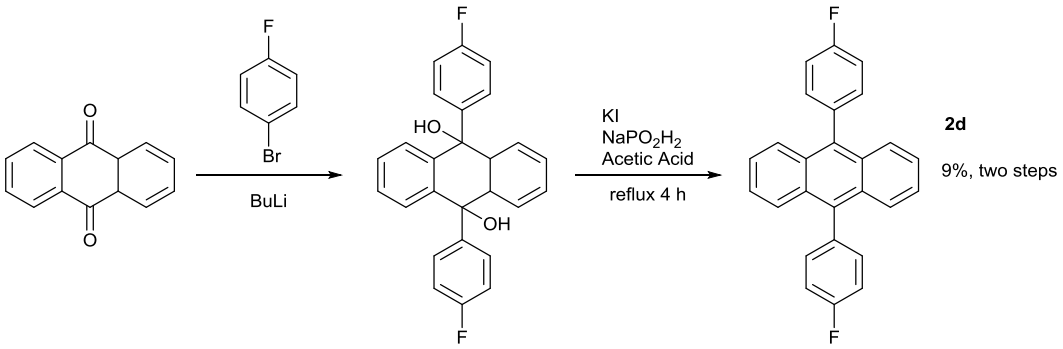

Figure 7.16 : Synthesis of diphenylanthracene emitter **2d** from anthraquinone

Nucleophilic attack by organolithium reagent formed from 4-fluorobromobenzene allowed the carbon scaffold to form, and the dihydroxy intermediate was isolated. The intermediate was reduced with potassium iodide and sodium hypophosphite in acetic acid providing the previously synthesised emitter **2d**, in 9% over two steps.

Clearly a route from the anthraquinone is possible and it can be assumed that, due to the increased electron withdrawing character of fluorine, the carbonyl group will be more susceptible to nucleophilic attack and so the first step proceed with increased efficiency.

To form the perfluoroanthraquinone tetrafluorophthalic anhydride was produced from commercially available tetrafluorophthalic anhydride.

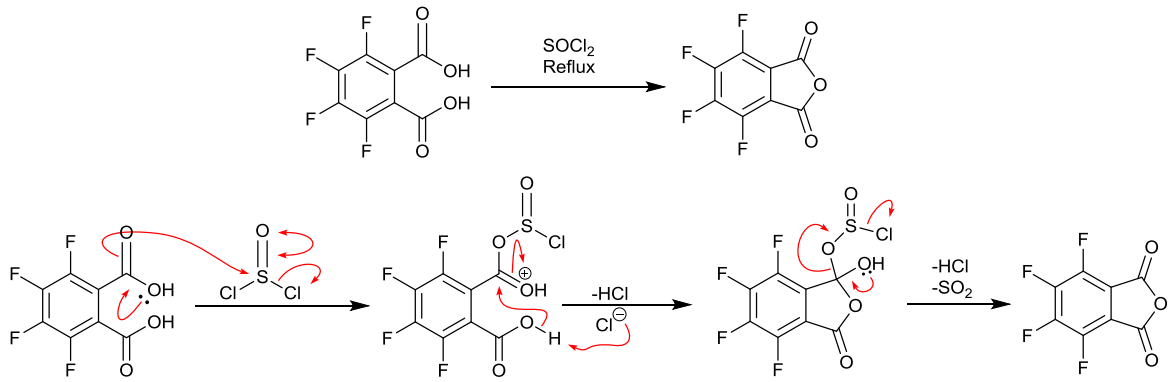

Figure 7.17 : Autodehydation reaction to form fluorinated intermediate tetrafluorophthalic anhydride

This dehydration reaction was carried out in neat thionyl chloride, heating at 90 °C overnight. Removal of the excess thionyl chloride *in vacuo* and sublimation of the resulting white solid allowed the desired intermediate in excellent yield. The sublimed material was a large (> 6 cm diameter) single crystal, a shard of which was used to assess crystal structure of the compound by x-ray crystallography.

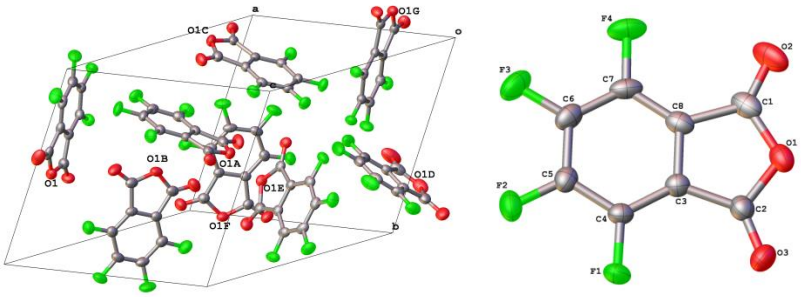

Figure 7.18 : Crystal structure of intermediate

The crystal was found to have eight crystallographically independent identical molecules in the unit cell, which is unusually high. This is likely a result of the sublimation technique used to form the unique crystal.

The anhydride intermediate is highly stable, and can be stored at room temperature for months without degradation.

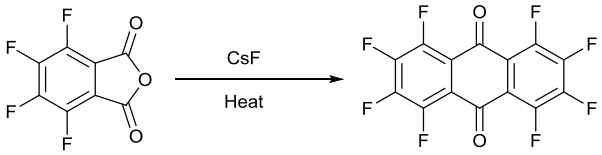

Figure 7.19 : Synthesis route to perfluoroanthraquinone

The anhydride was then subjected to a number of attempts to form 1,2,3,4,5,6,7,8-octafluoroanthraquinone by caesium fluoride in m-xylene and sulfolane.[3] This proved unsuccessful, and purification by sublimation produced less than 5% yield of the intended product. There is great difficulty in using sulfolane since its extremely high boiling point makes removal by vacuum distillation problematic. Multiple attempts were made to produce perfluoroanthraquinone with CeF in carius tubes with and without solvent, and in sulpholane at atmospheric pressure. All were unsuccessful in producing viable amounts for continuation of the synthesis in our hands.

7.3. Experimental

***24**, 9,9,10,10-tetrafluorodeoxyanthraquinone HRMS 5-46-2*

A solution of anthracene (0.502 g, 2.82 mmol) and selectfluor (3.138 g, 8.86 mmol, 3.1 equivalents) in acetonitrile (15 ml) in a microwave vial was heated to 60 °C for 60 s by microwave heating. The solution was allowed to cool and evaporated to dryness before addition of hexane and toluene (1:1), elution through a silica plug and evaporation to dryness gave 9,9,10,10-tetrafluorodeoxyanthraquinone (0.329 g, 46%) as a brown solid. MP (hexane) sublimes ~90 °C; δ_H (600 MHz, Chloroform-*d*) 7.95 (1 H, dd, *J* 5.8, 3.4), 7.67 (1 H, dd, *J* 5.9, 3.3); δ_C (151 MHz, Chloroform-*d*) 132.47 – 131.82 (m), 131.58 , 125.56 (d, *J* 3.6), 114.19 – 110.84 (m); δ_F (564 MHz, Chloroform-*d*) -81.10; MS (GCMS) 252.1 (M^+, 80%), 232.0 (100).

(1) Lendrem, D.; Owen, M.; Godbert, S. DOE (design of experiments) in development chemistry: potential obstacles. *Org. Process Res. Dev.* **2001**, *5*, 324–327.

(2) Leardi, R. Experimental design in chemistry: A tutorial. *Anal. Chim. Acta.* **2009**, *652*, 161–172.

(3) Tannaci, J. F.; Noji, M.; McBee, J.; Tilley, T. D. 9, 10-dichlorooctafluoroanthracene as a building block for n-type organic semiconductors. *J. Org. Chem.* **2007**, *72*, 5567–5573.

8. Summary, Conclusions and Future Work

This thesis has outlined the synthesis and advantages of fluorinated PAH molecular emitters for triplet-triplet annihilation up-conversion systems. These fluorinated molecules were constructed using aryl-aryl coupling techniques, as the fluorination of the reagents is increased a shift from Suzuki-Miyaura cross coupling reactions to the use of nucleophilic aromatic substation is required.

Octafluorotoluene is an excellent partner in nucleophlic substitution, since the reactive para site is blocked to further nucleophililic attack, and the electron withdrawing trifluoromethyl group further activates the ring to the initial attack.

Series of emitters based on 9-phenylanthracene, 9,10-bisphenylanthracene, 3,9(10)-diphenylperylene and 3,5,8-triarylBODIPY were successfully synthesised and their photophysical properties assessed with a view to their use in up-conversion systems. It was clear that fluorination increased the photostability of the emitter molecules while also providing good up-conversion ability. In one case the highly fluorinated derivative 3,9(10)-di-((4-trifluoromethyl)perfluorophenyl)perylene was a more effective emitter in an up-conversion system than the non-fluorinated 3,9(10)-diphenylperylene parent compound, allowing an extremely high up-conversion external quantum yield (16%), and having a high efficiency (21%) with a very low transition between weak and strong up-conversion limits (0.1 $W.cm^{-2}$). Furthermore when incorporated into nanoparticles this system exhibited a high up-conversion external quantum yield (0.9%) when compared to rare-earth up-conversion systems.

Emitters based on the 3,5,8-triarylBODIPY were successfully synthesised by a multi-step method, but are not effective in triplet-triplet up-conversion systems, despite the highly fluorinated derivative (3,5-(3,4,5-trifluorophenyl))-8-(perfluorophenyl)BODIPT being an excellent emissive molecule with high fluorescence quantum yield (93%) and good solubility in organic solvents.

The fluorination of polyaromatic hydrocarbon molecules by direct fluorination procedures (including elemental fluorine) was undertaken. This brought about the previously unreported 9,9,10,10-tetrafluorodeoxyanthraquinone, formed through action of both selectfluor's "F^{+}" providing cation and the BF_4^- anion upon anthracene. This reaction is general for anthracene derivatives with substitution in either of the 9 and 10 positions.

Finally approaches to emitter molecules with fluorinated polyaromatic hydrocarbon units were investigated, both anthracene and rubrene were considered. While these investigations were not completed they hold promise for a new range of fluorinated dyes suitable for organic electronic applications.

During the work the possibilities for Class C TTA emitter molecules were touched upon, indicating that emitters that have high fluorescence yields could be paired in a dyad with those that allow a high TTT yield. In the future a fluorinated Class C emitter containing a BODIPY emissive unit could have a high up-conversion potential. Other possibilities include macromolecules that could allow close alignment in space between sensitizer and emitter molecules in solids and liquids.